

***Characterisation and Performance of
Fibre-Reinforced Composite Restorations***

A thesis submitted to the University of Manchester for the
degree of

Doctor of Philosophy

in the Faculty of Medical and Human Sciences

2015

Ala'a AL-Haddad

School of Dentistry

List of Contents

List of Contents	2
List of Figures.....	9
List of Tables.....	15
List of Abbreviations	16
Abstract	18
Declaration	20
Copyright Statement	21
The Author	22
Dedication	24
Acknowledgment	25
Chapter 1: Review of the literature.....	26
1.1 Composites:.....	27
1.1.1 Introduction:	27
1.1.2 Dental resin-composites:.....	27
1.1.2.1 Resin matrix:	27
1.1.2.2 Inorganic Fillers:	32
1.1.2.3 Coupling agent:	33
1.1.3 Classification of resin composites:	34
1.2 Fibre-reinforced Composites (FRC):.....	36
1.2.1 Background:	36
1.2.2 Definition and classification:	37
1.2.3 Rationale:	37
1.2.4 Clinical applications:	38
1.2.5 Mechanical performance and influencing factors:	39
1.2.5.1 Reinforcing-fibre type:	39

1.2.5.2	Matrix and resin system:	43
1.2.5.3	Impregnation:	46
1.2.5.4	Interfacial adhesion:.....	47
1.2.5.5	Fibre orientation:	50
1.2.5.6	Volume and weight fractions:	54
1.2.5.7	The fibre geometry (placement):.....	55
1.2.6	Physico-mechanical properties of fibre-reinforced composite.....	57
1.2.6.1	Thermal properties:.....	57
1.2.6.2	Bond strength:	59
1.2.6.3	Hardness:.....	63
1.2.6.4	Edge Strength:.....	68
1.2.6.5	Fatigue:	70
1.2.6.6	Wear resistance:	75
1.3	summary:.....	80
1.4	References:	81
Chapter 2:	Aims and Objectives.....	105
2.1	Aims of the study:.....	106
Chapter 3:	General Methodology	108
3.1	INTRODUCTION	109
3.2	Materials:.....	109
3.3	Measurement of Hardness and Irradiance (Chapter 4):	111
3.3.1	Vickers hardness measurement:	111
3.3.1.1	Rationale:	111
3.3.1.2	Pilot Study:.....	112
3.3.1.3	Materials and Methodology:	112
3.3.2	Irradiance measurement:.....	113
3.4	Edge strength measurement (Chapter 5):.....	116

3.4.1.1	Rationale:	116
3.4.1.2	Pilot Study.....	116
3.4.1.3	Materials and Methodology:	117
3.5	Shear bond strength measurement (Chapter 6):	119
3.5.1.1	Rationale:	120
3.5.1.2	Materials and Methodology:	120
3.6	Load-bearing capacity of FRC-FPDs (Chapter 7):	123
3.6.1.1	Rationale:	123
3.6.1.2	Materials and Methodology:	124
3.7	Wear Measurement (Chapter 8):	127
3.7.1.1	Rationale:	127
3.7.1.2	Pilot study:	128
3.7.1.3	Materials and Methodology:	128
3.8	Load bearing capacity of Metal-free crowns (Chapter 9):.....	131
3.8.1.1	Rationale:	131
3.8.1.2	Materials and Methodology:	131
Chapter 4: Influence of Fibre-Reinforced Composite on Microhardness and Light Transmittance. 134		
4.1	Abstract:	135
4.2	Introduction:	136
4.3	Materials and methods:	137
4.3.1	Materials:	137
4.3.2	Microhardness assessment:	138
4.3.3	Irradiance measurements:	139
4.3.4	Statistical analysis:	140
4.4	Results:.....	141
4.5	Discussion:	145

4.6	Conclusions:	149
4.7	References:	150
Chapter 5: Effect of Fibre-Reinforcement and Orientation on The Edge-Strength of Direct Resin Composites		153
5.1	Abstract:	154
5.2	Introduction:	155
5.3	Materials and Methods:.....	156
5.3.1	Specimen preparation:	157
5.3.2	Edge strength testing:.....	158
5.3.3	Fractography:.....	158
5.3.4	Statistical analysis:	158
5.4	Results:.....	159
5.5	Discussion:	163
5.6	Conclusions:	166
5.7	References:	167
Chapter 6: Influence of Fibre-Reinforced Composite on Shear Bond strength with Ceramic and Metal Substrates.		170
6.1	Abstract:	171
6.2	Introduction:	172
6.3	Materials and methods:	173
6.3.1	Specimen preparation	175
6.3.2	Surface treatment and bonding procedure:	175
6.3.3	Bonding procedure:	175
6.3.4	Thermocycling:.....	177
6.3.5	Shear bond testing:	177
6.3.6	Statistical analysis:	177
6.4	Results:.....	178

6.5	Discussion:	181
6.6	Conclusion:.....	185
6.7	Referances:	186
Chapter 7: Fracture Load of Fibre-Reinforced Composite Bridges after <i>in-vitro</i> Chewing Simulation.....		
		189
7.1	Abstract	190
7.2	Introduction:	191
7.3	Materials and methods:	192
7.3.1	Specimen preparation:	194
7.3.2	FRC-FPD fabrication:	194
7.3.3	Chewing simulation:	197
7.3.4	Static loading to fracture:	198
7.3.5	Statistical analysis:	198
7.4	Results:.....	199
7.4.1	Quantitative findings.....	199
7.4.2	Qualitative findings:	204
7.5	Discussion:	205
7.6	Conclusions:	208
7.7	Referances:	209
Chapter 8: Quantitative Wear Evaluation of Metal-Free Crowns Using Intraoral Scanner <i>in-vitro</i>		
		212
8.1	Abstract:	213
8.2	Introduction:	214
8.3	Materials and methods:	216
8.3.1	Specimen Preparation:	216
8.3.2	Crown fabrication:	217
8.3.3	Wear simulation:	219

8.3.4	Wear analysis:	219
8.3.5	Statistics:	220
8.4	Results:	223
8.5	Discussion:	224
8.6	Conclusions:	227
8.7	Acknowledgements:.....	227
8.8	References:	228
Chapter 9: Load-Bearing Capacity of Fibre-Reinforced Composite Crowns in Comparison with Machined Alternatives.....		231
9.1	Abstract:	232
9.2	Introduction:	233
9.3	Methodology:	234
9.3.1	Specimen Preparation:	235
9.3.2	Crown fabrication:	235
9.3.3	Dynamic fatigue:	238
9.3.4	Static loading:.....	240
9.3.5	Statistical analysis:	240
9.4	Results:.....	241
9.5	Discussion:	243
9.6	Conclusion:.....	245
9.7	References:	246
Chapter 10: General Discussion, Implications, Recommendations for Future Work and Conclusions.....		249
10.1	General discussion:	250
10.2	Implications:	255
10.3	Recommendation for future work:.....	256
10.4	Conclusions:	257

10.5 References:	258
Appendix I:	261

Word Count: 48,469

List of Figures

Figure 1.1: Dimethacrylate molecules mostly used in dental resin-composites.....	29
Figure 1.2: Free-radical polymerization reaction of methacrylate-based composites. A) benzoyl peroxide readily splits to form two identical free radicals which can initiate polymerisation, B) reaction of a benzoyl peroxide radical with methylmethacrylate to form a new radical species, C) structural formulas of Camphoroquinone and D) dimethylamino ethylmethacrylate, commonly-used photo-activator and accelerator, respectively.....	30
Figure 1.3: Structural formula of Silorane molecule	31
Figure 1.4: Methacryloxypropyl trimethoxysilane	33
Figure 1.5: Classification of dental resin-composite.	35
Figure 1.6: Chemical structure of silane molecule connecting reinforcing-fibre with its matrix by Siloxane bridge.	50
Figure 1.7: Reinforcing efficiency (Krenchel factor K_{θ}) of fibres with different fibre orientation [44]. A) Unidirectional fibre orientation resulting in anisotropic materials with $K_{\theta}=1$, B) Unidirectional fibre orientation resulting in anisotropic materials with $K_{\theta}= 0$, C) Bidirectional fibre (woven) mat resulting in an orthotropic material with $K_{\theta}= 0.5$, D) Bidirectional fibre ($45^{\circ}/45^{\circ}$ bias) resulting in an orthotropic material with $K_{\theta}= 0.25$, E) Random fibres orientation resulting in an isotropic material with $K_{\theta}= 0.2$, providing the fibres are longer than critical length for that fibre type.....	51
Figure 1.8: Influence of fibre misalignment on the tensile strength of continuous unidirectional FRC [44].	52
Figure 1.9: Schematic representation of an efficient fibre placement at the tension side of a restoration.	56
Figure 2.1: General outline for the research.....	107
Figure 3.1: Flowchart showing the study protocol in Chapter 4	111
Figure 3.2: FM-700 microhardness tester (A), with a representative specimen ready for testing (B).	113

Figure 3.3: Schematic diagram showing the geometry of specimens tested for microhardness and the three points of interest measured on top/bottom surfaces.	113
Figure 3.4: MARC resin calibrator used for irradiance measurement, A) its main parts, B) LED curing unit during the baseline measurement and C) the mould assembly placed on top sensor prior to irradiance measurement.....	114
Figure 3.5: Schematic diagram showing the mould assembly on the top sensor of spectrometer during irradiance measurements. The same assembly was used during the baseline measurement of curing light in order to calculate the light attenuation occurred purely because of FRC and PRC.	115
Figure 3.6: Graph showing the irradiance versus time for one representative specimen for each group during the direct light curing for 20s.....	115
Figure 3.7: Diagram showing the study protocol in Chapter 5.	116
Figure 3.8: Schematic diagram showing the geometry of specimens tested for edge-strength and the two reading points on top surface (0.5mm distance from each edge).	117
Figure 3.9: CK10 edge-strength machine and its main parts (A) during the testing of one representative specimen (B).	118
Figure 3.10: Flowchart showing the study protocol in Chapter 6.....	119
Figure 3.11: Flowchart showing the bonding substrates, surface treatments, testing procedure, and fracture analysis followed in Chapter 6.....	121
Figure 3.12: Flowchart showing the study protocol in Chapter 7.	123
Figure 3.13: Flowchart showing the methodology followed in Chapter 7.....	126
Figure 3.14: Flowchart showing the study protocol in Chapter 8.....	127
Figure 3.15: 3M True Definition Scanner.....	128
Figure 3.16: Snapshot of Geomagic Control software during wear analysis.....	130
Figure 3.17: Wear analysis of a representative specimen relying on superimposition of three successive digital scans, A) 3D comparison performed, B) vertical wear measurement in the wear facet after the completion of C1 phase, and C) C2 phase....	130
Figure 3.18: Diagram showing the study protocol in Chapter 9.	131
Figure 3.19: Flowchart showing the preparation and cyclic loading of crown specimens, A) preparation of master mould, B) duplicated acrylic teeth coated with wax layer, C)	

mounted teeth in epoxy resin base and the wax coating is substituted with PVS layer, D) a specimen assembly ready for crown cementation, E) surface treatment (silica coating) for acrylic teeth and crowns using Cojet repair system, F) cementation of crowns using self-adhesive cement (RelyX Unicem 2), G) one representative specimen after cementation and thermocycling, H) mounted in the chewing simulator for cyclic loading and I) following the completion of cyclic loading..... 132

Figure 3.20: Static loading of one representative crown specimen using the steel ball indenter of Zwick Z020 machine..... 133

Figure 3.21: The mode of fracture of three representative crown specimens, A) Lava Zirconia, B) Lava Ultimate and C) FRC-Sinfony. * indicates the origin of fracture, while indicates crack propagation..... 133

Figure 4.1: Light curing unit assembly on the MARC Resin Calibrator using BenchMARC controller. 140

Figure 4.2: Schematic diagram showing the mould assembly on the spectrometer's top sensor during irradiance measurement..... 140

Figure 4.3: Bar chart showing mean (SD) VHN for top and bottom surface for all groups immediately post-cure and after 48h water storage..... 142

Figure 4.4: Graph showing the irradiance versus time for one representative specimen of each group during direct light curing (20s)..... 143

Figure 4.5: Scatter plot showing the positive correlation between the mean irradiance values and the bottom/top hardness ratio for all tested groups (R^2 Cubic= 0.974). This plot explains that the bottom/top VHN ratio, as an indicator of the depth of cure, tends to increase exponentially as a consequence of increasing irradiance value transmitted to specimen bottom surface. Such correlation concurs the idea that the incorporation of FRC within PRC tends to reduce depth of cure (bottom/top VHN ratio) by reducing the irradiance level transmitted to specimen bottom surface. Even at higher levels of irradiance, the consequential increase in VHN ratio plateaus out, owing to many factors affecting the degree of conversion within the bottom surface, including material type, distribution and quantity of fillers, quantity of photoinitiator, translucency and thickness of specimen, which can hinder any further light transmittance or material polymerization. 144

Figure 5.1: Bar chart showing the mean (SD) edge strength for all tested groups..... 161

Figure 5.2: Mode of failure for three representative specimens (top view where the load was perpendicularly applied), A) minimal chipping, B) edge fracture and C) edge/bulk fracture. Arrow head indicates crack propagation within specimen bulk. 162

Figure 5.3: Mode of failure for three representative specimens (side view of specimen edge), A) minimal chipping, B) edge fracture and C) edge/bulk fracture. Large arrow head indicates crack propagation within specimen bulk. Small arrow head indicates fracture line at edge surface. 162

Figure 5.4: Two representative fractured specimens made of XB with A) no reinforcement (control) and B) unidirectional FRC. 162

Figure 6.1: Two representative specimens. A) ceramic substrate and B) Co-Cr metal substrate..... 176

Figure 6.2: Bar chart showing mean (SD) shear bond strength for all groups according to their substrate and surface treatment..... 179

Figure 6.3: Examples of the failure modes observed following SBS testing, A) cohesive fracture in bidirectional FRC layer with metal, B) cohesive fracture in unidirectional FRC layer with ceramic, C) mixed adhesion/cohesion fracture at the ceramic interface with no reinforcement. 180

Figure 7.1: Diagrams showing A) the specimen assembly and dimensions of inlay cavities in each abutment, B) Type-I fibre framework, and C) Type-II framework. The dimensions of major connectors were 5mm height, 2.5mm width at premolar side and 3.5mm width at molar side. The clearance of the pontic base from the PMMA base was 3mm, ensured by using a custom silicon index beneath the pontic during fabrication. 195

Figure 7.2: 3D representations of a specimen during the preparation, A) silica coating for the cavities to enhance adhesion, B) bonding of the main FRC framework within the inlay retainers using bonding agent (Viso-Bond) and flowable PFC (x-tra Base) , and C) full build-up for the pontic with packable bulk-fill PRC (X-tra fil). 196

Figure 7.3: One representative specimen mounted in CS 4.2 machine, A) during the cyclic loading with the stylus moving vertically to the central fossa and then obliquely over the buccal groove, and B) after the completion of cyclic loading. 197

Figure 7.4: Bar chart showing the mean (SD) values of static IF and FF values for all tested groups with (B) and without previous thermocycling and dynamic fatigue (A).. 200

Figure 7.5: Scatter plot showing the positive linear correlation between initial fracture and final fracture in both framework types.	201
Figure 7.6: Scatter plot showing the Weibull modulus (m) for both framework types.	202
Figure 7.7: Scatter plot showing the characteristic strength (σ_0) for both framework types.	203
Figure 7.8: Examples of the fracture modes observed in FRC-FPDs after static loading, A) horizontal cracks extending from underneath the major connectors to the central fossa (loading point), B) delamination fracture with a separation of a mesio-lingual veneering PRC and C) midline (catastrophic) fracture extending vertically between both retainers.	204
Figure 8.1: Fabricating materials used to prepare all specimens, A) Lava Zirconia, B) Lava Ultimate and C) Stick Net & Sinfony.	218
Figure 8.2: Occlusal views for one representative specimen from each group showing the wear facet (*) and its morphological changes after C0, C1 and C2 phases (using Geomagic Control software). LZ had the modest morphological changes, while LU had the largest.	220
Figure 8.3: A snapshot from the Geomagic software after the ‘Best Fit Alignment’ function was performed (top), the area of interest ‘common area’ was selected prior to the alignment (middle), and then the 3D Comparison performed and the deviations visualised via deviation spectrum (bottom).	221
Figure 8.4: 3D comparisons for one representative specimen in group LU, (Top) shows the mean wear value ‘W1’ within the wear facet (0.5mm radius) after phase C1, while (bottom) shows the cumulative wear W_C at the end of phase C2.	222
Figure 8.5: Graph showing the mean cumulative wear (μm) for all the tested groups.	223
Figure 9.1: Representative specimen assembly showing a duplicated abutment in epoxy resin base (2mm below CEJ) and surrounded with PVS layer (0.2mm thickness) to simulate PDL.	235
Figure 9.2: 3D impressions for the master preparation using 3M True Definition Scanner, A) Buccal view showing the shoulder finish line (1mm) and buccal cusp bevel, and B) bite registration with 1.5mm interocclusal clearance.	236

Figure 9.3: CS 4.2 chewing simulator machine with its two compartments (top), one representative specimen mounted in one compartment (left), the same specimen after the completion of cyclic loading with a spectacular wear facet (right). 239

Figure 9.4: One representative crown specimen mounted in the Zwick machine prior to static loading..... 240

Figure 9.5: Bar chart showing the mean load bearing capacity for all tested groups... 241

Figure 9.6: Fractured representative specimens from each group. Lava Zirconia:LZ (top) Lava Ultimate: LU (mid), FRC-S (bottom) 242

List of Tables

Table 1.1: Mechanical properties of particulate-reinforced composites [3].	39
Table 3.1: List of materials used to perform this research.....	110
Table 4.1: Materials used to prepare all specimens	138
Table 4.2: Mean (SD) values of Vickers Hardness (VHN) for all tested groups.	141
Table 4.3: Mean and Maximum (SD) values of irradiance (I_R), total energy (E_T) and time required to reach plateau for all tested groups.....	143
Table 5.1: Materials used to prepare all specimens.	157
Table 5.2 : Mean (SD) edge-strength values (N) for all groups.	159
Table 5.3: The mode of fracture for all groups.	160
Table 5.4: The efficiency of different fibre reinforcement represented by Cohn's d ($r_{y\lambda}$) values for every main group.	160
Table 6.1: Materials used in this study	174
Table 6.2: Mean (SD) shear bond strength for all the tested groups.	178
Table 6.3: Fracture mode distribution for all tested groups according to the surface treatment applied.	180
Table 7.1: Materials used to fabricate all specimens.	193
Table 7.2: Mean \pm SD values for initial fracture (IF) and final fracture (FF) loads for all tested groups.....	199
Table 7.3: The mode of fracture exhibited in all tested specimens.	204
Table 8.1: Materials used to fabricate all crowns in the study.	216
Table 8.2: Wear measurements (μm) for all specimens, using 3D analysis.	223
Table 9.1: Materials used to fabricate all crowns in the study.	234
Table 9.2: The mean (SD) load-bearing capacity (N) for all tested groups	241

List of Abbreviations

A	Area
°C	Centigrade
3D	Three-dimensional
ANOVA	Analysis of variance
Bis-EMA	2,2-bis[4-(2methaacrylyloxyethoxy)phenyl]propane
Bis-GMA	Bisphenol-A glycidyl methacrylate
CEJ	Cementoenamel junction
DC	Degree of conversion
ET	Total energy
FEA	Finite element analysis
FF	Final fracture
FMax	Maximum force
FPD	Fixed partial denture
FRC	Fibre-reinforced composite
FRC-S	Fibre-reinforced composite & Sinfony
gF	Gram Force
GPa	Gigapascal
h	Hour
HVN	Hardness Vickers Number
Hz	Hertz
IF	Initial Fracture
IR	Irradiance
ISO	International Standard Organization
J	Joule
Kg	Kilogram
k θ	Krenchel factor
LED	Light emitting diodes
LU	Lava Ultimate
LZ	Lava Zirconia
m	Weibull modulus
min	Minute
mm	Millimetre
μ m	Micrometer
MPa	Megapascal

N	Newton
n	Sample Size
nm	Nanometer
PMMA	Poly (methyl methacrylate)
PRC	Particulate-Reinforced Composite
PTFE	Polytetrafluoroethylene
PVS	Polyvenyl siloxane
r	Pearson's correlation coefficient
R ²	Simple correlation coefficient
RBC	Resin-based composite
r _{γλ}	Effect-size correlation
s	Second
SBS	Shear Bond Strength
SD	Standard Deviation
SEM	Scanning Electron Microscopy
Semi-IPN	Semi-Interpenetrating Polymer Network
TEGDMA	triethylene glycol dimethacrylate
UDMA	Urethane dimethacrylate
UHMWPE	Ultra-High Molecular Weight Polyethylene
UV	Ultraviolet
vol%	Volume Percentage
W	Watt
WC	Cumulative wear
wt%	Weight percentage
α	Significance level
σ _θ	Characteristic strength
∅	Diameter

Abstract

In the modern era of metal-free minimally-invasive dentistry, there is a growing tendency toward using metal-free restorative alternatives that provide not only excellent aesthetics but also enable superior durability. Fibre-reinforced composite (FRC) is one cost-effective alternative that fulfils the requirements of aesthetics and durability, and offers favourable physico-mechanical properties. Many FRC applications are well-documented in the literature, such as crowns and fixed partial dentures (FPD); however, their clinical implementation is still limited, owing to the lack of significant knowledge about their longevity, deterioration signs, optimum design and overall performance. This *in-vitro* research aimed to address these uncertainties by investigating the performance of FRC restorations, and the influence of fibre reinforcement on particular physico-mechanical properties, including surface hardness, edge-strength, shear bond strength, fatigue and wear resistance.

Basic testing models were used to investigate the effect of incorporating differently-oriented FRCs on the surface hardness, edge-strength and shear bond strength of particulate-reinforced composite (PRC). The results revealed that the incorporation of FRC significantly enhanced surface hardness (by 12 - 19 %) and edge-strength (by 27 - 75 %). However, this incorporation significantly reduced the shear bond strength (SBS) between PRC and other restorative materials, including lithium disilicate ceramic (10.9 ± 3.1 MPa) and Co-Cr metal alloy (12.8 ± 2.3 MPa), compared to the control (15.2 ± 3.6 MPa, 15.0 ± 3.7 MPa). The orientation of FRC was also found to affect the efficiency of reinforcement as bidirectional FRCs exhibited significantly higher hardness (76.8 ± 1.2 VHN), edge-strength (67.7 ± 8.2 N) and SBS (14.1 ± 3.9 MPa) values than unidirectional FRCs (72.4 ± 1.2 VHN, 56.8 ± 5.9 N, 9.8 ± 2.3 MPa).

Clinically-relevant testing models, employing accelerated aging techniques, were performed to investigate the fatigue and wear behaviours of anatomically-shaped FRC restorations *in-vitro*. Direct inlay-retained FRC-FPDs with two framework designs, were tested for their fatigue behaviour and load-bearing capacity. Type-I design (with an additional bidirectional FRC layer incorporated perpendicular to the loading direction) yielded significantly higher fatigue resistance (1144.0 ± 270.9 N) and load-bearing capacity (1598.6 ± 361.8) than Type-II design (with a woven FRC embedded around the pontic core) (716.6 ± 72.1 N, 1125.8 ± 278.2 N, respectively). However, Type-

II design exhibited fewer delamination failures. Both framework design and dynamic fatigue were found to have a significant influence ($p < 0.05$) on the load-bearing capacity of FRC-FPDs.

Additionally, the *in-vitro* fatigue and wear behaviours of FRC crowns, fabricated conventionally from bidirectional FRC and indirect PRC (Sinfony), were compared with those made of two CAD/CAM alternatives, namely Lava Zirconia (LZ) and Lava Ultimate (LU). A chewing simulator was employed to induce some fatigue wear in crowns, while an intraoral 3D scanner was used to quantify the resultant morphological changes. The results showed that FRC crowns had significantly lower mean cumulative wear ($233.9 \pm 100.4 \mu\text{m}$) than LU crowns ($348.2 \pm 52.0 \mu\text{m}$), but higher than LZ crowns ($16.4 \pm 1.5 \mu\text{m}$). The mean load bearing-capacity after fatigue simulation was also the highest for LZ crowns ($1997.8 \pm 260.2 \text{ N}$) compared with FRC ($1386.5 \pm 258.4 \text{ N}$) and LU crowns ($756.5 \pm 290.9 \text{ N}$).

Accordingly, the incorporation of FRC in resin-composite restorations is advocated since it increases surface hardness and marginal integrity, improves fatigue and wear behaviours, and enhances load-bearing capacity and overall performance.

Declaration

No portion of the work referred to in the thesis has been submitted in support of an application for another degree or qualification of this or any other university or other institute of learning.

Alaa AL-Haddad
2015

Copyright Statement

- i. The author of this thesis (including any appendices and/or schedules to this thesis) owns any copyright in it (the “Copyright”) and s/he has given The University of Manchester the right to use such Copyright for any administrative, promotional, educational and/or teaching purposes.
- ii. Copies of this thesis, either in full or in extracts and whether in hard or electronic copy, may be made only in accordance with the Copyright, Designs and Patents Act 1988 (as amended) and regulations issued under it or, where appropriate, in accordance with licensing agreements which the University has from time to time. This page must form part of any such copies made.
- iii. The ownership of certain Copyright, patents, designs, trade marks and other intellectual property (the “Intellectual Property”) and any reproductions of copyright works in the thesis, for example graphs and tables (“Reproductions”), which may be described in this thesis, may not be owned by the author and may be owned by third parties. Such Intellectual Property and Reproductions cannot and must not be made available for use without the prior written permission of the owner(s) of the relevant Intellectual Property and/or Reproductions.
- iv. Further information on the conditions under which disclosure, publication and commercialisation of this thesis, the Copyright and any Intellectual Property and/or Reproductions described in it may take place is available in the University IP Policy (see <http://documents.manchester.ac.uk/DocuInfo.aspx?DocID=487>), in any relevant Thesis restriction declarations deposited in the University Library, The University Library’s regulations (see <http://www.manchester.ac.uk/library/aboutus/regulations>) and in The University’s policy on Presentation of Theses.

The Author

I graduated from the University of Jordan in 2008, gaining a BDS with a GPA of 3.65 out of 4 (Excellent). I worked then as a teaching assistant at the same university between 2009 and 2010 in the department of Fixed Prosthodontics. I was awarded a scholarship to continue my postgraduate study abroad, and so joined the University of Manchester in 2010. I enrolled in a one year full-time MSc Fixed and Removable Prosthodontics programme, which I finished with Merit. In September 2011, I enrolled in a full-time four-year clinical PhD (Doctor of Clinical Dental Science in Fixed and Removable Prosthodontics). In 2014, I won the Paffenberger Student Research Award (2nd prize) for research work I presented at the Academy of Dental Materials annual meeting (Bologna, Italy). I am also a journal reviewer for Dental Materials. During my PhD study, I also attended several scientific meetings:

- British Society of Prosthodontics meeting in Liverpool in April 2012.
- ADI Team Congress meeting in Manchester in May 2013.
- British Society of Prosthodontics meeting in Dundee in April 2014.
- British Society of Prosthodontics meeting in London in March 2015.

I also presented my research work at the following meetings:

- 22nd European Dental Materials Conference in Birmingham in August 2013. (Poster presentation titled: the influence of fibre-reinforced composite on edge-strength).
- IADR/PER Congress in Dubrovnik (Croatia), in September 2014. (Poster presentation titled: Fracture load of Fibre-reinforced composite bridges after chewing simulation, Abstract number: 501).
- Academy of Dental Materials annual meeting in Bologna (Italy) in October 2014. (Poster presentation titled: Fracture of fibre-reinforced composite crowns verses CAD/CAM alternatives).
- ADR/AADR/CADR General Session & Exhibition in Boston (USA), in March 2015. (Oral presentation titled: Quantitative Wear Evaluation OF Metal-Free Crowns Using True Definition Scanner).
- 23rd European Dental Materials Conference in Nuremberg (Germany) in August 2015. (Poster presentation titled: Influence of fibre-reinforcement on shear bond strength with ceramic/metal substrates).

In addition, another research work will be presented in the following meeting:

- Academy of Dental Materials annual meeting in Maui, Hawaii (USA) in October 2015. (Poster presentation titled: Influence of fibre-reinforced composite on microhardness and light transmittance).

I am currently in the process of submitting my research to a variety of scientific dental journals.

Dedication



In The Name of ALLAH,

and with His Blessing,

The All-knowing, The Most-Wise.

This thesis is dedicated to my beloved wife, **Alaa**, for all the sacrificial care she gave me throughout my study. Without you in my life, this work would not have been possible.

I would also like to dedicate this work to my parents, **Mohammad** and **Seham**, for their support and encouragement during all stages of this work. You are the inspiration of my achievements.

This thesis is also dedicated to my dearly son, **Karam**, and my siblings **Bahaa**, **Deyaa**, **Doaa** and **Baraa**.

Acknowledgment

All praises are due to ALLAH for his merciful guidance throughout my life and during my stay in Manchester.

I would like to express my sincere gratitude and deepest respect to my supervisors **Dr. Nick Silikas** and **Prof. Julian Satterthwaite** for all invaluable support they offered me throughout my project. I appreciate all the time, energy and motivation you have given me to complete this work.

My genuine appreciation is to *the University of Jordan, Amman, Jordan* for giving the opportunity to pursue my postgraduate study at the University of Manchester.

My thanks are also due to my friends **Ahmad El-Ma`aita, Muayed Zankuli, Ruwaida Alshali, Kold Al-Ahdal** and **Hanan Alsunbul** for their support and advice throughout the years.

Sincere gratitude is due to **Mr Ahmad Hjazi** for all invaluable help and support he offered to me throughout the years I spent in Manchester.

Chapter 1: Review of the literature

1.1 COMPOSITES:

1.1.1 Introduction:

A composite is defined as a material composed of two or more chemically discrete constituents or phases separated by a definite interface [1, 2]. Major phases in a composite material are the reinforcement phases (discontinuous) embedded within a continuous phase, termed as a matrix [3]. The reinforcing phase is usually harder and tougher than the matrix, and thus aids in improving the overall properties. Although the discrete phases maintain their integrity within the composite, the resultant properties may not be completely related to those of their constituents [4]. This is attributed to the synergistic influence of volume fraction, geometric orientation, distribution and interactions of the constituents on the resultant properties [5]. Taking into account all such parameters, it is possible to a certain extent to tailor the properties of a composite material according to particular requirements [2, 6]. Accordingly, researchers in many fields continuously develop synthetic composites in order to address an extensive range of demands [1, 7, 8]. In dentistry, resin-composite materials are principally being developed as restorative materials with properties similar to that of the tooth structure being replaced.

1.1.2 Dental resin-composites:

In the context of dental materials science, resin composite is defined as “a highly cross-linked polymeric material reinforced by a dispersion of amorphous silica, glass, crystalline, or organic resin filler particles and/or short fibres bonded to the matrix by a coupling agent” [9]. From the definition, a dental resin composite is typically produced from three distinct components: polymer resin matrix (the continuous phase), inorganic filler particles (the dispersed phase) and coupling agents (the interfacial phase). The presence of each component at a certain percentage is fundamental to achieve a successful resin-composite restoration [5, 9].

1.1.2.1 Resin matrix:

The matrix is the chemically active component of the resin-composite material. It is composed of one or more monomer/oligomers transformed into a cross-linked hard polymer by means of chemical or photochemical polymerization [10]. In the contemporary resin-composites, the matrix is commonly formulated from methacrylate molecules [10], although other molecules with higher functionality are also employed

[11, 12]. Monomers originally used in resin-composites were based on mono-methacrylate monomers, such as MMA [methylmethacrylate], which tend to produce a relatively linear polymer network and offer inadequate properties in terms of strength, polymerization shrinkage and water degradation. However, dimethacrylate monomers are the most widely used nowadays due to the fact that they have higher molecular weight and form a highly cross-linked polymer network, which solves many of the drawbacks of the predecessor monomers [12].

A variety of aromatic and aliphatic dimethacrylates has been employed as a monomer system for dental resin-composites (Figure 1.1). The most commonly used monomers are bisphenol-A-glycidyl dimethacrylate (Bis-GMA), ethoxylated Bis-GMA (Bis-EMA) and urethane dimethacrylate (UDMA) [10, 13]. Co-monomers with low molecular weight and viscosity, such as triethylene glycol dimethacrylate (TEGDMA) or ethylene glycol dimethacrylate (EGDMA), are also incorporated as a diluent to lower the viscosity of resin systems [10-14]. As the viscosity of the resin matrix decreases, more reinforcing fillers may be incorporated accordingly [10]. Moreover, an improvement in cross-linking between polymer chains can occur, leading to enhanced resistance of solvent degradation and faster polymerization. Nevertheless, a high percentage of low molecular weight dimethacrylates is detrimental as it increases the polymerization shrinkage [5, 10].

Polymerization of methacrylate-based composites depends on free radical reaction (Figure 1.2) [3]. The initiator (e.g. benzoyl peroxide) is converted into free radicals by the influence of accelerator (e.g. dimethylamino ethylmethacrylate (DMAEM)) or photo-activator (e.g. camphoroquinone (CQ)) [15]. Inhibitors (e.g. butylated hydroxytoluene) and stabilizers (e.g. benzophenones) are also incorporated to prevent premature polymerization and darkening with age, respectively [9]. The polymerization results from the conversion of double bonds within the monomers by the influence of free radicals, yielding a highly cross-linked polymeric network [16]. However, such polymerisation reaction is exothermic and associated with volumetric shrinkage, which can cumulatively cause harm to tooth structure [17, 18]. Susceptibility to oxygen inhibition is another drawback of free radical reaction, which leads to premature termination of polymerization and unpolymerized monomer remains. The unpolymerized monomers may leach from resin-composite restorations, and so raise biocompatibility concerns [19].

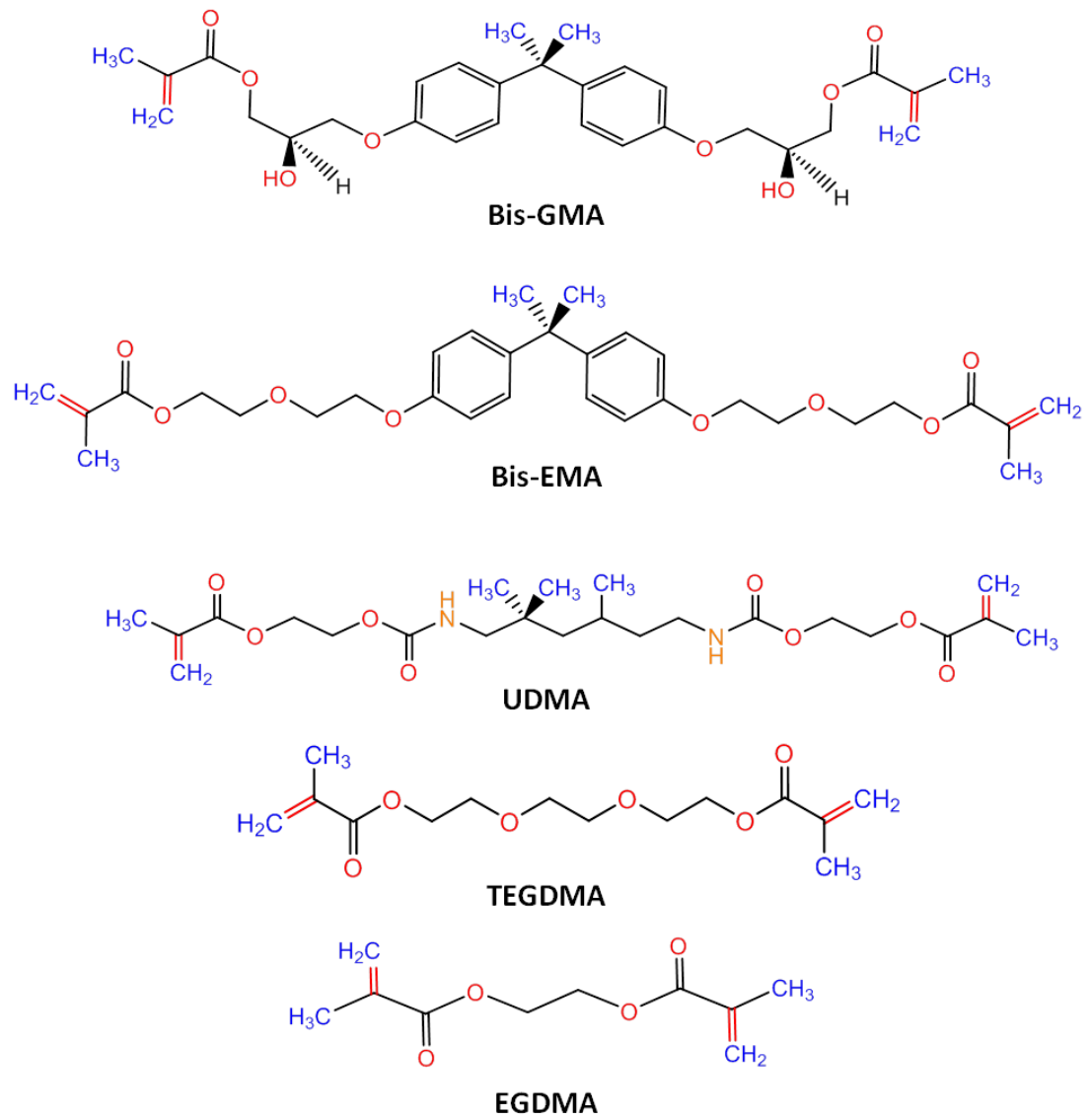


Figure 1.1: Dimethacrylate molecules mostly used in dental resin-composites.

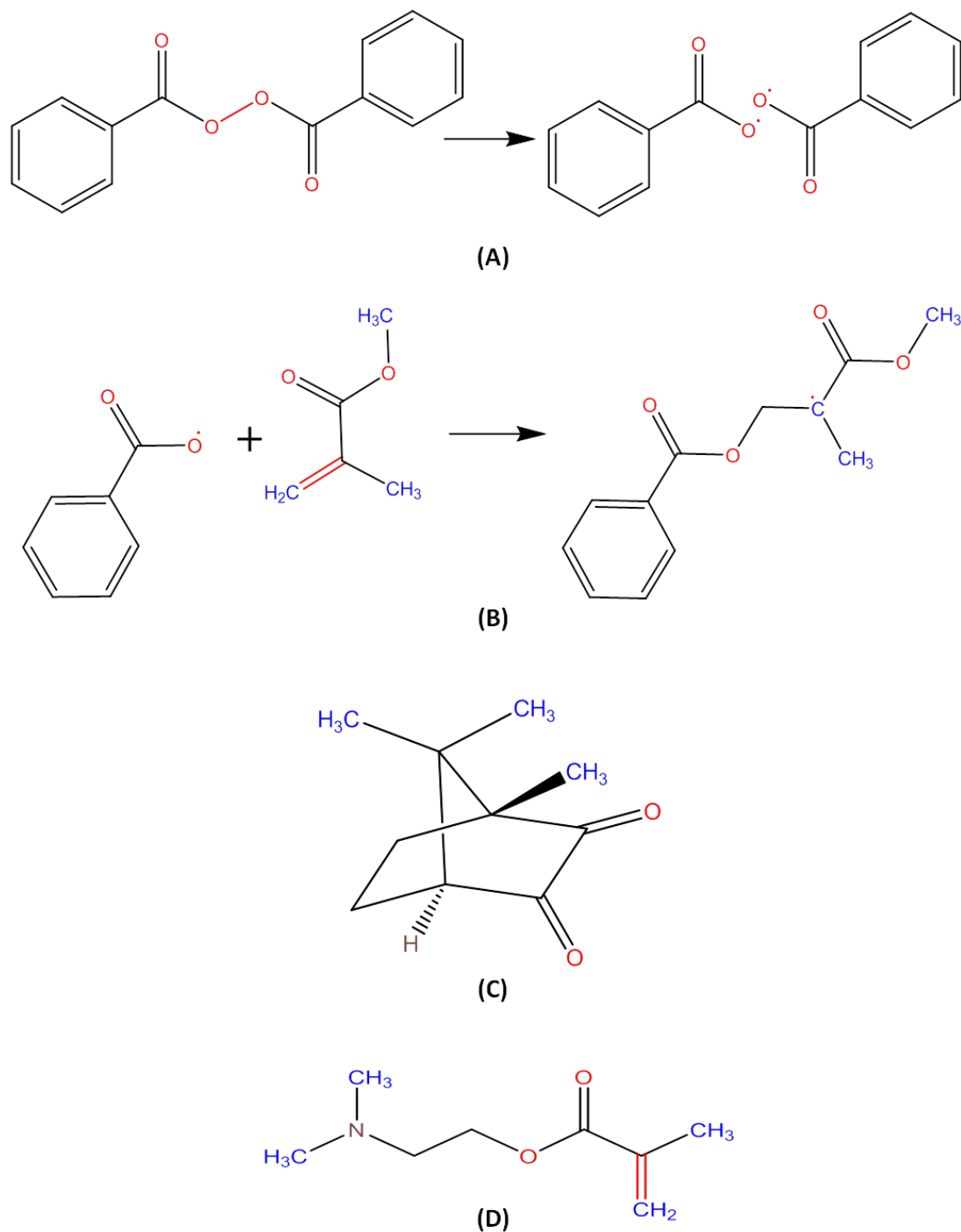


Figure 1.2: Free-radical polymerization reaction of methacrylate-based composites. A) benzoyl peroxide readily splits to form two identical free radicals which can initiate polymerisation, B) reaction of a benzoyl peroxide radical with methylmethacrylate to form a new radical species, C) structural formulas of Camphoroquinone and D) dimethylamino ethylmethacrylate, commonly-used photo-activator and accelerator, respectively.

Recently, several alternative resin systems have been developed to overcome the drawbacks of methacrylate-based composites. Silorane is an example of such alternatives (Figure 1.3). This molecule is a hybrid monomer developed from the reaction of siloxane and oxirane molecules. The siloxane molecule provides the hydrophobic characteristics, while the oxirane molecule represents the active site for polymerisation [20]. The polymerisation is based on a cationic ring-opening reaction, which develops a lower shrinkage polymeric network compared with that resulted from the free radical reaction [21]. Studies comparing methacrylate-based composites with silorane-based alternatives reported that the latter offer higher hydrophobicity, lower polymerization shrinkage, reduced oxygen sensitivity and better biocompatibility [19, 22-24]. Other new alternative monomers, such as dimer acid-based dimethacrylates, tricyclodecane urethane and organically-modified ceramics (ormocers) were also introduced to the market [21].

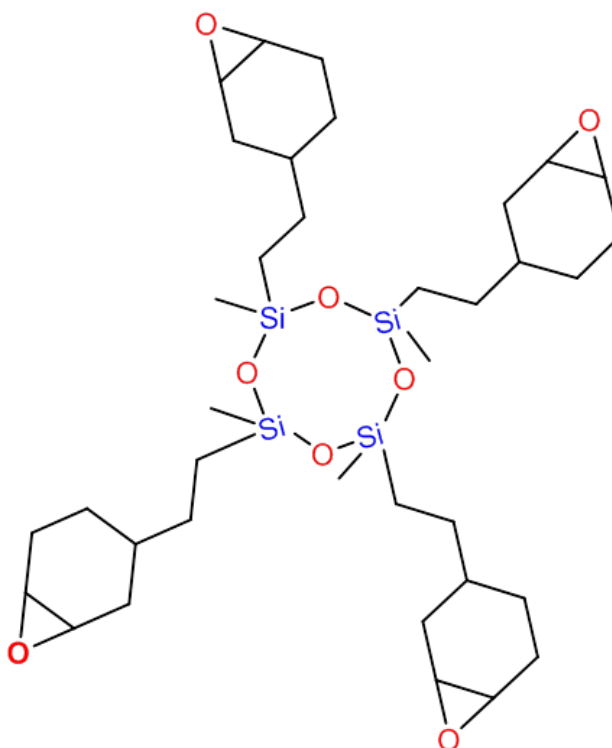


Figure 1.3: Structural formula of Silorane molecule

1.1.2.2 Inorganic Fillers:

The addition of inorganic fillers to dental resins was introduced in the 1950s [25-28]. Since then, it has gained wide acceptance due to its positive influence on many physico-mechanical properties [5, 11, 14, 29, 30]. Higher strength, improved stiffness, enhanced thermal diffusivity, reduced polymerization shrinkage, better rheological properties, improved wear resistance and superior aesthetics are some advantages of the incorporated fillers [5, 14, 30-40]. Nevertheless, the incorporation of too much filler may compromise the resultant properties and produce resin-composites with reduced degree of conversion (DC), increased viscosity, higher brittleness and worse handling [5, 41]. Moreover, the fillers should have a refractive index within the range of that for resin systems. A mismatch in the refractive index between fillers and resins can increase the light scattering and reduce its transmittance within the material, which result in visually opaque materials as well as curing problems [14, 42, 43].

The reinforcing fillers incorporated within resin composites can be in two forms, particles and fibres. Accordingly, resin-composites can be classified into particulate-reinforced composite (PRC) and fibre-reinforced composite (FRC) [3, 44]. PRCs are generally isotropic, meaning that they have similar mechanical and physical properties in all directions [6]. However, the specially oriented reinforcing fibres within FRCs offer anisotropy and result in different mechanical and physical properties in different directions [1, 3, 7, 45, 46]. In PRC, the most commonly used filler particles are quartz, colloidal silica, and silica glass containing barium, strontium and zirconium [47, 48]. Filler particles with various sizes are also used, ranging from 0.1nm to 100µm diameter [49]. According to such sizes, resin-composites are broadly classified into four main types. These types are macrofilled composite (1-100µm) [50], microfilled composite (~3µm) [51], hybrid (0.4-1.5µm) [52] and nanofilled composite (20-75nm) [53]. Furthermore, resin composite can be classified by the volume fraction of fillers into compact-filled (>60 vol% fillers) and midway-filled composite (<60 vol% fillers) [51, 54, 55]. In FRC, long continues and short discontinues fibres are used as reinforcing fillers. Different types of fibres are also employed, including glass, polyethylene and carbon [56-59].

1.1.2.3 Coupling agent:

To achieve optimum reinforcement and stress distribution within resin-composites, the reinforcing fillers and resin matrix have to be well-adhered [40]. In dentistry, this adhesion is typically achieved by coating the surface of the filler with a silane coupling agent [60]. The silane (organosilane) is a bifunctional molecule capable of reacting with the fillers and resin monomers by the influence of its functional groups [61]. The overall reaction of silane with the fillers and resin system determines the quality of the interfacial phase; and therefore many properties of resin-composite [60, 62, 63]. Flexural and compressive strengths, hardness, fatigue, toughness, shear strength, polymerisation shrinkage and durability are all resin-composite properties significantly improved by an appropriate silanization [64-70]. Such improvements are attributed to the enhanced filler dispersion and wetting resulted from silanization, which also reduces viscosity and protects against hydrolytic degradation [61, 71].

The most commonly used organosilane in dental resin composites is 3-methacryloxypropyl trimethoxysilane (MPS) (Figure 1.4). This molecule forms covalent bonds with the fillers and resin matrix by its alkoxy silane and methacrylate functional groups, respectively. Other molecules, such as 3-acryloxypropyltrimethoxysilane (APM), and 10-methacryloxydecyltrimethoxysilane (MDS) are also employed in dental applications [61-64, 72]. The selection of a suitable silane molecule is based on the composition of the inorganic fillers. The availability and number of hydroxyl groups on the surface of fillers determine the reactivity with silane coupling agents, and so influence the selection [61, 73].

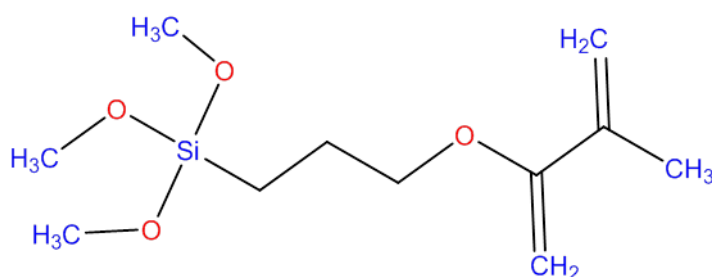


Figure 1.4: Methacryloxypropyl trimethoxysilane

1.1.3 Classification of resin composites:

There are many ways that have been proposed to classify dental resin composites (Figure 1.6). Firstly, according to the mode of activation, resin-composites can be classified into chemically-activated, light-activated and dual-cured composites. Light-activated composites can also be subdivided into direct (chair-side) and indirect (laboratory) composites. Secondly, according to the form of filler, resin-composites are grouped into either particulate-reinforced composite (PRC) or fibre-reinforced composite (FRC). PRCs can be classified according to their filler size into macrofilled, microfilled, hybrid and nanofilled composites. FRCs, however, are classified according to their fibre forms into continuous or discontinuous FRC. Thirdly, based on the viscosity, composites can be classified into flowable and packable composite. Other proposed ways of classification are according to the resin system (methacrylate-based, silorane-based and ormocer-based) [21], clinical applications (anterior, posterior or universal) and filling technique (incremental-fill or bulk-fill) [74].

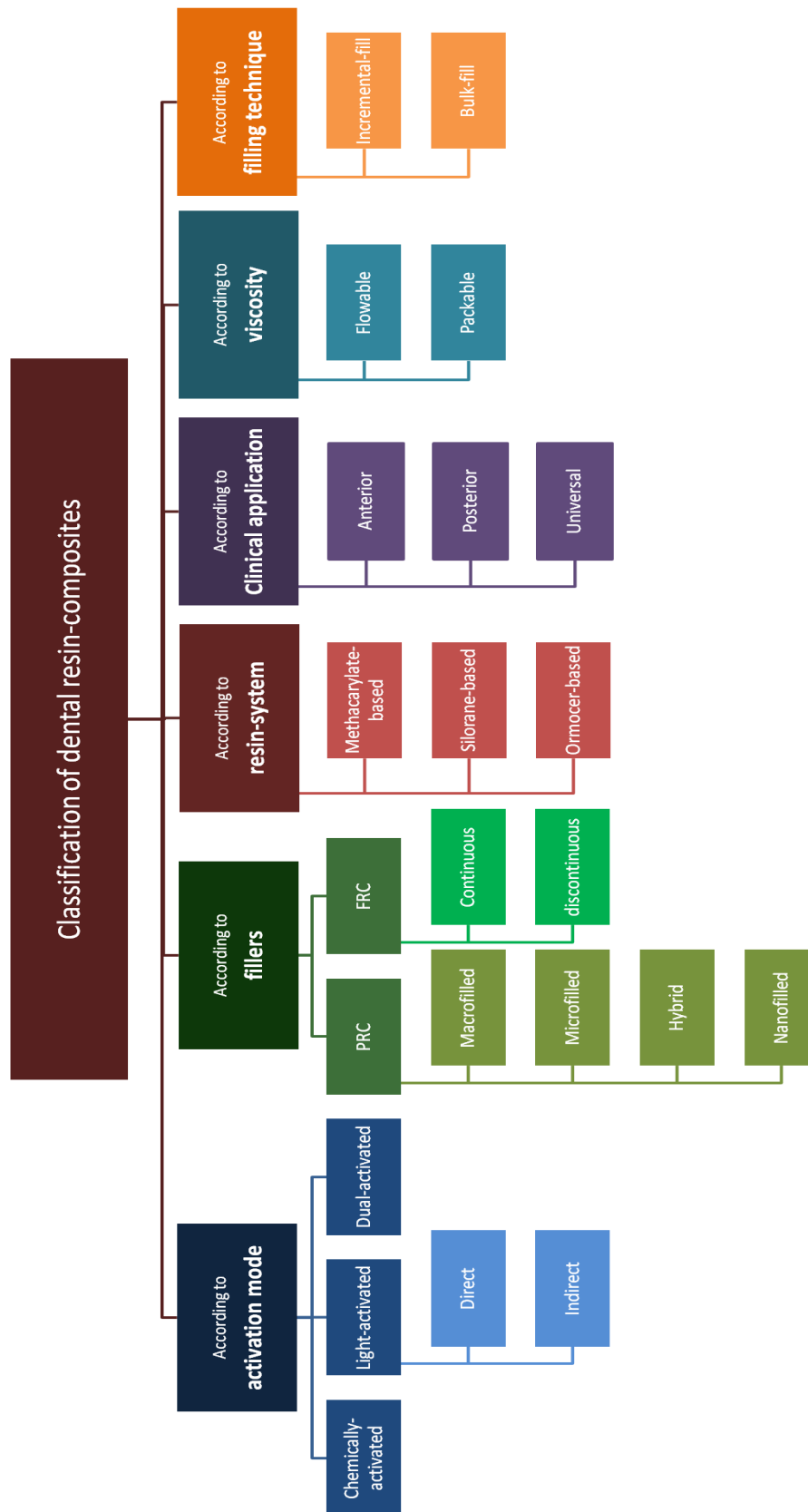


Figure 1.5: Classification of dental resin-composite.

1.2 FIBRE-REINFORCED COMPOSITES (FRC):

1.2.1 Background:

Despite the widespread acceptance particulate-reinforced composite [PRC] material has gained through recent years of the dental practice, its composition is still subject to continuous modification. Many investigations intended to improve the clinical performance of PRC and solve its drawbacks have been conducted in the literature [11]. Some of these drawbacks, like inadequate occlusal wear resistance and colour stability over time, have been successfully resolved in the contemporary resin-composite materials. However, other limitations, including poor wear and fatigue behaviours, polymerization shrinkage, and susceptibility to chemical degradation in the oral cavity, are still evident with a negative influence on the clinical performance, especially in highly-demanding situations when a material with additional levels of strength and aesthetics is required [3]. All of that, together with the ongoing desire for finding metal-free restorative alternatives, have made the conventional PRC far from ideal, and so motivated further searches for a more durable material with higher strength and adequate aesthetics.

Several subsequent advancements in resin-composites have consequently taken place. One advancement was the introduction of widely-accepted engineering technology, so-called 'Fibre-reinforcing Technology', into the dental field [75]. According to this technology, particular fractions of specific continuous fibres have the ability to reinforce the overlaying material and improve its mechanical properties; providing that the fibres are precisely oriented, carefully incorporated and well-bonded with the material [6, 7, 46]. This concept has been examined with a number of polymeric dental materials, such as denture base PMMA, and promising findings have been confirmed [46, 76]. With regard to the conventional dental composite resin material, the implementation of fibre reinforcement concept, combined with the ongoing development of dental adhesive techniques, have not only improved the mechanical properties but also yielded untraditional applications, like periodontal splints, fixed orthodontic retainers and prosthetic fixed partial dentures, a more broadly acceptance [45, 77-81].

Consequently, an increasing number of fibre-reinforced composites have become commercially available. By using FRC products, the era of aesthetic, metal-free, dentistry has become more developed and clinically applicable [29, 82]. However, the

lack of robust detailed information regarding the clinical performance of these newly developed materials is the major obstacle to their further spread.

1.2.2 Definition and classification:

Fibre-reinforced composite [FRC], as the name implies, is a composite material composed primarily of reinforcing fibres imbedded in a resin matrix [45]. The reinforcing fibres are numerous and offered in many different characteristics, including type, fraction, orientation, impregnation and architecture, which all have been claimed to remarkably influence the properties of resultant materials [6, 44].

The common classification of FRCs is according to fibre architecture (continuous or discontinuous), orientation (unidirectional, bidirectional, woven, braided or random), impregnation (pre-impregnated or dry) and type (glass, polyethylene or carbon) [44, 83].

1.2.3 Rationale:

In comparison with metal alloys, ceramics and other restorative materials used in dental practice recently, it is undeniable that conventional dental composite materials have a lot of desirable properties that enable their use in many clinical situations. Cost effectiveness, excellent aesthetics and translucency, non-corrosiveness, adequate adhesion to tooth structure, easy maintenance and minimal invasiveness are some encouraging properties [21, 84]. Conversely, brittleness, polymerisation shrinkage, hygroscopic expansion and mechanical inadequacies in terms of strength and stiffness, are examples of the negative properties that were unfortunately enough to restrict the exploitation of most high-demanding applications, like FPDs, endodontic posts and implant prostheses [85]. A desire of researchers to resolve the limitations of dental composite materials and expand their applications was the main motivation of dental FRC innovation [84, 85].

Complying with the engineering principles of material construction, a material is naturally stronger in the fibre form compared to its bulk [7]. The smaller diameter of a material in its fibre form as well as the preferential alignment of its molecular crystal structures tend to reduce the possibility of future critical defects and produce higher stiffness values [4, 7, 86]. Fibre reinforcing technology of plastics follows these principles and suggests that the reinforcement of a composite material can be possible by incorporating a fibrous reinforcing element. This fibrous reinforcing element has to

have the minimal mandatory aspect ratio (length: diameter), greater than 100, to present its full reinforcing potential [7]. Fortunately, many principles of fibre reinforcing technology of plastics have been implemented successfully in the dental field, and researchers were able to resolve many limitations of conventional dental composites and spread out their applications by relying on FRC [87].

The importance of dental FRC arises from the fact that such materials have a lot of desirable properties. Adding to the favourable properties of conventional dental composites, dental FRC also provide high values of strength and stiffness for a given weight of material, superior to those of most alloys, allowing minimally invasive techniques [78]. They also offer more desirable physical properties in terms of polymerisation shrinkage and thermal expansion as long as prostheses made of FRC are appropriately designed [88, 89]. Unlike conventional materials, the properties of FRC have the potential to be tailored according to the clinical situation [6]. This property gives FRC the potential to be employed in a variety of clinical situations, providing there is awareness of their basic structure and properties as well as appropriate understanding of the specific requirements of various clinical situations.

1.2.4 Clinical applications:

The implementation of FRC in the dental field has been slow compared with the industrial use. Early dental applications were restricted to denture bases due to the problems in aesthetics and handling [45, 75, 83]. With the recent advancement in manufacturing and polymerization methods, dental applications of FRC have been significantly expanded. Numerous FRC applications are well-documented in the literature, including crowns and fixed partial dentures (FPD) [78, 90, 91], periodontal splinting [80, 92-99], orthodontic treatments [81, 100-103], removable dentures [76, 87, 104], endodontic post applications [105-111], chair-side fillings [78, 112, 113], space maintainers [114] and implant supra-structure applications [58, 77, 115-120]. More recent applications include the utilization of FRCs as substructures for extra-oral prostheses [121-123], intermediate reinforcing layers within large resin-composite fillings [124-128], and implant fixtures [119, 129, 130].

1.2.5 Mechanical performance and influencing factors:

The chief indication of FRC is to improve the mechanical properties of resin-composite materials and strengthen their polymeric network. Rigidity, flexural strength and load-bearing capacity are considered the main mechanical properties of concern that have to be improved. This is not only because of the low values provided by conventional resin-composites (Table 1.1), but also for the dominating effect of such properties on clinical performance [2, 3, 131]. Improving such mechanical properties, however, cannot happen by simple incorporation of reinforcing fibres as there are many other factors ruling the process and affecting the performance.

Compressive strength	260 -300 MPa
Yield stress	160 -300 MPa
Tensile strength	40 -50 MPa
Flexural strength	80 -150 MPa
Modulus of elasticity	6 -14 GPa
Hardness	30 -90 VHN

Derek Hull stated about composite construction that “the essence of composite materials technology is the ability to put strong stiff fibres in the right place, in the right orientation and with the right volume fraction” [1]. The first symposium on fibre-reinforced plastics in dentistry (1998) also reported that the ability of reinforcing polymers is not as simple as placing a fibre into a plastic, but there exists a number of factors having power over this reinforcement efficacy, and influencing the overall performance of resultant materials [6]. Relevant studies have identified type of constituents, fibre orientation, fibre to matrix ratio, impregnation quality of fibre impregnation and adhesion with the resin, fibre/matrix interfacial adhesion and fibre location as major factors affecting the properties of reinforcement [44, 46].

1.2.5.1 Reinforcing-fibre type:

Different types of fibres have been used as reinforcement in FRC. In dentistry, reinforcing fibres made of glass, polyethylene, aramid and carbon are the most commonly used [132]. The unique structure of each type affects the mechanical properties of resultant materials [2, 132, 133].

I Glass Fibres:

Glass fibres are the most popular reinforcing-fibres in industrial and dental applications. Their popularity is attributed to their favourable mechanical properties, including high tensile strength, excellent impact and compressive strength, high modulus of elasticity and flexural strength [2]. Biocompatibility, high resistance to chemical degradation and relatively low cost have also contributed to their popularity, but the superior transparent appearance of the fibres that suits many aesthetic-demanding dental applications has much greater impact [134].

In the literature, the flexural strength of glass FRC varies between 420 and 1250 MPa depending on the composition of employed fibres and resin, as well as testing conditions [132, 135-141]. One study investigating the reinforcing effect of glass fibres has reported a consequent increase in the flexural strength of the unreinforced (control) composite by 364% after 6 days water storage [132]. Another study, however, has reported a higher reinforcing effect, up to 800%, when the specimens stored in dry conditions before flexural testing [135].

Glass fibres also have the potential to be uniformly stretched under stress to their breaking point and, interestingly, return to the original length upon stress removal without any yielding. This property, combined with the high mechanical strength, is what gives glass fibres the ability to store and release large energy levels during service [134]. All taken into account, FRC with glass fibres have been proposed to strengthen many dental restorations, prostheses and appliances prone to excessive occlusal load and/or requiring a high level of aesthetics [91, 142-144].

The microstructure of glass fibres has a three-dimensional network, composed of silicon, oxygen and other randomly aligned atoms [134]. Fractions of the raw composing materials are blended together and heated in an oven at 1600°C temperature to produce a fibre with particular chemical composition [134]. According to this chemical composition, dental glass reinforcing fibres are generally classified into two common types: E-glass and S-glass. Other less common glass fibres are also used like R-glass [56, 145].

A. *E-glass Fibre:*

Electrical glass fibre, so-called E-glass, is the most commonly used type. It has a calcium-alumino-borosilicate composition with 55 wt% SiO₂, 14.5 wt% Al₂O₃, 17 wt%

CaO, 4.5 wt% MgO, 8.5 wt% B₂O₃, and 0.5 wt% Na₂O. It has excellent strength and stiffness but low impact and fracture resistance [2].

B. S-glass Fibre:

High strength glass fibres, so-called S-glass, have the same density of E-glass fibres, but with a different chemical composition (64 wt% SiO₂, 26 wt% Al₂O₃ and 10 wt% MgO) [2]. It has the highest tensile strength among reinforcing-fibres and offers excellent wettability. However, due to their high processing cost, S-glass fibres are less commonly used than E-glass fibres. As a consequence, S₂-glass has been introduced with the same mechanical properties of S-glass but with lower cost [146].

II Ultrahigh molecular weight polyethylene (UHMWPE):

Polyethylene fibre is a thermoplastic polymeric material produced from long aligned chains of the monomer 'ethylene', and further shaped up to be in a fibre form [2]. The crystal structure of this fibre has been fashioned in many different ways to produce fibres with a different degree of branching, density, molecular weight and therefore mechanical properties. Considering the reinforcing effect, the ultra-high molecular weight polyethylene (UHMWPE) fibre was the type that gained a remarkable interest in the dental field due to its strength [124, 147].

UHMWPE fibres are chemically inert and white in colour with low density (0.94g/cm³) and excellent biocompatibility. They are made of highly-elongated and well-aligned chains, with a general molecular weight exceeding one million (mainly between 3x10⁶ – 6x10⁶) [148]. Such a structure is what intensifies the intermolecular interactions in fibres and allows effective load transfer [147, 149]. Many supporting studies comparing the mechanical properties among the different reinforcing fibres have showed that the impact strength of UHMWPE fibre in composites is 20 times greater than that of glass, aramid and carbon fibres [2, 132]. Therefore, UHMWPE fibres have been listed among the toughest reinforcing-fibres in dentistry yet.

Despite the favourable properties of UHMWPE fibres, they still have some weak points. Beside their low modulus of elasticity, limited tensile strength, high creep and low melting point (about 147°C), such fibres have been shown to have low surface energy and poor adhesion which makes the bonding between fibre and matrix unsatisfactory [2, 150-152]. Although surface treatment using electrical plasma technology or corona can enhance this adhesion with the resin matrix, practical limitations and high cost made

this option relatively unfeasible [153, 154]. Many previous studies have also reported difficulty in placing and manipulation of these fibres with enhanced levels of oral microorganisms retained on their surfaces [155-157]. As a consequence of such disadvantages, the applications of UHMWPE fibres tend to be relatively limited compared with glass fibres.

III Carbon/Graphite Fibres:

Carbon fibres are manufactured from carbon-rich organic fibre precursors (e.g. polyacrylonitrile, cellulose, pitch) through the application of controlled oxidation, carbonisation and graphitisation [2]. According to the manufacturing technique and carbonisation temperature, the resultant fibres may obtain a varying degree of amorphous carbon and crystalline graphite, and therefore can present with different structural composition and mechanical properties [134].

Carbon fibres have many favourable properties, including superior stiffness and compressive strength, high resistance to corrosion and fatigue, excellent adhesion and good handling properties. Nevertheless, low impact strength, major surface imperfections, high processing porosity and black colour are problems that tend to reduce their popularity compared with other fibres, especially in aesthetically demanding applications [2, 29, 134, 158, 159].

Carbon fibres have been used in several dental applications, including removable dentures [87, 160], restorative composite filling [161], implant-supported prostheses [77], interim FPDs [162], and dental implants [29]. However, due to their black colour and difficulties in manufacturing, their clinical use is now limited to prefabricated endodontic posts [163-165].

IV Aramid/Kevlar fibre:

Aramid fibres, commonly known as Kevlar fibres, are made of aromatic polyamide and formed by spinning liquid chemical blends into solid fibres. The resultant fibres are produced with a range of properties that are mainly high specific tensile strength, low density and good impact resistance [134]. However, due to their poor compressive strength, they are recommended to be used in a combination with other reinforcing-fibres in order to achieve satisfactory strength [2]. Previous studies using aramid fibres to reinforce PMMA [166-168] and resin-composite [133, 148] have confirmed a significant improvement in flexural strength.

Aramid fibres also offer other favourable properties, including thermal and chemical stability, high glass transitional temperature and excellent hardness [2]. However, they lack the effective bonding with resin matrix and slowly degrade when exposed to ultraviolet light [87]. Their bright yellow golden colour has also a detrimental effect on appearance and can limit their use in aesthetic-demanding situations [2]. During their incorporation within acrylic materials, Aramid fibres tend to spread laterally and unevenly, causing poor polishability, mucosal irritation and patient discomfort [169].

V Other fibres:

The literature contains other types of fibres used to reinforce dental applications. Nylon fibres, which are produced from polyamide, have gained some interest, owing to their high resistance to shock and repeated stressing. However, their mechanical properties are negatively influenced by water sorption [2]. A previous study comparing the reinforcing effect of nylon with glass and aramid fibres has reported that nylon fibres can increase the fracture toughness of PMMA, but not to the level of glass or aramid fibres [170]. Polyester fibres have been also used to reinforce PMMA dentures and improve impact strength; however, no effect on flexural strength and surface hardness was reported [171]. Fibres made of PMMA have been also used to strengthen dentures but no improvement in impact strength was achieved [172].

1.2.5.2 Matrix and resin system:

In respect of dental FRC, there exists a variety of resin matrices that have been proposed in the literature to impregnate the reinforcing fibres. Primarily, they are classified into linear thermoplastic matrix, cross-linked thermoset matrix or a combination of both together which forms a semi-interpenetrating polymer network (semi-IPN) [44, 137, 173, 174]. It is established that the different matrices of FRCs have different effects on mechanical properties. For example, many studies have reported that the modulus of elasticity of FRC impregnated with a cross-linked polymer matrix is higher than those impregnated by semi-IPN or a linear matrix [135, 141, 163]. However, toughness values are much greater with linear and semi-IPN matrices than cross-linked ones [175]. Moreover, the semi-IPN matrix of dental FRC presents advantages over cross-linked matrices in terms of handling properties and intraoral bonding of indirectly made restorations [175].

The viscosity of the FRC matrix is also critical for attaining optimum handling characteristics in the resultant materials [174, 176]. Reinforcing fibres impregnated with

a conventional matrix (with a low degree of viscosity) exhibit high memory, which means they tend to rebound once adapted to a curved surface. Such memory, resulting from the parallel run of continuous reinforcing fibres through the length of a FRC strip, contributes to a difficult adaptation process of FRC intraorally [83]. As a consequence, some researchers have preferred using a matrix with a high viscosity degree, produced by elimination of all diluents and other low viscosity components commonly added to the matrix system, in order to counteract such memory of fibres and ease the adaption [83, 174, 176]. Although highly viscous matrices neutralize the fibre memory, some studies have found that they adversely affect the handling and impregnation characteristics, and therefore a more sophisticated manufacturing process is required [45, 134, 177].

Methacrylate-based resin systems are the most popular matrix used to impregnate FRCs. By using such systems, the polymeric network formed around fibres can be linear with using mono-functional resin monomers (e.g. PMMA) [159, 174, 175, 178, 179] , cross-linked with using multifunctional monomer (e.g. Bis-GMA, UDMA) [83, 180] and urethane tetramethacrylate (UTMA) [139], or semi-IPN with combination monomers [46, 175, 177, 181, 182]. Other less popular, but effective, resin matrices have been also evaluated, including epoxy resin (Diglycidyl Ether of Biphenol-A (DGEBA)-based epoxy) [183], polyethylene terephthalate glycol (PETG), poly 1,4-cyclohexylene dimethylene terephthalate glycol (PCTG) [173] and polyamide [184].

I) Semi-Interpenetrating Polymer Network (semi-IPN) as dental FRCs matrix:

A. *Definition:*

Semi-interpenetrating polymer network matrix, or so-called semi-IPN, has been defined as “a polymer comprising one or more networks and one or more linear or branched polymers characterized by the penetration of at least one of the networks by at least some of the linear or branched macromolecules on the molecular scale” [181, 185]. The constituents of this matrix are not chemically dependent, and thus can be detached without breaking the chemical bond [186, 187]. Such independency has been claimed to be of remarkable significance when bonding of uncured resin material to fully-polymerised FRC is a demand [181].

B. Rationale:

Since dental FRCs are commonly used as a bonding substrate or framework, it is obligatory to have satisfactory bonding between this framework and resin materials used as either veneering PRC or resin-luting cement. The nature of impregnating matrix (either cross-linked or linear) of FRC frameworks has been reported to affect this bonding [44].

Apart from the effect of mechanical locking, the adhesion between unpolymerized resin material and polymerised FRCs substrate impregnated with cross-linked matrix can be obtained chemically by a free-radical polymerisation reaction [181, 188]. This reaction alone could be enough to achieve a durable bond if an unpolymerized surface layer, the so-called oxygen inhibited layer, was still available on the substrate surface. This layer has been proven to have some unreacted functional groups (C=C) responsible for keeping the polymerisation reaction active up to 24h after the initiation reaction [175, 181]. Obtaining such a layer in directly-made FRC substrates is easy. However, this is not the case with laboratory-made substrates that are usually delivered after 24h, and thereby, adequate bonding is not guaranteed [181]. On the other hand, when the FRC contains a linear impregnating matrix, the adhesion can be achieved by interdiffusion of the new unpolymerized resin monomers within this linear matrix, providing that the solubility parameter of the unpolymerized monomers is close enough to that of the linear matrix [175, 181, 189]. As the use of pure linear matrixes is infrequent in dental applications, the use of semi-IPN structures has been suggested instead [181].

FRC substrates impregnated with a semi-IPN structure contain both linear and cross-linked matrixes. Consequently, their adhesion with new monomers can be based on both free radical polymerisation and interdiffusion, which certainly gives a more predictable bonding [190]. The use of semi-IPN as a FRC impregnating matrix significantly enhances the dissolving depth and interdiffusion of adhesive resin monomers into FRC substrates compared with cross-linked matrix, and so promotes the bonding [189]. Additionally, semi-IPN matrix has been also proven to improve other properties such as glass transition temperature, elastic modulus and handling properties of fibres with high viscous resin [137, 181]. Many successful dental applications of semi-IPN have been reported in the literature, especially in repairing denture bases and laboratory-made fixed prostheses [44, 191].

1.2.5.3 Impregnation:

To acquire optimum reinforcement, fibres must be well impregnated with a matrix prior to their use. Effective impregnation, defined as total imbedding of the fibres with the resin, provides a successful interfacial adhesion which enables the stresses to be transferred effectively from the material to its reinforcing fibres. However, insufficient wetting can lead to void formation and premature failure [44].

I Methods of impregnation

The impregnation process itself can be done in two methods; either by hand or through a specially designed manufacturing procedure (pre-impregnation) [45]. The level of impregnation using the hand method was considered adequate until a desire for using resin systems with high viscosity (e.g. Bis-GMA) emerged [174, 176]. Such viscous resin, combined with its high volumetric polymerization shrinkage, hampers the effective impregnation, and leads to a major reduction in mechanical properties [6, 176]. Therefore, the use of fibres pre-impregnated by their manufacturers is recommended.

Different manufacturing methods have been introduced to optimize the impregnation of the fibres [45, 134, 177]. Most of them involve forming a FRC ‘prepreg’, a FRC strip combining both fibres and unpolymerized matrix, by pulling the fibre bundles through a tortuous path that forces the resin into fibre bundles [45, 192]. This procedure not only allows complete wetting of fibres with minimum void content, but also offers high fibre content with more control over the cross-sectional dimensions of the resultant prepregs [45, 192]. While many fibre characteristics, including their number, wetting, distribution and orientation, are well optimized in the prepregs, the flexibility remains sufficient for further shaping during their application. Once the fibres shaped, a final polymerization stabilizes the form and generates the mechanical properties [81, 192].

II Impregnating matrices and their effect:

The nature of the impregnating matrix affects not only the mechanical properties of FRC, but also water sorption, handling properties, bonding to unpolymerized resin and maintenance [44, 83, 132, 135, 193]. The degree of water sorption varies among different impregnating matrices used in dental FRC. Polymers with low water sorption potential, like bis-EMA and UDMA, are desirable to optimize the flexural properties of FRC [135, 193]. Matrices with high viscosity are also preferable since they facilitate the intraoral adaptation of FRC [83]. However, they tend to complicate the handling. To overcome this problem, pre-impregnation with porous PMMA was introduced [46].

This is based on pre-impregnating of the reinforcing fibres with a highly porous polymer during production [192]. Such porous pre-impregnated fibres still need further chair-side or laboratory wetting with an adhesive resin previous to any application [46, 181, 190]. Another technique of pre-impregnation, combining PMMA and dimethacrylate resins in a gel matrix, has been introduced to improve the handling and reduce the clinical steps [44]. Using this technique, previous studies have reported an increase (up to 70%) in the quantity of reinforcing fibres pre-impregnated in the resin matrix. Moreover, the bonding to unpolymerized resin and maintenance were also improved by enhancing interdiffusion and secondary-IPN formation [44, 190].

1.2.5.4 Interfacial adhesion:

I Introduction:

Bonding and adhesion are two interchangeable terms that describe the state of molecular/atomic attraction between two contacting substances promoted by physical or chemical interfacial forces [194]. In dentistry, adhesion has been defined as “the process of joining two dissimilar materials by means of an adhesive agent that solidifies during the bonding process”[9]. The substance that enhances adhesion and transfers load between two attracted substances is called adhesive. The material tending to adhere is called adherent, while the ‘substrate’ is the material to which the adherent is applied [9, 194].

Regarding FRCs, the interfacial adhesion between their constituents is one of the major factors determining the longevity and overall performance. This adhesion, especially in the interfacial region between the reinforcement and the matrix, is essential for obtaining optimal mechanical properties in the resultant FRC [44].

II Importance of interfacial adhesion:

The mechanical properties of FRCs are significantly affected by the strength and durability of interfacial adhesion. The tensile strength of FRCs is affected by the efficiency of the load transfer from the matrix to the reinforcing fibre at the interface [61]. Strong interfacial adhesion enables an effective transfer of stress from the polymer matrix to the reinforcing fibres [61, 195]. However, poor adhesion adversely affects mechanical properties, increases water sorption, and limits longevity [196].

The durability of FRCs is also affected by the interfacial adhesion as well as many environmental factors, such as temperature, moisture and loading stress [44]. With poor

interfacial adhesion, water accumulates over a period of time at the exposed fibre surfaces, leading to adhesion failure and strength reduction [135, 193, 195, 197]. Under normal circumstances, the affected fibres will consequently fracture at a lower load compared with their theoretical ultimate strength. Once the fracture occurred, the constituents lose their stored elastic energy in the region around broken fibre ends, resulting in further crack propagation along the interface and critical damage [195]. Consequently, a reduction in the durability and clinical performance of FRCs is inevitable.

FRCs are usually utilised as a bonding substrate that has to be veneered and cemented with different materials. Accordingly, the interfacial region between the matrix and reinforcement surfaces is not the only place that affects the properties of FRCs constructions. The interfacial adhesion at the interfaces between different materials or structural components is also influential [131]. The compatibility between the matrices of different interfaces is essential to achieve an effective adhesion [1]. In general, the key component for achieving enhanced mechanical properties in FRC applications is the ability of the constituents (fibres, matrix and veneering materials) to be effectively adhered together [44].

III Mechanisms of interfacial adhesions:

The interaction between the constituents of FRCs happens by several mechanisms, including mechanical adhesion, chemical adhesion and interdiffusion. In mechanical adhesion, the bond is produced by the physical interlocking between the matrix and fibre surfaces. This locking is mainly dependent on the surface topography of the fibres, but is unlikely to be adequate to withstand high loading situations [153]. On the other hand, chemical adhesion is formed by covalent bonding between the constituents. The strength of this adhesion depends on the number and type of covalent bonds formed, as well as the matrix type and fibre microstructure [44, 153]. A range of fibre surface treatments can also affect the strength of chemical adhesion [66, 67, 195].

Regarding the interdiffusion mechanism, the bond between constituents happens by the diffusion of active molecules from one surface into the molecular network of the other surface. The strength of this bond depends on the amount of diffusion (molecular entanglement together) and the number of molecular chains involved [153]. The degree of interdiffusion amount will depend on the involved constituents, their molecular conformation and the simplicity of the molecular motion, which can be enhanced by the

presence of solvents or plasticising agents [1]. One prominent example of this interdiffusion mechanism is the use of the semi-IPN phenomenon [175, 181, 186].

IV Interfacial adhesion enhancement:

Many surface treatments are available for enhancing the interfacial adhesion of FRCs [66, 67, 195]. Most of these treatments are based on increasing the frequency of mechanical interaction between the constituents and/or facilitating their chemical bonding [60, 62, 153, 198, 199]. Flame treatment and etchants (e.g. KMnO_2 , H_2O_2 , and $\text{K}_2\text{Cr}_2\text{O}_7$) are examples of effective surface treatments used to enhance the adhesion of a variety of reinforcing fibres. Such techniques, however, are not effective enough to be used with UHMWPE fibres, which are chemically inert and resist interactions with most polymer resins [153].

A significant improvement in the adhesion of UHMWPE fibres can be obtained by the use of 'gas plasma treatment'. In this technique, UHMWPE fibres are subjected to high temperature plasma treatment in the presence of gases (e.g. O_2 , NH_3 , N_2 , Ar, CO_2), causing significant surface modifications. Four modifications enhancing the adhesion have been recognized, including oxidation of the fibre surface, cross-linked skin formation and weak boundary layer removal, enhanced surface roughness and increased wettability [153]. Although such modifications have been reported transient [151, 200], manufacturers still use gas plasma as a predominant treatment with UHMWPE fibres [147, 150, 201]. Other surface treatments, such as corona discharge, chemical grafting, high energy laser, UV and gamma irradiation, are also efficiently used with UHMWPE fibres [154].

The use of coupling agents is another treatment mode employed to improve the surface energy and wettability of reinforcing fibres [60]. Owing to their bi-functionality, coupling agents can bond chemically with both the matrix and the fibres, resulting in a continuous interfacial connection [193]. Several coatings with different structures have been used as coupling agents, including rubber emulsions and polymeric solutions (e.g. polyurethane or polystyrene). However, silane-coupling agents are the most commonly used owing to their high predictable results [62, 66, 67, 199]. Silane molecule, with the general formula " $\text{Y}-\text{Si}(\text{X})_3$ ", contains two types of functional groups [153, 193]. The first type is the hydrolysable alkoxy groups (X) which, upon their hydrolysis to silanol, react with silanol groups present on the fibre surfaces, forming siloxane bridges as chemical bonds (Figure 1.6). The other type is the non-hydrolysable organofunctional

groups (Y), such as amino and methacrylate, that form a link with the matrix functional groups through chemical adhesion and interdiffusion [153]. The reaction with the fibre surfaces seems to be responsible for the hydrolytic damage resulting from water sorption, while the reaction with the matrix chiefly enhances the interfacial adhesion [193].

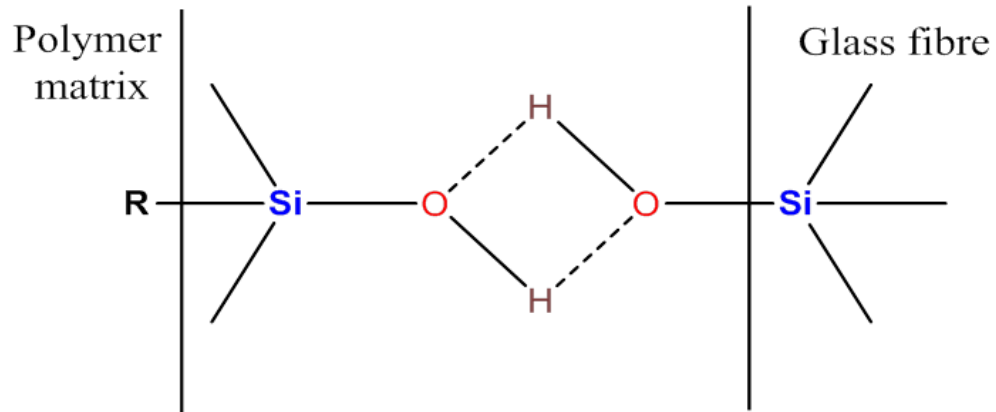


Figure 1.6: Chemical structure of silane molecule connecting reinforcing-fibre with its matrix by Siloxane bridge.

Treating reinforcing fibres with silane coupling agents generally improves the interfacial adhesion of FRCs. Silanization of glass fibres has been reported to increase the surface wettability [66, 67, 132, 197] and enhance the mechanical properties [66, 193, 199], providing there are complete wetting of the constituents and minimal void formation. However, silanization of UHMWPE fibres exhibits poor fibre wetting and unreliable interfacial adhesion [148, 196, 200]. Consequently, researchers recommended the use of silanized glass fibres instead of UHMWPE fibres in many adhesive applications [146, 151, 175].

1.2.5.5 Fibre orientation:

It is well established that the orientation of reinforcement, or the arrangement of fibres inside the matrix, influences the physic-mechanical properties of FRC [7, 44]. Many studies investigating the effect of constituent arrangement have revealed the significance of fibre orientation on FRC performance [44, 145, 202, 203]. Accordingly, understanding of this factor and its implications prior to the clinical application of FRCs is crucial for achieving desirable performance.

The reinforcing fibres of dental FRC are used in two forms, continuous (long) or discontinuous (short) [45]. According to the orientation, the continuous fibres can be categorized into unidirectional, bidirectional or randomly-oriented fibres [204]. The discontinuous fibres are either randomly oriented or aligned in one preferred direction

[45, 204]. The fibres with random orientation provide FRC with isotropy, which means the properties are uniform in all directions. On the other hand, the use of unidirectional and bidirectional fibres promotes anisotropic and orthotropic properties, respectively [7, 46]. Such properties are advantageous in certain applications requiring more effective reinforcement at one direction than the others [88].

The efficiency of reinforcement for FRC loaded at a given level is described by the Krenchel factor (K_θ) [3, 44, 205]. FRC has $K_\theta = 1$ (100%) when the fibres are oriented in one direction (unidirectional), giving the maximum level of reinforcement in that direction. However, due to the anisotropy produced, other directions of loading give different properties with $K_\theta = 0$ (Figure 1.7). By using bidirectional fibres arranged perpendicular to each other (weaves), the efficiency of reinforcement is reduced by 50% ($K_\theta = 0.5$), producing equal reinforcement in both directions of the fibres and orthotropic properties. However, for woven (45/45 bias) fibres, the efficiency of reinforcement drops to reach ($K_\theta = 0.25$). FRCs reinforced with randomly-oriented fibres have $K_\theta = 0.38$ when considered in flat surfaces, but the efficiency of reinforcement decreases ($K_\theta = 0.20$) in three dimensional structures [3, 44].

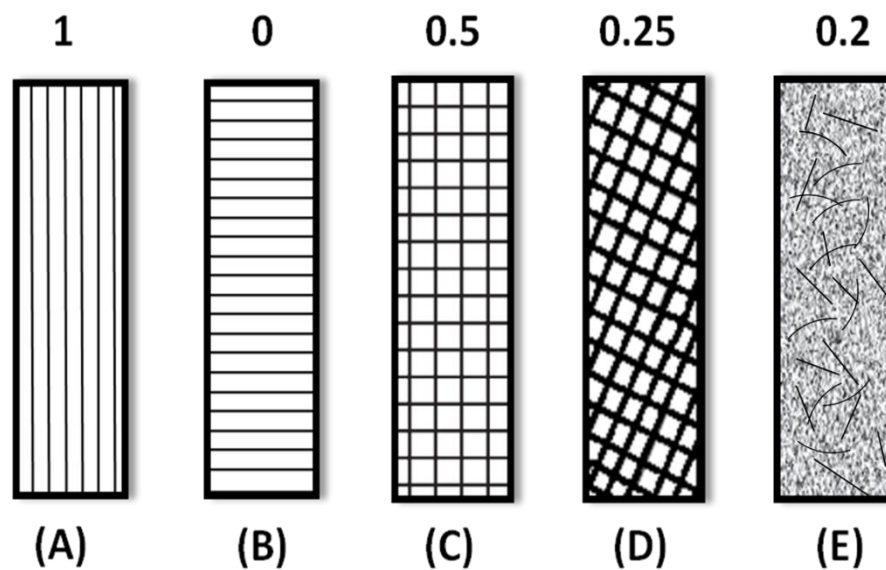


Figure 1.7: Reinforcing efficiency (Krenchel factor K_θ) of fibres with different fibre orientation [44]. A) Unidirectional fibre orientation resulting in anisotropic materials with $K_\theta=1$, B) Unidirectional fibre orientation resulting in anisotropic materials with $K_\theta= 0$, C) Bidirectional fibre (woven) mat resulting in an orthotropic material with $K_\theta= 0.5$, D) Bidirectional fibre (45°/45° bias) resulting in an orthotropic material with $K_\theta= 0.25$, E) Random fibres orientation resulting in an isotropic material with $K_\theta= 0.2$, providing the fibres are longer than critical length for that fibre type.

Many researchers have understood the implications of fibre orientation on the mechanical properties of FRC, and successfully implemented them in various applications [88, 89, 119, 145, 202, 203, 206]. Studies employing continuous unidirectional fibres have reported that such fibres provide the highest strength and stiffness values in the direction of the fibres [89, 120, 145, 164], and claimed their ultimate suitability for applications in which the direction of the highest load is known or likely to be single [6, 134]. Accordingly, the use of unidirectional fibres is emphasized in small sized dental appliances, like components (connector, retainer, pontic) of FPDs, which must be appropriately-designed to achieve satisfactory reinforcement and withstand heavy mastication. Nevertheless, a small fibre misalignment within such structures can significantly influence the resultant properties (Figure 1.8) [44].

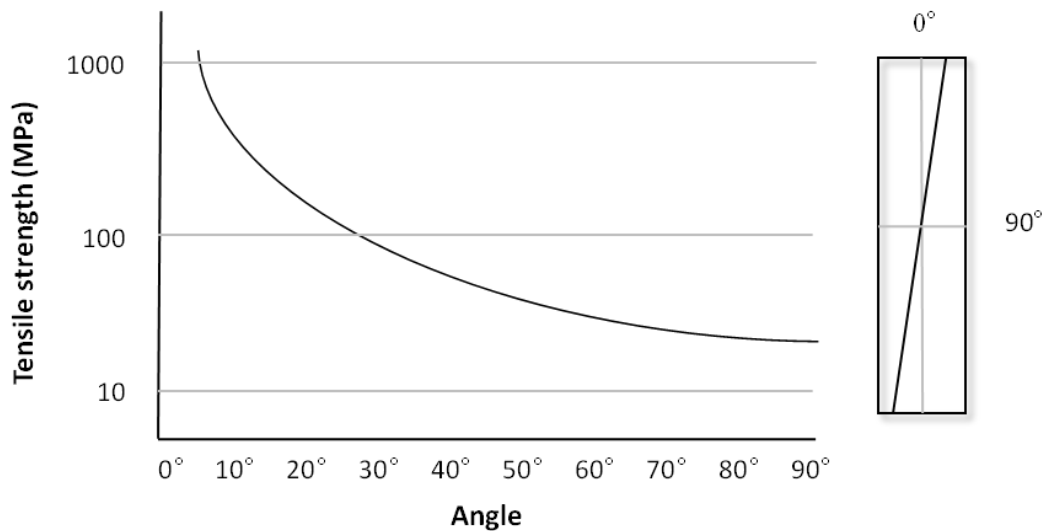


Figure 1.8: Influence of fibre misalignment on the tensile strength of continuous unidirectional FRC [44].

Alternatively, studies utilizing continuous bidirectional fibres have revealed a major drop in mechanical properties, but with an equal reinforcement in two directions rather than one [44, 144, 207-209]. Accordingly, authors have suggested using such fibres in cases where the direction of the load is unknown or limited space is available for using unidirectional fibres, as in overdentures or areas with small dimensions [44, 76, 177]. Additionally, woven fibres have been shown to act as a crack stopper and add toughness to the material by increasing the strain prior to fracture [177, 210]. From a clinical perspective, this property is desirable in situations where extra toughness is mandatory; for example, overdentures with thin regions over precision attachments need higher

toughness values to diminish the risk of perforation, and the margins of laboratory-made composite crowns that are high susceptible to cracks during fabrication and fitting [159, 177, 211-213]. Some authors have also suggested a combination between unidirectional and bidirectional fibres that allows different mechanical properties in the same construction. For example, the pontic of FPDs can be reinforced with continuous unidirectional fibres as it needs high strength and stiffness, while the margins of the retainers can be reinforced with woven fibres as they require more toughness [44]. Regarding to FRC with randomly-oriented fibres, studies have reported reduced reinforcement but equal mechanical properties in all directions of loading. Accordingly, such fibres have been proposed as a strategy to reinforce against multi-directional or unknown loads [143, 214-216].

Conversely, predicting the mechanical behaviour of discontinuous short fibres is complex due to the fact that the efficiency of load transfer depends on fibre length. It has been found that short fibres must have a minimal length equal to the critical length (L_c) to strengthen a material to their maximum potential [7, 217]. The use of short fibres, with a length significantly shorter than L_c , leads to matrix deformation and almost no stress transfer in the resultant FRC [218]. Even if the critical length of short fibres is fulfilled, they theoretically offer little maximum reinforcement ($K_0 = 0.2$) based on their random orientation [44]. Some techniques, like injection moulding, have been developed to specifically align the short fibres in FRC, and so enhance their reinforcement [219]. However, the results show no significant improvement in mechanical properties. This is explained by the fact that even when short fibres are oriented, their relatively-weak ends should carry the most load during stress transfer between the adjacent fibres [219]. In view of that, composite materials reinforced with short discontinuous fibres are theoretically weaker than those reinforced with long continuous fibres [7]. Nevertheless, many studies have used discontinuous fibres to reinforce various dental prostheses, including provisional crowns, FPDs, acrylic removable dentures or simple restorative fillings under heavy occlusion [57, 188, 214, 216, 220-223].

Fibre orientation also affects the physical properties of FRC, including thermal behaviour and polymerization shrinkage [88, 89]. Studies comparing the thermal expansion among FRCs with differently-oriented fibres have revealed that the coefficient of thermal expansion is significantly affected by the direction of the incorporated fibres. This has been attributed to the anisotropic nature of FRC that seems

to have an influence on many thermal properties [88, 190, 224]. Likewise, a study investigating the linear polymerization shrinkage strain of differently-oriented FRCs has claimed that the anisotropy of FRC also affects the polymerization shrinkage. The shrinkage in unidirectional FRC mainly occurred transversally to the fibre direction, but not longitudinally, whereas it occurred equally in both direction when bidirectional or randomly-oriented FRC used [89].

1.2.5.6 Volume and weight fractions:

The relative proportions of the constituents, expressed as weight or volume fractions, influence the mechanical properties and overall performance of FRC. Changing fibre content or matrix fraction of FRC can cause a considerable alteration in the overall behaviour [6, 131, 204, 225].

It is empirically established that there is an intimate relationship between the mechanical properties of FRC and the properties of its constituents. Some authors have addressed this relationship and generically termed as “the rule of mixtures” [204, 225], which is simply expressed as the following:

$$E_C = E_f V_f + E_m V_m \quad \text{Equation 1.1}$$

Where E_C is the overall property of the composite, E_f is the property of the fibres, V_f is the volume fraction of the fibres, E_m is the property of the matrix and V_m is the volume fraction of the matrix.

Although it has been shown that not all composites follow this relationship numerically, the rule of mixtures is still at the heart of our understanding of the relationship between the fractions of the constituents and the resultant mechanical properties [44]. Following this rule, many authors have proposed an explanatory theory about the performance of FRC, asserting that as a constituent amount increases, the performance of FRC shifts toward the behaviour of that constituent [1, 44, 131, 225]. Accordingly, the greater the fraction of reinforcing fibres, the more likely the fibrous mechanical properties [177].

Many previous studies have confirmed the effect of changing the reinforcement fraction on the mechanical properties of FRC [77, 135, 159, 177, 226, 227]. An increase in the flexural strength of FRC has been demonstrated as a result of increasing fibre content [228]. Higher stiffness has been also achieved by incorporating more fibres within composite structures [227]. A study comparing the flexural strength among FRCs with different fibre fractions (V_f : 12%, 23%, 36% or 45%) has also reported a significant

increase in flexural strength as the volume fraction increases [135]. Following a different perspective, other studies have highlighted the importance of using a controlled manufacturing process that allows more fibre incorporation ($V_f = 45\% - 65\%$) and higher flexural strength (up to 1250 MPa) [44, 139, 229], instead of using a manual incorporation method that allows only limited fibre reinforcement ($V_f = 5\% - 15\%$) and a modest increase in flexural strength [230]. A positive linear correlation has also been reported between the ultimate flexural strength and the fibre volume fraction (up to the level of 70 vol%) [44]. A recent study has also demonstrated a significant increase in the modulus of elasticity, toughness and load-bearing capacity (by 27%, 34%, 15% respectively) of E-glass FRC as a consequence of increasing the fibre volume fraction (from 51.7% to 61.7%) [231].

Several attempts have been made to manipulate the mechanical properties of FRC appliances by altering the fraction of their reinforcement. FRC-FPD is a common application benefited from the increase in the fibre framework. Previously, authors have minimally supported the idea of increasing fibre fraction during the designing of FRC-FPDs [232-234]. However, recent studies support this idea and highlight its importance. One study has reported a significant improvement in the strength and performance of interim FRC-FPDs as a consequence of increasing fibre content [235]. Another study comparing the clinical performance of FRC-FPDs made with low-volume and high-volume fibre frameworks, has reported lower survival rate (62%) and multiple signs of failure in the low-volume prostheses, in comparison with the survivability of the high-volume prostheses (95%), during the observation time (3.75 ± 0.4 years) [86]. A recent study has also exhibited a significant increase in the loads required for initiating and propagating fractures in FRC FPDs when high fibre volume fractions used.[215].

1.2.5.7 The fibre geometry (placement):

The fibre geometry, or the exact structural position of the reinforcing fibres, is also an important factor affecting the mechanical properties of FRC. An accurate placement of fibres within a structure can significantly enhance its performance [145].

In the literature, there are many attempts to investigate the influence of fibre geometry on the mechanical properties of FRC applications. A preliminary study considering the position of reinforcing fibres inside FRC dentures has revealed that there is a relationship between the fibre geometry and the mechanical properties of FRC [236]. Later, another study has confirmed this relationship and reported a significant change in

the performance of interim FPDs as a result of altering the position of reinforcing fibres [235]. One study has emphasised the placement of reinforcing fibres at the tensile side of FRC appliances (Figure 1.9); however, it has not reported any guidelines on the exact required position or thickness [44]. A later study has provided these guidelines by investigating the effect of placing fibres at five different distances from the tensile side on flexural strength, and indicated that the placement of fibres at the tensile side (0.0mm) significantly improves flexural strength.[237]. However, once the fibres have been moved away (1.5 mm from the tensile side), the flexural strength significantly reduced. This means that the placement of fibres within a range of 1.5 mm from the tensile side enables them to arrest the initiated crack at the tension side, while the fibres positioned further away allow sufficient room for this crack to travel and cause fracture [237].

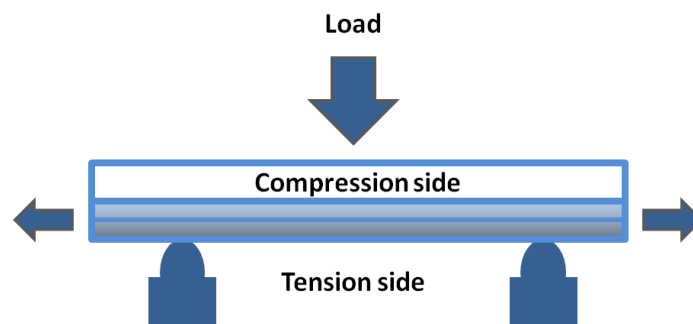


Figure 1.9: Schematic representation of an efficient fibre placement at the tension side of a restoration.

Recent studies have also emphasised the importance of tension side reinforcement on other mechanical properties and applications. [140, 145, 238]. The best load-bearing capacity of FRC-FPDs has been achieved when UHMWPE fibres were placed at the tension side of appliances [145]. An enhancement in the flexural strength of FRC-FPDs has been also exhibited as a consequence of reinforcing veneering composites at the tension side [140]. A higher flexural strength has been also exhibited in denture base polymers when reinforced at the tension side rather than the compression side [238]. Elastic modulus has been also increased as a result of locating unidirectional glass fibres at both tension and compression sides of appliances [239].

Collectively, these studies outline a critical role for fibre geometry during the performance of FRC appliances. Correctly-placed fibres at the tension side and perpendicular to the possible fracture line can act as crack stoppers and efficiently hamper crack propagation, leading to an improvement in mechanical properties and overall performance [91, 201, 202].

1.2.6 Physico-mechanical properties of fibre-reinforced composite

1.2.6.1 Thermal properties:

Dental restorative materials, including composites, are usually subjected to wide temperature fluctuations in situ. Such thermal variations, resulting from dietary habits, processing technique and an exothermic setting reaction, could be enough to reduce the mechanical properties of restorative materials and determine their future performance. Therefore, a considerable amount of attention has been given to the thermal properties of dental materials, especially thermal conductivity, diffusivity and expansion[3].

I Definition

Thermal conductivity is defined as “the rate of heat flow per unit temperature gradient”. It is a good indicator of dental materials that provide satisfactory thermal insulation and so lead to less harm to the surrounding tissues, such as the pulp [9]. However, this property is not practical enough to predict composite material behaviour as the most thermal stimuli encountered in the mouth are transitory in nature [3, 240]. Thermal diffusivity, on the other hand, which is “the thermal conductivity divided by material density and specific heat capacity”, gives a better indication about the response of resin-composite materials to transient thermal stimuli [9, 241]. It indicates that once transient thermal stimuli are applied, a certain amount of heat will be absorbed in raising the temperature of the material itself, which will effectively reduce the quantity of heat available to be transported through the material, and thereby, cause less harm to dental tissue [3]. According to this property, dental composite materials are generally considered adequate thermal insulators although their thermal diffusivity varies with their filler content. The larger the filler fraction, the higher the thermal diffusivity achieved [3, 241].

Thermal expansion is another important property for dental composites that affects their adhesion with tooth structures [9]. According to this property, a restorative material expands and contracts as a result of temperature rise and drop respectively, and so does the tooth structure [9]. The amount of expansion/contraction for each is depending on a specific value for each, termed as linear coefficient of thermal expansion (LCTE). LCTE is defined as the fractional change in the original length of a material for each degree centigrade change in temperature [3, 9], and expressed in the following equation:

$$LCTE (^{\circ}C^{-1}) = \frac{\Delta L/L_0}{\Delta T} \quad \text{Equation 1.2}$$

Where: **LCTE** is the linear coefficient of thermal expansion, ΔL is the change in length, L_0 is the original length and ΔT is the change in temperature.

A significant difference in LCTE values between the resin-composite restoration and the tooth structure leads to different dimensional changes which could adversely develop stresses at the tooth/restoration interface, resulting in bonding failure [9]. Small gaps might also develop subsequently at the margins, leading to microleakage, and allowing fluids containing bacteria to penetrate and cause harm to tooth structure [242, 243]. Moreover, a significant LCTE mismatch between the constituents of resin-composite material could result in increased tensile stresses at the filler/matrix interface, causing deterioration in physico-mechanical properties. Therefore, attempting to bond different materials or structures together with remarkable mismatch in their LCTE is impractical as the bond might not last [40]. Ideally, the ultimate combination of thermal properties for a resin-composite material would be a low value of diffusivity combined with a LCTE value similar to that for tooth substances in general, and close for each of the specific constituents [3].

II Thermal expansion of FRC:

It is well-established that each resin-composite material has its own specific thermal behaviour according to its unique composition. With regards to PRC, this behaviour is mainly dependent on the filler fraction as well as the chemical structure of the matrix [244, 245]. Resin-composites based on Bis-EMA exhibit the highest LCTE values, in comparison with those based on Bis-GMA, UDMA and TEGDMA. Additionally, an inverse linear relationship between LCTE and filler volume fraction has been reported, indicating a lower LCTE value with heavily-filled materials [245]. Many researchers have confirmed such inverse relationship when they studied the thermal properties of differently-filled resin-composite materials [36, 73, 246, 247]. Parameters, like thermal characteristics of the filler particles and the adhesion between filler and matrix, have been also suggested as influential factors [248]. Yet, one study has claimed that filler silianzation has no effect on the LCTE of resin-composites [73].

Other parameters influencing the thermal behaviour of composite materials have been introduced as a consequence of using reinforcing fibres instead of particles.

Accordingly, a more complex thermal behaviour was observed in FRC compared to PRC [7, 249, 250]. Fibre type and orientation are the main parameters influencing the thermal behaviour of FRC. E-glass fibres have the highest LCTE value (4.9°C^{-1}), in comparison with S-glass (2.5°C^{-1}), Carbon ($-1.45^{\circ}\text{C}^{-1}$) and Kevlar (-2°C^{-1}) fibres [2]. Fibre orientation will induce anisotropy in the thermal behaviour [88]. Unidirectional FRC has been found to have two different LCTE values in relation to the fibre direction. In the longitudinal direction, LCTE value is small owing to the mechanical restraints imposed by the length of reinforcing fibres. However, in the transverse direction, a significant increase in LCTE value exhibited as trivial mechanical restraints were forced by the thickness of reinforcing fibres [7, 249, 251]. The explanation for such behaviour is that the rigid fibres tend to limit the matrix expansion in the longitudinal direction, and thus impose it more than normal in the transverse direction [88]. From a clinical perspective, this behaviour is important to understand during the fabrication of FRC prosthesis as a variation in the thermal behaviour between FRC and PRC might aggravate their interfacial adhesion.

1.2.6.2 Bond strength:

I Definition

Adhesion has been defined as “the process of joining two dissimilar materials by means of an adhesive agent that solidifies during the bonding process”[9]. Four different mechanisms of adhesion have been identified, including mechanical adhesion, adsorption, diffusion and electrostatic adhesion [194]. Mechanical adhesion relies on interlocking (keying) of the adhesive into the irregularities of bonding surfaces to promote adhesion. In adsorption adhesion, the substrate and adherent surfaces chemically bonded by the influence of either primary (ionic and covalent) or secondary (hydrogen bonds, van der Waals, or dipole interaction) valence forces. Diffusion bonding is based on the interdiffusion and interlocking of mobile molecules (mainly polymer) from one surface into the molecular network of the other surface. This mechanism requires sufficient mobility and mutually solubility between the molecules of substances being bonded. Electrostatic adhesion involves the formation of an electrical double layer along the interface between metal and polymer substances, which promotes the total adhesion [194]. A combination of these mechanisms might be evident in many applications of restorative dentistry, like the formation of a hybrid layer

between resin-composite and tooth substances, and the adhesion in porcelain-fused-to-metal restorations [9].

II Measurements:

The bond strength of two materials is the measure of the load-bearing capacity of their adhesive joint [194]. The measurement usually involves the application of a load that would develop stresses at the interface between bonded substrates, and eventually lead to a failure [252]. The resultant failure modes are a mixture of cohesive, mixed and adhesive fractures [253].

Several testing setups have been used for the measurement, which can be classified based on the size of the bonding area into macro- or micro-bond strength tests [252, 253]. The followings are some of the most common testing setups used in the literature:

A. *Shear bond strength (SBS) test:*

This method relies on a shear load applied at the interface between bonded substrates, using a knife edge probe, and distributed axially to cause a bond failure. The shear bond strength (SBS) is a function of the applied load and bonded area, and calculated according the following equation:

$$SBS = \frac{F_{Max}}{A} \quad \text{Equation 1.3}$$

Where **SBS** is expressed in MPa (N/mm²), **F_{Max}** is the maximum failure load recorded in Newton (N) and **A** is the area of bonded interface (mm²).

In this *in-vitro* setup, the stress distribution is influenced by several factors, including the mechanical properties of bonded substances, the thickness of the adhesive layer, the design of their assembly, the load applied (i.e. cross head speed) and the storage condition (e.g. thermocycling) [253, 254]. However, this can lead to non-uniform stress distributions along the interface that may not be a true representation of shear force [255]. Recently, specific testing methods (e.g. wire loop) and jigs (e.g. SDI rig, Ultradent jig) have been developed in an attempt to standardise the testing procedure. Though, some variations in the testing parameters remain and still influence the final results that may be impossible to correlate between different studies [254]. Nevertheless, this test is considered a most popular tool for screening and comparing new adhesive materials, owing to its simplicity and feasibility [3].

B. Tensile bond strength (TBS) test:

This method involves the application of a tensile load perpendicularly to the adhesive surface. The tensile bond strength is calculated using the same equation of shear bond strength. However, the results are more variable, owing to the difficulty in specimen alignment [3]. Moreover, the plastic and elastic deformations occurred in a specimen as well as asymmetric stress concentrations along the interface might lead to imprecise and inconsistent measurements. The specimen height is crucial to consider during testing since it influences whether the stresses would be concentrated at the adhesive interface or not [255].

C. Micro-shear bond strength (μ SBS) test:

This method employs relatively-small specimens, with 1mm^2 cross-sectional areas, for the measurement of bond strength [254]. Using small bonded areas has many advantages, like the simplicity of specimen fabrication and the possibility of regional mapping across the surface. However, some difficulties in the measurements have been reported as the smaller specimens, in combination with a relative thick adhesive layer, may cause considerable bending and non-uniform loading at the interface [253]. Also, the accuracy of measurement may exacerbate when materials with low modulus of elasticity are tested [254, 255]. According to FEA, both SBS and μ SBS have been found to provide the same non-uniform stress distribution and equivalent underestimated bond strength values [253]. However, the final results of μ SBS might even be less representative than those of SBS [256].

D. Micro-tensile bond strength (μ TBS) test:

This test follows the same principle as the TBS test; however, it employs small specimens (1mm^2) with specific designs (hourglass, stick or dumbbell) for the measurement of bond strength [254]. Such test configuration has been found the best to represent clinical bond strength since it allows uniform stress distributions along the bonding interface [257]. Studies reviewing this test setup have reported that most failures occurred at the interface between the bonded substrates [257, 258]. However, it still has some disadvantages, like technique sensitivity and specimen fragility. Some surface flaws and micro-cracks might also be introduced as a consequence of specimen preparation, leading to weak bond and underestimated strength [254, 258]. Accordingly, high coefficient of variance has been reported when this technique was used [254, 258]. Comparing the micro-bond strength tests with their macro-scale counterparts, the latter

show lesser strength values that are attributable to the high probability of flaws existing in larger specimens [257].

III Bond strength of FRC:

The applications of FRCs are mostly adhesive in nature, which require being bonded to different substrates in the oral cavity to be functional [259]. An optimum bonding of FRC with the supporting substrates and veneering layers is therefore essential to ensure superior stress distribution and excellent performance. Two interfaces appear to be necessary in FRC restorations. The first is the adhesion of the FRC to the supporting structures, like tooth substance or other restorations, and the second is the adhesion of the FRC to the overlying materials [260].

Several factors have been identified in the literature influencing the bond strength between FRC and tooth substance. Parameters like FRC type, orientation and resin impregnation are claimed to be influential [261, 262]. Glass FRCs have been reported to provide better adhesion than those based on UHMWP [175]. This is due to the fact that UHMWP fibres exhibit low surface energy and wettability during resin impregnation that might lead to weak adhesion [2, 150-152]. However, due to the hygroscopic nature of glass FRCs, it is claimed that they are more seriously affected by the adverse effects of water sorption, leading to a progressive degradation in adhesion as well as mechanical properties [197]. Studies comparing the bond strength between different FRC types have shown controversial findings. One study has reported that UHMWP FRCs had the highest SBS values when they were bonded to enamel [263]. Another study has also confirmed this finding in both enamel and dentine, and reported that UHMWP FRCs exhibit significantly better SBS than those made of glass [262]. However, a recent study has shown that glass FRCs tend to provide better SBS than other types although the difference is not significant [261]. Regarding to the effect of fibre orientation and impregnating matrix, the literature was more conclusive. Most previous studies have reported significantly better SBS values for bidirectional FRCs compared with other orientations [125, 203, 206, 261-265]. FRC pre-impregnated with highly viscous matrix exhibit more favourable interfacial adhesion than that with low viscosity, leading to better adaptation and adhesion [83, 174, 176]. Likewise, the use of FRCs with semi-IPN matrix is advocated as they tend to allow better bonding with resin-based adhesive systems during the cementation [44, 132, 181].

Another factor influencing the bond strength of FRC is the bonding technique. Studies investigating the influence of different adhesive systems used to bond FRCs have found a significant variation in SBS values [266]. However, this variation may not be significant [264, 267]. Some authors have advocated the use of flowable resin-composite as a base underneath FRCs in order to facilitate the adaptation and enhance the bond strength [267]. However, this practice has been reported to have no significant influence on SBS [265]. Likewise, the use of a silicon forming aid during the direct application of FRCs is also suggested to facilitate the adaptation of fibres and reduce the adhesive failure [264].

The nature of bonding substrate is also a significant factor that influences bond strength. Studies comparing the bond strength of FRC with tooth substances have reported significantly higher values with enamel [206, 262, 268]. This variation is mainly attributed to the hydrophilic nature of dentine and the consequent adhesive mechanism that formulates a relatively weak bonding interface [262, 265]. Although the FRC/tooth interface is still considered the weakest link in the adhesive joint, the presence of FRC within that interface is beneficial [125, 269]. An improvement in SBS has been reported as a consequence of incorporating an intermediate FRC layer at the interface. This improvement has been found significant in some studies [262-264], while others have reported the opposite [206, 261, 265, 268]. Though, most studies have agreed that a favourable alteration in stress dynamics at the interface would result from the FRC incorporation, leading to more repairable fractures [125, 206, 262-264, 266, 268, 270, 271]. The same concept can also be adapted when FRCs are bonded with other restorative materials, like dental ceramics and metal alloys [127, 128, 270, 272-274]. However, limited information is available about the factors influencing the adhesion of FRC with such bonding substrates.

1.2.6.3 Hardness:

I Definition

The hardness of a material is defined as the resistance of its surface to plastic deformation that could be a consequence of indentation, scratching, machining or abrasion [40, 218]. By definition, the hardness is considered as a surface property that results from an interaction of many other properties. Accordingly, it is used to give an indication of material behaviour in terms of polishability, abrasiveness to opposing dentition, abrasion wear and scratching resistance [3, 9]. In relation to resin-composite

materials, the hardness can be used as an indirect indicator of the degree of conversion (DC) and depth of cure (DoC) [275-279].

II Hardness measurement:

Many laboratory tests are used to measure the surface hardness of materials. Early hardness tests were exclusively designed to rank the ability of one material to scratch another relying on a qualitative ordinal scale (Mohs scale). Recently, quantitative hardness tests have been developed which based on an indenter being forced to deform the surface of the test material [3, 40]. Several measuring methods based on surface indentation are described in the literature. Such methods can be classified according to many parameters, including the indenter's size (micro or macro), shape (sphere, cone or pyramid,), material (steel, tungsten, carbide, or diamond), the method of application (static or dynamic) and the amount of load (nano-, micro- or macro-hardness) [40, 218]. The followings are some of the most common methods employed:

A. *Brinell hardness test:*

This is the oldest method used to measure the hardness. It involves the use of a small spherical steel indenter (Brinell ball), under a specific load (500 – 3000kgf), to produce a circular indentation [40, 218]. A light microscope is used to measure the indentation's diameter which converted into the Brinell hardness number (kgf/mm²) according to the following equation:

$$HBN = \frac{2P}{\pi D(D - \sqrt{D^2 - d^2})} \quad \text{Equation 1.4}$$

Where **HBN** is the Brinell hardness number (kgf/mm²), **P** is the applied force (kgf), **D** (mm) is the indenter diameter (mm), and **d** is the diameter of indentation (mm).

However, this method has some limitations due to the indenter's spherical shape which produces a variation in the relative geometry of the indentation with different loads [40]. One limitation is that the hardness values cannot be directly comparable when different loads or diameter balls are used. Another limitation is that it is only suitable for measuring certain materials that meet specific testing requirements (the diameter (d) ranges between 25% -60% of D). Accordingly, this method is limited to measure the hardness of metal alloys in dental researches [40].

B. Rockwell hardness test:

Rockwell hardness test relies on measuring the penetration depth of an indenter instead of the diameter of the resultant indentation. The indenter used can have different shapes (spherical or conical) and be made of different materials (steel, tungsten, carbide, or diamond) [40]. The Rockwell hardness number (RHN) is determined by comparing the depth of penetration under a large load with that caused by an initial minor preload. The main advantages of this test are the versatility and the quickness of reading (10-15s). However, fulfilling the test requirements is essential to ensure precise measurements. The specimen thickness must be at least ten times the indentation depth, whereas the inter-indentation allowance and distance from the specimen edge should equal three indentation diameters at least [40]. Both Brinell and Rockwell hardness tests are classified as macro-hardness tests.

C. Vickers hardness test:

The Vickers hardness test follows the same principle of testing as the Brinell test; however, it uses different indenter shape to overcome the continuous variation in the Brinell indentation geometry. The Vickers indenter is a square-based pyramid diamond indenter whose opposite sides meet at the apex at an angle of 136°. This indenter is forced into a surface under a certain load, and maintained for a specific dwell time (normally 10-15s) to induce a square-shaped indentation. The surface area of the indentation is determined microscopically by measuring the average length of both diagonals (*d*) [40]. The Vickers hardness number (HVN) is obtained according to the following equation:

$$HVN = \frac{2F}{d^2} \cdot \sin\left(\frac{136^\circ}{2}\right) = \frac{1.854F}{d^2} \quad \text{Equation 1.5}$$

Where **F** is the applied force (kgf) and **d** is the average length of both diagonals (mm).

The main advantages of the Vickers hardness test is that the geometry of the indentation remains identical regardless of the loading applied or material tested. Accordingly, this method can investigate a large range of materials [40]. Dental resin composites are commonly tested using this method [277, 280-284].

D. Knoop hardness test:

This method employs similar testing procedure and measuring principle as that of the Vickers hardness test. However, it uses instead a rhombic-based pyramidal diamond indenter, with seven times longer diagonals than its width, to induce a swallow elongated indentation. The sides of this indentation tend to spring back due to elasticity, whereas the ends of the long diagonal remain measurable. Therefore, this method is applicable to investigate brittle materials in which the recovery will be across the short diagonal [40]. The Knoop hardness (H_K) is calculated according to the following equation:

$$H_K = \frac{14.23F}{d^2} \quad \text{Equation 1.6}$$

Where F is the applied force (kgf) and d is the length of the long diagonal (mm).

With all microhardness tests, it is imperative to consider during testing the boundaries of the plastically deformed zone, which extends as much as twice the diagonal size of the indentation and 10 times the depth [40]. In view of that, successive tests should be separated by more than 4 times their width to avoid measuring already deformed areas, and far enough from the edge to be fully contained. Additionally, it is important to know that the hardness values are highly correlated, yet, not interchangeable as all of indenters have a varying geometry [40]. With respect to dental resin composite materials, the hardness methods with micro/nano indenters are the most applicable to use since they are able to discriminate between the different constituents and induce the deformation in a tiny specified spot [285].

III Hardness of dental resin-composite material:

Due to the nature of resin-composite material, several factors have been identified affecting the hardness. Relating to the inorganic phase, parameters like filler fraction, size and shape have been confirmed as strong influential factors. Many studies have reported an improvement in the hardness values as a consequence of increasing filler content [33, 41, 275, 286, 287]. Other studies investigating the effect of filler size have shown that the micro-filled resin-composites tend to be harder than those reinforced with hybrid or fine particles, providing that they have similar filler volume fractions [288, 289]. On the other hand, resin composites with nano-particles tend to be more heavily filled than those with larger particles, and therefore have higher hardness [33,

280, 290]. In relation to filler morphology, resin-composite materials with spherical particles have been found to have higher hardness, and sometimes higher filler loading, in comparison with those with irregularly shaped fillers [33].

The organic matrix also has some parameters that influence the hardness. The chemical composition of monomers and their relative proportion affect the degree of polymerisation and many mechanical properties [291-295]. Composite materials based on UDMA resins have been reported to exhibit higher hardness than those based on Bis-GMA. This is attributable to the lower viscosity and increased flexibility of UDMA that cause a higher degree of monomer conversion compared to the rigid Bis-GMA monomers [291]. Increasing the proportion of the TEGDMA monomer, up to certain level, have also reported to improve the hardness due to the fact that it enhances the molecular mobility and degree of conversion [291]. The density of polymeric network is another influential factor. Previous studies have reported high hardness values in resin-composites with high-density polymeric networks, like ormocer-based composites [277].

The type of photoinitiator also influences the hardness of resin-composites. Studies investigating the effect of the photoinitiator type on hardness have exhibited significantly lower hardness values by using phenyl propanedione instead of camphorquinone [296-298]. Likewise, resin-composites with aliphatic amine have shown higher hardness values than those with aromatic amines [299].

The hardness of resin-composites is also affected by the storage medium and temperature [292, 300, 301]. Water sorption and its diffusion within the organic matrix can lead to several consequences, like matrix cracking, interfacial de-bonding, filler dissolution and dislodgment, which cumulatively reduce the hardness [302]. In contrast, the temperature of the oral cavity has been reported to increase the hardness as the heat increases the degree of conversion and so the overall polymerisation [295]. A previous study has reported higher hardness values for the resin-composites stored in dry condition at 37°C than those stored in wet conditions at 23°C [302]. Other factors related to the specimen preparation and testing technique have been also found affecting the hardness. Light intensity [303], curing technique [304], material thickness [305] and surface roughness [286] are among such factors that should be carefully considered during the hardness testing.

IV Hardness of FRC:

There is limited information available about the effect of FRCs on the surface hardness. One recent study comparing the hardness between one conventional resin-composite material and an experimental FRC material made of random short E-glass fibres has reported that the latter material has lower hardness and depth of cure [278]. Unfortunately, this study has not considered the effect of fibre type and orientation on the findings. Another unpublished study investigating the influence of unidirectional E-glass FRC on the hardness of indirect resin-composites has claimed a significant improvement in the hardness as a consequence of FRC incorporation [306]. However, this study has not considered the influence of other parameters, like fibre type, orientation and matrix on the hardness values. Therefore, the literature is still considered inconclusive in this area.

1.2.6.4 Edge Strength:

I Definition:

Edge-strength is a concept that indicates the ability of material fine margins to resist fracture or abrasion [307]. This concept was introduced in 1966 when it was used to investigate the strength of gold restorations [308]. Subsequently, researchers have employed it to study the performance of various materials, like amalgam, composite and ceramics, [309-311]. It is also used to reflect how a particular material is able to maintain its marginal integrity upon clinical loading [312-314].

II Rationale:

It is known that restorative materials are relatively weaker at the edge, in comparison with other places. The edge also tends to be highly-susceptible to temperature changes and frequent mechanical loading that promote its fracture [314]. In view of this, clinical precautions to avoid the materials being loaded at their margins are always advisable. Nevertheless, this is not always achievable; especially when such margins are subjected to heavy unanticipated eccentric loading which disrupts their integrity and causes fracture.

Although such a marginal fracture is often a minimal chipping and could cause no detrimental effect on the retention of a restoration, the resultant disruption in marginal integrity might have several negative consequences. Marginal microleakage, tooth sensitivity, secondary caries, staining and aesthetic problems, as well as an increasing

tendency of catastrophic marginal fractures, are all serious consequences causing patient/dentist hassle and necessitating urgent clinical intervention [313, 314]. Therefore, it is pragmatic to consider enhancing the marginal integrity of restorations, especially at the design stage, in order to improve their longevity.

III Measurement:

To date, the measurement of edge-strength has been developed through a variety of documented techniques [308-312, 315, 316]. One technique has been recently proposed, and claimed to be simple, reliable and highly-standardized [317]. In this technique, a static load is applied at certain distances from the edges of a specimen to induce fracture. A dedicated machine with built-in acoustic sensor is usually employed to detect signals released at any fracture point and determine the force. The maximum fracture-inducing force measured at 0.5mm from the edge is used to represent the edge-strength value.[314, 318].

Several studies have employed this technique to investigate the edge-strength of restorative materials, such as acrylic polymers, packable and flowable resin-composites. [314, 317, 318]. The results have showed that an excellent degree of reliability can be offered by this technique. Nevertheless, many parameters have been identified affecting the measurement, including the geometry of the applied force, its distance from the edge, the angle of application , the edge design and the fracture toughness of the tested material [309, 313, 319, 320].

IV Edge strength of FRC:

In the literature, there are many studies of materials that have gained additional strength and benefits from being fibre-reinforced [4, 84, 177, 211]. PMMA used to fabricate provisional fixed prostheses is one of such materials in which the strength has been tripled by incorporating glass reinforcing fibres[177]. The strength and durability of PRC have also been improved by being fibre-reinforced, enabling their utilization in many high-demanding situations like restoring posterior teeth and replacing missing teeth [84, 90, 321, 322]. Interestingly, most of such improvements have been confirmed in terms of flexural strength and fracture toughness but not in edge-strength. This is because that most researchers tended to follow the protocols of ISO standard (ISO-4049) that are intended to investigate relatively large surface areas and preclude edges.

Limited studies have been identified investigating the edge-strength of FRC. One study has reported a significant improvement (43%) in the edge-strength of indirect PRC as a consequence of incorporating unidirectional FRC at the margins. [313]. Another unpublished study investigating the effect of incorporating unidirectional FRC on the edge strength of three indirect PRC has also reported a significant enhancement in both dry and wet storage conditions [306]. However, no study has considered investigating the effect of other parameters, like fibre type or orientation, on edge-strength.

1.2.6.5 Fatigue:

I Definition

Fatigue is defined as “a form of failure that occurs in structures subjected to dynamic and fluctuating stresses” [218]. It also represents the reduction of material strength caused by repeatedly applied loads [3]. Although the applied loads would be far below the threshold that causes material fracture when measured individually in direct compressive, tensile or flexural tests, they are still able to cause failure over a period of time. This is due to the formation of sub-critical cracks (microcracks) that consequently concentrate at structural flaws and slowly propagate until catastrophic fracture or yielding eventually occurred [3, 218, 323]. For dental materials, the fatigue behaviour is important to understand as it helps determining the clinical performance and longevity of their application.

II Measurements:

In order to measure the fatigue behaviour of a material, a test should be designed to simulate as many as possible the conditions affecting that material during service [218]. Stress level, pattern and frequency as well as other geometrical and environmental factors have to be duplicated during testing. The following are some common techniques used to investigate the fatigue behaviour of dental materials:

A. Staircase method:

The staircase method entails a series of tests at certain stress levels for a predetermined number of cycles to induce fatigue failure [218, 324-326]. In the initial test, the stress level is usually set at two thirds of the static tensile strength of specimens. The test is then repeated at higher or lower stress levels if the specimens survived or failed respectively. The results are plotted as the peak stress versus the number of cycles on a logarithmic scale, so-called S/N plot [40]. This plot is used to compare the fatigue

behaviour between materials by determining the fatigue life which is the number of cycles to cause failure at a specified stress level. The fatigue strength can also be specified which represents “the stress level at which failure will occur for some specified number of cycles” [218]. For some materials, the fatigue limit below which fatigue failure will not occur is also determined [3, 40, 218].

Two types of fatigue behaviour can be identified from the plot. One is termed low-cycle fatigue as it is associated with high stress levels that produce elastic and some plastic strain during each cycle, leading to failure at a relatively low number of cycles. The other is called high-cycle fatigue which is associated with lower stress levels wherein deformations are purely elastic that require a large number of cycles to cause failure [40]. A concern with this method is that the cross-over behaviour, in which some materials with better high-cycle fatigue than low-cyclic fatigue, can induce large scattering within the findings and so unreliability [327, 328]. Another concern is that this method requires a large number of identical specimens to enhance reliability, which tends to be expensive and time-consuming [40].

B. Rolling ball method:

This method involves the use of a rolling ruby ball to apply a complex pattern of stresses, mainly compressive, on the surface of the tested material to induce surface fatigue [328]. Consequently, subsurface cracks develop and ultimately reach the surface before being observed as open fissures. Later, the fissures may be filled with water and propagate to cause fracture. The final outcome of this method is referred to as ‘the fatigue life’ which is the time taken for the surface degradation to happen [329]. Scanning electron microscope is also used to confirm that the fatigue mechanism was responsible for the failure [328, 329]. This method is considered simple, reproducible and not time-consuming as it uses a relatively small number of specimens. Therefore, it has been used frequently for comparing the surface fatigue behaviour of resin-composite materials [329, 330].

C. Masticatory fatigue simulation method:

The main principle of this method is to simulate the masticatory force and its cyclic loading pattern on the tested specimens in order to induce fatigue failure [331-334]. Computerized chewing simulator machines are usually used to perform not only the cyclic loading but also thermocyclic aging. The investigator determines the test parameters, like biting force, loading pattern and number of cycles, prior to

commencing the test on specimens until fracture occurred. If the specimens survived the cyclic loading, a static loading is used to cause failure [331]. The results are used to define the survival rate of tested specimens or the corresponding reduction in their fracture resistance [335]. This method is a simple and reliable technique with high clinical relevance that many researchers in dental field favour [336-338].

III Fatigue of resin-composite:

Understanding the fatigue behaviour of resin-composite materials is essential for their clinical practice as fatigue is the most common cause of clinical failure [3]. The fatigue process is characterized by three distinct steps. The first step is the crack initiation wherein a microcrack forms at a point of high stress concentration like voids or surface flaws. The second step is the crack propagation in which the microcrack grows and propagates within the matrix around the fillers with each stress cycle. The third step is the final failure which occurs once the microcrack reached a critical size and advanced rapidly to cause catastrophic fracture [218, 323, 326, 339, 340].

Several factors influence the fatigue behaviour of resin-composites, which can be classified into compositional, geometrical and environmental factors [339]. The filler content, matrix type, interfacial strength and microstructure are common compositional factors dominantly affecting the fatigue behaviour [327]. Many authors have claimed that resin-composites with high-filler content tend to have better fatigue strength than those with lower content [34, 341-343]. This can be attributed to the reduced distance between filler particles and high localised polymerisation stresses developed around them, leading to hindered crack propagation [341, 342]. However, other authors have reported that resin-composites with intermediate levels of filler content (30 – 50%) have higher contact fatigue resistance compared with those heavily-filled [328, 329, 339]. This can be explained by the brittleness developed as a consequence of high filler content, leading to a high susceptibility for crack growth [329]. Regarding to microstructure, one study has reported better fatigue resistance in nanofilled PRCs in comparison with nanohybrid and microhybrid resin-composites [344].

The matrix and its density also influence fatigue behaviour of resin-composites. Composites containing UDMA monomers tend to provide superior fatigue behaviour than those based purely on Bis-GMA/TEGDMA monomers. This is attributed to the ability of urethane linkage to form hydrogen bonds within the polymeric network and restrict the sliding of its parts in relation to each other [293, 345]. Regarding to matrix

density, composites with relatively rigid matrices exhibit better static fatigue behaviour than those with more flexible matrices [339, 346]. Likewise, homogeneous matrices with uniformly distributed particles tend to provide enhanced fatigue behaviour [327]

Furthermore, the strength of the interface between matrix and fillers affects fatigue behaviour since it regulates how cracks would propagate [339, 342]. Therefore, an enhancement in the interfacial adhesion is advocated in order to suppress the crack propagation. Studies using filler silanization to improve the interfacial adhesion within resin-composites have consequently reported a significant enhancement in fatigue behaviour [329, 339].

Surface quality and geometrical discontinuity also have an influence on fatigue behaviour. The presence of structural flaws, like voids or notches, near the surface can act as a stress raiser and initiate crack formation [218, 323]. Sharp edges, small scratches, grooves and air bubbles severely concentrate the stress and dramatically reduce the fatigue life [330]. Therefore, improving the surface finish of resin-composite restorations by polishing and avoiding sharp edges during fabrication are essential to enhance fatigue behaviour and longevity [339].

Environmental factors like the mode of applied load [330], thermal fluctuation [347] and storage medium [348, 349] also affect fatigue behaviour of resin-composite materials. Applying cyclic masticatory loading, instead of monotonic static or dynamic loadings, can significantly reduce the fatigue life [326, 330, 350]. Employing thermocycling in water baths as an artificial ageing approach also leads to a considerable reduction in overall strength [351-356]. This is because of the fluctuating thermal stresses induced from dimensional expansions and/or contractions, which led to enhanced degradation and thermal fatigue [218, 355]. Water also tends to be absorbed into the defects and voids within the surface of resin-composites, causing plasticization and hydrolytic degradation in the matrix as well as interfacial adhesion [327, 339, 352, 355, 357]. Consequently, enhanced crack propagation and reduced fatigue life have been reported in studies using water storage [326, 327, 357]. Regarding to storage time, one study has found a logarithmic relationship between water storage time and fatigue strength.[358].

IV Fatigue of FRC:

The fatigue mechanism of FRCs is relatively similar to that of PRCs, except when the cracks reach the reinforcing fibres [359, 360]. Under cyclic loading, the induced stresses

and initiated microcracks swiftly propagate through the matrix to reach the fibre interface. At that point, the stresses tend to divide and travel along the interface, causing failure in the local matrix and separation of the dispersed fibre. The stresses are then transferred to neighbouring fibres, causing their rupture [323, 327]. Once a critical density of single-fibre failures is achieved, localised damage develops within particular domains. Such damages are called "brush-like cracking", from which the final failure would advance [327, 361]. The presence of such damage changes the compliance of the material bulk and deteriorates its load-bearing capacity ahead of the occurrence of final failure [362]. Accordingly, the fatigue life of FRC might be determined by the localized damage occurred around the reinforcing fibres as well as the corresponding alteration in load-bearing capacity.

Additional factors also influence the fatigue life of FRC besides those affecting PRC. The fibre microstructure regulates the distribution of cracks along the interface rather than the direction of applied load [360]. The speed of crack propagation is also governed by microstructure as well as the stress intensity [361]. The strength gradient at the fibre/matrix interface also influences the crack propagation rate rather than the matrix alone [327]. In terms of fibre orientation, unidirectional FRC has higher fatigue life than bidirectional when tested in 3-point bending configuration [184]. However, the latter exhibits better fatigue behaviour when tested using compressive loading [207]. Moreover, the type of fibres and their position in relation to the applied force also affects fatigue behaviour. Glass FRCs exhibit higher fatigue strength than other types like UHMWP or polyaramid [184]. Lower fatigue resistance is generally exhibited when the reinforcing fibres are incorporated within the compression side rather than the tension side [145, 327, 363]. From a clinical viewpoint, all of these factors should be carefully considered during the fabrication of FRC restorations to ensure optimum fatigue behaviour.

Studies comparing the fatigue behaviour of different resin-composites have confirmed that FRCs generally exhibit better fatigue resistance than PRCs [83, 164, 184, 207, 323, 360, 364, 365]. One study has reported that plain FRCs have a significantly higher fatigue limit ($1606 \pm 235\text{N}$) than plain PRCs ($740 \pm 45\text{N}$) [207]. Combination materials made of FRC and PRC also exhibit superior fatigue limit than plain PRCs, which indicates that the incorporation of FRC within PRC tends to improve the fatigue resistance [184, 207]. This is explained by the fact that the reinforcing fibres act as a stress-bearing component "by activating crack-stopping or crack-deflecting

mechanisms” [207, 360]. Clinically, enhanced longevity and performance of resin-composite restorations have been reported as a consequence of FRC incorporation [78, 83, 86, 90, 91, 201, 229, 269, 322, 366, 367]. However, scant attention has been paid to compare the fatigue behaviour and performance of FRC restorations with other alternatives [368, 369]. Such comparison would be beneficial to enhance the understanding of FRC and improve their clinical practice.

1.2.6.6 Wear resistance:

I Definition:

Wear is defined as “the gradual loss of substance resulting from the mechanical interaction between two contacting surfaces in a relative motion” [370]. In the oral cavity, wear is described as a continuous physiological process that affects both teeth and restorative materials at a low estimated annual rate. However, it could become pathological under certain circumstances, like parafunctional habits and high acid consumption, leading to excessive amplification of the wear rate and severe aggravation in the functionality and appearance [371].

The mechanism of wear in the oral cavity is simultaneously influenced by various tribological parameters, including the mechanical properties of articulating surfaces, their roughness and topography, the abrasive nature of food, chewing behaviour as well as other environmental factors [370, 372, 373]. Consequently, several wear mechanisms have been identified in the oral cavity, which tend to occur in a combination [374]. According to its mechanism, the wear can be classified into:

A. Attrition:

This type of wear is the result of direct sliding action between antagonistic teeth or restorations during mastication or any other occlusal movements. It is usually described as a two-body wear as long as there is no intermediate layer transmitting forces between the interlocking surfaces [372, 375]. This type is the most obvious in patients who have parafunctional habits, like clenching or grinding [376].

B. Abrasion:

This type represents a three-body wear which occurs in the presence of abrasive particles, like a bolus of food or toothpaste, as an intermediate layer between the relatively moving surfaces [370, 375, 377, 378]. Under normal circumstances, this type is considered more clinically relevant than two-body wear since the time of direct

contact between opposing structures is limited during the day compared with the time spent on food chewing and teeth brushing [377].

C. Fatigue wear:

This type occurs as a consequence of the repetitive loads of mastication, which cause intermittent stresses within the contacting surfaces [372, 379]. Such stresses provoke surface microcracks that spread to subsurface regions, inducing chipping and separation in the affected structure [376]. The degree of fatigue wear is mainly affected by the fatigue strength of contacting materials [380].

D. Corrosive wear:

This type is related to chemical reactions that soften superficial microstructures and facilitate their scrapping away with antagonistic contacts [370, 376, 381]. Accordingly, the presence of chemical or corrosive medium in the oral environment raises the wear rate dramatically [381].

II Measurement:

Investigating the tribological behaviours of dental materials *in-vitro* involves two consecutive processes; wear simulation and wear assessment. For wear simulation, two approaches have been used in the literature. One approach is by attempting to closely mimic all wear conditions in the mouth, like the cyclic masticatory loading and oral environment, in order to achieve clinically relevant results [382, 383]. The other approach relies on isolating certain wear mechanisms or influencing factors to investigate their effect on wear behaviour [374, 384, 385]. The latter approach is the most advocated as there is no *in-vitro* method which can accurately simulate the clinical wear. The lack of precision in wear measuring methods makes the comparison and correlation between different studies unattainable [374].

A multitude of testing machines has been developed to simulate wear *in-vitro*. These machines can be classified according to the mode of action into toothbrushing machines, two-body and three-body wear machines [385]. Toothbrushing machines rely on a toothbrush/dentifrice abrasion concept to simulate tooth cleaning and sliding wear [386, 387]. However, two-body wear machines have been developed and used in different configurations, including pin-on-disk tribometer [388], ball-and-crater [389], reciprocating sliding-wear test [390], two-body wear rotating countersample [391], oscillating friction and wear test rig [392]. Yet, three-body machines are the most

frequently used, owing to their most accurate simulation of clinical wear [385]. Alabama [393], ACTA [394], OHSU [395], Zurich [396], MTS [374] and Willytec Munich wear simulators [397] are among the most cited three-body wear machines in the dental literature. Different antagonist types (enamel, stainless steel, steatite and ceramic) [379] and shapes (cylindrical and spherical) [376], lubricants (artificial saliva, deionised water) [398], and abrasive media (rice, millet seeds, poppy seeds and PMMA beads) [399] have also been used with the intention of achieving the best clinical simulation. Recently, a chewing robot has also been developed, aiming to simulate chewing patterns and tooth-food-tooth interactions with a combination of different wear mechanisms [400].

With regard to wear assessment *in-vitro*, a variety of methods has been also employed. Weight loss [384], profilometrical tracings [38, 401, 402], photomicrographs [403], micro-CT [404] and 3D laser scanning [405] are among the most practiced methods. Surface matching software used to superimpose sequential 3D scans is another method that is considered the most accurate [406]. On the other hand, wear assessment *in-vivo* can be performed either directly or indirectly. Direct techniques are mainly tooth wear indices using predefined criteria to qualitatively assess the degree of wear [407]. Although it is not always feasible, direct quantitative findings can be also achieved relying on objective physical measurements, such as the height of cusp, depth of groove and area of facet [408, 409]. However, indirect techniques are considered simpler and more reliable to quantify clinical tooth wear. Nevertheless, such techniques depend on impressions, gypsum casts or epoxy resin dies for image acquisition, which could create many inherent errors [410-412]. Accordingly, direct intraoral scanning of affected teeth would be the potential gold standard for wear measurement since it would decrease the number of steps and enhance accuracy.

III Wear resistance of resin composite material:

It is established that the wear behaviour of resin-composite restorations is an important indicator of their clinical performance [376]. Ideally, restorations should have wear resistance similar to that of tooth substance in order to prevent any subsequent instability in the occlusion [413]. In the posterior area, the average estimated wear rate for enamel is about 20-40µm per year [414], while it is typically 0.1 to 0.2 mm more for resin-composite restorations over 10 years [9]. Such differential wear rate has clinical importance as it may affect the functionality and appearance of restored teeth [9, 414,

415]. Loss of contour, exposure of cavity margins, increase in surface roughness and staining, leaching of monomers and inhalation of worn filler particles, are all potential problems caused by the wear of resin composite restoration [415, 416]. Therefore, most modern resin-composite products have been developed in an attempt to improve wear behaviour and address corresponding problems.

Wear behaviour of resin-composites is known to be mainly dependent on compositional features, such as filler size, shape, fraction, matrix formulation and interfacial strength [376, 401, 402]. Resin-composites with finer particles and higher content have been reported to result in reduced interparticle spacing and thereby enhanced wear resistance [284, 395, 417]. One study has found that nano-composites exhibit smoother and lesser wear facets than hybrid and micro-filled composites [418]. Another study has also confirmed that smaller particles for a fixed-volume-fraction of filler cause reduced wear [37]. However, some researchers have reported the relationship between wear and particle size to be non-linear, especially for nanocomposites [5, 380]. While some studies have exhibited significantly better wear resistance in nano-composites [283, 387], others reported lesser wear in microhybrid resin-composites [401, 419]. This is possibly due to the reduced preferential load support that nano-fillers can provide, indicating that wear behaviour of resin-composites is not purely dependent on filler size [380]. In terms of filler fraction, most studies have reported an increase in wear resistance as a consequence of increasing the filler loading [5, 32, 284, 382, 402].

The shape and hardness of filler particles also influence wear behaviour. Resin-composites with irregularly shaped particles exhibit higher wear resistance than those with spherical particles [37]. This is attributed to the higher specific area for adhesion that irregular particles can provide compared to regular particles. Accordingly, the debonding and separation of spherical particles from the resin matrix as a result of wear were more frequent [37, 420]. Resin-composites with relatively soft fillers, like barium glass, also display better wear behaviour than those with harder fillers, like quartz. This is because that the softer particles tend to partially absorb the loading stresses during their transmittance within the matrix [421]. Furthermore, the matrix viscosity also affects the wear resistance since a lesser wear rate has been reported when the viscosity of resin increased [422].

Interestingly, the resin matrix and filler particles have different wear patterns as they do not abrade at the same rate [423]. Due to the fact that the matrix is much softer than the

inorganic phase, it tends to be preferentially abraded during the mastication. As the matrix wears down, the filler particles become more exposed to the wear action, leading to their plucking from the matrix at an exponential rate [423]. The smaller the filler particles, the reduced plucking and surface degradation that occur during chewing, and thus the lesser degree of abrasive wear. Likewise, the stronger the adhesion between the fillers and the matrix, the higher the wear resistance achieved [14]. Accordingly, manufacturers of resin-composites rely on silanization to improve adhesion between the different polymeric phases [422].

IV Wear resistance of FRC:

Despite the high wear resistance developed in contemporary resin-composite materials, they are still considered not suitable as durable restorations in patients with active tooth wear [371]. Other metal-free alternatives, like dental ceramics, tend to be more favourable although they also have disadvantages [397]. High differential wear resistance and aggressiveness to opposing dentition are the main drawbacks of ceramics that would produce severe tooth sensitivity and occlusal imbalance [378, 397]. Precious metal alloys are considered the gold standard to restore worn teeth since their wear behaviour is comparable to enamel [413, 424]. However, their poor aesthetic is the main drawback. Accordingly, there is no ideal restorative material that can offer low differential wear resistance with enamel as well as excellent aesthetics [413].

FRC has been developed with the intention of improving wear behaviour of resin-composites; for example, long and short fibres have been incorporated within PRCs to enhance wear behaviour as well as other mechanical properties [59, 207]. Long fibres provide superior wear resistance since they can reinforce the matrix better than short fibres [425]. The fibre fraction, however, has non-linear relationship with the wear behaviour since a low wear resistance has been reported in FRCs with low and high fibre content. This is explained by the inadequate support provided to the matrix by the low fibre content, and the excessive fibres clustering within the matrix caused by the high fibre content [425, 426]

In comparison with PRC, FRC tends to have a lesser wear resistance. This is because of the enhanced plucking of fibre particles that makes the matrix more prone to further degradation and increases wear rates [284]. However, some recent studies have reported the opposite since FRC tends to exhibit enhanced fatigue wear and superior mechanical properties [259, 323]. Some authors have also suggested FRC restorations as an option

to restore heavily worn teeth, owing to their superior mechanical properties, excellent longevity and maintainability [371]. Nevertheless, the wear behaviour of FRC has not been compared with that of other well-practiced alternatives used to restore heavily worn tooth structure, leading to uncertainty about its indication in such cases.

1.3 SUMMARY:

Fibre reinforced composite has many dental applications as a restorative material, owing to its superior mechanical properties and excellent aesthetics. However, it is not as well-practiced clinically as other metal-free alternatives due to many uncertainties about its clinical performance. A lack of information about the effect of fibre reinforcement and its orientation on surface hardness, marginal integrity, bonding strength with other restorative substrates has been identified. Scarce attention has been also paid to study the corresponding effect of the wear and fatigue behaviours of FRC restorations on longevity and overall performance. Moreover, limited studies have considered comparing the performance of FRC restorations and other well-practiced alternatives in an attempt to provide a meaningful context to the findings.

1.4 REFERENCES:

1. Hull D, Clyne TW. *An Introduction to Composite Materials*. 2nd ed. Cambridge: Cambridge University Press; 1996.
2. Barbucci R. *Integrated Biomaterials Science*. New York ; London: Kluwer Academic/Plenum; 2002.
3. McCabe JF, Walls A. *Applied Dental Materials*. 9th ed. Oxford: Blackwell; 2008.
4. Piggott MR. *Load Bearing Fibre Composites*. 2nd ed. Boston: Kluwer Academic Publishers; 2002.
5. Ferracane JL. Resin Composite--State of the Art. *Dent Mater*, 2011; **27**: 29-38.
6. Isaac D. Engineering Aspects of the Structure and Properties of Polymer-Fibre Composites. In: *The First International Symposium on Fibre-Reinforced Plastics in Dentistry*. Edited by Vallittu pK. Turku,Finland; 1998.
7. Nielsen L. *Mechanical Properties of Polymers and Composites Vol 1*. [S.l.]: Marcel Dekker; 1974.
8. Fernandes CP, Chevitaese O. The Orientation and Direction of Rods in Dental Enamel. *J Prosthet Dent*, 1991; **65**: 793-800.
9. Anusavice KJ, Phillips RWSodm. *Phillips' Science of Dental Materials*. 11th ed. St. Louis, Mo. : Saunders; 2003.
10. Peutzfeldt A. Resin Composites in Dentistry: The Monomer Systems. *Eur J Oral Sci*, 1997; **105**: 97-116.
11. Moszner N, Salz U. New Developments of Polymeric Dental Composites. *Prog Polymer Sci*, 2001; **26**: 535-576.
12. Moszner N, Fischer UK, Angermann J, Rheinberger V. A Partially Aromatic Urethane Dimethacrylate as a New Substitute for Bis-GMA in Restorative Composites. *Dent Mater*, 2008; **24**: 694-699.
13. Ruyter IE, Sjøvik IJ. Composition of Dental Resin and Composite Materials. *Acta Odontologica Scandinavica*, 1981; **39**: 133-146.
14. Ferracane JL. Current Trends in Dental Composites. *Crit Rev Oral Biol Med*, 1995; **6**: 302-318.
15. Ruyter. Monomer Systems and Polymerization. In: *Posterior Composite Resin Dental Restorative Materials* Edited by Vanherle; G, Smith D: Peter Szulc Publishing CO; 1985. pp. 35-109.
16. Andrzejewska E. Photopolymerization Kinetics of Multifunctional Monomers. *Prog Polymer Sci*, 2001; **26**: 605-665.
17. Kleverlaan CJ, Feilzer AJ. Polymerization Shrinkage and Contraction Stress of Dental Resin Composites. *Dent Mater*, 2005; **21**: 1150-1157.
18. Dogan A, Hubbezoglu I, Dogan OM, Bolayir G, Demir H. Temperature Rise Induced by Various Light Curing Units through Human Dentin. *Dent Mater J*, 2009; **28**: 253-260.
19. Shawkat ES, Shortall AC, Addison O, Palin WM. Oxygen Inhibition and Incremental Layer Bond Strengths of Resin Composites. *Dent Mater*, 2009; **25**: 1338-1346.
20. Eick JD, Kotha SP, Chappelow CC, Kilway KV, Giese GJ, Glaros AG, Pinzino CS. Properties of Silorane-Based Dental Resins and Composites Containing a Stress-Reducing Monomer. *Dent Mater*, 2007; **23**: 1011-1017.

21. Ilie N, Hickel R. Resin Composite Restorative Materials. *Aust Dent J*, 2011; **56 Suppl 1**: 59-66.
22. Weinmann W, Thalacker C, Guggenberger R. Siloranes in Dental Composites. *Dent Mater*, 2005; **21**: 68-74.
23. Kostoryz EL, Zhu Q, Zhao H, Miller M, Eick JD. Assessment of the Relative Skin Sensitization Potency of Siloranes and Bis-GMA Using the Local Lymph Node Assay and Qsar Predicted Potency. *J Biomed Mater Res A*, 2006; **79**: 684-688.
24. Ilie N, Jelen E, Clementino-Luedemann T, Hickel R. Low-Shrinkage Composite for Dental Application. *Dent Mater J*, 2007; **26**: 149-155.
25. Knock, Glenn. Dental Materials and Methods. *US Patent*, 1951; **2**: 139.
26. Bowen RL. Properties of a Silica-Reinforced Polymer for Dental Restorations. *J Am Dent Assoc*, 1963; **66**: 57-64.
27. Cook WD, Beech DR, Tyas MJ. Resin-Based Restorative Materials—a Review. *Aust Dent J*, 1984; **29**: 291-295.
28. Bowen RL. Effect of Particle Shape and Size Distribution in a Reinforced Polymer. *J Am Dent Assoc*, 1964; **69**: 481-495.
29. Stein PS, Sullivan J, Haubenreich JE, Osborne PB. Composite Resin in Medicine and Dentistry. *J Long Term Eff Med Implants*, 2005; **15**: 641-654.
30. Miyasaka T. Effect of Shape and Size of Silanated Fillers on Mechanical Properties of Experimental Photo Cure Composite Resins. *Dent Mater J*, 1996; **15**: 98-110.
31. Emami N, Sjö Dahl M, Söderholm K-JM. How Filler Properties, Filler Fraction, Sample Thickness and Light Source Affect Light Attenuation in Particulate Filled Resin Composites. *Dent Mater*, 2005; **21**: 721-730.
32. Lim BS, Ferracane JL, Condon JR, Adey JD. Effect of Filler Fraction and Filler Surface Treatment on Wear of Microfilled Composites. *Dent Mater*, 2002; **18**: 1-11.
33. Kim KH, Ong JL, Okuno O. The Effect of Filler Loading and Morphology on the Mechanical Properties of Contemporary Composites. *J Prosthet Dent*, 2002; **87**: 642-649.
34. Htang A, Ohsawa M, Matsumoto H. Fatigue Resistance of Composite Restorations: Effect of Filler Content. *Dent Mater*, 1995; **11**: 7-13.
35. Braem M, Finger W, Van Doren VE, Lambrechts P, Vanherle G. Mechanical Properties and Filler Fraction of Dental Composites. *Dent Mater*, 1989; **5**: 346-349.
36. Hashinger DT, Fairhurst CW. Thermal Expansion and Filler Content of Composite Resins. *J Prosthet Dent*, 1984; **52**: 506-510.
37. Turssi CP, Ferracane JL, Vogel K. Filler Features and Their Effects on Wear and Degree of Conversion of Particulate Dental Resin Composites. *Biomaterials*, 2005; **26**: 4932-4937.
38. Suzuki S, Leinfelder KF, Kawai K, Tsuchitani Y. Effect of Particle Variation on Wear Rates of Posterior Composites. *Am J Dent*, 1995; **8**: 173-178.
39. Oysaed H, Ruyter IE. Water Sorption and Filler Characteristics of Composites for Use in Posterior Teeth. *J Dent Res*, 1986; **65**: 1315-1318.
40. Darvell BW. *Materials Science for Dentistry*. 9th ed. Oxford: Woodhead Publishing; 2009.
41. McCabe JF, Wassell RW. Hardness of Model Dental Composites – the Effect of Filler Volume Fraction and Silanation. *J Mater Sci - Mater Med*, 1999; **10**: 291-294.

42. Shortall AC, Palin WM, Burtscher P. Refractive Index Mismatch and Monomer Reactivity Influence Composite Curing Depth. *J Dent Res*, 2008; **87**: 84-88.
43. Watts DC, Cash AJ. Analysis of Optical Transmission by 400-500 Nm Visible Light into Aesthetic Dental Biomaterials. *J Dent*, 1994; **22**: 112-117.
44. Vallittu PK. Strength and Interfacial Adhesion of FRC-Tooth System. In: *The Second International Symposium on Fibre-Reinforced Plastics in Dentistry, Symposium Book on the Scientific Workshop on Dental Fibre-Reinforced Composite on 13 October 2001*. Edited by Vallittu PK. Nijmegen, Netherlands 2001.
45. Goldberg AJ, Burstone CJ. The Use of Continuous Fiber Reinforcement in Dentistry. *Dent Mater*, 1992; **8**: 197-202.
46. Vallittu PK. Experience of Using Glass Fibers with Multiphase Acrylic Resin Systems. Theoretical Background and Clinical Examples In: *The First Symposium on Fiber Reinforced Plastics in Dentistry*. Edited by PK V. Turku, Finland: University of Turku, Institute of dentistry; 1998.
47. Muller H, Olsson S, Soderholm KJ. The Effect of Comonomer Composition, Silane Heating, and Filler Type on Aqueous TEGDMA Leachability in Model Resin Composites. *Eur J Oral Sci*, 1997; **105**: 362-368.
48. Halvorson RH, Erickson RL, Davidson CL. The Effect of Filler and Silane Content on Conversion of Resin-Based Composite. *Dent Mater*, 2003; **19**: 327-333.
49. Beun S, Glorieux T, Devaux J, Vreven J, Leloup G. Characterization of Nanofilled Compared to Universal and Microfilled Composites. *Dent Mater*, 2007; **23**: 51-59.
50. Ferracane JL, Greener EH. Fourier Transform Infrared Analysis of Degree of Polymerization in Unfilled Resins--Methods Comparison. *J Dent Res*, 1984; **63**: 1093-1095.
51. Lutz F, Phillips RW. A Classification and Evaluation of Composite Resin Systems. *J Prosthet Dent*, 1983; **50**: 480-488.
52. Combe EC, Burke FJ. Contemporary Resin-Based Composite Materials for Direct Placement Restorations: Packables, Flowables and Others. *Dent Update*, 2000; **27**: 326-332, 334-326.
53. Chen MH. Update on Dental Nanocomposites. *J Dent Res*, 2010; **89**: 549-560.
54. Khan AM, Suzuki H, Nomura Y, Taira M, Wakasa K, Shintani H, Yamaki M. Characterization of Inorganic Fillers in Visible-Light-Cured Dental Composite Resins. *J Oral Rehabil*, 1992; **19**: 361-370.
55. Willems G, Lambrechts P, Braem M, Celis JP, Vanherle G. A Classification of Dental Composites According to Their Morphological and Mechanical Characteristics. *Dent Mater*, 1992; **8**: 310-319.
56. Vallittu PK. Compositional and Weave Pattern Analyses of Glass Fibers in Dental Polymer Composites. *J Prosthodont*, 1998; **7**: 170-176.
57. Kamath G, Bhargava K. Comparison of Impact Strength of Acrylic Resin Reinforced with Kevlar and Polyethylene Fibres. *Indian J Dent Res*, 2002; **13**: 108-111.
58. Bergendal T, Ekstrand K, Karlsson U. Evaluation of Implant-Supported Carbon/Graphite Fiber-Reinforced Poly (Methyl Methacrylate) Prostheses. A Longitudinal Multicenter Study. *Clin Oral Implants Res*, 1995; **6**: 246-253.
59. Garoushi S, Vallittu PK, Lassila LV. Short Glass Fiber Reinforced Restorative Composite Resin with Semi-Inter Penetrating Polymer Network Matrix. *Dent Mater*, 2007; **23**: 1356-1362.

60. Matinlinna JP, Lassila LV, Ozcan M, Yli-Urpo A, Vallittu PK. An Introduction to Silanes and Their Clinical Applications in Dentistry. *Int J Prosthodont*, 2004; **17**: 155-164.
61. Plueddemann EP. *Silane Coupling Agents*. 2nd ed. New York: Plenum Press; 1991.
62. Antonucci JMD, S.H.; Fowler, B.O.; Xu, H.H.K.; McDonough, W.G. . Chemistry of Silanes: Interfaces in Dental Polymers and Composites. *J Res Natl Inst Stand Techno*, 2005; **110**: 541-558.
63. Mohsen NM, Craig RG. Effect of Silanation of Fillers on Their Dispersability by Monomer Systems. *J Oral Rehabil*, 1995; **22**: 183-189.
64. Takahashi JMA, J.W. Stansbury. Effect of Silane Coupling Agent and Filler on Composite Durability. *J Dent Res*, 1999; **1999**: 549.
65. Matinlinna JP, Vallittu PK. Silane Based Concepts on Bonding Resin Composite to Metals. *J Contemp Dent Pract*, 2007; **8**: 1-8.
66. Debnath S, Wunder SL, McCool JI, Baran GR. Silane Treatment Effects on Glass/Resin Interfacial Shear Strengths. *Dent Mater*, 2003; **19**: 441-448.
67. Vallittu PK. Curing of a Silane Coupling Agent and Its Effect on the Transverse Strength of Autopolymerizing Polymethylmethacrylate-Glass Fibre Composite. *J Oral Rehabil*, 1997; **24**: 124-130.
68. Labella R, Braden M, Deb S. Novel Hydroxyapatite-Based Dental Composites. *Biomaterials*, 1994; **15**: 1197-1200.
69. Gao X, Jensen RE, Li W, Deitzel J, McKnight SH, Gillespie JW. Effect of Fiber Surface Texture Created from Silane Blends on the Strength and Energy Absorption of the Glass Fiber/Epoxy Interphase. *J Compos Mater*, 2008; **42**: 513-534.
70. Wilson KS, Antonucci JM. Interphase Structure-Property Relationships in Thermoset Dimethacrylate Nanocomposites. *Dent Mater*, 2006; **22**: 995-1001.
71. Soderholm KJ. Degradation of Glass Filler in Experimental Composites. *J Dent Res*, 1981; **60**: 1867-1875.
72. Mohsen NM, Craig RG. Hydrolytic Stability of Silanated Zirconia-Silica-Urethane Dimethacrylate Composites. *J Oral Rehabil*, 1995; **22**: 213-220.
73. Soderholm KJ. Influence of Silane Treatment and Filler Fraction on Thermal Expansion of Composite Resins. *J Dent Res*, 1984; **63**: 1321-1326.
74. Ilie N, Bucuta S, Draenert M. Bulk-Fill Resin-Based Composites: An in Vitro Assessment of Their Mechanical Performance. *Oper Dent*, 2013; **38**: 618-625.
75. Smith DC. Recent Developments and Prospects in Dental Polymers. *J Prosthet Dent*, 1962; **12**: 1066-1078.
76. Narva KK, Vallittu PK, Helenius H, Yli-Urpo A. Clinical Survey of Acrylic Resin Removable Denture Repairs with Glass-Fiber Reinforcement. *Int J Prosthodont*, 2001; **14**: 219-224.
77. Ruyter IE, Ekstrand K, Björk N. Development of Carbon/Graphite Fiber Reinforced Poly(Methyl Methacrylate) Suitable for Implant-Fixed Dental Bridges. *Dent Mater*, 1986; **2**: 6-9.
78. Vallittu PK, Sevelius C. Resin-Bonded, Glass Fiber-Reinforced Composite Fixed Partial Dentures: A Clinical Study. *J Prosthet Dent*, 2000; **84**: 413-418.
79. Freilich MA, Duncan JP, Meiers JC, Goldberg AJ. Preimpregnated, Fiber-Reinforced Prostheses. Part I. Basic Rationale and Complete-Coverage and Intracoronal Fixed Partial Denture Designs. *Quintessence Int*, 1998; **29**: 689-696.

80. Meiers JC, Duncan JP, Freilich MA, Goldberg AJ. Preimpregnated, Fiber-Reinforced Prostheses. Part II. Direct Applications: Splints and Fixed Partial Dentures. *Quintessence Int*, 1998; **29**: 761-768.
81. Freudenthaler JW, Tischler GK, Burstone CJ. Bond Strength of Fiber-Reinforced Composite Bars for Orthodontic Attachment. *Am J Orthod Dentofacial Orthop*, 2001; **120**: 648-653.
82. Jokstad A, Gokce M, Hjortsjo C. A Systematic Review of the Scientific Documentation of Fixed Partial Dentures Made from Fiber-Reinforced Polymer to Replace Missing Teeth. *Int J Prosthodont*, 2005; **18**: 489-496.
83. Freilich MA, Karmaker AC, Burstone CJ, Goldberg AJ. Development and Clinical Applications of a Light-Polymerized Fiber-Reinforced Composite. *J Prosthet Dent*, 1998; **80**: 311-318.
84. Freilich MA, Meiers JC. Fiber-Reinforced Composite Prostheses. *Dent Clin North Am*, 2004; **48**: viii-ix, 545-562.
85. Zimmerli B, Strub M, Jeger F, Stadler O, Lussi A. Composite Materials: Composition, Properties and Clinical Applications. A Literature Review. *Schweiz Monatsschr Zahnmed*, **120**: 972-986.
86. Freilich MA, Meiers JC, Duncan JP, Eckrote KA, Goldberg AJ. Clinical Evaluation of Fiber-Reinforced Fixed Bridges. *J Am Dent Assoc*, 2002; **133**: 1524-1534; quiz 1540-1521.
87. Vallittu PK. A Review of Fiber-Reinforced Denture Base Resins. *J Prosthodont*, 1996; **5**: 270-276.
88. Tezvergil A, Lassila LV, Vallittu PK. The Effect of Fiber Orientation on the Thermal Expansion Coefficients of Fiber-Reinforced Composites. *Dent Mater*, 2003; **19**: 471-477.
89. Tezvergil A, Lassila LV, Vallittu PK. The Effect of Fiber Orientation on the Polymerization Shrinkage Strain of Fiber-Reinforced Composites. *Dent Mater*, 2006; **22**: 610-616.
90. Behr M, Rosentritt M, Handel G. Fiber-Reinforced Composite Crowns and FPDs: A Clinical Report. *Int J Prosthodont*, 2003; **16**: 239-243.
91. van Heumen CC, Kreulen CM, Creugers NH. Clinical Studies of Fiber-Reinforced Resin-Bonded Fixed Partial Dentures: A Systematic Review. *Eur J Oral Sci*, 2009; **117**: 1-6.
92. Miller TE. A New Material for Periodontal Splinting and Orthodontic Retention. *Compend Contin Educ Dent*, 1993; **14**: 800-806.
93. Strassler HE, Serio CL. Esthetic Considerations When Splinting with Fiber-Reinforced Composites. *Dent Clin North Am*, 2007; **51**: 507-524.
94. Yildirim OG, Ataoglu HKN, Karaman AI. An Alternative Method for Splinting of Traumatized Teeth: Case Reports. *Dent Traumatol*, 2006; **22**: 345-349.
95. Trushkowsky R. Fiber Reinforced Composite Bridge and Splint Replacing Congenitally Missing Teeth. *NY State Dent J*, 2004; **70**: 34-38.
96. Strassler HE, Brown C. " Periodontal Splinting with a Thin, High-Modulus Polyethylene Ribbon". *Compend Contin Educ Dent*, 2001; **22**: 696-704.
97. Strassler HE, Haeri A, Gultz JP. New Generation Bonded Reinforcing Materials for Anterior Periodontal Tooth Stabilization and Splinting. *Dent Clin North Am*, 1999; **43**: 105-126.

98. Christensen G. Reinforcement Fibers for Splinting Teeth. *CRA Newsletter*, 1997; **21**: 01-Feb.
99. Miller TE, F H, DN R. Immediate and Indirect Woven Polyethylene Ribbon-Reinforced Periodontal-Prosthetic Splint a Case Report. *Quintessence Int*, 1995; **26**: 267-271.
100. Tahmasbi S, Heravi F, Moazzami SM. Fracture Characteristics of Fibre Reinforced Composite Bars Used to Provide Rigid Orthodontic Dental Segments. *Aust Orthod J*, 2007; **23**: 104-108.
101. Karaman AI, Kir N, Belli S. Four Applications of Reinforced Polyethylene Fiber Material in Orthodontic Practice. *Am J Orthod Dentofacial Orthop*, 2002; **121**: 650-654.
102. Iniguez I, Strassler HE. Polyethylene Ribbon and Fixed Orthodontic Retention and Porcelain Veneers: Solving an Esthetic Dilemma. *J Esthet Dent*, 1998; **10**: 52-59.
103. Ohtonen J, Vallittu PK, Lassila LV. Effect of Monomer Composition of Polymer Matrix on Flexural Properties of Glass Fibre-Reinforced Orthodontic Archwire. *Eur J Orthod*.
104. Nakamura M, Takahashi H, Hayakawa I. Reinforcement of Denture Base Resin with Short-Rod Glass Fiber. *Dent Mater J*, 2007; **26**: 733-738.
105. Le Bell AM, Tanner J, Lassila LV, Kangasniemi I, Vallittu PK. Depth of Light-Initiated Polymerization of Glass Fiber-Reinforced Composite in a Simulated Root Canal. *Int J Prosthodont*, 2003; **16**: 403-408.
106. Turker SB, Alkumru HN, Evren B. " Prospective Clinical Trial of Polyethylene Fiber Ribbon-Reinforced, Resin Composite Post-Core Build-up Restorations". *Int J Prosthodont*, 2007; **20**: 55-56.
107. Piovesan EM, Demarco FF, Cenci MS, Pereira-Cenci T. Survival Rates of Endodontically Treated Teeth Restored with Fiber-Reinforced Custom Posts and Cores: A 97 Month Study. *Int J Prosthodont*, 2007; **20**: 633-639.
108. Naumann M, Preuss A, Frankenberger R. Reinforcement Effect of Adhesively Luted Fiber Reinforced Composite Versus Titanium Posts. *Dent Mater*, 2007; **23**: 138-144.
109. Le Bell-Ronnlof AM, Lahdenpera M, Lassila LV, Vallittu PK. Bond Strength of Composite Resin Luting Cements to Fiber-Reinforced Composite Root Canal Posts. *J Contemp Dent Pract*, 2007; **8**: 17-24.
110. Newman MP, Yaman P, Dennison J, Rafter M, al e. Fracture Resistance of Endodontically Treated Teeth Restored with Composite Posts. *J Prosthet Dent*, 2003; **89**: 360-367.
111. Bijelic J, Garoushi S, Vallittu PK, Lassila LV. Fracture Load of Tooth Restored with Fiber Post and Experimental Short Fiber Composite. *Open Dent J*, 2011; **5**: 58-65.
112. Ahlstrand WM, Finger WJ. Direct and Indirect Fiber-Reinforced Fixed Partial Dentures: Case Reports. *Quintessence Int*, 2002; **33**: 359-365.
113. Belvedre P, Turner W. Direct Fiber-Reinforced Composite Bridges. *Dent Today*, 2002; **21**: 88-94.
114. Kargul B, Caglar E, Kabalay U. Glass Fiber-Reinforced Composite Resin as Fixed Space Maintainers in Children: 12-Month Clinical Follow-Up. *J Dent Child (Chic)*, 2005; **72**: 109-112.
115. Bjork N, Ekstrand K, Ruyter IE. Implant-Fixed, Dental Bridges from Carbon/Graphite Fibre Reinforced Poly(Methyl Methacrylate). *Biomaterials*, 1986; **7**: 73-75.

116. Meiers JC, Freilich MA. Use of a Prefabricated Fiber-Reinforced Composite Resin Framework to Provide a Provisional Fixed Partial Denture over an Integrating Implant: A Clinical Report. *J Prosthet Dent*, 2006; **95**: 14-18.
117. Ballo AM, Narhi TO, Akca EA, Ozen T, Syrjanen SM, Lassila LV, Vallittu PK. Prepolymerized vs. In Situ-Polymerized Fiber-Reinforced Composite Implants--a Pilot Study. *J Dent Res*, **90**: 263-267.
118. Duncan JP, Freilich MA, Latvis CJ. Fiber-Reinforced Composite Framework for Implant-Supported Overdentures. *J Prosthet Dent*, 2000; **84**: 200-204.
119. Ballo A, Lassila LV, Narhi T, Vallittu PK. In Vitro Mechanical Testing of Glass Fiber-Reinforced Composite Used as Dental Implants. *J Contemp Dent Pract*, 2008; **9**: 41-48.
120. Keulemans F, Lassila LV, Garoushi S, Vallittu PK, Kleverlaan CJ, Feilzer AJ. The Influence of Framework Design on the Load-Bearing Capacity of Laboratory-Made Inlay-Retained Fibre-Reinforced Composite Fixed Dental Prostheses. *J Biomech*, 2009; **42**: 844-849.
121. Kurunmaki H, Kantola R, Hatamleh MM, Watts DC, Vallittu PK. A Fiber-Reinforced Composite Prosthesis Restoring a Lateral Midfacial Defect: A Clinical Report. *J Prosthet Dent*, 2008; **100**: 348-352.
122. Hatamleh MM, Watts DC. Fibre Reinforcement Enhances Bonding of Soft Lining to Acrylic Dental and Maxillofacial Prostheses. *Eur J Prosthodont Restor Dent*, 2008; **16**: 116-121.
123. Patil PG. Modified Technique to Fabricate a Hollow Light-Weight Facial Prosthesis for Lateral Midfacial Defect: A Clinical Report. *J Adv Prosthodont*, **2**: 65-70.
124. Belli S, Erdemir A, Ozcopur M, Eskitascioglu G. The Effect of Fibre Insertion on Fracture Resistance of Root Filled Molar Teeth with MOD Preparations Restored with Composite. *Int Endod J*, 2005; **38**: 73-80.
125. Fennis WM, Tezvergil A, Kuijs RH, Lassila LV, Kreulen CM, Creugers NH, Vallittu PK. In Vitro Fracture Resistance of Fiber Reinforced Cusp-Replacing Composite Restorations. *Dent Mater*, 2005; **21**: 565-572.
126. Eronat N, Candan U, Turkun M. Effects of Glass Fiber Layering on the Flexural Strength of Microfill and Hybrid Composites. *J Esthet Restor Dent*, 2009; **21**: 171-178; discussion 179-181.
127. Bagis B, Ustaomer S, Lassila LV, Vallittu PK. Provisional Repair of a Zirconia Fixed Partial Denture with Fibre-Reinforced Restorative Composite: A Clinical Report. *J Can Dent Assoc*, 2009; **75**: 133-137.
128. Turkaslan S, Tezvergil-Mutluay A. Intraoral Repair of All Ceramic Fixed Partial Denture Utilizing Preimpregnated Fiber Reinforced Composite. *Eur J Dent*, 2008; **2**: 63-68.
129. Ballo AM, Cekic-Nagas I, Ergun G, Lassila L, Palmquist A, Borchardt P, Lausmaa J, Thomsen P, Vallittu PK, Narhi TO. Osseointegration of Fiber-Reinforced Composite Implants: Histological and Ultrastructural Observations. *Dent Mater*, 2014; **30**: e384-395.
130. Vallittu PK, Narhi TO, Hupa L. Fiber Glass-Bioactive Glass Composite for Bone Replacing and Bone Anchoring Implants. *Dent Mater*, 2015; **31**: 371-381.
131. Herakovich C. *Mechanics of Fiber Composites* Wiley and Sons; 1998.
132. Ellakwa AE, Shortall AC, Marquis PM. Influence of Fiber Type and Wetting Agent on the Flexural Properties of an Indirect Fiber Reinforced Composite. *J Prosthet Dent*, 2002; **88**: 485-490.

133. Uzun G, Keyf F. The Effect of Fiber Reinforcement Type and Water Storage on Strength Properties of a Provisional Fixed Partial Denture Resin. *J Biomater Appl*, 2003; **17**: 277-286.
134. Murphy JM. *The Reinforced Plastics Handbook*. 2nd ed. Oxford: Elsevier Advanced Technology; 1998.
135. Lassila LVJ, Nohrström T, Vallittu PK. The Influence of Short-Term Water Storage on the Flexural Properties of Unidirectional Glass Fiber-Reinforced Composites. *Biomaterials*, 2002; **23**: 2221-2229.
136. Alander P, Lassila LV, Tezvergil A, Vallittu PK. Acoustic Emission Analysis of Fiber-Reinforced Composite in Flexural Testing. *Dent Mater*, 2004; **20**: 305-312.
137. Vakiparta M, Yli-Urpo A, Vallittu PK. Flexural Properties of Glass Fiber Reinforced Composite with Multiphase Biopolymer Matrix. *J Mater Sci Mater Med*, 2004; **15**: 7-11.
138. Alander P, Lassila LV, Vallittu PK. The Span Length and Cross-Sectional Design Affect Values of Strength. *Dent Mater*, 2005; **21**: 347-353.
139. Lassila LV, Tezvergil A, Lahdenpera M, Alander P, Shinya A, Vallittu PK. Evaluation of Some Properties of Two Fiber-Reinforced Composite Materials. *Acta Odontol Scand*, 2005; **63**: 196-204.
140. Gohring TN, Gallo L, Luthy H. Effect of Water Storage, Thermocycling, the Incorporation and Site of Placement of Glass-Fibers on the Flexural Strength of Veneering Composite. *Dent Mater*, 2005; **21**: 761-772.
141. Bouillaguet S, Schutt A, Alander P, Schwaller P, Buerki G, Michler J, Cattani-Lorente M, Vallittu PK, Krejci I. Hydrothermal and Mechanical Stresses Degrade Fiber-Matrix Interfacial Bond Strength in Dental Fiber-Reinforced Composites. *J Biomed Mater Res B Appl Biomater*, 2006; **76**: 98-105.
142. Ootaki M, Shin-Ya A, Gomi H, et al. Optimum Design for Fixed Partial Dentures Made of Hybrid Composite with Glass Fiber Reinforcement by Finite Element Analysis: Effect of Vertical Reinforced Thickness on Fiber Frame. *Dent Mater J*, 2007; **26**: 280-289.
143. Garoushi S, Vallittu PK, Lassila LV. Fracture Resistance of Short, Randomly Oriented, Glass Fiber-Reinforced Composite Premolar Crowns. *Acta Biomater*, 2007; **3**: 779-784.
144. Garoushi SK, Lassila LV, Tezvergil A, Vallittu PK. Fiber-Reinforced Composite Substructure: Load-Bearing Capacity of an Onlay Restoration and Flexural Properties of the Material. *J Contemp Dent Pract*, 2006; **7**: 1-8.
145. Dyer SR, Lassila LV, Jokinen M, Vallittu PK. Effect of Fiber Position and Orientation on Fracture Load of Fiber-Reinforced Composite. *Dent Mater*, 2004; **20**: 947-955.
146. Goldberg AJ, Freilich MA. An Innovative Pre-Impregnated Glass Fiber for Reinforcing Composites. *Dent Clin North Am*, 1999; **43**: 127-133.
147. Rudo DN, Karbhari VM. Physical Behaviors of Fiber Reinforcement as Applied to Tooth Stabilization. *Dent Clin North Am*, 1999; **43**: 7-35.
148. Ellakwa A, Shortall A, Shehata M, Marquis P. Influence of Bonding Agent Composition on Flexural Properties of an Ultra-High Molecular Weight Polyethylene Fiber-Reinforced Composite. *Open Dent J*, 2002; **27**: 184-191
149. Ward I. The Preparation, Structure and Properties of Ultra-High Modulus Flexible Polymers. In: *Key Polymers Properties and Performance*: Springer Berlin / Heidelberg; 1985. pp. 1-70.

150. Vallittu PK. Ultra-High-Modulus Polyethylene Ribbon as Reinforcement for Denture Polymethyl Methacrylate: A Short Communication. *Dent Mater*, 1997; **13**: 381-382.
151. Bae JM, Kim KN, Hattori M, Hasegawa K, Yoshinari M, Kawada E, Oda Y. The Flexural Properties of Fiber-Reinforced Composite with Light-Polymerized Polymer Matrix. *Int J Prosthodont*, 2001; **14**: 33-39.
152. Gutteridge DL. Reinforcement of Poly(Methyl Methacrylate) with Ultra-High-Modulus Polyethylene Fibre. *J Dent*, 1992; **20**: 50-54.
153. Kim J-K, Mai YW. *Engineered Interfaces in Fiber Reinforced Composites*. Amsterdam ; Oxford: Elsevier; 1998.
154. Bahramian N, Atai M, Naimi-Jamal MR. Ultra-High-Molecular-Weight Polyethylene Fiber Reinforced Dental Composites: Effect of Fiber Surface Treatment on Mechanical Properties of the Composites. *Dent Mater*, 2015; **31**: 1022-1029.
155. Tanner J, Carlen A, Soderling E, Vallittu PK. Adsorption of Parotid Saliva Proteins and Adhesion of Streptococcus Mutans Atcc 21752 to Dental Fiber-Reinforced Composites. *J Biomed Mater Res B Appl Biomater*, 2003; **66**: 391-398.
156. Taner B, Dogan A, Tincer T, Akinay AE. A Study on Impact and Tensile Strength of Acrylic Resin Filled with Short Ultra-High Molecular Weight Polyethylene Fibers. *J Oral Sci*, 1999; **41**: 15-18.
157. Cheng YY, Chow TW. Fabrication of Complete Denture Bases Reinforced with Polyethylene Woven Fabric. *J Prosthodont*, 1999; **8**: 268-272.
158. Bowman AJ, Manley TR. The Elimination of Breakages in Upper Dentures by Reinforcement with Carbon Fibre. *Br Dent J*, 1984; **156**: 87-89.
159. DeBoer J, Vermilyea SG, Brady RE. The Effect of Carbon Fiber Orientation on the Fatigue Resistance and Bending Properties of Two Denture Resins. *J Prosthet Dent*, 1984; **51**: 119-121.
160. Schreiber CK. Polymethylmethacrylate Reinforced with Carbon Fibres. *Br Dent J*, 1971; **130**: 29-30.
161. Yazdanie N, Mahood M. Carbon Fiber Acrylic Resin Composite: An Investigation of Transverse Strength. *J Prosthet Dent*, 1985; **54**: 543-547.
162. Larson WR, Dixon DL, Aquilino SA, Clancy JM. The Effect of Carbon Graphite Fiber Reinforcement on the Strength of Provisional Crown and Fixed Partial Denture Resins. *J Prosthet Dent*, 1991; **66**: 816-820.
163. Lassila LV, Tanner J, Le Bell AM, Narva K, Vallittu PK. Flexural Properties of Fiber Reinforced Root Canal Posts. *Dent Mater*, 2004; **20**: 29-36.
164. Drummond JL, Bapna MS. Static and Cyclic Loading of Fiber-Reinforced Dental Resin. *Dent Mater*, 2003; **19**: 226-231.
165. Torbjorner A, Karlsson S, Syverud M, Hensten-Pettersen A. Carbon Fiber Reinforced Root Canal Posts. Mechanical and Cytotoxic Properties. *Eur J Oral Sci*, 1996; **104**: 605-611.
166. Mullarky RH. Aramid Fiber Reinforcement of Acrylic Appliances. *J Clin Orthod*, 1985; **19**: 655-658.
167. Vallittu PK, Lassila VP. Reinforcement of Acrylic Resin Denture Base Material with Metal or Fibre Strengtheners. *J Oral Rehabil*, 1992; **19**: 225-230.
168. Uzun G, Hersek N, Tincer T. Effect of Five Woven Fiber Reinforcements on the Impact and Transverse Strength of a Denture Base Resin. *J Prosthet Dent*, 1999; **81**: 616-620.

169. Foo SH, Lindquist TJ, Aquilino SA, Schneider RL, Williamson DL, Boyer DB. Effect of Polyaramid Fiber Reinforcement on the Strength of 3 Denture Base Polymethyl Methacrylate Resins. *J Prosthodont*, 2001; **10**: 148-153.
170. John J, Gangadhar SA, Shah I. Flexural Strength of Heat-Polymerized Polymethyl Methacrylate Denture Resin Reinforced with Glass, Aramid, or Nylon Fibers. *J Prosthet Dent*, 2001; **86**: 424-427.
171. Chen SY, Liang WM, Yen PS. Reinforcement of Acrylic Denture Base Resin by Incorporation of Various Fibers. *J Biomed Mater Res*, 2001; **58**: 203-208.
172. Jagger D, Harrison A, Jagger R, Milward P. The Effect of the Addition of Poly(Methyl Methacrylate) Fibres on Some Properties of High Strength Heat-Cured Acrylic Resin Denture Base Material. *J Oral Rehabil*, 2003; **30**: 231-235.
173. Goldberg AJ, Burstone CJ, Hadjinikolaou I, Jancar J. Screening of Matrices and Fibers for Reinforced Thermoplastics Intended for Dental Applications. *J Biomed Mater Res*, 1994; **28**: 167-173.
174. Vallittu PK. Impregnation of Glass Fibres with Polymethylmethacrylate Using a Powder-Coating Method. *Appl Compos Mater*, 1995; **2**: 51-58.
175. Vallittu PK. Interpenetrating Polymer Networks (IPNs) in Dental Polymers and Composites. In: *Adhesion Aspects in Dentistry*. Edited by J. Matinlinna, Mittal KL; 2009. pp. 62-74.
176. Vallittu PK. The Effect of Void Space and Polymerization Time on Transverse Strength of Acrylic-Glass Fibre Composite. *J Oral Rehabil*, 1995; **22**: 257-261.
177. Vallittu PK. Flexural Properties of Acrylic Resin Polymers Reinforced with Unidirectional and Woven Glass Fibers. *J Prosthet Dent*, 1999; **81**: 318-326.
178. Segerstrom S, Meric G, Knarvang T, Ruyter IE. Evaluation of Two Matrix Materials Intended for Fiber-Reinforced Polymers. *Eur J Oral Sci*, 2005; **113**: 422-428.
179. Ekstrand K, Ruyter IE, Wellendorf H. Carbon/Graphite Fiber Reinforced Poly(Methyl Methacrylate): Properties under Dry and Wet Conditions. *J Biomed Mater Res*, 1987; **21**: 1065-1080.
180. Karmaker AC, Dibenedetto AT, Goldberg AJ. Extent of Conversion and Its Effect on the Mechanical Performance of Bis-GMA/Pegdma-Based Resins and Their Composites with Continuous Glass Fibres. *J Mater Sci Mater Med*, 1997; **8**: 369-374.
181. Lastumaki TM, Lassila LV, Vallittu PK. The Semi-Interpenetrating Polymer Network Matrix of Fiber-Reinforced Composite and Its Effect on the Surface Adhesive Properties. *J Mater Sci Mater Med*, 2003; **14**: 803-809.
182. Lastumaki TM, Kallio TT, Vallittu PK. The Bond Strength of Light-Curing Composite Resin to Finally Polymerized and Aged Glass Fiber-Reinforced Composite Substrate. *Biomaterials*, 2002; **23**: 4533-4539.
183. Malquarti G, Berruet RG, Bois D. Prosthetic Use of Carbon Fiber-Reinforced Epoxy Resin for Esthetic Crowns and Fixed Partial Dentures. *J Prosthet Dent*, 1990; **63**: 251-257.
184. Bae JM, Kim KN, Hattori M, Hasegawa K, Yoshinari M, Kawada E, Oda Y. Fatigue Strengths of Particulate Filler Composites Reinforced with Fibers. *Dent Mater J*, 2004; **23**: 166-174.
185. Jones RG, Kahovec J, Stepto R, Wilks ES, Hess M, Kitayama T, Metanomski WV. 1: Glossary of Basic Terms in Polymer Science (1996). In: *Compendium of Polymer Terminology and Nomenclature: Iupac Recommendations 2008*: The Royal Society of Chemistry; 2009. pp. 3-21.

186. Sperling LH. Interpenetrating Polymer Networks: An Overview. In: *Interpenetrating Polymer Networks*: American Chemical Society; 1994. pp. 3-38.
187. Sperling LH, Mishra V. The Current Status of Interpenetrating Polymer Networks. *Polym Adv Technol*, 1996; **7**: 197-208.
188. Garoushi S, Vallittu PK, Lassila LV. Use of Short Fiber-Reinforced Composite with Semi-Interpenetrating Polymer Network Matrix in Fixed Partial Dentures. *J Dent*, 2007; **35**: 403-408.
189. Wolff D, Geiger S, Ding P, Staehle HJ, Frese C. Analysis of the Interdiffusion of Resin Monomers into Pre-Polymerized Fiber-Reinforced Composites. *Dent Mater*, 2012; **28**: 541-547.
190. Kallio TT, Lastumaki TM, Vallittu PK. Bonding of Restorative and Veneering Composite Resin to Some Polymeric Composites. *Dent Mater*, 2001; **17**: 80-86.
191. Vallittu PK, Ruyter IE. Swelling of Poly(Methyl Methacrylate) Resin at the Repair Joint. *Int J Prosthodont*, 1997; **10**: 254-258.
192. Vallittu PK. Polymer-Fibre Prepreg, a Method for the Preparation Thereof as Well as the Use of Said Prepreg. In: 1998. pp. 10.
193. Iglesias JG, Gonzalez-Benito J, Aznar AJ, Bravo J, Baselga J. Effect of Glass Fiber Surface Treatments on Mechanical Strength of Epoxy Based Composite Materials. *J Colloid Interface Sci*, 2002; **250**: 251-260.
194. Jorge Perdigão, Swift EJ. Fundamental Concepts of Enamel and Dentin Adhesion. In: *Sturdevant's Art and Science of Operative Dentistry*. Edited by T.M. Roberson, H. Heymann, Swift J. Fifth ed: Mosby Elsevier; 2006.
195. DiBenedetto AT. Tailoring of Interfaces in Glass Fiber Reinforced Polymer Composites: A Review. *Mater Sci Eng*, 2001; **302**: 74-82.
196. Miettinen VM, Vallittu PK, Docent DT. Water Sorption and Solubility of Glass Fiber-Reinforced Denture Polymethyl Methacrylate Resin. *J Prosthet Dent*, 1997; **77**: 531-534.
197. Miettinen VM, Narva KK, Vallittu PK. Water Sorption, Solubility and Effect of Post-Curing of Glass Fibre Reinforced Polymers. *Biomaterials*, 1999; **20**: 1187-1194.
198. Shimizu H, Tsue F, Chen ZX, Takahashi Y. Effect of Surface Preparation on the Failure Load of a Highly Filled Composite Bonded to the Polymer-Monomer Matrix of a Fiber-Reinforced Composite. *J Prosthodont*, 2009; **18**: 255-258.
199. Yenisey M, Kulunk S. Effects of Chemical Surface Treatments of Quartz and Glass Fiber Posts on the Retention of a Composite Resin. *J Prosthet Dent*, 2008; **99**: 38-45.
200. Takagi K, Fujimatsu H, Usami H, Ogasawara S. Adhesion between High Strength and High Modulus Polyethylene Fibers by Use of Polyethylene Gel as an Adhesive. *J Adhes Sci Technol*, 1996; **10**: 869-882.
201. van Heumen CC, Kreulen CM, Bronkhorst EM, Lesaffre E, Creugers NH. Fiber-Reinforced Dental Composites in Beam Testing. *Dent Mater*, 2008; **24**: 1435-1443.
202. Shi L, Fok AS. Structural Optimization of the Fibre-Reinforced Composite Substructure in a Three-Unit Dental Bridge. *Dent Mater*, 2009; **25**: 791-801.
203. Lassila LV, Tezvergil A, Dyer SR, Vallittu PK. The Bond Strength of Particulate-Filler Composite to Differently Oriented Fiber-Reinforced Composite Substrate. *J Prosthodont*, 2007; **16**: 10-17.
204. Agarwal BD, Broutman LJ. *Analysis and Performance of Fiber Composites*. 2nd ed. New York ; Chichester: Wiley; 1990.

205. Krenchel H. *Fibre Reinforcement; Theoretical and Practical Investigations of the Elasticity and Strength of Fibre-Reinforced Materials*. Copenhagen: Akademisk forlag; 1964.
206. Tezvergil A, Lassila LV, Vallittu PK. The Shear Bond Strength of Bidirectional and Random-Oriented Fibre-Reinforced Composite to Tooth Structure. *J Dent*, 2005; **33**: 509-516.
207. Garoushi S, Lassila LV, Tezvergil A, Vallittu PK. Static and Fatigue Compression Test for Particulate Filler Composite Resin with Fiber-Reinforced Composite Substructure. *Dent Mater*, 2007; **23**: 17-23.
208. Garoushi S, Lassila LV, Tezvergil A, Vallittu PK. Load Bearing Capacity of Fibre-Reinforced and Particulate Filler Composite Resin Combination. *J Dent*, 2006; **34**: 179-184.
209. Goncu Basaran E, Ayna E, Uctasli S, Vallittu PK, Lassila LV. Load-Bearing Capacity of Fiber Reinforced Fixed Composite Bridges. *Acta Odontol Scand*.
210. Vallittu PK, Narva K. Impact Strength of a Modified Continuous Glass Fiber--Poly(Methyl Methacrylate). *Int J Prosthodont*, 1997; **10**: 142-148.
211. Aydin C, Yilmaz H, Caglar A. Effect of Glass Fiber Reinforcement on the Flexural Strength of Different Denture Base Resins. *Quintessence Int*, 2002; **33**: 457-463.
212. Keulemans F, De Jager N, Kleverlaan CJ, Feilzer AJ. Influence of Retainer Design on Two-Unit Cantilever Resin-Bonded Glass Fiber Reinforced Composite Fixed Dental Prostheses: An in Vitro and Finite Element Analysis Study. *J Adhes Dent*, 2008; **10**: 355-364.
213. Xie Q, Lassila LV, Vallittu PK. Comparison of Load-Bearing Capacity of Direct Resin-Bonded Fiber-Reinforced Composite FPDs with Four Framework Designs. *J Dent*, 2007; **35**: 578-582.
214. Lastumaki TM, Lassila LV, Vallittu PK. Flexural Properties of the Bulk Fiber-Reinforced Composite Dc-Tell Used in Fixed Partial Dentures. *Int J Prosthodont*, 2001; **14**: 22-26.
215. Dyer SR, Sorensen JA, Lassila LV, Vallittu PK. Damage Mechanics and Load Failure of Fiber-Reinforced Composite Fixed Partial Dentures. *Dent Mater*, 2005; **21**: 1104-1110.
216. Garoushi S, Vallittu PK, Lassila LV. Fracture Toughness, Compressive Strength and Load-Bearing Capacity of Short Glass Fibre-Reinforced Composite Resin. *Chin J Dent Res*, 2011; **14**: 15-19.
217. Marom G, Weinberg A. The Effect of the Fibre Critical Length on the Thermal Expansion of Composite Materials. *J Mater Sci*, 1975; **10**: 1005-1010.
218. Callister WD. *Materials Science and Engineering : An Introduction*. 7th ed. New York ; Chichester: Wiley; 2007.
219. Chen PE. Strength Properties of Discontinuous Fiber Composites. *Polym Eng Sci*, 1971; **11**: 51-56.
220. Garoushi SK, Vallittu PK, Lassila LV. Short Glass Fiber-Reinforced Composite with a Semi-Interpenetrating Polymer Network Matrix for Temporary Crowns and Bridges. *J Contemp Dent Pract*, 2008; **9**: 14-21.
221. Garoushi S, Vallittu PK, Watts DC, Lassila LV. Polymerization Shrinkage of Experimental Short Glass Fiber-Reinforced Composite with Semi-Inter Penetrating Polymer Network Matrix. *Dent Mater*, 2008; **24**: 211-215.
222. Garoushi S, Vallittu PK, Lassila LV. Direct Restoration of Severely Damaged Incisors Using Short Fiber-Reinforced Composite Resin. *J Dent*, 2007; **35**: 731-736.

223. Garoushi SK, Lassila LV, Vallittu PK. Short Fiber Reinforced Composite: The Effect of Fiber Length and Volume Fraction. *J Contemp Dent Pract*, 2006; **7**: 10-17.
224. Adams RD. Compositional Effects of Fibre Reinforced Composites on the Coefficient of Thermal Expansion. In: *Materials Characterization by Thermomechanical Analysis Astm Stp 1136*. Edited by Riga A, Neag C: American Society for Testing and Materials 1991. pp. 150-160.
225. Barbero EJ. *Introduction to Composite Materials Design, Second Edition*; 2010.
226. Vallittu PK. Some Aspects of the Tensile Strength of Undirectional Glass Fibre-Polymethyl Methacrylate Composite Used in Dentures. *J Oral Rehabil*, 1998; **25**: 100-105.
227. Rosentritt M. Fibre Reinforced Composite in Vitro Behaviour. In: *The Second International Symposium on Fire-Reinforced Plastics in Dentistry, Symposium Book on Scientific Workshop*. Edited by Vallittu PK; 2001.
228. Vallittu PK, Lassila VP, Lappalainen R. Acrylic Resin-Fiber Composite--Part I: The Effect of Fiber Concentration on Fracture Resistance. *J Prosthet Dent*, 1994; **71**: 607-612.
229. Freilich MA. *Fiber-Reinforced Composites in Clinical Dentistry*. Chicago ; London: Quintessence; 2000.
230. Karacaer O, Polat TN, Tezvergil A, Lassila LV, Vallittu PK. The Effect of Length and Concentration of Glass Fibers on the Mechanical Properties of an Injection- and a Compression-Molded Denture Base Polymer. *J Prosthet Dent*, 2003; **90**: 385-393.
231. Abdulmajeed AA, Närhi TO, Vallittu PK, Lassila LV. The Effect of High Fiber Fraction on Some Mechanical Properties of Unidirectional Glass Fiber-Reinforced Composite. *Dent Mater*, 2011; **27**: 313-321.
232. Zanghellini G. Fiber-Reinforced Framework and Ceromer Restorations: A Technical Review. *Signature*, 1997; **4**: 1-5.
233. Samadzadeh A, Kugel G, Hurley E, Aboushala A. Fracture Strengths of Provisional Restorations Reinforced with Plasma-Treated Woven Polyethylene Fiber. *J Prosthet Dent*, 1997; **78**: 447-451.
234. Altieri JV, Burstone CJ, Goldberg AJ, Patel AP. Longitudinal Clinical Evaluation of Fiber-Reinforced Composite Fixed Partial Dentures: A Pilot Study. *J Prosthet Dent*, 1994; **71**: 16-22.
235. Nohrstrom TJ, Vallittu PK, Yli-Urpo A. The Effect of Placement and Quantity of Glass Fibers on the Fracture Resistance of Interim Fixed Partial Dentures. *Int J Prosthodont*, 2000; **13**: 72-78.
236. Vallittu PK. Glass Fiber Reinforcement in Repaired Acrylic Resin Removable Dentures: Preliminary Results of a Clinical Study. *Quintessence Int*, 1997; **28**: 39-44.
237. Ellakwa A, Shortall A, Marquis P. Influence of Fibre Position on the Flexural Properties and Strain Energy of a Fibre-Reinforced Composite. *J Oral Rehabil*, 2003; **30**: 679-682.
238. Narva KK, Lassila LV, Vallittu PK. The Static Strength and Modulus of Fiber Reinforced Denture Base Polymer. *Dent Mater*, 2005; **21**: 421-428.
239. Dyer SR, Lassila LV, Jokinen M, Vallittu PK. Effect of Cross-Sectional Design on the Modulus of Elasticity and Toughness of Fiber-Reinforced Composite Materials. *J Prosthet Dent*, 2005; **94**: 219-226.
240. Brady AP, Lee H, Orlowski JA. Thermal Conductivity Studies of Composite Dental Restorative Materials. *J Biomed Mater Res*, 1974; **8**: 471-485.

241. Watts DC, McAndrew R, Lloyd CH. Thermal Diffusivity of Composite Restorative Materials. *J Dent Res*, 1987; **66**: 1576-1578.
242. Bullard RH, Leinfelder KF, Russell CM. Effect of Coefficient of Thermal Expansion on Microleakage. *J Am Dent Assoc*, 1988; **116**: 871-874.
243. Momoi Y, Iwase H, Nakano Y, Kohno A, Asanuma A, Yanagisawa K. Gradual Increases in Marginal Leakage of Resin Composite Restorations with Thermal Stress. *J Dent Res*, 1990; **69**: 1659-1663.
244. Wypych G. *Handbook of Fillers*. 3rd ed. Toronto: ChemTec Pub; 2010.
245. Sideridou I, Achilias DS, Kyrikou E. Thermal Expansion Characteristics of Light-Cured Dental Resins and Resin Composites. *Biomaterials*, 2004; **25**: 3087-3097.
246. Vaidyanathan J, Vaidyanathan TK, Wang Y, Viswanadhan T. Thermoanalytical Characterization of Visible Light Cure Dental Composites. *J Oral Rehabil*, 1992; **19**: 49-64.
247. Versluis A, Douglas WH, Sakaguchi RL. Thermal Expansion Coefficient of Dental Composites Measured with Strain Gauges. *Dent Mater*, 1996; **12**: 290-294.
248. Yamaguchi R, Powers JM, Dennison JB. Thermal Expansion of Visible-Light-Cured Composite Resins. *Oper Dent*, 1989; **14**: 64-67.
249. Schapery. Thermal Expansion Coefficients of Composite Materials Based on Energy Principles. *J Comp Mater*, 1968; **2**: 115-118.
250. Holliday L, Robinson J. Review: The Thermal Expansion of Composites Based on Polymers. *J Mater Sci*, 1973; **8**: 301-311.
251. Theocaris PS, Papanicolaou GC, Spathis GD. Physical Model for the Thermal Expansion Behaviour of Fibre-Reinforced Viscoelastic Composites. *Fibre Sci Technol*, 1981; **15**: 187-197.
252. Burke FJ, Hussain A, Nolan L, Fleming GJ. Methods Used in Dentine Bonding Tests: An Analysis of 102 Investigations on Bond Strength. *Eur J Prosthodont Restor Dent*, 2008; **16**: 158-165.
253. Armstrong S, Geraldeli S, Maia R, Raposo LH, Soares CJ, Yamagawa J. Adhesion to Tooth Structure: A Critical Review of "Micro" Bond Strength Test Methods. *Dent Mater*, 2010; **26**: e50-62.
254. Van Meerbeek B, Peumans M, Poitevin A, Mine A, Van Ende A, Neves A, De Munck J. Relationship between Bond-Strength Tests and Clinical Outcomes. *Dent Mater*, 2010; **26**: e100-121.
255. Ferracane JL, Dossett JM, Pelogia F, Macedo MRP, Hilton TJ. Navigating the Dentin Bond Strength Testing Highway: Lessons and Recommendations. *J Adhes Sci Technol*, 2009; **23**: 1007-1022.
256. Placido E, Meira JB, Lima RG, Muench A, de Souza RM, Ballester RY. Shear Versus Micro-Shear Bond Strength Test: A Finite Element Stress Analysis. *Dent Mater*, 2007; **23**: 1086-1092.
257. Scherrer SS, Cesar PF, Swain MV. Direct Comparison of the Bond Strength Results of the Different Test Methods: A Critical Literature Review. *Dent Mater*, 2010; **26**: e78-93.
258. Pashley DH, Carvalho RM, Sano H, Nakajima M, Yoshiyama M, Shono Y, Fernandes CA, Tay F. The Microtensile Bond Test: A Review. *J Adhes Dent*, 1999; **1**: 299-309.
259. Nayar S, Ganesh R, Santhosh S. Fiber Reinforced Composites in Prosthodontics: A Systematic Review. *J Pharm Bioallied Sci*, 2015; **7**: S220-S222.

260. Chen Y, Li H, Fok A. In Vitro Validation of a Shape-Optimized Fiber-Reinforced Dental Bridge. *Dent Mater*, 2011; **27**: 1229-1237.
261. Juloski J, Beloica M, Goracci C, Chieffi N, Giovannetti A, Vichi A, Vulicevic ZR, Ferrari M. Shear Bond Strength to Enamel and Flexural Strength of Different Fiber-Reinforced Composites. *J Adhes Dent*, 2013; **15**: 123-130.
262. Ilday N, Seven N. The Influence of Different Fiber-Reinforced Composites on Shear Bond Strengths When Bonded to Enamel and Dentin Structures. *J Dent Sci*, 2011; **6**: 107-115.
263. Meiers JC, Kazemi RB, Donadio M. The Influence of Fiber Reinforcement of Composites on Shear Bond Strengths to Enamel. *J Prosthet Dent*, 2003; **89**: 388-393.
264. Cekic-Nagas I, Ergun G, Tezvergil A, Vallittu PK, Lassila LV. Effect of Fiber-Reinforced Composite at the Interface on Bonding of Resin Core System to Dentin. *Dent Mater J*, 2008; **27**: 736-743.
265. Tezvergil A, Lassila LV, Vallittu PK. Strength of Adhesive-Bonded Fiber-Reinforced Composites to Enamel and Dentin Substrates. *J Adhes Dent*, 2003; **5**: 301-311.
266. Scribante A, Cacciafesta V, Sfondrini MF. Effect of Various Adhesive Systems on the Shear Bond Strength of Fiber-Reinforced Composite. *Am J Orthod Dentofacial Orthop*, 2006; **130**: 224-227.
267. Brauchli L, Pintus S, Steineck M, Lüthy H, Wichelhaus A. Shear Modulus of 5 Flowable Composites to the Everstick Ortho Fiber-Reinforced Composite Retainer: An in-vitro Study. *Am J Orthod Dentofacial Orthop*, 2009; **135**: 54-58.
268. Ergun G, Cekic I, Lassila LV, Vallittu PK. Bonding of Lithium-Disilicate Ceramic to Enamel and Dentin Using Orthotropic Fiber-Reinforced Composite at the Interface. *Acta Odontol Scand*, 2006; **64**: 293-299.
269. Badakar CM, Shashibhushan KK, Naik NS, Reddy VV. Fracture Resistance of Microhybrid Composite, Nano Composite and Fibre-Reinforced Composite Used for Incisal Edge Restoration. *Dent Traumatol*, 2011; **27**: 225-229.
270. Fennis WMM, Kreulen CM, Tezvergil A, Lassila LVJ, Vallittu PK, Creugers NHJ. In Vitro Repair of Fractured Fiber-Reinforced Cusp-Replacing Composite Restorations. *Int J Dent*, 2011; **2011**.
271. Turkaslan S, Tezvergil-Mutluay A, Bagis B, Shinya A, Vallittu PK, Lassila LV. Effect of Intermediate Fiber Layer on the Fracture Load and Failure Mode of Maxillary Incisors Restored with Laminate Veneers. *Dent Mater J*, 2008; **27**: 61-68.
272. Liang Chen, Suh BI. Bonding of Resin Materials to All-Ceramics: A Review. *Curr. Res. Dent*, 2012; **3**: 7-17.
273. Dehghani M, Ahrari F. The Effect of Surface Treatment with Er: Yag Laser on Shear Bond Strength of Orthodontic Brackets to Fiber-Reinforced Composite. *J Clin Exp Dent*, 2014; **6**: e379-383.
274. Asakawa Y, Takahashi H, Kobayashi M, Iwasaki N. Effect of Components and Surface Treatments of Fiber-Reinforced Composite Posts on Bond Strength to Composite Resin. *J Mech Behav Biomed Mater*, 2013; **26**: 23-33.
275. Alshali RZ, Salim NA, Satterthwaite JD, Silikas N. Post-Irradiation Hardness Development, Chemical Softening, and Thermal Stability of Bulk-Fill and Conventional Resin-Composites. *J Dent*, 2015; **43**: 209-218.
276. Alrahlah A, Silikas N, Watts DC. Post-Cure Depth of Cure of Bulk Fill Dental Resin-Composites. *Dent Mater*, 2014; **30**: 149-154.
277. Marghalani HY. Post-Irradiation Vickers Microhardness Development of Novel Resin Composites. *Mat Res*, 2010; **13**: 81-87.

278. Garoushi S, Vallittu PK, Lassila LV. Depth of Cure and Surface Microhardness of Experimental Short Fiber-Reinforced Composite. *Acta Odontol Scand*, 2008; **66**: 38-42.
279. Ferracane JL. Correlation between Hardness and Degree of Conversion During the Setting Reaction of Unfilled Dental Restorative Resins. *Dent Mater*, 1985; **1**: 11-14.
280. Poggio C, Lombardini M, Gaviati S, Chiesa M. Evaluation of Vickers Hardness and Depth of Cure of Six Composite Resins Photo-Activated with Different Polymerization Modes. *J Conserv Den*, 2012; **15**: 237-241.
281. Bucuta S, Ilie N. Light Transmittance and Micro-Mechanical Properties of Bulk Fill vs. Conventional Resin Based Composites. *Clin Oral Investig*, 2014; **18**: 1991-2000.
282. Finan L, Palin WM, Moskwa N, McGinley EL, Fleming GJP. The Influence of Irradiation Potential on the Degree of Conversion and Mechanical Properties of Two Bulk-Fill Flowable Rbc Base Materials. *Dent Mater*, 2013; **29**: 906-912.
283. Cao L, Zhao X, Gong X, Zhao S. An in Vitro Investigation of Wear Resistance and Hardness of Composite Resins. *Int J Clin Exp Med*, 2013; **6**: 423-430.
284. Manhart J, Kunzelmann KH, Chen HY, Hickel R. Mechanical Properties of New Composite Restorative Materials. *J Biomed Mater Res*, 2000; **53**: 353-361.
285. Angker L, Swain MV. Nanoindentation: Application to Dental Hard Tissue Investigations. *Journal of Materials Research*, 2006; **21**: 1893-1905.
286. Ferracane JL, Berge HX, Condon JR. In Vitro Aging of Dental Composites in Water--Effect of Degree of Conversion, Filler Volume, and Filler/Matrix Coupling. *J Biomed Mater Res*, 1998; **42**: 465-472.
287. Hosseinalipour M, Javadpour J, Rezaie H, Dadras T, Hayati AN. Investigation of Mechanical Properties of Experimental Bis-GMA/TEGDMA Dental Composite Resins Containing Various Mass Fractions of Silica Nanoparticles. *J Prosthodont*, 2010; **19**: 112-117.
288. Schwartz JI, Soderholm KJ. Effects of Filler Size, Water, and Alcohol on Hardness and Laboratory Wear of Dental Composites. *Acta Odontol Scand*, 2004; **62**: 102-106.
289. Valente LL, Peralta SL, Ogliari FA, Cavalcante LM, Moraes RR. Comparative Evaluation of Dental Resin Composites Based on Micron- and Submicron-Sized Monomodal Glass Filler Particles. *Dent Mater*, 2013; **29**: 1182-1187.
290. de Moraes RR, Goncalves Lde S, Lancellotti AC, Consani S, Correr-Sobrinho L, Sinhoreti MA. Nanohybrid Resin Composites: Nanofiller Loaded Materials or Traditional Microhybrid Resins? *Oper Dent*, 2009; **34**: 551-557.
291. Nicolae LC, Shelton RM, Cooper PR, Martin RA, Palin WM. The Effect of UDMA/TEGDMA Mixtures and Bioglass Incorporation on the Mechanical and Physical Properties of Resin and Resin-Based Composite Materials. *Conference Papers in Science*, 2014; **2014**: 5.
292. Gajewski VES, Pfeifer CS, Fróes-Salgado NRG, Boaro LCC, Braga RR. Monomers Used in Resin Composites: Degree of Conversion, Mechanical Properties and Water Sorption/Solubility. *Braz Dent J*, 2012; **23**: 508-514.
293. Asmussen E, Peutzfeldt A. Influence of UEDMA BisGMA and TEGDMA on Selected Mechanical Properties of Experimental Resin Composites. *Dent Mater*, 1998; **14**: 51-56.
294. Goncalves F, Kawano Y, Pfeifer C, Stansbury JW, Braga RR. Influence of BisGMA, TEGDMA, and BisEMA Contents on Viscosity, Conversion, and Flexural Strength of Experimental Resins and Composites. *Eur J Oral Sci*, 2009; **117**: 442-446.

295. Pereira SnG, Osorio R, Toledano M, Cabrerizo-VÃ-lchez MA, Nunes TG, Kalachandra S. Novel Light-Cured Resins and Composites with Improved Physicochemical Properties. *Dent Mater*, 2007; **23**: 1189-1198.
296. Cramer NB, Stansbury JW, Bowman CN. Recent Advances and Developments in Composite Dental Restorative Materials. *J Dent Res*, 2011; **90**: 402-416.
297. Schneider LFJ, Pfeifer CSC, Consani S, Prah SA, Ferracane JL. Influence of Photoinitiator Type on the Rate of Polymerization, Degree of Conversion, Hardness and Yellowing of Dental Resin Composites. *Dent Mater*, 2008; **24**: 1169-1177.
298. Brandt WC, Tomaselli Lde O, Correr-Sobrinho L, Sinhoreti MA. Can Phenyl-Propanedione Influence Knoop Hardness, Rate of Polymerization and Bond Strength of Resin Composite Restorations? *J Dent*, 2011; **39**: 438-447.
299. Furuse AY, Mondelli J, Watts DC. Network Structures of Bis-GMA/TEGDMA Resins Differ in Dc, Shrinkage-Strain, Hardness and Optical Properties as a Function of Reducing Agent. *Dent Mater*, 2011; **27**: 497-506.
300. van Groeningen G, Jongebloed W, Arends J. Composite Degradation in Vivo. *Dent Mater*, 1986; **2**: 225-227.
301. Yap AU, Tan SH, Wee SS, Lee CW, Lim EL, Zeng KY. Chemical Degradation of Composite Restoratives. *J Oral Rehabil*, 2001; **28**: 1015-1021.
302. Watts DC, Amer OM, Combe EC. Surface Hardness Development in Light-Cured Composites. *Dent Mater*, 1987; **3**: 265-269.
303. Sobrinho LC, Goes MF, Consani S, Sinhoreti MA, Knowles JC. Correlation between Light Intensity and Exposure Time on the Hardness of Composite Resin. *J Mater Sci Mater Med*, 2000; **11**: 361-364.
304. Yazici AR, Kugel G, Gul G. The Knoop Hardness of a Composite Resin Polymerized with Different Curing Lights and Different Modes. *J Contemp Dent Pract*, 2007; **8**: 52-59.
305. Price RB, Rizkalla AS, Hall GC. Effect of Stepped Light Exposure on the Volumetric Polymerization Shrinkage and Bulk Modulus of Dental Composites and an Unfilled Resin. *Am J Dent*, 2000; **13**: 176-180.
306. Elgergeni K. A Laboratory Investigation of the Failure and Reinforcement of Fibre-Reinforced Resin Composite Bridgework: University of Manchester; 2007.
307. Mosby. *Mosby's Dental Dictionary*. 2nd Edition ed: Elsevier; 2007.
308. Iwaku M, Nagata N, Hosoda H, Fusayama T. Edge Strength of Powdered Gold Fillings. *J Dent Res*, 1966; **45**: 1468-1472.
309. Flanders LA, Quinn JB, Wilson Jr OC, Lloyd IK. Scratch Hardness and Chipping of Dental Ceramics under Different Environments. *Dent Mater*, 2003; **19**: 716-724.
310. Mahler DB, Terkla LG, Van Eysden J, Reisbick MH. Marginal Fracture Vs Mechanical Properties of Amalgam. *J Dent Res*, 1970; **49**: 1452-1457.
311. Bryant RW, Mahler DB, Engle JH. A Comparison of Methods for Evaluating the Marginal Fracture of Amalgam Restorations. *Dent Mater*, 1985; **1**: 235-237.
312. Hoard RJ, Eichmiller FC, Parry EE, Giuseppetti AA. Edge-Bevel Fracture Resistance of Three Direct-Filling Materials. *Oper Dent*, 2000; **25**: 182-185.
313. Ereifej N, Silikas N, Watts DC. Edge Strength of Indirect Restorative Materials. *J Dent*, 2009; **37**: 799-806.
314. Watts DC, Issa M, Ibrahim A, Wakiaga J, Al-Samadani K, Al-Azraqi M, Silikas N. Edge Strength of Resin-Composite Margins. *Dent Mater*, 2008; **24**: 129-133.

315. Ferracane JL, Condon JR. In Vitro Evaluation of the Marginal Degradation of Dental Composites under Simulated Occlusal Loading. *Dent Mater*, 1999; **15**: 262-267.
316. Tsitrou EA, Northeast SE, van Noort R. Brittleness Index of Machinable Dental Materials and Its Relation to the Marginal Chipping Factor. *J Dent*, 2007; **35**: 897-902.
317. Kim SH, Watts DC. In Vitro Study of Edge-Strength of Provisional Polymer-Based Crown and Fixed Partial Denture Materials. *Dent Mater*, 2007; **23**: 1570-1573.
318. Baroudi K, Silikas N, Watts DC. Edge-Strength of Flowable Resin-Composites. *J Dent*, 2008; **36**: 63-68.
319. Quinn J, Mohan R. Geometry of Edge Chips Formed at Different Angles. In: *Mechanical Properties and Performance of Engineering Ceramics and Composites: Ceramic Engineering and Science Proceedings*: John Wiley & Sons, Inc.; 2008. pp. 85-92.
320. Quinn JB, Sundar V, Parry EE, Quinn GD. Comparison of Edge Chipping Resistance of Pfm and Veneered Zirconia Specimens. *Dent Mater*, 2010; **26**: 13-20.
321. Kargul B, Caglar E, Kabalay U. Glass Fiber Reinforced Composite Resin Space Maintainer: Case Reports. *J Dent Child*, 2003; **70**: 258-261.
322. Bohlsen F, Kern M. Clinical Outcome of Glass-Fiber-Reinforced Crowns and Fixed Partial Dentures: A Three-Year Retrospective Study. *Quintessence Int*, 2003; **34**: 493-496.
323. Drummond JL. Degradation, Fatigue, and Failure of Resin Dental Composite Materials. *J Dent Res*, 2008; **87**: 710-719.
324. Brandao L, Adabo GL, Vaz LG, Saad JR. Compressive Strength and Compressive Fatigue Limit of Conventional and High Viscosity Posterior Resin Composites. *Braz Oral Res*, 2005; **19**: 272-277.
325. Draughn RA. Compressive Fatigue Limits of Composite Restorative Materials. *J Dent Res*, 1979; **58**: 1093-1096.
326. Lohbauer U, Horst Tvd, Frankenberger R, KrÄmer N, Petschelt A. Flexural Fatigue Behavior of Resin Composite Dental Restoratives. *Dent Mater*, 2003; **19**: 435-440.
327. Baran G, Boberick K, McCool J. Fatigue of Restorative Materials. *Crit Rev Oral Biol Med*, 2001; **12**: 350-360.
328. McCabe JF, Abu Kasim NH, Cleary S. A Rolling-Ball Device for Producing Surface Fatigue and Its Application to Dental Materials. *J Mater Sci*, 1997; **32**: 283-287.
329. McCabe JF, Wang Y, Braem M. Surface Contact Fatigue and Flexural Fatigue of Dental Restorative Materials. *J Biomed Mater Res*, 2000; **50**: 375-380.
330. Fujii K, Carrick TE, Bicker R, McCabe JF. Effect of the Applied Load on Surface Contact Fatigue of Dental Filling Materials. *Dent Mater*, 2004; **20**: 931-938.
331. Kheradmandan S, Koutayas SO, Bernhard M, Strub JR. Fracture Strength of Four Different Types of Anterior 3-Unit Bridges after Thermo-Mechanical Fatigue in the Dual-Axis Chewing Simulator. *J Oral Rehabil*, 2001; **28**: 361-369.
332. Nie E-M, Chen X-Y, Zhang C-Y, Qi L-L, Huang Y-H. Influence of Masticatory Fatigue on the Fracture Resistance of the Pulpless Teeth Restored with Quartz-Fiber Post-Core and Crown. *In J Oral Sci*, 2012; **4**: 218-220.
333. Stawarczyk B, Ender A, Trottmann A, Ozcan M, Fischer J, Hammerle CH. Load-Bearing Capacity of CAD/CAM Milled Polymeric Three-Unit Fixed Dental Prostheses: Effect of Aging Regimens. *Clin Oral Investig*, 2012; **16**: 1669-1677.
334. Beuer F, Steff B, Naumann M, Sorensen JA. Load-Bearing Capacity of All-Ceramic Three-Unit Fixed Partial Dentures with Different Computer-Aided Design

- (CAD)/Computer-Aided Manufacturing (CAM) Fabricated Framework Materials. *Eur J Oral Sci*, 2008; **116**: 381-386.
335. Heintze SD, Cavalleri A, Zellweger G, Buchler A, Zappini G. Fracture Frequency of All-Ceramic Crowns During Dynamic Loading in a Chewing Simulator Using Different Loading and Luting Protocols. *Dent Mater*, 2008; **24**: 1352-1361.
 336. Heintze SD, Albrecht T, Cavalleri A, Steiner M. A New Method to Test the Fracture Probability of All-Ceramic Crowns with a Dual-Axis Chewing Simulator. *Dent Mater*, 2011; **27**: e10-19.
 337. Stappert CF, Ozden U, Gerds T, Strub JR. Longevity and Failure Load of Ceramic Veneers with Different Preparation Designs after Exposure to Masticatory Simulation. *J Prosthet Dent*, 2005; **94**: 132-139.
 338. Cleuren KM, Vandamme K, Naert I. Fracture Strength of Resin-Bonded Dental Prostheses with a Rigid Versus Nonrigid Joint. An in Vitro Study. *Int J Prosthodont*, 2009; **22**: 140-142.
 339. Lohbauer U, Belli R, Ferracane JL. Factors Involved in Mechanical Fatigue Degradation of Dental Resin Composites. *J Dent Res*, 2013; **92**: 584-591.
 340. Shah MB, Ferracane JL, Kruzic JJ. Mechanistic Aspects of Fatigue Crack Growth Behavior in Resin Based Dental Restorative Composites. *Dent Mater*, 2009; **25**: 909-916.
 341. Drummond JL. Cyclic Fatigue of Composite Restorative Materials. *J Oral Rehabil*, 1989; **16**: 509-520.
 342. Lohbauer U, Frankenberger R, Kramer N, Petschelt A. Strength and Fatigue Performance Versus Filler Fraction of Different Types of Direct Dental Restoratives. *J Biomed Mater Res B Appl Biomater*, 2006; **76**: 114-120.
 343. Abe Y, Braem MJ, Lambrechts P, Inoue S, Takeuchi M, Van Meerbeek B. Fatigue Behavior of Packable Composites. *Biomaterials*, 2005; **26**: 3405-3409.
 344. Curtis AR, Palin WM, Fleming GJ, Shortall AC, Marquis PM. The Mechanical Properties of Nanofilled Resin-Based Composites: The Impact of Dry and Wet Cyclic Pre-Loading on Bi-Axial Flexure Strength. *Dent Mater*, 2009; **25**: 188-197.
 345. Papadogiannis Y, Lakes RS, Palaghias G, Helvatjoglu-Antoniades M, Papadogiannis D. Fatigue of Packable Dental Composites. *Dent Mater*, 2007; **23**: 235-242.
 346. El-Safty S, Silikas N, Akhtar R, Watts DC. Nanoindentation Creep Versus Bulk Compressive Creep of Dental Resin-Composites. *Dent Mater*, 2012; **28**: 1171-1182.
 347. Ayatollahi MR, Yahya MY, Karimzadeh A, Nikkhooyifar M, Ayob A. Effects of Temperature Change and Beverage on Mechanical and Tribological Properties of Dental Restorative Composites. *Materials Science and Engineering: C*, 2015; **54**: 69-75.
 348. Lohbauer U, Frankenberger R, Kramer N, Petschelt A. Time-Dependent Strength and Fatigue Resistance of Dental Direct Restorative Materials. *J Mater Sci Mater Med*, 2003; **14**: 1047-1053.
 349. Han L, Okamoto A, Fukushima M, Okiji T. Evaluation of Flowable Resin Composite Surfaces Eroded by Acidic and Alcoholic Drinks. *Dent Mater J*, 2008; **27**: 455-465.
 350. Lin L, Drummond JL. Cyclic Loading of Notched Dental Composite Specimens. *Dent Mater*, 2009; **26**: 207.
 351. Janda R, Roulet JF, Latta M, Rüttermann S. The Effects of Thermocycling on the Flexural Strength and Flexural Modulus of Modern Resin-Based Filling Materials. *Dent Mater*, 2006; **22**: 1103-1108.

352. Morresi AL, D'Amario M, Capogreco M, Gatto R, Marzo G, D'Arcangelo C, Monaco A. Thermal Cycling for Restorative Materials: Does a Standardized Protocol Exist in Laboratory Testing? A Literature Review. *J Mech Behav Biomed Mater*, 2014; **29**: 295-308.
353. Ernst CP, Canbek K, Euler T, Willershausen B. In Vivo Validation of the Historical in Vitro Thermocycling Temperature Range for Dental Materials Testing. *Clin Oral Investig*, 2004; **8**: 130-138.
354. Cenci MS, Pereira-Cenci T, Donassollo TA, Sommer L, Strapasson A, Demarco FF. Influence of Thermal Stress on Marginal Integrity of Restorative Materials. *J Appl Oral Sci*, 2008; **16**: 106-110.
355. De Munck J, Van Landuyt K, Coutinho E, Poitevin A, Peumans M, Lambrechts P, Van Meerbeek B. Micro-Tensile Bond Strength of Adhesives Bonded to Class-I Cavity-Bottom Dentin after Thermo-Cycling. *Dent Mater*, 2005; **21**: 999-1007.
356. Gale MS, Darvell BW. Thermal Cycling Procedures for Laboratory Testing of Dental Restorations. *J Dent*, 1999; **27**: 89-99.
357. Shah MB, Ferracane JL, Kruzic JJ. R-Curve Behavior and Toughening Mechanisms of Resin-Based Dental Composites: Effects of Hydration and Post-Cure Heat Treatment. *Dent Mater*, 2009; **25**: 760-770.
358. Yamamoto M, Takahashi H. Tensile Fatigue Strength of Light Cure Composite Resins for Posterior Teeth. *Dent Mater J*, 1995; **14**: 175-184.
359. Horst JJ, Spoormaker JL. Fatigue Fracture Mechanisms and Fractography of Short-Glassfibre-Reinforced Polyamide 6. *J Mater Sci*, 1997; **32**: 3641-3651.
360. Garoushi SK, Lassila LV, Vallittu PK. Fatigue Strength of Fragmented Incisal Edges Restored with a Fiber Reinforced Restorative Material. *J Contemp Dent Pract*, 2007; **8**: 9-16.
361. Bolotin VV. *Mechanics of Fatigue*. Boca Raton ; London: CRC Press; 1999.
362. Dyer KP, Isaac DH. Fatigue Behaviour of Continuous Glass Fibre Reinforced Composites. *Composites Part B: Engineering*, 1998; **29**: 725-733.
363. Ellakwa AE, Shortall AC, Shehata MK, Marquis PM. The Influence of Fibre Placement and Position on the Efficiency of Reinforcement of Fibre Reinforced Composite Bridgework. *J Oral Rehabil*, 2001; **28**: 785-791.
364. Rocca G, Saratti C, Poncet A, Feilzer A, Krejci I. The Influence of Frcs Reinforcement on Marginal Adaptation of CAD/CAM Composite Resin Endocrowns after Simulated Fatigue Loading. *Odontology*, 2015: 1-13.
365. Garoushi S, Kaleem M, Shinya A, Vallittu PK, Satterthwaite JD, Watts DC, Lassila LVJ. Creep of Experimental Short Fiber-Reinforced Composite Resin. *Dent Mater J*, 2012; **31**: 737-741.
366. van Heumen CCM, Tanner J, van Dijken JWV, Pikaar R, Lassila LVJ, Creugers NHJ, Vallittu PK, Kreulen CM. Five-Year Survival of 3-Unit Fiber-Reinforced Composite Fixed Partial Dentures in the Posterior Area. *Dent Mater*, 2010; **26**: 954-960.
367. Göhring TN, Roos M. Inlay-Fixed Partial Dentures Adhesively Retained and Reinforced by Glass Fibers: Clinical and Scanning Electron Microscopy Analysis after Five Years. *Eur J Oral Sci*, 2005; **113**: 60-69.
368. Belli R, Geinzer E, Muschweck A, Petschelt A, Lohbauer U. Mechanical Fatigue Degradation of Ceramics Versus Resin Composites for Dental Restorations. *Dent Mater*, 2014; **30**: 424-432.

369. Erkmen E, Meriç G, Kurt A, Tunç Y, Eser A. Biomechanical Comparison of Implant Retained Fixed Partial Dentures with Fiber Reinforced Composite Versus Conventional Metal Frameworks: A 3D FEA Study. *J Mech Behav Biomed Mater*, 2011; **4**: 107-116.
370. Mair LH, Stolarski TA, Vowles RW, Lloyd CH. Wear: Mechanisms, Manifestations and Measurement. Report of a Workshop. *J Dent*, 1996; **24**: 141-148.
371. Mehta SB, Banerji S, Millar BJ, Suarez-Feito JM. Current Concepts on the Management of Tooth Wear: Part 4. An Overview of the Restorative Techniques and Dental Materials Commonly Applied for the Management of Tooth Wear. *Br Dent J*, 2012; **212**: 169-177.
372. Hahnel S, Schultz S, Trempler C, Ach B, Handel G, Rosentritt M. Two-Body Wear of Dental Restorative Materials. *J Mech Behav Biomed Mater*, 2011; **4**: 237-244.
373. Wang L, Liu Y, Si W, Feng H, Tao Y, Ma Z. Friction and Wear Behaviors of Dental Ceramics against Natural Tooth Enamel. *J Eur Ceram Soc*, 2012; **32**: 2599-2606.
374. Heintze SD. How to Qualify and Validate Wear Simulation Devices and Methods. *Dent Mater*, 2006; **22**: 712-734.
375. Mehl C, Scheibner S, Ludwig K, Kern M. Wear of Composite Resin Veneering Materials and Enamel in a Chewing Simulator. *Dent Mater*, 2007; **23**: 1382-1389.
376. Turssi CP, de Moraes Purquerio B, Serra MC. Wear of Dental Resin Composites: Insights into Underlying Processes and Assessment Methods—a Review. *J Biomed Mater Res*, 2003; **65B**: 280-285.
377. McCabe JF, Molyvda S, Rolland SL, Rusby S, Carrick TE. Two-and Three-Body Wear of Dental Restorative Materials. *Int Dent J*, 2002; **52**: 406-416.
378. Amer R, Kürklü D, Kateeb E, Seghi RR. Three-Body Wear Potential of Dental Yttrium-Stabilized Zirconia Ceramic after Grinding, Polishing, and Glazing Treatments. *J Prosthet Dent*, 2014; **112**: 1151-1155.
379. Heintze SD, Zellweger G, Cavalleri A, Ferracane J. Influence of the Antagonist Material on the Wear of Different Composites Using Two Different Wear Simulation Methods. *Dent Mater*, 2006; **22**: 166-175.
380. Turssi CP, Ferracane JL, Ferracane LL. Wear and Fatigue Behavior of Nano-Structured Dental Resin Composites. *J Biomed Mater Res*, 2006; **78B**: 196-203.
381. Sarkar NK. Internal Corrosion in Dental Composite Wear. *J Biomed Mater Res*, 2000; **53**: 371-380.
382. Condon JR, Ferracane JL. Evaluation of Composite Wear with a New Multi-Mode Oral Wear Simulator. *Dent Mater*, 1996; **12**: 218-226.
383. DeLong R, Douglas WH. Development of an Artificial Oral Environment for the Testing of Dental Restoratives: Bi-Axial Force and Movement Control. *J Dent Res*, 1983; **62**: 32-36.
384. Hu X, Harrington E, Marquis PM, Shortall AC. The Influence of Cyclic Loading on the Wear of a Dental Composite. *Biomaterials*, 1999; **20**: 907-912.
385. Lambrechts P, Debels E, Van Landuyt K, Peumans M, Van Meerbeek B. How to Simulate Wear?: Overview of Existing Methods. *Dent Mater*, 2006; **22**: 693-701.
386. Wang L, Garcia FC, Amarante de Araujo P, Franco EB, Mondelli RF. Wear Resistance of Packable Resin Composites after Simulated Toothbrushing Test. *J Esthet Restor Dent*, 2004; **16**: 303-314; discussion 314-305.
387. Teixeira EC, Thompson JL, Piascik JR, Thompson JY. In Vitro Toothbrush-Dentifrice Abrasion of Two Restorative Composites. *J Esthet Restor Dent*, 2005; **17**: 172-180; discussion 181-172.

388. Nagarajan VS, Jahanmir S, Thompson VP. In Vitro Contact Wear of Dental Composites. *Dent Mater*, 2004; **20**: 63-71.
389. Souza JAd, Dolavale LC, Camargo SAdS. Wear Mechanisms of Dental Composite Restorative Materials by Two Different in-vitro Methods. *Mat Res*, 2012; **16**: 333-340.
390. Ramalho A, Antunes PV. Reciprocating Wear Test of Dental Composites against Human Teeth and Glass. *Wear*, 2007; **263**: 1095-1104.
391. Hu X, Marquis PM, Shortall AC. Two-Body in Vitro Wear Study of Some Current Dental Composites and Amalgams. *J Prosthet Dent*, 1999; **82**: 214-220.
392. Willems G, Celis JP, Lambrechts P, Braem M, Roos JR, Vanherle G. In Vitro Vibrational Wear under Small Displacements of Dental Materials Opposed to Annealed Chromium-Steel Counterbodies. *Dent Mater*, 1992; **8**: 338-344.
393. Heintze SD, Barkmeier WW, Latta MA, Rousson V. Round Robin Test: Wear of Nine Dental Restorative Materials in Six Different Wear Simulators - Supplement to the Round Robin Test of 2005. *Dent Mater*, 2011; **27**: e1-9.
394. Reich SM, Petschelt A, Wichmann M, Frankenberger R. Mechanical Properties and Three-Body Wear of Veneering Composites and Their Matrices. *J Biomed Mater Res*, 2004; **69**: 65-69.
395. Clelland NL, Pagnotto MP, Kerby RE, Seghi RR. Relative Wear of Flowable and Highly Filled Composite. *J Prosthet Dent*, 2005; **93**: 153-157.
396. Göhring TN, Besek MJ, Schmidlin PR. Attritional Wear and Abrasive Surface Alterations of Composite Resin Materials in Vitro. *J Dent*, 2002; **30**: 119-127.
397. Kunzelmann KH, Jelen B, Mehl A, Hickel R. Wear Evaluation of MZ100 Compared to Ceramic CAD/CAM Materials. *Int J Comput Dent*, 2001; **4**: 171-184.
398. Kaidonis JA, Richards LC, Townsend GC, Tansley GD. Wear of Human Enamel: A Quantitative in Vitro Assessment. *J Dent Res*, 1998; **77**: 1983-1990.
399. Lawson NC, Cakir D, Beck P, Litaker MS, Burgess JO. Characterization of Third-Body Media Particles and Their Effect on in Vitro Composite Wear. *Dent Mater*, 2012; **28**: e118-e126.
400. Raabe D, Alemzadeh K, Harrison AL, Ireland AJ. The Chewing Robot: A New Biologically-Inspired Way to Evaluate Dental Restorative Materials. *Conf Proc IEEE Eng Med Biol Soc*, 2009: 6050-6053.
401. Yesil ZD, Alapati S, Johnston W, Seghi RR. Evaluation of the Wear Resistance of New Nanocomposite Resin Restorative Materials. *J Prosthet Dent*, 2008; **99**: 435-443.
402. Suzuki S, Nagai E, Taira Y, Minesaki Y. In Vitro Wear of Indirect Composite Restoratives. *J Prosthet Dent*, 2002; **88**: 431-436.
403. Clelland NL, Agarwala V, Knobloch LA, Seghi RR. Wear of Enamel Opposing Low-Fusing and Conventional Ceramic Restorative Materials. *J Prosthodont*, 2001; **10**: 8-15.
404. Bedini R, Pecci R, Notarangelo G, Zuppante F, Persico S, Di Carlo F. Microtomography Evaluation of Dental Tissue Wear Surface Induced by in Vitro Simulated Chewing Cycles on Human and Composite Teeth. *Ann Ist Super Sanita*, 2012; **48**: 65-70.
405. Heintze SD, Cavalleri A, Forjanic M, Zellweger G, Rousson V. Wear of Ceramic and Antagonist--a Systematic Evaluation of Influencing Factors in Vitro. *Dent Mater*, 2008; **24**: 433-449.
406. DeLong R. Intra-Oral Restorative Materials Wear: Rethinking the Current Approaches: How to Measure Wear. *Dent Mater*, 2006; **22**: 702-711.

407. López-Frías FJ, Castellanos-Cosano L, Martín-González J, Llamas-Carreras JM, Segura-Egea JJ. Clinical Measurement of Tooth Wear: Tooth Wear Indices. *J Clin Exp Dent*, 2012; **4**: e48-e53.
408. Al-Omiri MK, Sghaireen MG, Alzarea BK, Lynch E. Quantification of Incisal Tooth Wear in Upper Anterior Teeth: Conventional Vs New Method Using Toolmakers Microscope and a Three-Dimensional Measuring Technique. *J Dent*, 2013; **41**: 1214-1221.
409. Al-Omiri MK, Harb R, Abu Hammad OA, Lamey PJ, Lynch E, Clifford TJ. Quantification of Tooth Wear: Conventional Vs New Method Using Toolmakers Microscope and a Three-Dimensional Measuring Technique. *J Dent*, 2010; **38**: 560-568.
410. Rodriguez JM, Austin RS, Bartlett DW. A Method to Evaluate Profilometric Tooth Wear Measurements. *Dent Mater*, 2012; **28**: 245-251.
411. Schlueter N, Ganss C, De Sanctis S, Klimek J. Evaluation of a Profilometrical Method for Monitoring Erosive Tooth Wear. *Eur J Oral Sci*, 2005; **113**: 505-511.
412. Azzopardi A, Bartlett DW, Watson TF, Sherriff M. The Measurement and Prevention of Erosion and Abrasion. *J Dent*, 2001; **29**: 395-400.
413. Yip KH, Smales RJ, Kaidonis JA. Differential Wear of Teeth and Restorative Materials: Clinical Implications. *Int J Prosthodont*, 2004; **17**: 350-356.
414. Lambrechts P, Braem M, Vuylsteke-Wauters M, Vanherle G. Quantitative in Vivo Wear of Human Enamel. *J Dent Res*, 1989; **68**: 1752-1754.
415. Heintze SD. Predictability of Clinical Wear by Laboratory Wear Methods for the Evaluation of Dental Restorative Materials [Doctor of Philosophy]. Groningen; 2010:223.
416. Gatti AM, Rivasi F. Biocompatibility of Micro- and Nanoparticles. Part I: In Liver and Kidney. *Biomaterials*, 2002; **23**: 2381-2387.
417. Bayne SC, Taylor DF, Heymann HO. Protection Hypothesis for Composite Wear. *Dent Mater*, 1992; **8**: 305-309.
418. Yap AU, Tan CH, Chung SM. Wear Behavior of New Composite Restoratives. *Oper Dent*, 2004; **29**: 269-274.
419. Barucci-Pfister N, Gohring TN. Subjective and Objective Perceptions of Specular Gloss and Surface Roughness of Esthetic Resin Composites before and after Artificial Aging. *Am J Dent*, 2009; **22**: 102-110.
420. Xu HH, Quinn JB, Giuseppetti AA, Eichmiller FC, Parry EE, Schumacher GE. Three-Body Wear of Dental Resin Composites Reinforced with Silica-Fused Whiskers. *Dent Mater*, 2004; **20**: 220-227.
421. Luhrs AK, Geurtsen W. The Application of Silicon and Silicates in Dentistry: A Review. *Prog Mol Subcell Biol*, 2009; **47**: 359-380.
422. Musanje L, Ferracane JL, Ferracane LL. Effects of Resin Formulation and Nanofiller Surface Treatment on in Vitro Wear of Experimental Hybrid Resin Composite. *J Biomed Mater Res B Appl Biomater*, 2006; **77**: 120-125.
423. Sarac D, Sarac YS, Kulunk S, Ural C, Kulunk T. The Effect of Polishing Techniques on the Surface Roughness and Color Change of Composite Resins. *J Prosthet Dent*, 2006; **96**: 33-40.
424. Ekfeldt A, Oilo G. Wear of Prosthodontic Materials--an in Vivo Study. *J Oral Rehabil*, 1990; **17**: 117-129.

425. Callaghan DJ, Vaziri A, Nayeb-Hashemi H. Effect of Fiber Volume Fraction and Length on the Wear Characteristics of Glass Fiber-Reinforced Dental Composites. *Dent Mater*, 2006; **22**: 84-93.
426. Suresha B, Chandramohan G, Dayananda Jawali N, Siddaramaiah. Effect of Short Glass Fiber Content on Three-Body Abrasive Wear Behaviour of Polyurethane Composites. *J Compos Mater*, 2007; **41**: 2701-2713.

Chapter 2: Aims and Objectives

2.1 AIMS OF THE STUDY:

The main aim of the following series of studies was to improve the understanding of fibre-reinforced composite restorations and their clinical performance by investigating selected physico-mechanical properties.

The specific objectives of this research were:

- To investigate the influence of fibre reinforcement and orientation on surface hardness and light-transmittance.
- To investigate the effect of incorporating differently-oriented FRCs on the edge-strength.
- To examine the effect of fibre-reinforcement on shear bond strength between resin-composite material and ceramic/metal substrates.
- To determine the consequence of dynamic fatigue and framework design on the ultimate load-bearing capacity of direct inlay FRC FPDs.
- To compare the wear behaviour and fracture resistance of FRC crowns and other metal free alternatives.

A systematic approach of testing has been followed to address the knowledge gap identified in this research. Six in-vitro experiments were performed as shown in Figure 2.1:

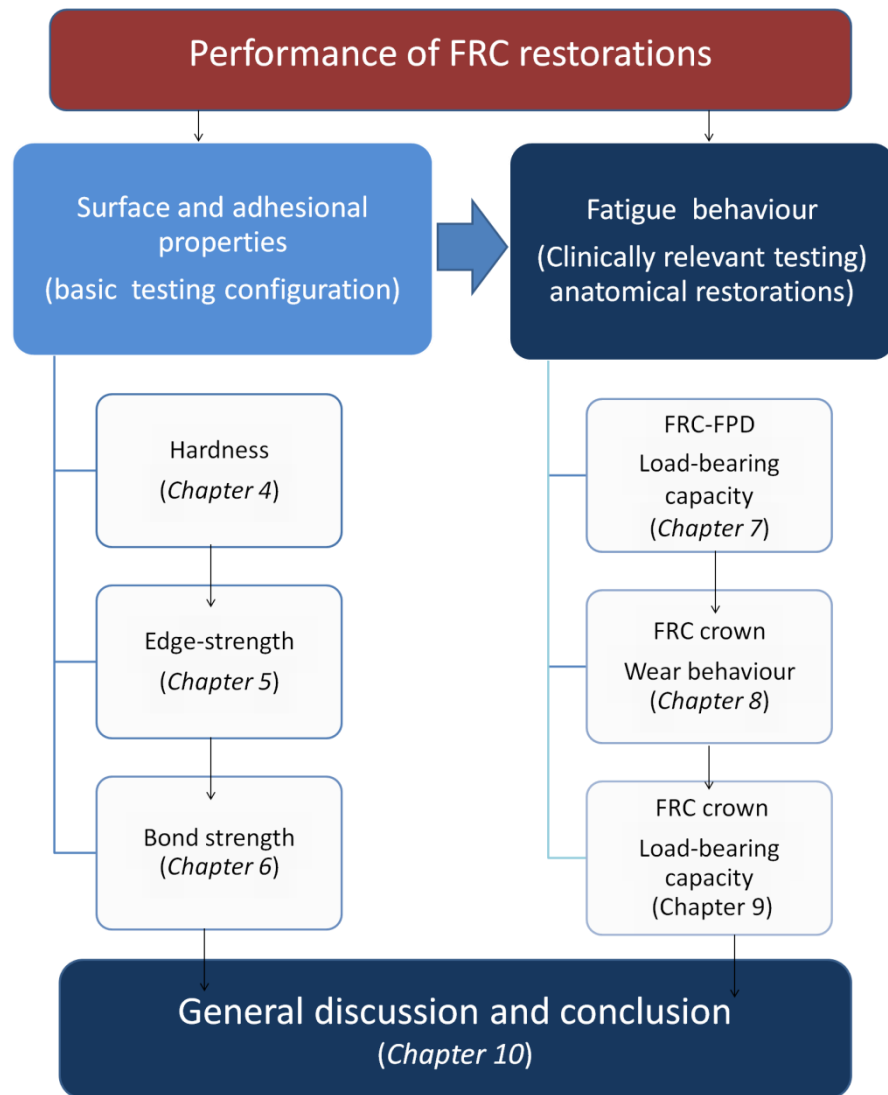


Figure 2.1: General outline for the research.

Chapter 3: General Methodology

3.1 INTRODUCTION

A variety of standard and novel methodologies were utilized to address the objectives of the current research. All the methodologies are fully described in their relevant chapters.

The standard techniques applied were:

1. Vickers hardness method to measure the surface microhardness using a microhardness tester (FM-700). (Chapter 4)
2. Edge-strength testing using a compression testing machine (CK10). (Chapter 5)
3. Shear bond strength (SBS) testing using a universal testing machine (Zwick Z020). (Chapter 6)
4. Static load-to-fracture testing to measure the load-bearing capacity of FRC restorations using a universal testing machine. (Chapter 7 and Chapter 9)

The new techniques applied were:

1. The use of a laboratory grade spectrometer (MARC Resin Calibrator) to measure the influence of fibre reinforcement on light transmittance. (Chapter 3)
2. The use of a chewing simulator machine (CS 4.2) to simulate the masticatory loading on FRC restorations and induce the corresponding wear and dynamic fatigue. (Chapter 7-9)
3. The use of an intraoral 3D scanner (3M True Definition Scanner) to quantify and compare the wear induced in FRC crowns and other CAD/CAM alternatives. (Chapter 8)

3.2 MATERIALS:

Different material categories were used to execute this research. Each category contains various types of materials that differ in their composition or structures. Table 3.1 shows all the materials used in this research classified according to their main category.

Table 3.1: List of materials used to perform this research

Category	Material	Description	Manufacturer
Fibre-reinforced composites	Everstick [®] C&B	Pre-impregnated unidirectional E-glass fibres	<i>Stick Tech Ltd, Turku, Finland</i>
	EverStick [®] Net	Pre-impregnated bidirectional E-glass fibres	<i>Stick Tech Ltd, Turku, Finland</i>
	Stick [®]	Non-impregnated unidirectional E-glass fibres	<i>Stick Tech Ltd, Turku, Finland</i>
	Stick [®] Net	Non-impregnated bidirectional E-glass fibres	<i>Stick Tech Ltd, Turku, Finland</i>
	Construct [™]	Non-impregnated woven UHMWP fibres	<i>Kerr, CA, USA</i>
Particle-reinforced composites	X-tra [®] fil	Posterior packable microhybrid composite (Bulk-fill)	<i>Voco, Cuxhaven, Germany</i>
	Grandio [®]	Universal packable nanohybrid composite (Increment-fill)	<i>Voco, Cuxhaven, Germany</i>
	Herculite Ultra [®]	Universal packable nanohybrid composite for Enamel (Increment-fill)	<i>Kerr, CA, USA</i>
	X-tra base	Universal flowable nanohybrid composite (Bulk-fill)	<i>Voco, Cuxhaven, Germany</i>
	Grandioso Flow	Universal flowable nanohybrid composite (Increment -fill)	<i>Voco, Cuxhaven, Germany</i>
Machined crown materials	Lava [®] Zirconia	Pre-sintered Zirconia-based ceramic	<i>3M-ESPE, Seefeld, Germany</i>
	Lava [®] Ultimate	Resin nano-ceramic	<i>3M-ESPE, Seefeld, Germany</i>
	IPS e.max press	Silicate-based ceramic.	<i>Ivoclar Vivadent, Schaan, Liechtenstein</i>
	Incise LaserPFM	Laser-sintered Co-Cr metal alloys	<i>Renishaw plc, Gloucestershire, UK</i>
Coupling and bonding agents	ESPE [®] Sil	Silane coupling agent	<i>3M-ESPE, Seefeld, Germany</i>
	Stick [®] Resin	Unfilled light-cured resin	<i>Stick Tech Ltd, Turku, Finland</i>
	Visio-Bond [®]	One bottle bonding agent	<i>3M-ESPE, Seefeld, Germany</i>
Surface Treatments	Cojet [®] Sand	Silicatized airborne sand	<i>3M-ESPE, Seefeld, Germany</i>
	Porcelain Etchant	9.5% buffered Hydrofluoric acid gel	<i>BISCO Inc, Illinois, USA</i>

3.3 MEASUREMENT OF HARDNESS AND IRRADIANCE (CHAPTER 4):

The specific study protocol followed to investigate the influence of FRC and their orientation on the surface hardness and light transmittance is outlined in Figure 3.1.

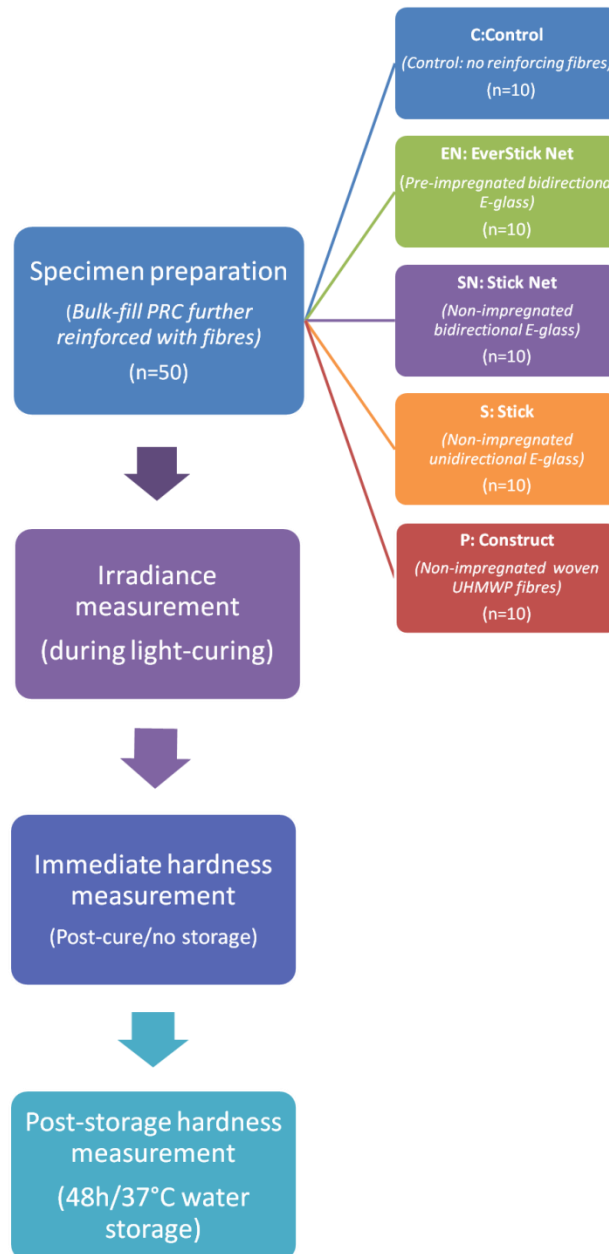


Figure 3.1: Flowchart showing the study protocol in Chapter 4

3.3.1 Vickers hardness measurement:

3.3.1.1 Rationale:

The microhardness, as a property, was investigated in this study to give an indication about the effect of incorporating FRC on surface hardness, degree of conversion (DC)

and depth of cure (DoC). Among all hardness tests, the Vickers hardness test was selected due to many reasons, including popularity, simplicity, versatility and high accuracy as the geometry of its indentation remains identical regardless of the loading applied or material tested. Moreover, it is able to discriminate between the different constituents of composite materials and induce the deformation in tiny specified spot. Immediate and post-cure VHN were compared to investigate the effect of FRC on post-cure polymerization

3.3.1.2 Pilot Study:

A pilot study was executed to confirm sample size and determine specimen geometry. Prior data indicated to study 5 specimens in each group to be able to reject the null hypothesis with associated 0.8 power ($1-\beta$) and 0.05 type-I error (α). Disc-shaped specimens (8 x 3 mm) were initially considered; however, they did not yield consistent results. This was due to the difficulties of incorporating standardized volume fractions of the reinforcing fibres within the specimens, especially around the edges. Consequently, rectangular-shaped specimens (5 x 5 x 3 mm) were prepared instead to ensure adequate fibre reinforcement incorporated within the entire specimen.

3.3.1.3 Materials and Methodology:

Four FRCs and one bulk-fill PRC were selected to prepare the required specimens. The chosen FRC materials (EN, SN, P and S) were commercially available for aesthetic restorations, and different in terms of type (E-glass Vs UHMWP), orientation (unidirectional, bidirectional or woven) and impregnation (non-impregnated Vs pre-impregnated). The selected PRC (XF) was a bulk-fill composite in order to facilitate specimen placement and curing in one cycle (20s) through the whole thickness (3mm). The 3-mm thickness was used instead of up to 4mm thickness advertised by the manufacturer in order to ensure full light penetration even with the presence of FRC.

Fifty rectangular-shaped specimens made of FRC-PRC were allocated into five equal groups (n=10) according to the type of FRC used. Half of the specimens (n=5) in each group were immediately used to determine the initial top and bottom Vickers hardness number (VHN), while the remaining specimens were stored in distilled water (48h/37°C) before being tested. A microhardness tester (*FM-700, Future Tech Corp., Japan*) was employed to measure top and bottom VHN for each specimen (Figure 3.2). Three readings were taken per surface; the first at the centre point (x2.5, y2.5) and the

other two readings at (x1.5, y1.5) and (x3.5, y3.5) points (Figure 3.3). Initially, the automated hardness machine was calibrated according to specific testing parameters (300gF, 10s dwell). The built-in microscopy was used to select the point of interest at the surface. The Vickers diamond indenter was applied at that point with 10s dwells in order to induce an indentation. For each indentation, both diagonals were measured using the microscope. The machine automatically calculated the corresponding hardness value and presented it as VHN.

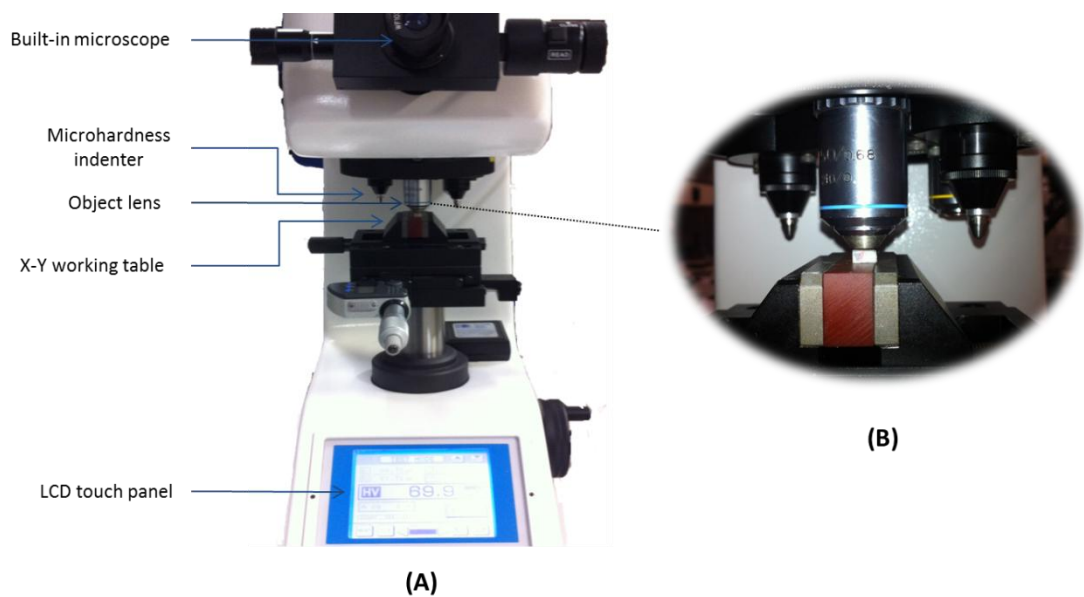


Figure 3.2: FM-700 microhardness tester (A), with a representative specimen ready for testing (B).

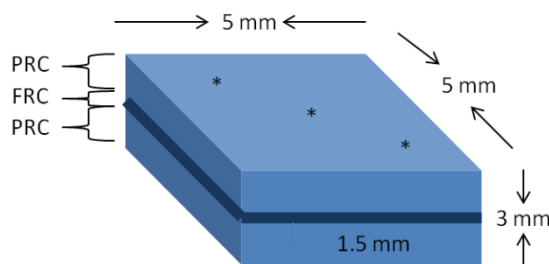


Figure 3.3: Schematic diagram showing the geometry of specimens tested for microhardness and the three points of interest measured on top/bottom surfaces.

3.3.2 Irradiance measurement:

In order to study the effect of fibre reinforcement and its orientation on light transmittance, a laboratory grade NIST-referenced USB-4000 spectrometer (*MARC Resin Calibrator v.3, Blue-Light Analytics Inc., Halifax, NS, Canada*) was employed (Figure 3.4.A). The top sensor (4mm diameter) was used to measure irradiance (I_R) and

total energy (E_T) delivered to the bottom surface of specimen during curing. These values indicated the amount of light attenuation that occurred as a consequence of incorporating FRC within PRC, in comparison with the control (without FRC). New specimens with the same geometry used in hardness experiment were fabricated from each group using the same technique. This was to help find any correlation between hardness and irradiance. delivered to bottom surface.

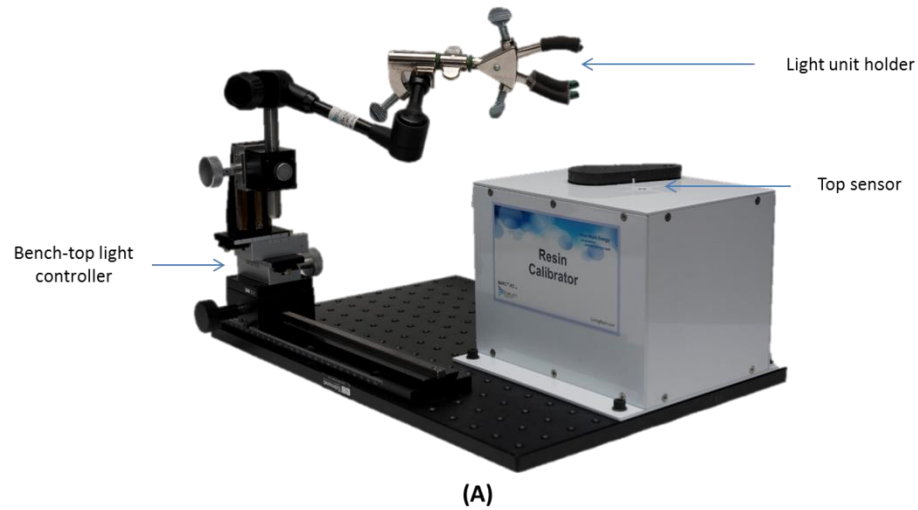


Figure 3.4: MARC resin calibrator used for irradiance measurement, A) its main parts, B) LED curing unit during the baseline measurement and C) the mould assembly placed on top sensor prior to irradiance measurement.

Initially, an LED curing unit (*EliparTMS10*, 3M-ESPE, USA) was assessed for its spectrum type (single-peak), wavelength range (420–480 nm), and mean output I_R (1764 mW/cm^2) (Appendix I), when its tip was in a direct contact with the top sensor (Figure 3.4.B). Taking into account the separation between the light tip and sensor, the thickness of empty mould (3mm), base glass slide (1mm) and top glass cover (0.1mm) during curing, a baseline measurement of I_R was further assessed (1032 mW/cm^2) (Figure 3.4.C and Figure 3.5). Later, the irradiance curve for three specimens in each group was monitored during light curing for 20s (Figure 3.6). Mean/maximum I_R

(mW/cm^2) and E_T (J/cm^2) values were measured for each specimen. Additionally, the curing-time required to reach the plateau in I_R spectrums was also recorded. This indicated the time required to achieve initial polymerization at bottom surface for each group. Statistical analysis using 1-way ANOVA (Tukey's Post hoc) was performed to detect any significant difference between groups.

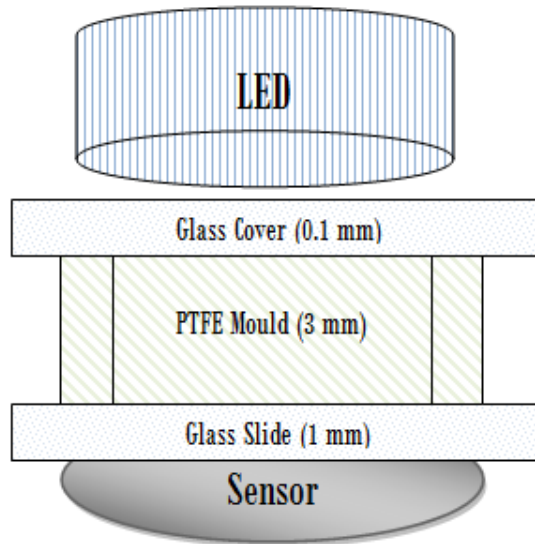


Figure 3.5: Schematic diagram showing the mould assembly on the top sensor of spectrometer during irradiance measurements. The same assembly was used during the baseline measurement of curing light in order to calculate the light attenuation occurred purely because of FRC and PRC.

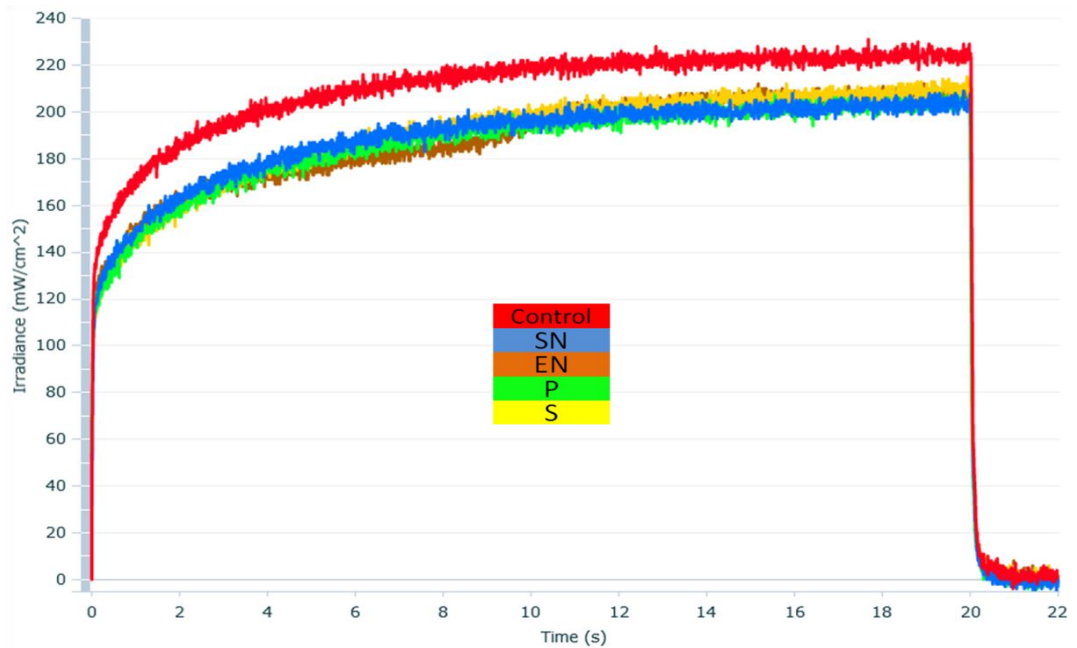


Figure 3.6: Graph showing the irradiance versus time for one representative specimen for each group during the direct light curing for 20s

3.4 EDGE STRENGTH MEASUREMENT (CHAPTER 5):

The influence of FRC and their orientation on the edge strength was investigated using the protocol below (Figure 3.7):

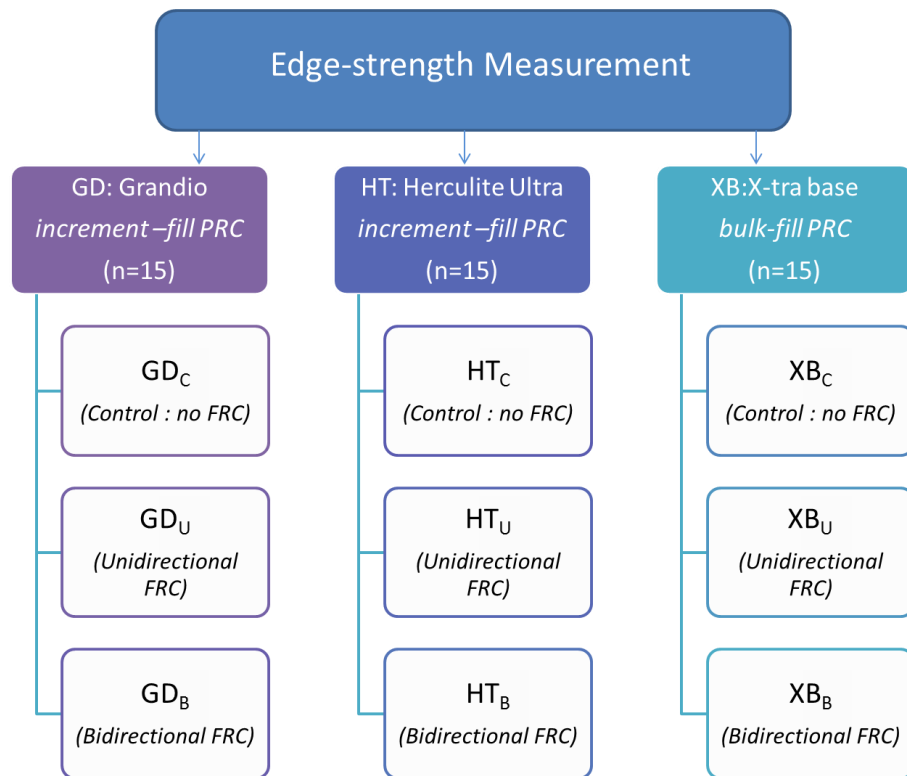


Figure 3.7: Diagram showing the study protocol in Chapter 5.

3.4.1.1 Rationale:

Edge strength, as a surface property, was investigated in this study to give an indication about the influence of FRC on marginal integrity and deterioration resistance. Using a dedicated machine (CK10), edge strength test was performed due to its simplicity and popularity, and so to facilitate comparison of the results with previous studies.

3.4.1.2 Pilot Study

A pilot study was conducted to determine sample size, specimen geometry and testing parameters. For 0.8 power probability and 0.05 type-I error, the required sample size capable of detecting a true difference between groups was calculated to be 3 specimens for each subgroup. Both disc-shaped (12 x 2 mm) and rectangular-shaped (12.5 x 4 x 2 mm) specimens were attempted in the pilot study. The results of the latter, however, were more consistent as the fraction of reinforcing fibres incorporated at the edges was better standardized, especially with the unidirectional FRCs. Different testing parameters, including cross head speed (0.5 and 1 mm/min), location of applied force

(0.5mm distance from the margins or corners) and number of readings per edge (1 -3 readings), were also attempted. The most consistent preliminary data were achieved with 1 mm/min cross head speed and two readings per specimen (one at 0.5mm distance from each edge) (Figure 3.8). Accordingly, forty five rectangular-shaped specimens were allocated into three equal groups (n=15) and subgroups (n=5), and then tested using the latter testing parameters.

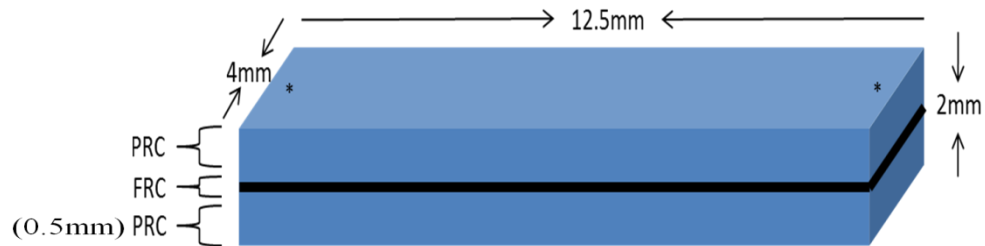


Figure 3.8: Schematic diagram showing the geometry of specimens tested for edge-strength and the two reading points on top surface (0.5mm distance from each edge).

3.4.1.3 Materials and Methodology:

The specimens were prepared from three PRCs and two FRCs using a sectional stainless steel mould. The PRCs were chosen to represent three different categories: a universal increment-fill packable resin-composite (*Grandio, Voco*), an Enamel-replacing increment-fill packable resin-composite (*Herculite Ultra, Kerr*), and a universal bulk-fill flowable resin-composite (*X-tra Base, Voco*). The FRCs were chosen with two different orientations: unidirectional FRC (*Everstick C&B, Stick Tech Ltd*) and bidirectional FRC (*Everstick Net, Stick Tech Ltd*).

The designated FRC was incorporated within PRC as an intermediate layer at 1.5mm depth in each specimen, and extended to include the margins. A specialised edge-strength testing machine (*CK10, Engineering Systems, Nottingham, UK*) was used to measure the edge-strength values for all specimens (Figure 3.9). At first, the machine was calibrated for the required testing parameters (1 mm/min cross head speed). A specimen was located within the designated holder on the X-Y table, and the built-in microscope was used to determine the point of interest for the measurement. A Vickers diamond indenter was used to apply static vertical compressive load at 0.5mm distance from the centre of each edge until fracture occurred. The edge strength value, represented by the maximum fracture-inducing force (N), was recorded for both edges in every specimen. The average value per specimen was used in the statistical analysis.

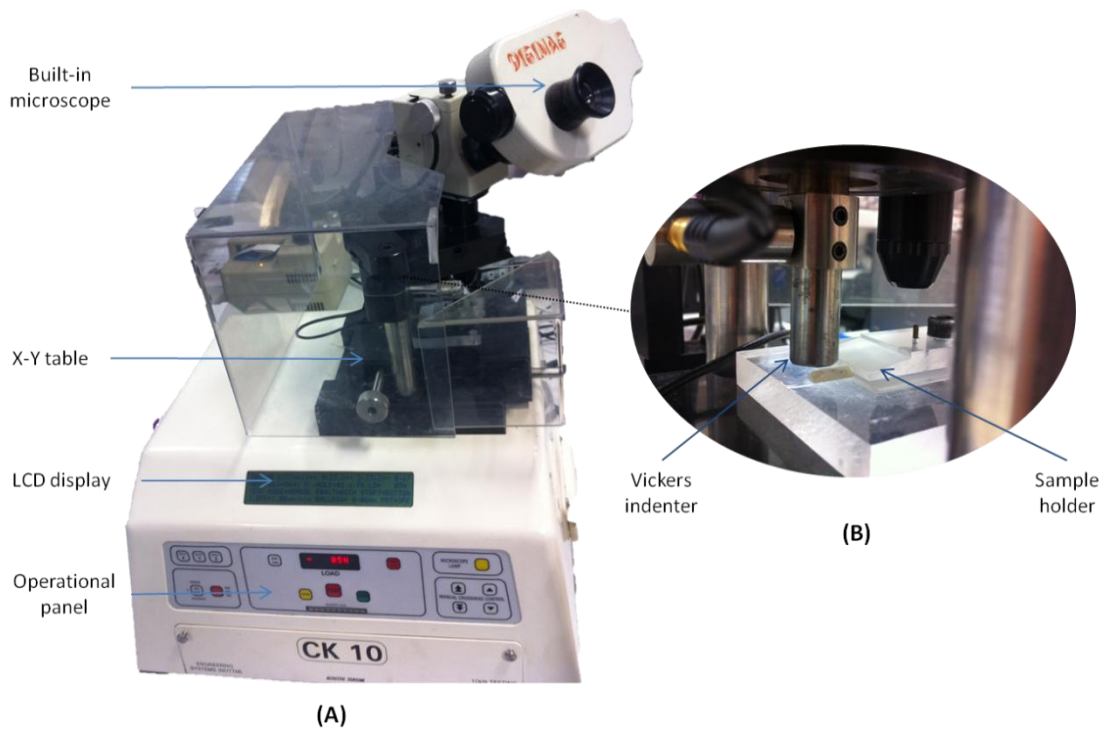


Figure 3.9: CK10 edge-strength machine and its main parts (A) during the testing of one representative specimen (B).

3.5 SHEAR BOND STRENGTH MEASUREMENT (CHAPTER 6):

The effect of incorporating an intermediate FRC layer on shear bond strength (SBS) between resin-composite and ceramic/metal substrates was investigated following the study protocol below (Figure 3.10):

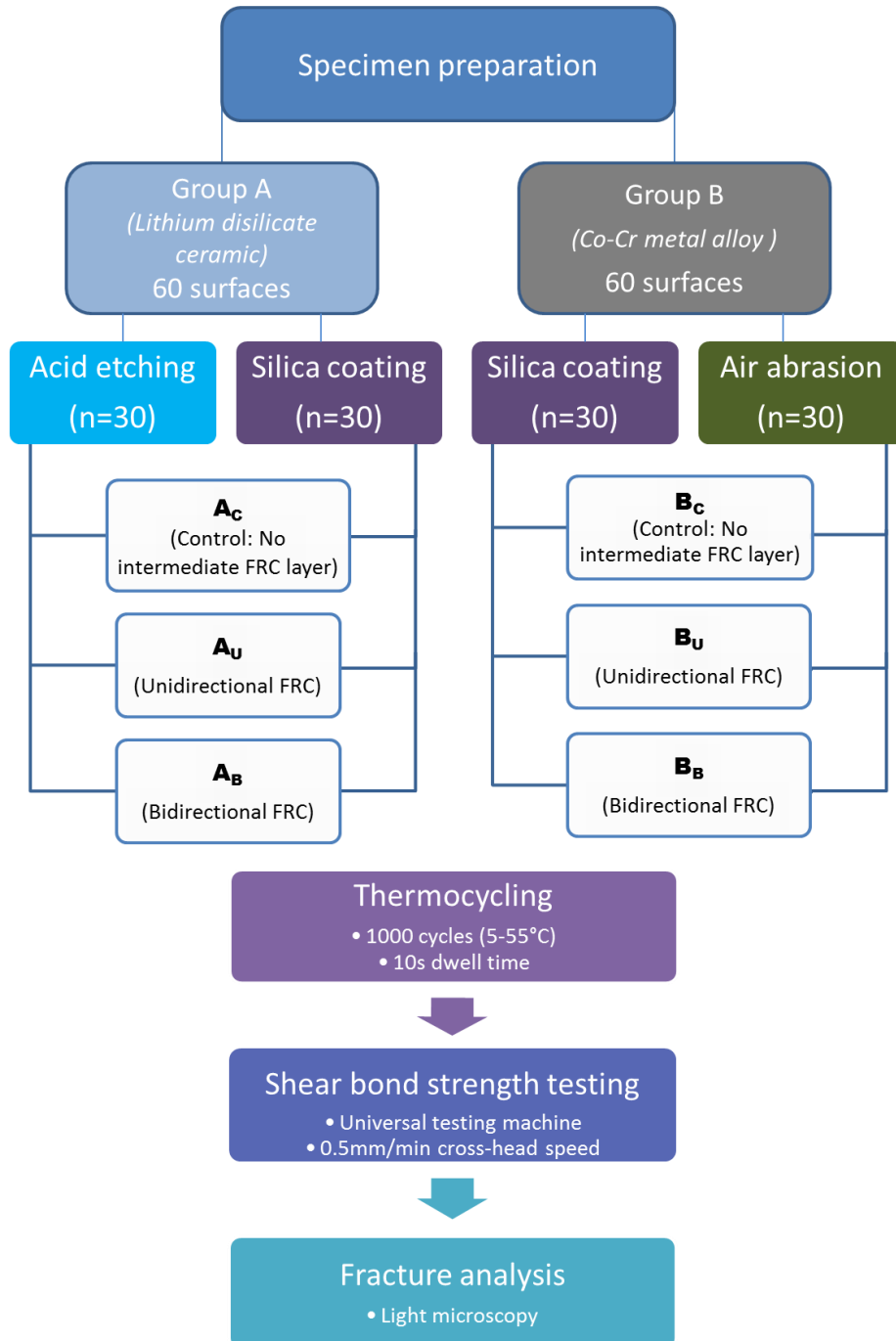


Figure 3.10: Flowchart showing the study protocol in Chapter 6

3.5.1.1 Rationale:

Shear bond strength was investigated to give an indication about how FRC will influence the adhesion when it is employed as intermediate layer to reinforce veneering PRC. Such effect was previously investigated when the bonding substrate was tooth substance (Enamel and Dentine). However, this effect has not been tested when the bonding substrate is another restorative material, such as ceramic or metal. Accordingly, two restorative materials, as a representative of their main categories, were chosen as bonding substrates. Among different tests investigating bond strength, a shear bond strength test was selected due to its simplicity and feasibility as screening tool for comparing new materials.

3.5.1.2 Materials and Methodology:

The ceramic (*IPS e.max press, Ivoclar Vivadent*) and metal (*Incise LaserPFM, Renishaw plc*) substrates (n=30 each) were prepared using CAD/CAM technology as disc-shaped specimens (16 x 2 mm). The dimensions of specimens were chosen to fit the metal housing used to hold specimen during shear bond testing.

Different surface treatments were applied on each side of a specimen, followed with bonding agent application. Ceramic specimens (Group A) were treated with silica-coating on one side and hydrofluoric acid (HF) etching on the other, while metal specimens (Group B) were treated with silica-coating and air-abrasion (Figure 3.11). All surfaces were treated with saline before being bonded to enhance surface wetting and adhesion.

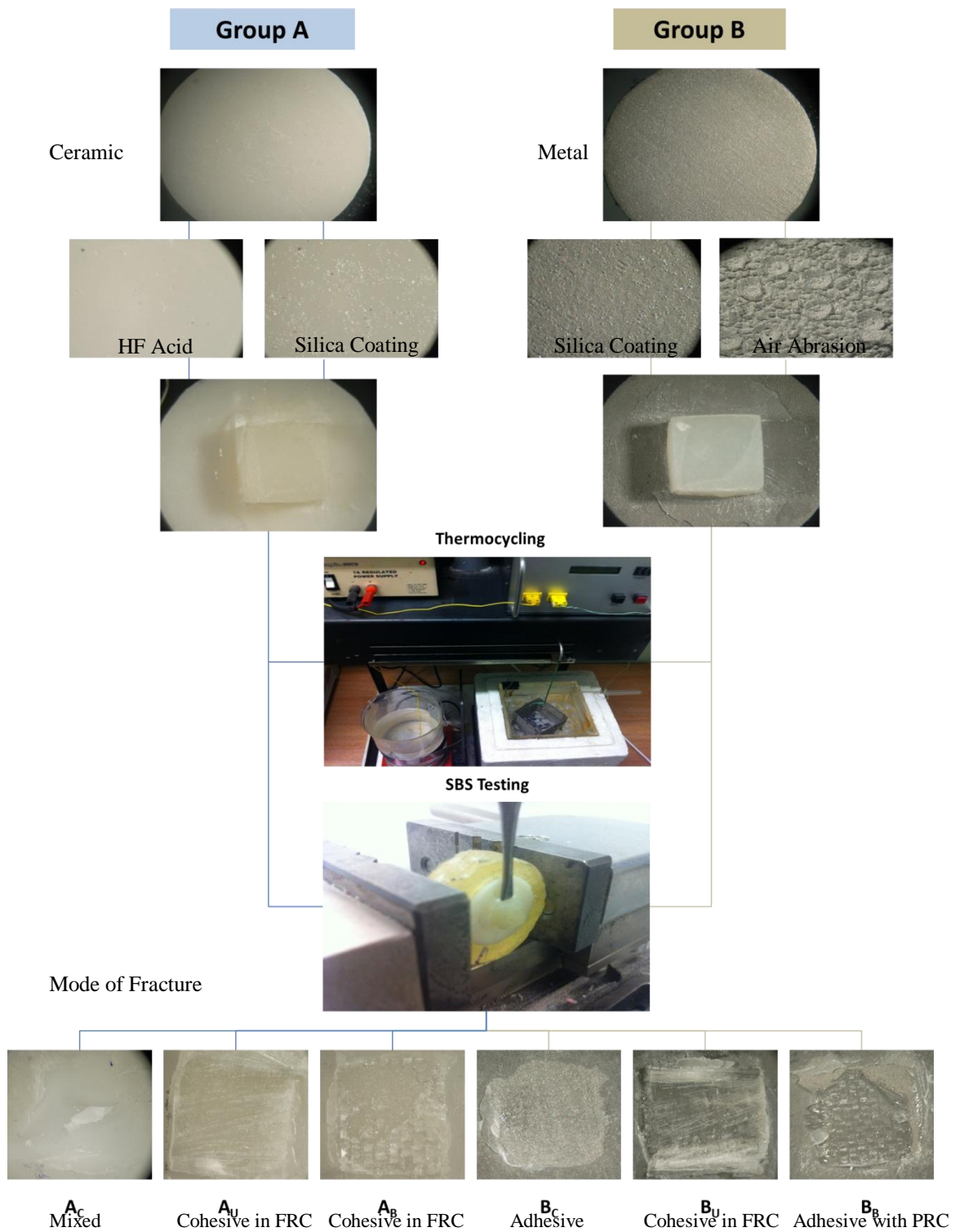


Figure 3.11: Flowchart showing the bonding substrates, surface treatments, testing procedure, and fracture analysis followed in Chapter 6.

The bonding procedure started with the application of a resin bonding agent to the bonding surface and then light-cured for 10s. A layer of flowable resin composite was applied as a base prior to the application of the designated FRC layer in order to facilitate FRC adaptation, and then both light cured together (20s). One increment of bulk-fill PRC was then applied, covered with a glass slide and light cured (20s). Thermocycling (1000 cycles, 5-55°C, 10s dwell) was performed later for all specimens using a dedicated thermocycling machine to simulate oral environment and induce artificial aging. The Zwick/Roell Z020 universal testing machine (*Zwick GmbH, Ulm, Germany*) with a single-sided chisel indenter was employed to apply shear loading (0.5 mm/min crosshead speed) along the adhesive interface between resin composite and metal/ceramic materials in every specimen in an attempt to standardize stress distribution along the interface. The shear bond strength (MPa) was then calculated according the following equation:

$$SBS = \frac{F_{Max}}{A} \quad \text{Equation 3.1}$$

Where F_{Max} is the ultimate load-to failure (N) and A is the bonded area (mm^2).

The debonded surfaces were examined under light microscopy with high magnification (x30) in order to assess the failure mode. The mode of failure was reported for each specimen and classified as adhesive failure within the substrate interface, adhesive within PRC interface, cohesive failure within FRC and mixed adhesive/cohesive failure. A series of two-way ANOVA (Tukey's Post hoc) was used to investigate the influence of material substrate, surface treatment and FRC orientation on SBS.

3.6 LOAD-BEARING CAPACITY OF FRC-FPDS (CHAPTER 7):

Twenty inlay-retained FRC-FPDs with two different framework designs were prepared and tested following the protocol below (Figure 3.12):

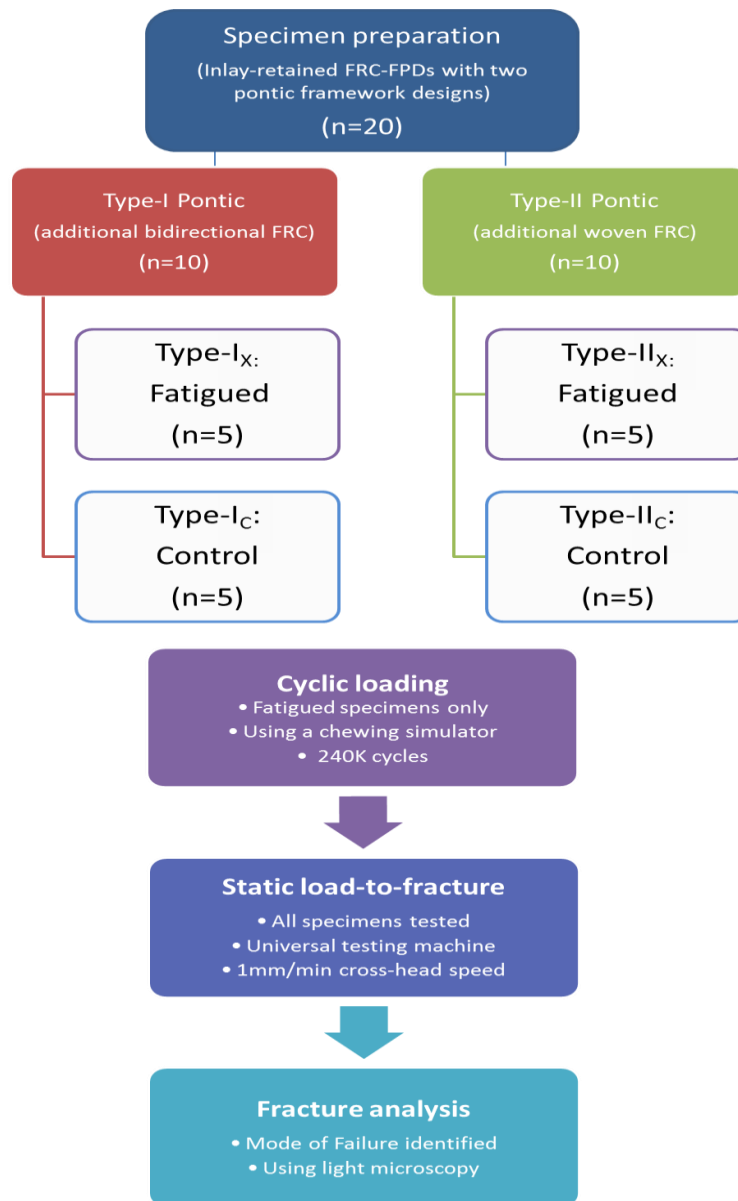


Figure 3.12: Flowchart showing the study protocol in Chapter 7.

3.6.1.1 Rationale:

Specimens in this research were fabricated in anatomical form rather than using simple bar specimens. This was with intention to simulate all the loading stresses affecting the performance of FRC-FPDs in the oral cavity. Three different FPD designs could be fabricated using FRC. The first design is the conventional design which relies on the full preparation of abutments and uses two full crowns as retainers. This design is the strongest, yet, the most destructive. The second design is the prep-less design which

relies purely on the adhesion of retainers to the buccal and lingual surfaces of abutments. This design is the most conservative, yet, the weakest as its retainers can be subjected to highly destructive shear loading beyond the tolerance of the bond strength with tooth structures. The third design is the inlay-retained FPD which is the most documented and practiced as it relies on one inlay retainer at both abutments for support and retention. This design is minimally-invasive and allows adequate support and retention from the adjacent abutments. Accordingly, it was chosen to fabricate the FRC-FPDs specimens in this research.

3.6.1.2 Materials and Methodology:

At first, two artificial teeth (mandibular 2nd premolar and 2nd molar) were prepared as master abutments for a 3-unit inlay-retained FPD on an artificial mandible (Figure 3.13, a). A vacuum-formed matrix was formed beforehand to standardize the morphology of all fabricated FPDs (Figure 3.13, b). Both master abutments were duplicated using a silicone duplicating material (*Gemini, Bracon, East Sussex, UK*) (Figure 3.13, c-d). Following the duplication, twenty identically-prepared acrylic premolars and molars were harvested. The duplicated teeth were pre-coated with 0.2 mm-thickness wax prior to their mounting within an epoxy-resin base (*B&K Resins Ltd, Bromley, UK*) in order to simulate PDL space. A standardised position of abutment teeth simulating the average space of missing lower 1st molar, with 11mm pontic space and 2mm base support below CEJ, was ensured through the mounting process using the vacuum-formed index. Once the base has been set, the wax coatings were replaced by light-bodied impression material (*Aquasil LV, Dentsply, USA*) to reproduce PDL elasticity. Twenty identical assemblies were fabricated and used to support FRC-FPDs (Figure 3.13, e).

Twenty FRC-FPDs (n=20) were directly-fabricated over the mounted teeth, utilizing two bundles of woven ultrahigh molecular weight (UHMW) polyethylene fibres (*Construct, Kerr*) as the main supporting framework (Figure 3.13, g-h). Prior to the fibre adaptation, the inlay cavities were pre-treated with silica coating and silanization (*Cojet™ system, 3M-ESPE*) according to the manufacturer's instruction (Figure 3.13, f) in order to enhance the adhesion of acrylic teeth, followed by the application of a bonding agent (*Visio-Bond, 3M-ESPE*). Later, resin-composite (*X-tra fill, Voco*) was adapted between the fibres to build the pontic core and then cured for 20s (Figure 3.14, i).

Two types of pontics with different additional reinforcing fibres were subsequently fabricated. Type-I (n=10) had a bidirectional E-glass fibre sheet (6 X 5 mm) (*Everstick Net, Stick Tech Ltd*) perpendicularly-adhered to the core with the intention of implementing further support for the occlusal veneering PRC and suppress crack propagation. Type-II had an additional 10mm fibre bundle of the polyethylene fibres (*Construct, Kerr*) wrapped around the core in an inverted U-shape fashion with the intention of increasing the support for the buccal, occlusal, and lingual veneering PRC and reduce delamination fracture.

The final specimen shape was reproduced in a standardised way. The veneering PRC (*X-tra fill, Voco*) was applied and cured through the clear vacuum matrix for 20s from each surface. (Figure 3.14, j). Finishing and polishing using coarse/medium finishing discs (*OptiDisc, Kerr, Switzerland*) were performed for all specimens, which were then stored in water (37 °C, 48 hours) prior to further testing to simulate the oral environment..

Half of the specimens were cyclicly loaded using a chewing simulator machine (*CS-4.2, SD Mechatronic, Germany*) to simulate the effect of clinical mastication and dynamic fatigue *in-vitro* (Figure 3.14, k-m), while the remaining specimens were control. Later, all the specimens were statically loaded to fracture in a universal testing machine (*Zwick Z020, Zwick/Roell GmbH, Germany*) with a steel ball indenter at the central fossa (Figure 3.14, n-o). Initial failure (IF) and final failure (FF) loads were recorded for each specimen, and then used in the statistical analysis. Initial failure was identified from the stress vs strain curve during the static loading at the point of initial drop in stress. Final failure was identified from the same curve at the point of abrupt drop in stress.

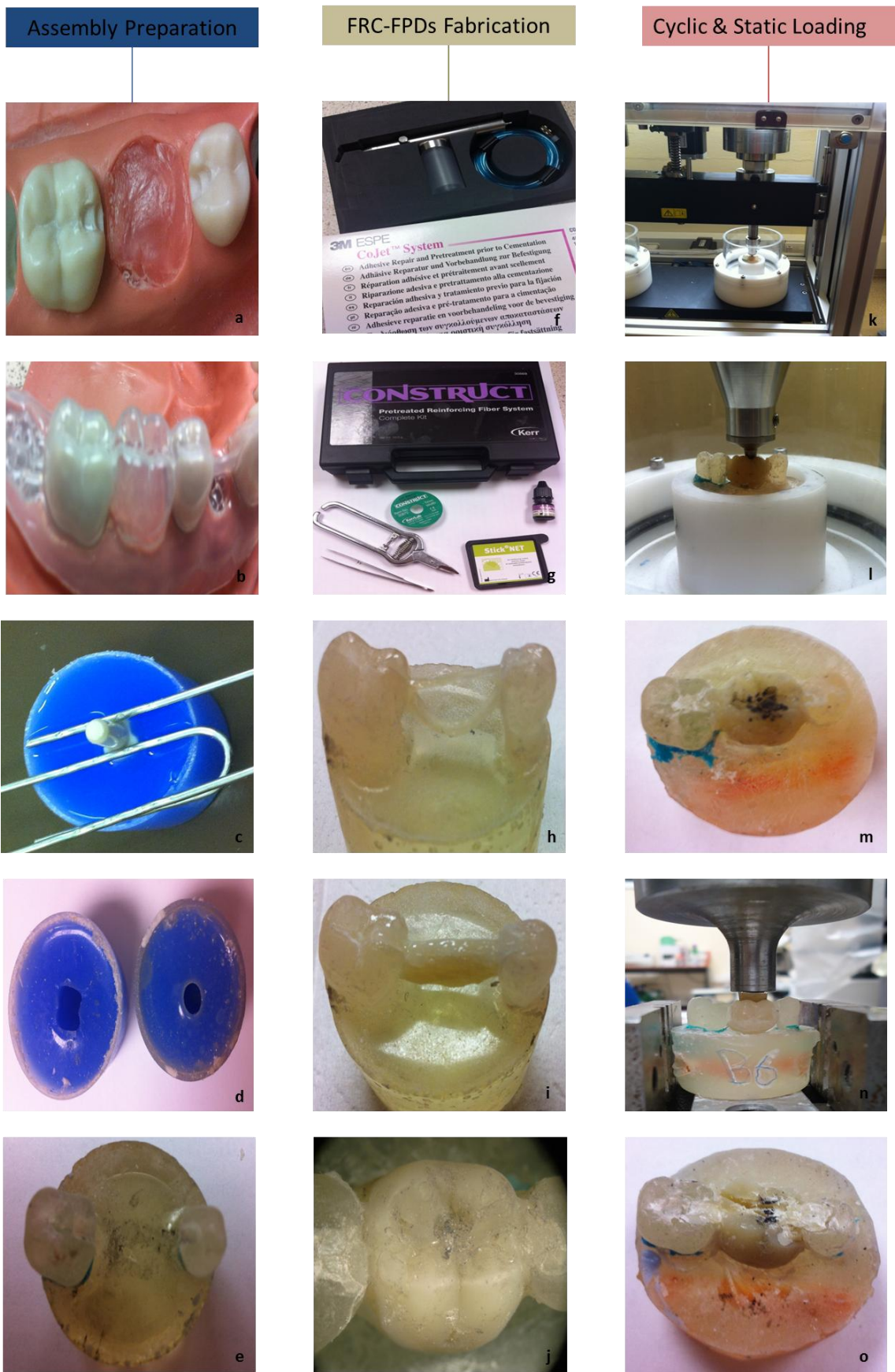


Figure 3.13: Flowchart showing the methodology followed in Chapter 7

3.7 WEAR MEASUREMENT (CHAPTER 8):

Fifteen single posterior crowns were subjected to dynamic fatigue in a chewing simulator machine to induce a degree of wear following a standardized protocol (Figure 3.14). The resultant morphological changes were monitored and compared using a 3D scanner marketed for intraoral use (*3M True Definition Scanner, 3M-ESPE, Germany*) (Figure 3.15).

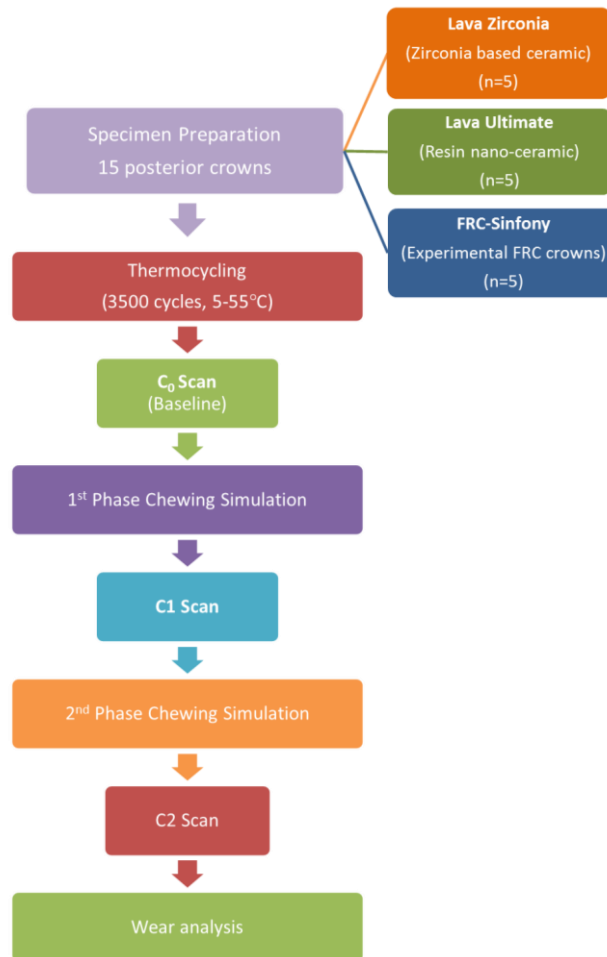


Figure 3.14: Flowchart showing the study protocol in Chapter 8

3.7.1.1 Rationale:

The ability of FRC to enhance many mechanical properties of PRC has been proven in the literature. However, no study has investigated the influence of incorporating FRC on wear behavior and resistance. New PRCs were introduced to the market claiming the best wear resistance. However, they have not been compared with PRC further reinforced with FRC. Accordingly, this experiment attempted to compare the wear behavior of FRC-PRC combination, as a system, with different metal-free restorative materials with best document wear resistance.

Digital scanners have been used to monitor and measure wear indirectly relying on impressions, casts and epoxy dies. However, in this study, a scanner intended for intraoral use was employed to monitor morphological changes directly on the teeth without the need for intermediate steps that induce many inherent errors.

3.7.1.2 Pilot study:

A pilot study was conducted to check the validity of using the intraoral scanner as a direct wear monitoring device. A baseline 3D scan was taken for one monolithic zirconia crown without any alteration. A minimal degree of wear was then induced at the central fossa using a high speed air turbine with a coarse grit diamond bur. Another scan was then taken and compared with the baseline, using surface matching software. Deviations in the order of 10µm were able to be detected using this technique. Accordingly, a full scale study was then executed.

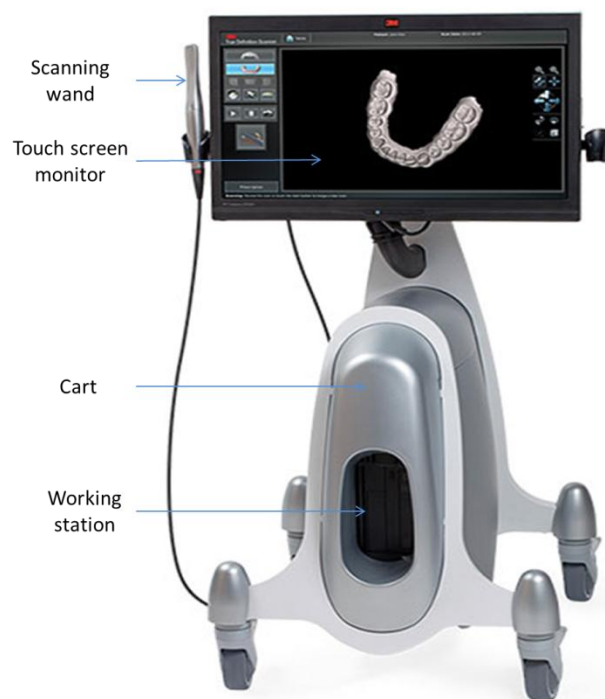


Figure 3.15: 3M True Definition Scanner

3.7.1.3 Materials and Methodology:

Fifteen mandibular first molar crowns (n=15) with the same occlusal morphology and dimensions were fabricated from three different metal-free materials. In Group A (n=5), CAD/CAM monolithic all-ceramic crowns were manufactured from Lava™ Zirconia (3M-ESPE), whereas in Group B (n=5) Lava™ Ultimate (3M-ESPE) was used instead.

Both materials were chosen as a representative of their main categories (Lava Zircoina (LZ): Ceramic, Lava Ultimate (LU): PRC), and have been claimed to have high wear resistance by their manufacturers. Group C (n=5) included the experimental crowns that were made conventionally from laboratory PRC (*Sinfony*, 3M-ESPE) and bidirectional FRC sheet (*Stick Net*, *Stick Tech Ltd*). All crowns were adhesively cemented (*RelyX Unicem 2*, 3M-ESPE) on identical assemblies representing a prepared lower first molar tooth and its supporting structure.

Thermocycling aging (3500 cycles, 5-55°C, 10s dwell) was performed to simulate the oral environment, and a baseline scan (C_0) was taken for each specimen. Wear was then induced using a chewing simulator (CS 4.2) in two consecutive phases (240K cycles each). Two scans (C_1 , C_2) were taken after the completion of each phase to calculate the resultant wear corresponding to each phase. Geomagic Control 2014 software (*Geomagic*, 3D System Corporation, USA) was used to superimpose the digital scans and quantify the degree of wear for all specimens (Figure 3.16). Three wear values (W_1 , W_2 and W_C) were recorded per specimen; W_1 represents the resultant wear of phase C_1 , W_2 represents the resultant wear of phase C_2 , and W_C is the cumulative wear (Figure 3.17). All such values were used in the statistical analysis.

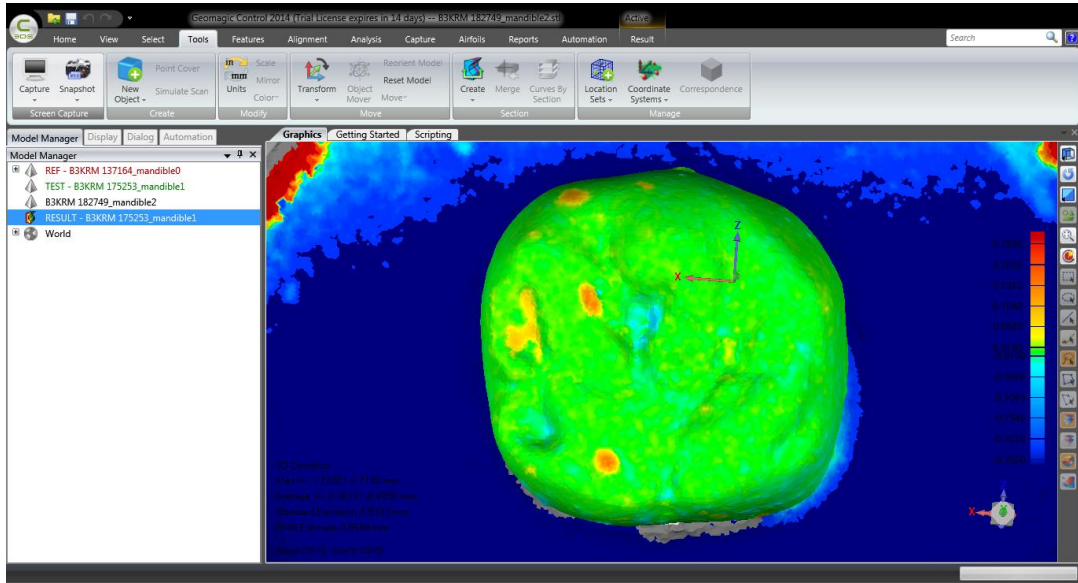


Figure 3.16: Snapshot of Geomagic Control software during wear analysis.

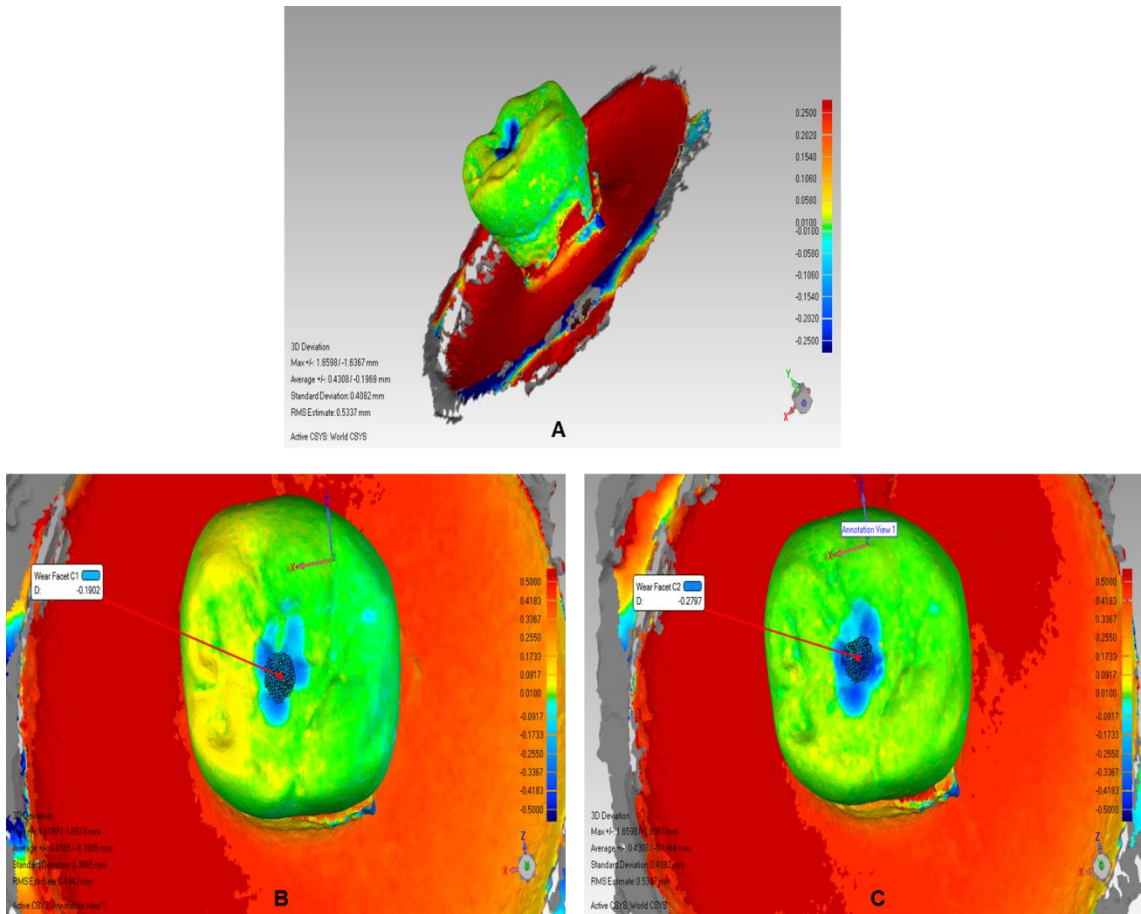


Figure 3.17: Wear analysis of a representative specimen relying on superimposition of three successive digital scans, A) 3D comparison performed, B) vertical wear measurement in the wear facet after the completion of C1 phase, and C) C2 phase

3.8 LOAD BEARING CAPACITY OF METAL-FREE CROWNS (CHAPTER 9):

Thirty posterior single crowns made of three metal-free materials were prepared and tested following the protocol below (Figure 3.18):

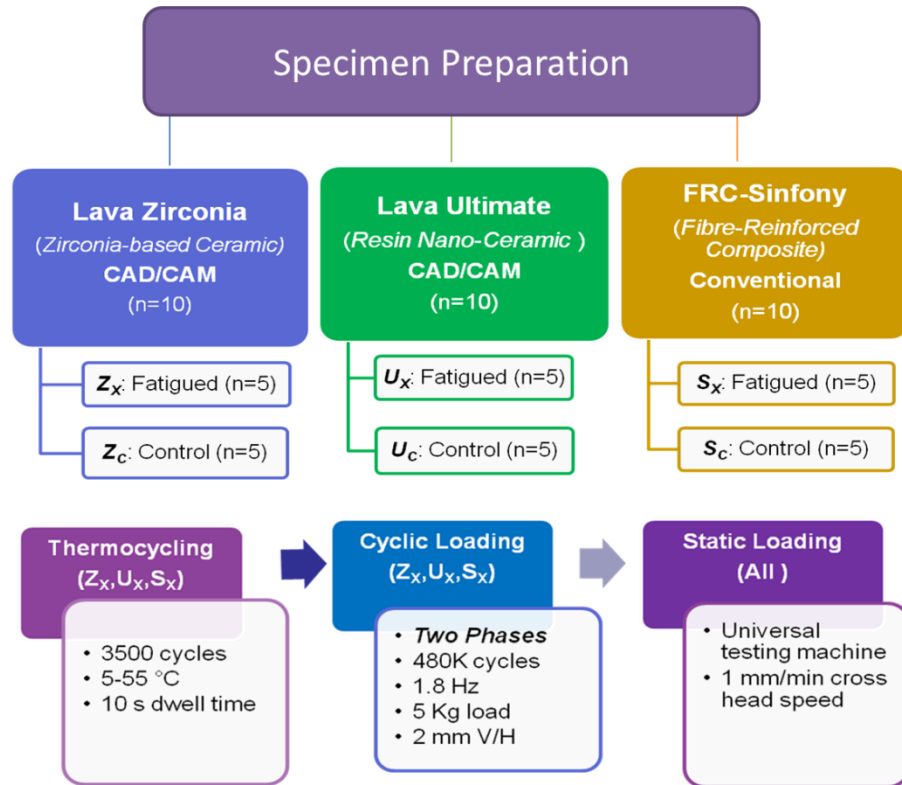


Figure 3.18: Diagram showing the study protocol in Chapter 9.

3.8.1.1 Rationale:

This study was performed as a continuation of the previous study to compare the fatigue behaviour and load-bearing capacity between the three metal-free crown fabricating systems. The fatigue behaviour of FRC crowns is not well-documented in the literature, and so this study was intended to investigate the fatigue behaviour of FRC using the masticatory fatigue simulation method. This method is a simple and reliable technique with high clinical relevance that many researchers in dental field favour.

3.8.1.2 Materials and Methodology:

Crowns were cemented adhesively on thirty identical assemblies simulating the clinical environment. Half of the specimens were dynamically fatigued by thermocycling and chewing simulator machines (Figure 3.19). Later, all the specimens were statically loaded to fracture in a universal testing machine (Zwick Z020, Zwick/Roell GmbH,

Germany) with a steel ball indenter (Figure 3.20), and the mode of fracture was observed (Figure 3.21). The maximum load-to-fracture was recorded for each specimen and used in the statistical analysis.

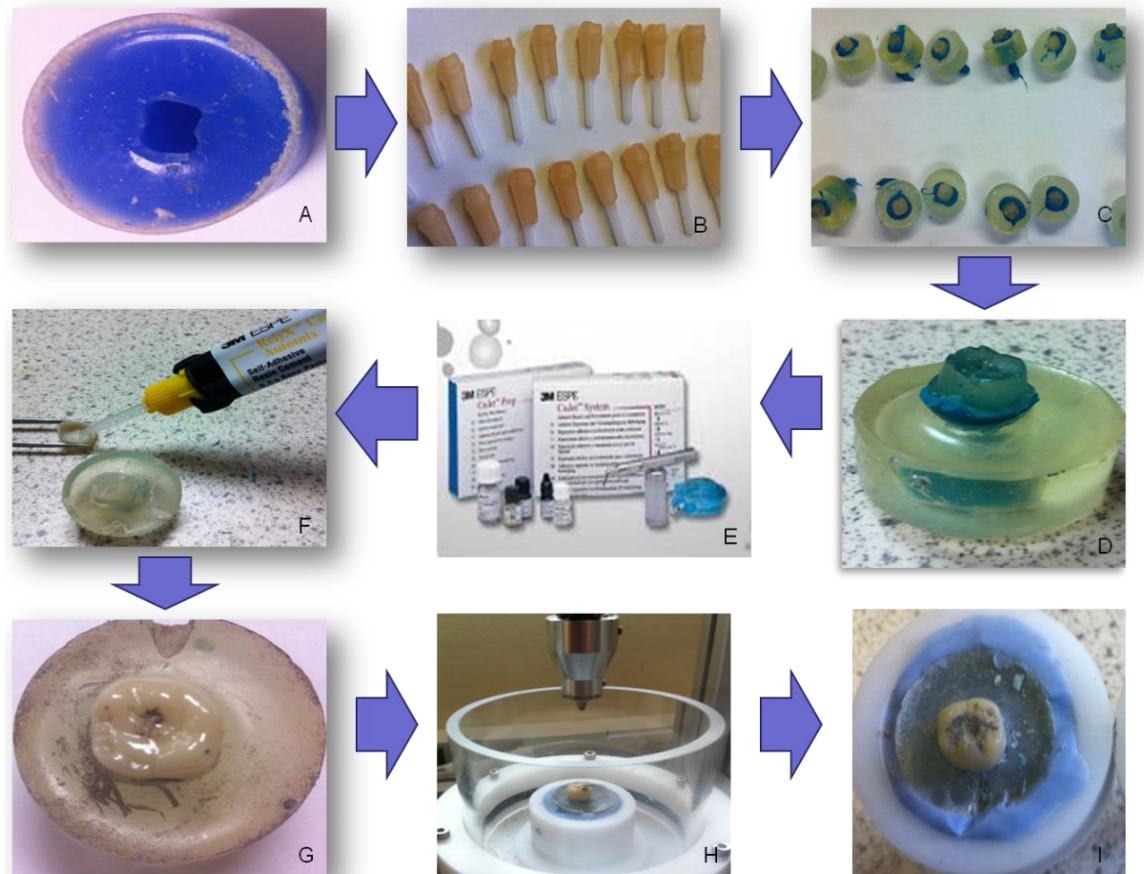


Figure 3.19: Flowchart showing the preparation and cyclic loading of crown specimens, A) preparation of master mould, B) duplicated acrylic teeth coated with wax layer, C) mounted teeth in epoxy resin base and the wax coating is substituted with PVS layer, D) a specimen assembly ready for crown cementation, E) surface treatment (silica coating) for acrylic teeth and crowns using Cojet repair system, F) cementation of crowns using self-adhesive cement (RelyX Unicem 2), G) one representative specimen after cementation and thermocycling, H) mounted in the chewing simulator for cyclic loading and I) following the completion of cyclic loading.

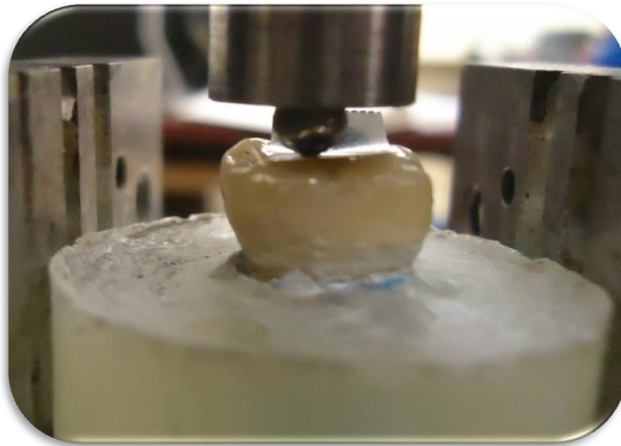


Figure 3.20: Static loading of one representative crown specimen using the steel ball indenter of Zwick Z020 machine.

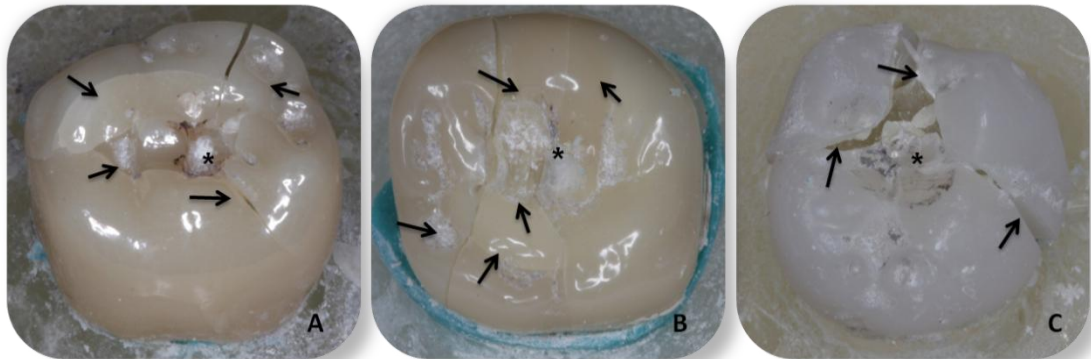


Figure 3.21: The mode of fracture of three representative crown specimens, A) Lava Zirconia, B) Lava Ultimate and C) FRC-Sinfony. * indicates the origin of fracture, while ↗ indicates crack propagation.

**Chapter 4: Influence of Fibre-Reinforced Composite
on Microhardness and Light Transmittance.**

4.1 ABSTRACT:

Objectives: To i) measure and compare the top and bottom initial and 48h post-cure Vickers microhardness (VHN) for one bulk-fill resin-composite after incorporating different fibre-reinforced composite (FRC), and ii) investigate the effect of fibre reinforcement on microhardness and light transmittance.

Methods: Fifty rectangular-shaped specimens (5 x 5 X 3 mm) made from a bulk-fill resin-composite (*X-tra fill, Voco*) were divided into five groups (n=10). No reinforcing-fibres was used to reinforce Group C (control), while pre-impregnated (*EverStick Net, StickTech Ltd*) and non-impregnated bidirectional E-glass fibres (*Stick Net, Stick Tech Ltd*), plasma-treated woven polyethylene fibres (*Construct, Kerr*) and unidirectional E-glass fibres (*Stick, Stick Tech Ltd*) were incorporated at 1.5mm depth to reinforce groups (EN, SN, P, S), respectively. An LED light (*EliparTMS10, 3M-ESPE*) was utilized to cure all specimens (20s) from the top surface only. Vickers microhardness (VHN) for top and bottom surfaces was measured immediately post-cure for half of specimens, while the remaining was tested after water storage (48h/37°C). A spectrometer (*MARC Resin Calibrator, Blue-Light Analytics*) was employed to measure mean irradiance (I_R) and total energy (E_T) delivered to specimen bottom surface during light-curing. One-way ANOVA (*Tukey's Post-hoc*) and independent t-test were used to detect any significant difference among the groups ($\alpha=0.05$).

Results: Group C had the lowest initial (64.4 ± 2.0 VHN) and post-cure (75.2 ± 1.4 VHN) microhardness but the highest bottom/top ratio (98.5%), I_R (207 ± 4.5 mW/cm²) and E_T (4.2 ± 0.1 J/cm²). For fibre-reinforced groups, SN had the highest initial microhardness (76.8 ± 1.6 VHN), bottom/top ratio (97.2%), I_R (190 ± 8.6 mW/cm²) and E_T (3.9 ± 0.2 J/cm²) while S had the lowest values (72.4 ± 1.2 VHN, 93.5%, 183 ± 7.4 mW/cm², 3.7 ± 0.2 J/cm²). Fibre-reinforcement significantly improved top-bottom VHN but reduced bottom/top ratio, I_R and E_T values. Storage condition significantly enhanced microhardness for all groups.

Conclusion: The use of FRC can improve the microhardness of bulk-fill resin-composite without affecting post-cure polymerisation. However, it tends to attenuate light transmittance to bottom surfaces that might require longer irradiation-time to compensate.

4.2 INTRODUCTION:

Since their first introduction to dentistry in the late 1970s, visible light-cured resin-based composites (RBCs) have been in constant evaluation [1, 2]. Many efforts to improve their physico-mechanical properties are based on increasing the extent of polymerisation, or the so-called 'degree of conversion' (DC) [3-6]. Superior mechanical properties [7], improved adhesion to tooth structure [8] and enhanced biocompatibility with a reduced level of residual monomers and free radicals [9] can be achievable if the DC is adequate through the entire bulk of RBCs. Material thickness and light intensity influence the DC [1, 10]. A light that transmits through RBC can only reach a certain depth due to scattering and absorption, leading to reduced DC and unsatisfactory properties at deep layers [9-14]. Therefore, it is crucial to enhance light transmittance in depth to achieve adequate DC and desirable properties.

Light transmittance in RBC is influenced by several factors, including filler size and distribution [6, 15-17], resin type and photoinitiators [2, 4, 13], shade and translucency [13, 18, 19], light intensity and irradiation time [15, 20-23]. Studies addressing these factors have developed effective irradiation methods (e.g. LED and plasma curing units) and new RBCs that facilitates photoactivation and enhances light transmittance [2, 5, 14, 15, 22-25]. One latest development is a resin-composite material intended for posterior 'bulk-fill'. This material can be applied in increments up to 4mm thickness owing to its unique composition that allows excellent light penetration [26, 27] and skipping of the time-consuming layering technique [21, 28]. It also reduces polymerization shrinkage [29, 30], cusp deflection [31] and microleakage [32], and improves marginal integrity [33] as well as other mechanical properties [25, 34], in comparison with conventional RBC. Accordingly, bulk-fill RBCs have been used in many high-demanding applications [35].

One potential application of bulk-fill RBC is to accompany fibre-reinforced composite (FRC) in order to replace posterior missing teeth. This combination of materials is believed to provide superior mechanical properties without impairing aesthetics, providing that translucent reinforcing fibres, like glass and polyethylene, are used [36]. However, the presence of reinforcing-fibres in the path of the curing light can attenuate light penetration, and probably reduces DC. Few studies have confirmed the negative effect of FRC on light transmittance but no study reported the influence of fibre orientation [37, 38]. Surface hardness can be used as an indirect indicator to investigate

the influence on light transmittance [34, 39-41]. Ideally, the ratio between top and bottom hardness for RBC should be 1 with optimal light transmittance. However, the light attenuation resulted from the reinforcing-fillers reduces DC and leads to a drop in the bottom/top ratio. The minimal acceptable bottom/top ratio equals 0.8, indicating the least acceptable DC in RBCs [39, 40, 42].

The main aim of this study was to investigate the influence of incorporating different FRCs within bulk-fill RBC on microhardness and light transmittance. The influence of 'FRC type', 'post-irradiation storage' on top and bottom microhardness was also examined. Four null hypotheses were formulated: i) the incorporation of FRC within bulk-fill material has no significant effect on its initial and post-irradiation microhardness, ii) there is no significant difference in the bottom/top hardness ratio as a consequent of FRC incorporation, iii) the mean irradiance and total energy received by the bottom surface of bulk-fill RBC would not be significantly influenced by the FRC orientation and iv) there exists no correlation between the bottom/top hardness ratio and degree of irradiance.

4.3 MATERIALS AND METHODS:

4.3.1 Materials:

Four commercial FRCs with different types, orientation and impregnation and one bulk-fill PRC were investigated by assessing the variation in Vickers microhardness and irradiance delivered to the bottom surface. Top and bottom Vickers hardness number (VHN) were measured immediately post-cure and after 48h water storage for all specimens, while all I_R values were taken during the light curing process. The materials used to prepare all specimens, their descriptions, compositions and manufacturers are listed in Table 4.1.

Table 4.1: Materials used to prepare all specimens

Materials	Description	Composition	Lot No.	Manufacturer
Stick®Net (SN)	Non-impregnated bidirectional fibres	Non-silanated mesh E-glass fibres, porous PMMA	20140920	<i>Stick Tech Ltd, Turku, Finland</i>
EverStick®Net (EN)	Pre-impregnated bidirectional fibres	Silanated mesh E-glass fibres, PMMA, Bis-GMA	120424	<i>Stick Tech Ltd, Turku, Finland</i>
Construct™ (P)	Non-impregnated woven fibres	Cold gas plasma-treated pre-silanated with unfilled resin polyethylene fibres	2960366	<i>Kerr, CA, USA</i>
Stick® (S)	Non-impregnated unidirectional fibres	Silanated longitudinal E-glass fibres, porous PMMA	120523	<i>Stick Tech Ltd, Turku, Finland</i>
X-tra®fil (C)	Packable bulk-fill posterior micro-hybrid composite	86 wt% filler (barium-boron-alumina-silicate glass), Bis-GMA,UDMA,TEGDMA	1209351/ universal shade	<i>VOCO GmbH, Cuxhaven, Germany</i>
Stick® Resin	Unfilled light-cured resin	Bis-GMA, TEGDMA	120321I	<i>Stick Tech Ltd, Turku, Finland</i>

PMMA: poly methyl methacrylate, Bis-GMA: bisphenol A dimethacrylate, TEGDMA: triethylene glycol dimethacrylate.

4.3.2 Microhardness assessment:

Fifty rectangular bar-shaped specimens (5 x 5 x 3 mm) made of a bulk-fill RBC (*X-tra fill, Voco*) and reinforced by FRC were prepared using standardized polytetrafluoroethylene (PTFE) mould. Five equal groups (n=10) were allocated according to the type of FRC used. For Groups EN and SN, pre-impregnated (*EverStick Net, Stick Tech Ltd*) and non-impregnated bidirectional E-glass FRCs (*Stick Net, Stick Tech Ltd*) were used respectively. Specimens in Groups S and P were reinforced by incorporating non-impregnated unidirectional E-glass (*Stick, Stick Tech Ltd*) and woven polyethylene (*Construct, Kerr*) FRC respectively, whereas Group C specimens had no incorporated FRC layer incorporated (control). All the non-impregnated FRCs were impregnated by a resin (*Stick Resin, Stick Tech*) for 5min prior to their implementation.

After applying a separating medium (petroleum jelly) to the mould, an initial increment of RBC (1.5mm thickness) was packed into the mould against a glass slide on a non-reflective background surface. The designated intermediate FRC layer was then incorporated as an intermediate layer and spread to the entire area to ensure appropriate adaptation prior to the application of final RBC increment. The mould was then slightly

overfilled with RBC and the excess was removed by firmly adapting another glass slide on the top. Each specimen was then light-cured for 20s from the top surface using a LED light curing unit (*EliparTMS10, 3M-ESPE, USA*) under a standard curing mode. The light curing unit had a 10mm-tip placed centrally over specimens with a direct contact. Immediately after the curing, the specimen was gently pushed out from the mould, and any excess flash was removed using 1000-grit silicon polishing sandpaper. A permanent marker was used (at the sides) to identify the top surface.

Half of the specimens in each group (n=5) were immediately used to determine the initial top and bottom Vickers hardness number (VHN), while the remaining specimens were stored in distilled water (37°C, 48h) before being dried up (23°C, 1h) and measured for their top and bottom VHN. A microhardness instrument (*FM-700, Future Tech Corp., Japan*) with a Vickers diamond indenter was used. Three sequential measurements were taken for each surface with 300gf fixed load applied for 10s (dwell time). Bottom/top surface hardness ratios were then calculated for each specimen.

4.3.3 Irradiance measurements:

In order to assess the variation in light transmittance, the irradiance (I_R) and total energy (E_T) received by the bottom surface during light-curing (20s) were measured for all five groups. A laboratory grade NIST-referenced USB-4000 spectrometer (*MARC Resin Calibrator v.3, Blue-Light Analytics Inc., Halifax, NS, Canada*) was employed for all the measurements (Figure 4.1). The same light-curing unit was used to deliver the required curing energy; the unit was mounted on a specific bench-top curing light controller (*BenchMARCTM, Blue-Light Analytics Inc., Halifax, NS, Canada*) in order to standardise the position and curing distance.

At first, the light curing unit was assessed for its spectrum type (single-peak), wavelength range (420–480 nm), and mean output I_R (1764 mW/cm^2) when its tip was in a direct contact with the spectrometer top sensor (4mm ϕ). Taking into account the separation between the light tip and sensor, the thickness of empty mould (3mm), base glass slide (1mm) and top glass cover (0.1mm) during curing, a baseline measurement of I_R was further assessed (Figure 4.2). For the measurements of each group, three fresh specimens were directly light-cured (20s) over the sensor, and the real-time irradiance spectrums were monitored. Mean/maximum I_R (mW/cm^2) and E_T (J/cm^2) values were recorded for each specimen. Additionally, the curing-time required to reach the plateau in irradiance spectrums was also recorded.

4.3.4 Statistical analysis:

The data for all groups were collected and analysed statistically using SPSS 22.0 (IBM SPSS Statistics, SPSS Inc., Chicago, IL, USA). Paired and independent t-tests were used to compare top and bottom VHN, initial and 48h post-cure VHN for each group, respectively. Two-way analysis of variance (ANOVA) was used to assess the significance of 'FRC type', 'post-cure storage' on VHN. One-way ANOVA (Tukey's post hoc) was performed to detect any significant difference in initial VHN, 48h post-cure VHN, bottom/top ratio, mean I_R and E_T for each group. Scatter plot and Pearson correlation analysis were performed to test the relationship between bottom/top ratio and mean I_R values. The level of significance for all tests was set at $\alpha=0.05$.

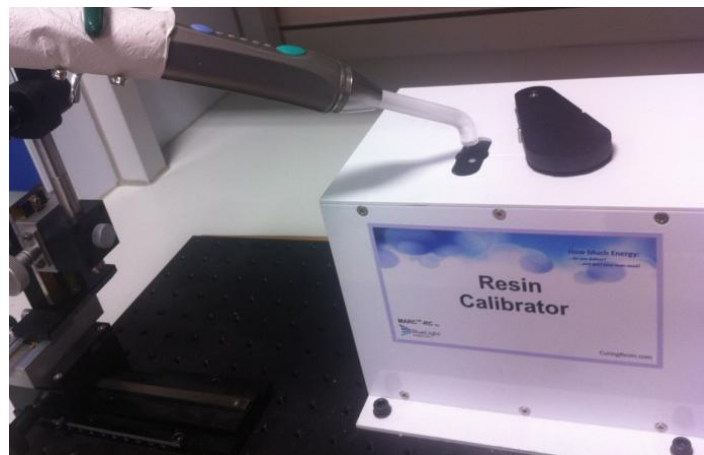


Figure 4.1: Light curing unit assembly on the MARC Resin Calibrator using BenchMARC controller.

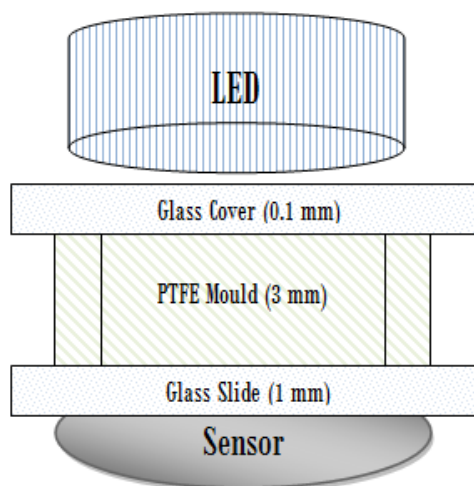


Figure 4.2: Schematic diagram showing the mould assembly on the spectrometer's top sensor during irradiance measurement.

4.4 RESULTS:

Mean (SD) VHN for all tested groups are shown in Table 4.2, and presented graphically in Figure 4.3. Group SN had the highest initial top and bottom values (76.8-74.7) while Group EN had the highest post-cure values (85.6-80.1). Group S had the lowest bottom/top microhardness ratio (92.7-93.5 %) whereas Group C had the highest (97.2-98.3%). All groups exhibited significantly higher top and bottom VHN after 48h of water storage compared to their initial VHN ($p < 0.001$). All FRC groups had significantly better initial and post-cure VHN than the control group ($p < 0.05$). Bottom VHN values were significantly lower than top initial VHN for all FRC groups ($p < 0.001$), while there was no significant difference for the control group ($p = 0.104$). Both FRC type and post-cure storage had a significant influence on VHN ($p < 0.001$). With regards to the bottom/top ratio, the differences between the groups was significant ($p < 0.001$), and Group C had the highest ratio (98.5%).

Table 4.2: Mean (SD) values of Vickers Hardness (VHN) for all tested groups.

Group	Initial (VHN)			48h post-cure (VHN)		
	Top	Bottom	B/T (%)	Top	Bottom	B/T (%)
C: Control	64.4±2.0 ^{a,1}	63.3±1.9 ^{a,1}	98.3 ^a	75.2±1.4 ^{a,1}	73.1±0.8 ^{a,2}	97.2 ^a
SN: StickNet	76.8±1.2 ^{b,1}	74.7±1.6 ^{b,2}	97.2 ^{a,b}	82.9±1.8 ^{b,1}	79.1±1.9 ^{b,c,2}	95.4 ^b
EN: Everstick Net	72.9±1.1 ^{c,1}	69.7±0.9 ^{c,2}	95.6 ^{b,c}	85.6±1.8 ^{b,1}	80.1±1.4 ^{b,2}	94.6 ^b
P: Construct	73.2±0.9 ^{c,1}	69.1±0.9 ^{c,2}	94.4 ^{c,d}	83.5±1.2 ^{b,1}	77.8±1.4 ^{c,2}	93.1 ^c
S: Stick	72.4±1.2 ^{c,1}	67.7±1.4 ^{c,2}	93.5 ^d	84.0±1.7 ^{b,1}	77.9±1.8 ^{c,2}	92.7 ^c

**Different superscript letters and numbers indicate a significant difference within the same column and row, respectively.*

Mean and maximum irradiance (mW/cm^2), total energy (J/cm^2) and time required to reach plateau are reported for all groups in Table 4.3. The real-time I_R spectrums during light-curing for a representative specimen from each group were superimposed and presented in Figure 4.4. Group C had the highest mean I_R values ($207\text{-}231 \text{ mW}/\text{cm}^2$), E_T ($4.2 \text{ J}/\text{cm}^2$) and shortest curing-time to reach plateau (12s), while Group S had the lowest values (I_R : $183\text{-}215 \text{ mW}/\text{cm}^2$, E_T : $3.7 \text{ J}/\text{cm}^2$) and longest time (16s). Bottom/top VHN ratio was positively correlated to mean I_R values measured by the resin calibrator, with Pearson correlation coefficient of 0.876 ($p = 0.052$) and linear regression analysis (R^2) value of 0.767 (Figure 4.5).

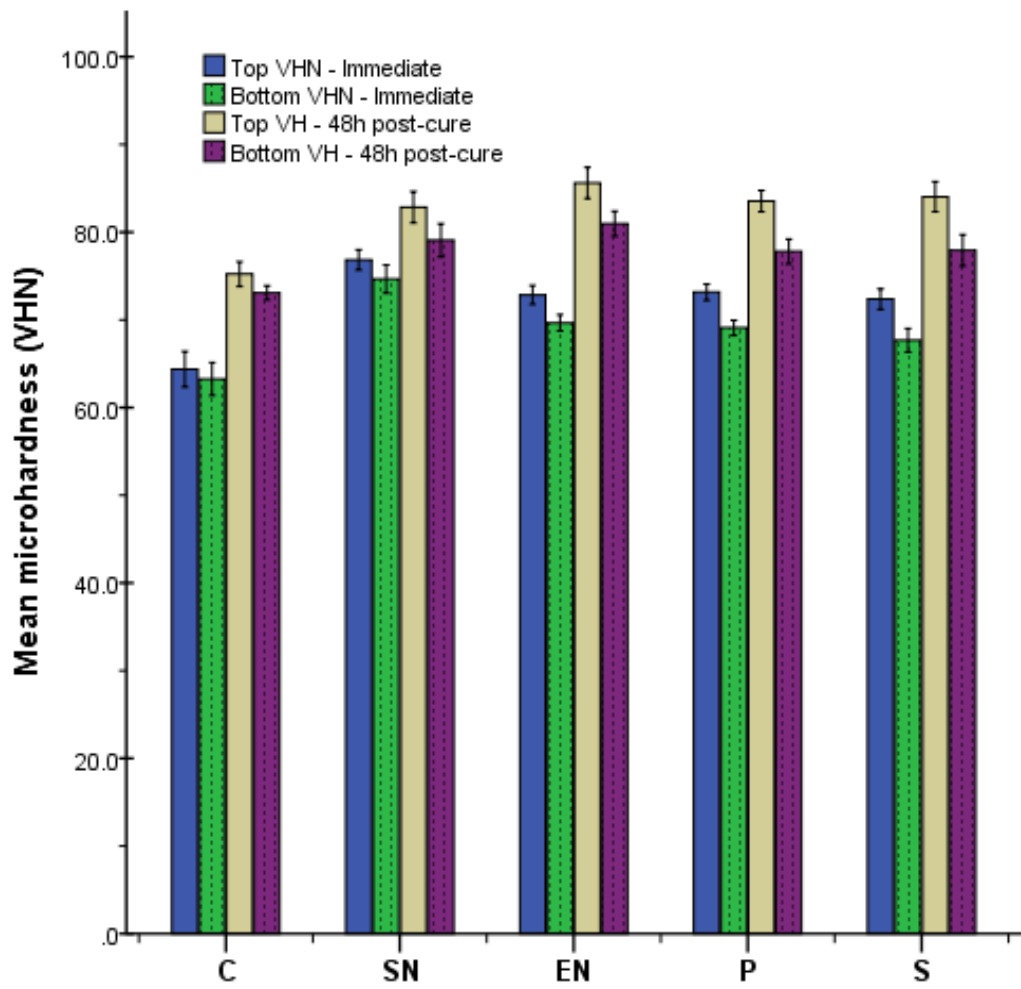


Figure 4.3: Bar chart showing mean (SD) VHN for top and bottom surface for all groups immediately post-cure and after 48h water storage.

Table 4.3: Mean and Maximum (SD) values of irradiance (I_R), total energy (E_T) and time required to reach plateau for all tested groups.				
Group	Mean I_R (mW/cm ²)	Max I_R (mW/cm ²)	E_T (J/cm ²)	Time(s)
C: Control	207.0±4.5 ^a	231.0±8.5 ^a	4.2±0.1 ^a	12
SN: Stick Net	190.0±8.6 ^{a,b}	217.0±7.6 ^a	3.9±0.2 ^{a,b}	14
EN: Everstick Net	186.0±5.1 ^b	217.0±3.6 ^a	3.8±0.1 ^b	15
P: Construct	183.0±6.6 ^b	211.0±5.2 ^a	3.7±0.2 ^b	16
S: Stick	183.0±7.4 ^b	215.0±9.2 ^a	3.7±0.2 ^b	16

**Different superscript letters indicate a significant difference within same column.
**Baseline mean/max I_R with empty mould: 1032/1065 mW/cm², $E_T = 21.1$ J/cm².*

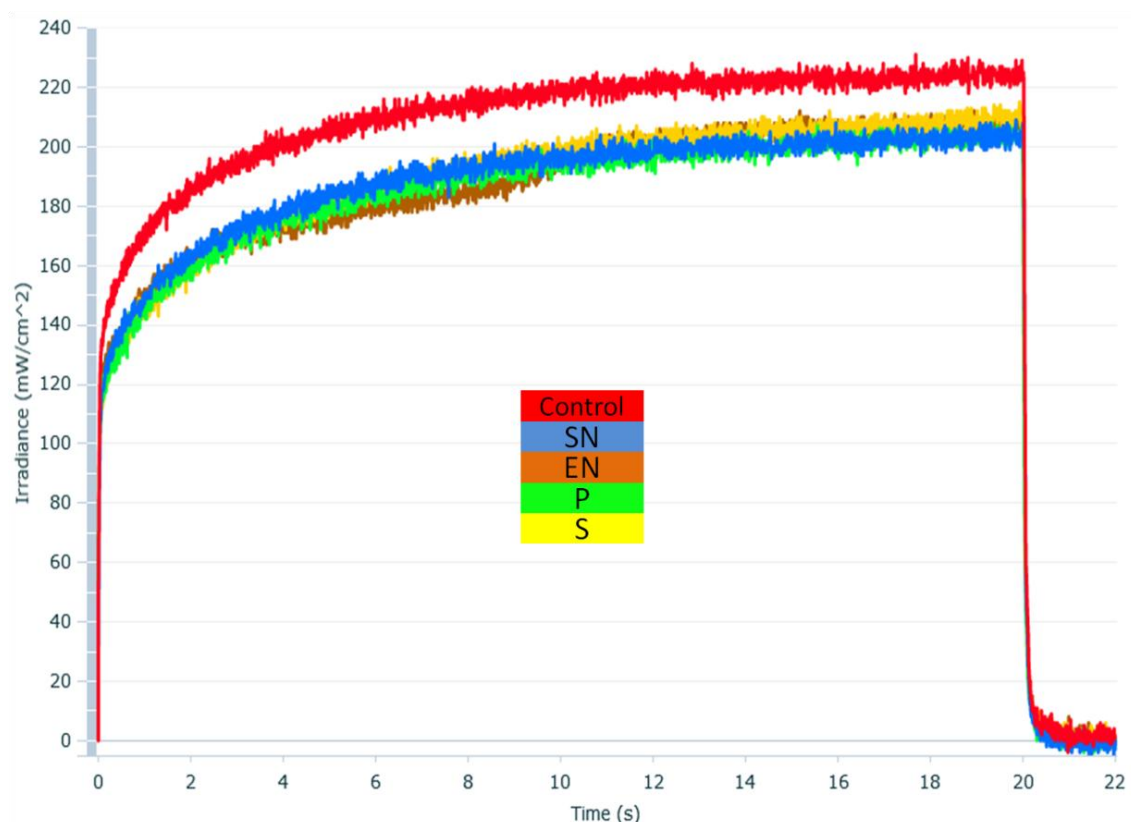


Figure 4.4: Graph showing the irradiance versus time for one representative specimen of each group during direct light curing (20s).

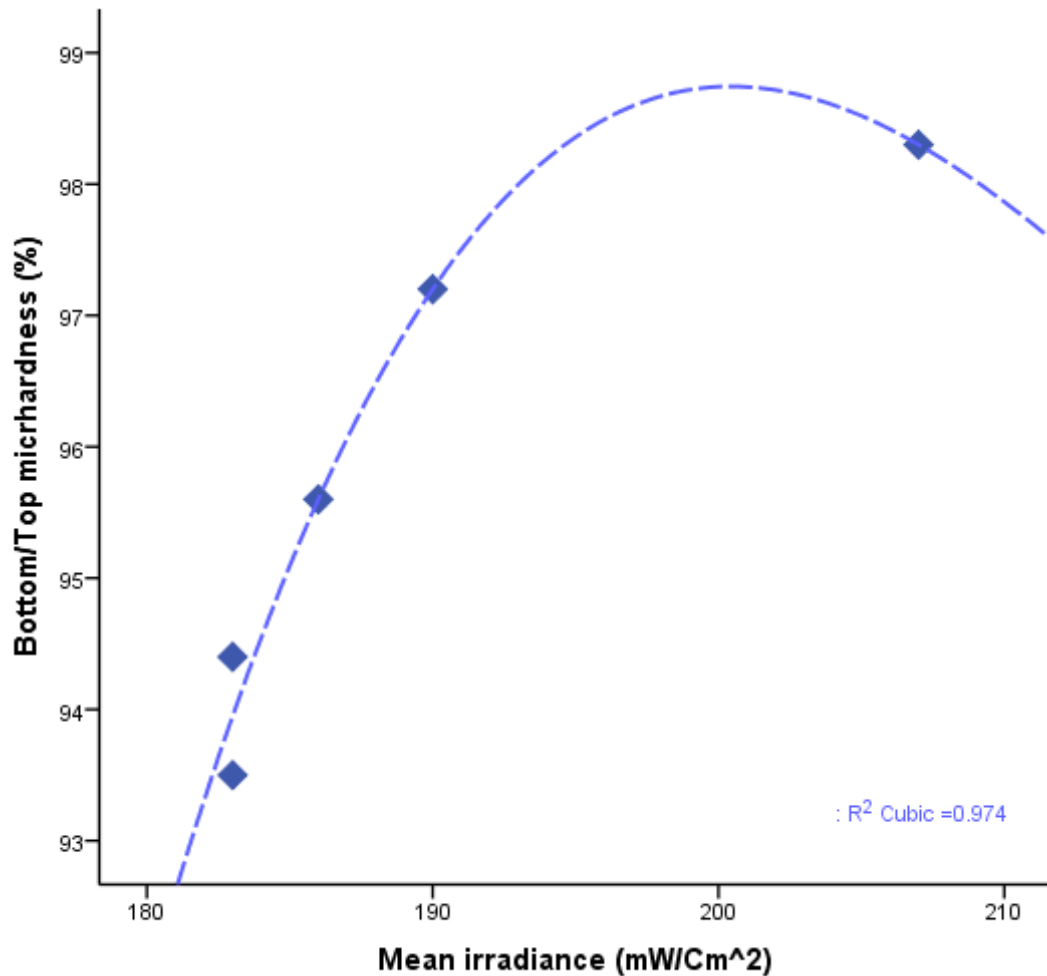


Figure 4.5: Scatter plot showing the positive correlation between the mean irradiance values and the bottom/top hardness ratio for all tested groups (R^2 Cubic= 0.974). This plot explains that the bottom/top VHN ratio, as an indicator of the depth of cure, tends to increase exponentially as a consequence of increasing irradiance value transmitted to specimen bottom surface. Such correlation concurs the idea that the incorporation of FRC within PRC tends to reduce depth of cure (bottom/top VHN ratio) by reducing the irradiance level transmitted to specimen bottom surface. Even at higher levels of irradiance, the consequential increase in VHN ratio plateaus out, owing to many factors affecting the degree of conversion within the bottom surface, including material type, distribution and quantity of fillers, quantity of photoinitiator, translucency and thickness of specimen, which can hinder any further light transmittance or material polymerization.

4.5 DISCUSSION:

This study was designed to demonstrate the consequence of incorporating FRC within bulk-fill material on microhardness and light transmittance. The first null hypothesis was rejected as FRC groups were found to have a significant influence on initial and post-cure VHN. All specimens incorporated with FRC also exhibited significantly improved top and bottom VHN compared with the control, which can be attributed to the effect of additional filler content.

As confirmed in the literature, increasing filler content in conventional RBCs enhances mechanical properties, such as flexural strength, fracture toughness and microhardness [6, 17, 43, 44]. However, this increase could be detrimental for light transmittance and thus depth of cure [1, 16, 23]. Bulk-fill resin-composite materials, which follow the same principle, have been reported to provide superior mechanical properties with the high-filled versions, though low depth of cure compared with the low-filled versions [24, 28, 34]. Accordingly, in the present study, one bulk-fill material was chosen, which had the highest filler content (86 wt%) on the market, to prepare all specimens and investigate the influence of adding further fillers in fibre form. The results reported for the unreinforced (control) group in this study (63.3-75.2 VHN) were comparable to those reported in a previous study investigating the same material (70 VHN) [28]. A significant improvement in VHN was also reported as a consequence of FRC incorporation. Top and bottom VHN significantly increased with the presence of additional reinforcing FRC layer, which is attributed to the resultant increase in filler content. This finding agrees with a previous study investigating the mechanical properties of FRC-RBC material and explaining that the improvement in strength is a result of the increase in filler fraction [45].

The current study also showed that 48h water storage significantly increased VHN for all groups regardless of the FRC used ($p < 0.001$). This finding is consistent with many previous studies reporting an improvement in the VHN over a period of 1h up to one week of post-cure storage at 37°C [34, 42, 46]. Such improvement in VHN is attributed to post-irradiation polymerization which tends to increase the cross-linking reaction and degree of conversion within the resin matrix [3, 34, 42, 47]. The choice of water as a storage medium is also influential since it causes sorption and hygroscopic expansion, which can cumulatively increase deterioration rate and reduce strength [39, 47, 48]. However, the current study reported no harm for such short term water storage on VHN,

which seems to be neutralised by post-irradiation polymerization. Moreover, the presence of FRC seems to have no influence on post-cure polymerization as the mean increase percentages in post-cure microhardness were comparable for both reinforced (15%) and control groups (16 %).

Consistent with many previous studies investigating the microhardness and depth of cure for bulk-fill RBCs [24, 27, 28, 34, 39], the present study showed that the VHN for the top surface was higher than that for the bottom surface at 3mm thickness, with the bottom/top hardness ratio exceeding 90% for all specimens. In comparison with the minimal acceptable ratio (80%) suggested in the literature for light-cured RBCs [39, 40, 42], the high ratio reported herein indicates adequate light transmittance in all tested groups. It can also be inferred that the incorporated FRC layer generally has no significant influence on the depth of cure of bulk-fill composites. This finding is in good agreement with a recent study investigating the curing behaviour of commercial bulk-fill FRC and reporting an effective depth of cure up to 6mm with 20s light-curing cured [49]. Another previous study investigating the microhardness and depth of cure of experimental FRC, have also demonstrated comparable values to those of control RBC when a longer curing time (40s) was performed [38]. The statistical analysis comparing the initial top and bottom surface VHN in the present study showed a significant difference for all FRC groups ($p < 0.001$), while the difference in control group was found non-significant ($p = 0.104$). This indicates that FRCs can slightly attenuate light transmittance through the bulk of specimen irrespective of their orientation or type. Analysis of the bottom/top VHN ratio among the groups was also supportive for this finding as the control group exhibited a significantly higher ratio than FRC groups; hence the second null hypothesis rejected.

The results of the irradiance test show that all groups had a significant difference in the mean I_R and E_T values, which supports the rejection of the third null hypothesis. Lower I_R and E_T values were detected for the reinforced specimens in relation to the control, indicating that the incorporation of FRC has a negative influence on light transmittance. Similar results have been previously reported in the literature with the incorporation of short random reinforcing-fibres that enhanced light scattering and reduced depth of cure [38, 49]. The depth of cure of RBC light-cured through a layer of unidirectional FRC has also reduced in a previous study [37], and a longer irradiation time to compensate for the light attenuation has been suggested. All such findings can be explained by understanding the physics of light transmittance.

According to the Beer-Lambert Law [11, 12], some scattering and absorption occurs when a beam of light is transmitted through a material, such as RBC. This was evident in the current study by the substantial difference (80%) in the light intensity between the baseline (1032 mW/cm^2) and during specimen curing (207 mW/cm^2). Additional scattering and absorption happen due to the presence of FRC layer that tends to introduce a barrier with a mismatching reflective index along the path of light, leading to less irradiance delivered to the bottom surface in a given time [11-13, 37]. This reduction in irradiance means that there would be less energy available at the bottom surface to initiate polymerization, in comparison with the top surface, which also explains the significant difference between top and bottom VHN in FRC groups.

Analysis of the irradiance (Figure 4.4) for different groups also explains these findings. The spectrums of FRC groups had a tendency to follow a similar path and reach a lower level of maximum irradiance compared with that of the control group. The 'plateau' status of irradiance was also reached later in all FRC curves, suggesting that more irradiation time is needed to compensate for light attenuation and reach the same level of polymerisation as the control. It can be also noted that the use of 20s light-curing time is sufficient to reach an effective polymerisation for the whole depth of specimens even with FRC incorporation.

The fourth null hypothesis was also rejected as a strong correlation (Pearson correlation coefficient (r) = 0.876, $p=0.052$) was found between the I_R values and corresponding bottom/top VH ratio for all groups. A tendency toward higher microhardness ratio with higher I_R value was also seen in the positive cubic relationship detected ($R^2=0.767$). In the control group, bottom surfaces tend to receive I_R and E_T comparable to those received by top surfaces; hence the highest bottom/top VHN ratio. In contrast, the incorporated unidirectional FRC in Group S tends to reduce light transmittance and energy delivered to bottom surfaces, leading to reduced DC and bottom/top VHN ratio.

The orientation of FRC was also found to have an influence on light transmittance. Comparing the VHN ratio and I_R values among FRC groups, the bidirectional FRCs used in SN and EN groups seem to enable deeper light transmittance than woven (Group P) and unidirectional FRC (Group S) despite the non-significant difference. The relatively high I_R values for the bidirectional FRC groups indicate that the light is less attenuated, in comparison with the other FRC groups, with a higher amount of energy delivered to the bottom surface and higher bottom/top VHN ratios. The densely

compacted microstructure observed for unidirectional and woven FRCs [50], in addition to the large thickness in relation bidirectional FRC, are potential explanations for the degree of light attenuation. In terms of the influence of FRC orientation on microhardness, the findings were inconclusive. Group SN with bidirectional FRC was found to have a significantly higher initial top VHN than other groups. However, no significant difference in post-cure VHN was detected among FRC groups.

This study followed a unique protocol to investigate the correlation between surface hardness and irradiance. However, it has some limitations. Ideally, the same specimen should be prepared and tested for its irradiance, initial VHN and post-cure VHN successively. Nevertheless, different specimens were used herein in order to standardize the time between light curing and immediate VHN measurement, and to avoid measuring already deformed areas in the successive tests following 48h water storage.

Overall, the incorporation of fibre within the bulk-fill RBC increased filler fraction and so improved the initial and post-cure VHN. Nevertheless, the degree of improvement in post-cure VHN was not dependent on the incorporated FRC since a comparable improvement was observed in the control group after storage. Light transmittance was also significantly influenced by FRC as reduced bottom/top VH ratios, mean I_R and E_T values were detected in FRC groups. From a clinical perspective, the incorporation of FRC within bulk-fill RBC might be a potential option to further improve mechanical properties without affecting aesthetics and DC. Though, longer curing time is required to compensate for the light attenuation and energy lost. Using FRC with bidirectional orientation is advocated as it tends to increase microhardness and allow better light transmittance.

4.6 CONCLUSIONS:

Within the limitations of this study, the following can be concluded:

- 1- FRC incorporation and post-cure storage significantly improve the top and bottom VHN for bulk-fill RBC.
- 2- The extent of improvement in post-cure VHN is not influenced by the incorporated FRC.
- 3- FRC incorporation significantly reduces irradiance and energy levels delivered to the bottom surface of RBC, and so a longer irradiation time is needed to achieve adequate polymerisation.
- 4- A strong relationship exists between bottom/top VHN ratio and irradiance delivered to the bottom surface of bulk-fill RBC.

4.7 REFERENCES:

1. dos Santos GB, Alto RV, Filho HR, da Silva EM, Fellows CE. Light Transmission on Dental Resin Composites. *Dent Mater*, 2008; **24**: 571-576.
2. Santini A, Gallegos IT, Felix CM. Photoinitiators in Dentistry: A Review. *Prim Dent J*, 2013; **2**: 30-33.
3. Alshali RZ, Silikas N, Satterthwaite JD. Degree of Conversion of Bulk-Fill Compared to Conventional Resin-Composites at Two Time Intervals. *Dent Mater*, 2013; **29**: e213-217.
4. Ikemura K, Endo T. A Review of the Development of Radical Photopolymerization Initiators Used for Designing Light-Curing Dental Adhesives and Resin Composites. *Dent Mater J*, 2010; **29**: 481-501.
5. Guiraldo RD, Consani S, Consani RL, Berger SB, Mendes WB, Sinhoreti MA, Correr-Sobrinho L. Comparison of Silorane and Methacrylate-Based Composite Resins on the Curing Light Transmission. *Braz Dent J*, 2010; **21**: 538-542.
6. Kim KH, Ong JL, Okuno O. The Effect of Filler Loading and Morphology on the Mechanical Properties of Contemporary Composites. *J Prosthet Dent*, 2002; **87**: 642-649.
7. Finan L, Palin WM, Moskwa N, McGinley EL, Fleming GJP. The Influence of Irradiation Potential on the Degree of Conversion and Mechanical Properties of Two Bulk-Fill Flowable Rbc Base Materials. *Dent Mater*, 2013; **29**: 906-912.
8. Van Ende A, De Munck J, Van Landuyt KL, Poitevin A, Peumans M, Van Meerbeek B. Bulk-Filling of High C-Factor Posterior Cavities: Effect on Adhesion to Cavity-Bottom Dentin. *Dent Mater*, 2013; **29**: 269-277.
9. Ferracane JL. Elution of Leachable Components from Composites. *J Oral Rehabil*, 1994; **21**: 441-452.
10. Pianelli C, Devaux J, Bebelman S, Leloup G. The Micro-Raman Spectroscopy, a Useful Tool to Determine the Degree of Conversion of Light-Activated Composite Resins. *J Biomed Mater Res*, 1999; **48**: 675-681.
11. Watts DC, Cash AJ. Analysis of Optical Transmission by 400-500 Nm Visible Light into Aesthetic Dental Biomaterials. *J Dent*, 1994; **22**: 112-117.
12. Emami N, Sjö Dahl M, Söderholm K-JM. How Filler Properties, Filler Fraction, Sample Thickness and Light Source Affect Light Attenuation in Particulate Filled Resin Composites. *Dent Mater*, 2005; **21**: 721-730.
13. Shortall AC, Palin WM, Burtscher P. Refractive Index Mismatch and Monomer Reactivity Influence Composite Curing Depth. *J Dent Res*, 2008; **87**: 84-88.
14. Leprince JG, Leveque P, Nysten B, Gallez B, Devaux J, Leloup G. New Insight into the "Depth of Cure" of Dimethacrylate-Based Dental Composites. *Dent Mater*, 2012; **28**: 512-520.
15. Kramer N, Lohbauer U, Garcia-Godoy F, Frankenberger R. Light Curing of Resin-Based Composites in the LED Era. *Am J Dent*, 2008; **21**: 135-142.
16. Arikawa H, Kanie T, Fujii K, Takahashi H, Ban S. Effect of Filler Properties in Composite Resins on Light Transmittance Characteristics and Color. *Dent Mater J*, 2007; **26**: 38-44.
17. Li Y, Swartz ML, Phillips RW, Moore BK, Roberts TA. Materials Science Effect of Filler Content and Size on Properties of Composites. *J Dent Res*, 1985; **64**: 1396-1403.

18. Gaglianone LA, Lima AF, Araujo LS, Cavalcanti AN, Marchi GM. Influence of Different Shades and LED Irradiance on the Degree of Conversion of Composite Resins. *Braz Oral Res*, 2012; **26**: 165-169.
19. Guiraldo RD, Consani S, Consani RL, Berger SB, Mendes WB, Sinhoreti MA. Light Energy Transmission through Composite Influenced by Material Shades. *Bull Tokyo Dent Coll*, 2009; **50**: 183-190.
20. Haenel T, Hausnerová B, Steinhaus J, Price RBT, Sullivan B, Moeginger B. Effect of the Irradiance Distribution from Light Curing Units on the Local Micro-Hardness of the Surface of Dental Resins. *Dent Mater*, 2015; **31**: 93-104.
21. Ilie N, Bucuta S, Draenert M. Bulk-Fill Resin-Based Composites: An in Vitro Assessment of Their Mechanical Performance. *Oper Dent*, 2013; **38**: 618-625.
22. Rahiotis C, Patsouri K, Silikas N, Kakaboura A. Curing Efficiency of High-Intensity Light-Emitting Diode (LED) Devices. *J Oral Sci*, 2010; **52**: 187-195.
23. Bhamra GS, Fleming GJP, Darvell BW. Influence of LED Irradiance on Flexural Properties and Vickers Hardness of Resin-Based Composite Materials. *Dent Mater*, 2010; **26**: 148-155.
24. Ilie N, Stark K. Curing Behaviour of High-Viscosity Bulk-Fill Composites. *J Dent*, 2014; **42**: 977-985.
25. Ilie N, Keßler A, Durner J. Influence of Various Irradiation Processes on the Mechanical Properties and Polymerisation Kinetics of Bulk-Fill Resin Based Composites. *J Dent*, 2013; **41**: 695-702.
26. Bucuta S, Ilie N. Light Transmittance and Micro-Mechanical Properties of Bulk Fill vs. Conventional Resin Based Composites. *Clin Oral Investig*, 2014; **18**: 1991-2000.
27. Czasch P, Ilie N. In Vitro Comparison of Mechanical Properties and Degree of Cure of Bulk Fill Composites. *Clin Oral Investig*, 2013; **17**: 227-235.
28. Leprince JG, Palin WM, Vanacker J, Sabbagh J, Devaux J, Leloup G. Physico-Mechanical Characteristics of Commercially Available Bulk-Fill Composites. *J Dent*, 2014; **42**: 993-1000.
29. El-Damanhoury H, Platt J. Polymerization Shrinkage Stress Kinetics and Related Properties of Bulk-Fill Resin Composites. *Oper Dent*, 2014; **39**: 374-382.
30. Marovic D, Taubock TT, Attin T, Panduric V, Tarle Z. Monomer Conversion and Shrinkage Force Kinetics of Low-Viscosity Bulk-Fill Resin Composites. *Acta Odontol Scand*, 2014: 1-7.
31. Moorthy A, Hogg CH, Dowling AH, Grufferty BF, Benetti AR, Fleming GJ. Cuspal Deflection and Microleakage in Premolar Teeth Restored with Bulk-Fill Flowable Resin-Based Composite Base Materials. *J Dent*, 2012; **40**: 500-505.
32. Scotti N, Comba A, Gambino A, Paolino DS, Alovise M, Pasqualini D, Berutti E. Microleakage at Enamel and Dentin Margins with a Bulk Fills Flowable Resin. *Eur J Dent*, 2014; **8**: 1-8.
33. Roggendorf MJ, Kramer N, Appelt A, Naumann M, Frankenberger R. Marginal Quality of Flowable 4-mm Base vs. Conventionally Layered Resin Composite. *J Dent*, 2011; **39**: 643-647.
34. Alshali RZ, Salim NA, Satterthwaite JD, Silikas N. Post-Irradiation Hardness Development, Chemical Softening, and Thermal Stability of Bulk-Fill and Conventional Resin-Composites. *J Dent*, 2015; **43**: 209-218.
35. Margeas RC. Bulk-Fill Materials: Simplify Restorations, Reduce Chairtime. *Compend Contin Educ Dent*, 2015; **36**: e1-4.

36. Vallittu PK. Flexural Properties of Acrylic Resin Polymers Reinforced with Unidirectional and Woven Glass Fibers. *J Prosthet Dent*, 1999; **81**: 318-326.
37. Fennis WM, Ray NJ, Creugers NH, Kreulen CM. Microhardness of Resin Composite Materials Light-Cured through Fiber Reinforced Composite. *Dent Mater*, 2009; **25**: 947-951.
38. Garoushi S, Vallittu PK, Lassila LV. Depth of Cure and Surface Microhardness of Experimental Short Fiber-Reinforced Composite. *Acta Odontol Scand*, 2008; **66**: 38-42.
39. Alrahlah A, Silikas N, Watts DC. Post-Cure Depth of Cure of Bulk Fill Dental Resin-Composites. *Dent Mater*, 2014; **30**: 149-154.
40. Flury S, Hayoz S, Peutzfeldt A, Hüsler J, Lussi A. Depth of Cure of Resin Composites: Is the Iso 4049 Method Suitable for Bulk Fill Materials? *Dent Mater*, 2012; **28**: 521-528.
41. Aguiar FH, Andrade KR, Leite Lima DA, Ambrosano GM, Lovadino JR. Influence of Light Curing and Sample Thickness on Microhardness of a Composite Resin. *Clin Cosmet Investig Dent*, 2009; **1**: 21-25.
42. Watts DC, Amer OM, Combe EC. Surface Hardness Development in Light-Cured Composites. *Dent Mater*, 1987; **3**: 265-269.
43. Willems G, Lambrechts P, Braem M, Celis JP, Vanherle G. A Classification of Dental Composites According to Their Morphological and Mechanical Characteristics. *Dent Mater*, 1992; **8**: 310-319.
44. Braem M, Finger W, Van Doren VE, Lambrechts P, Vanherle G. Mechanical Properties and Filler Fraction of Dental Composites. *Dent Mater*, 1989; **5**: 346-349.
45. Garoushi S, Lassila LV, Tezvergil A, Vallittu PK. Load Bearing Capacity of Fibre-Reinforced and Particulate Filler Composite Resin Combination. *J Dent*, 2006; **34**: 179-184.
46. Marghalani HY. Post-Irradiation Vickers Microhardness Development of Novel Resin Composites. *Mat Res*, 2010; **13**: 81-87.
47. Truffier-Boutry D, Demoustier-Champagne S, Devaux J, Biebuyck J-J, Mestdagh MI, Larbanois P, Leloup Gt. A Physico-Chemical Explanation of the Post-Polymerization Shrinkage in Dental Resins. *Dent Mater*, 2006; **22**: 405-412.
48. Milleding P, Ahlgren F, Wennerberg A, Ortengren U, Karlsson S. Microhardness and Surface Topography of a Composite Resin Cement after Water Storage. *Int J Prosthodont*, 1998; **11**: 21-26.
49. Li X, Pongprueksa P, Van Meerbeek B, De Munck J. Curing Profile of Bulk-Fill Resin-Based Composites. *J Dent*, 2015.
50. Karbhari VM, Strassler H. Effect of Fiber Architecture on Flexural Characteristics and Fracture of Fiber-Reinforced Dental Composites. *Dent Mater*, 2007; **23**: 960-968.

**Chapter 5: Effect of Fibre-Reinforcement and
Orientation on the Edge-Strength of Direct Resin
Composites**

5.1 ABSTRACT:

Objectives: To evaluate the effect of incorporating differently-oriented fibre-reinforced composites (FRCs) on the edge-strength of direct particulate-reinforced composites (PRCs).

Methods: Forty five rectangular-shaped specimens (12.5 x 4 x 2 mm) made of different FRC-PRC combinations were allocated into three equal groups (n=15): GD (*Grandio, Voco*), HT (*Herculite Ultra, Kerr*) and XB (*X-tra base, Voco*). Each group was subdivided into three subgroups (n=5) according to the incorporated FRC. Subgroups X and B were reinforced with unidirectional (*Everstick C&B, Stick Tech Ltd*) and bidirectional (*Everstick Net, Stick Tech Ltd*) E-glass FRCs respectively, while subgroup C had no fibre reinforcement (control). Specimens were tested with an edge-strength machine (*CK10, Engineering Systems*) by applying compressive load (1 mm/min crosshead speed) at 0.5mm from the margin. The force-to-failure (N) was recorded and two readings were obtained per specimens. Two-way ANOVA and Tukey's post hoc tests were used to detect any significant difference among groups ($\alpha=0.05$).

Results: The edge strength value (N) significantly improved after the incorporation of FRC in all groups ($p<0.05$). XB_B had the highest edge strength value (420.2 ± 47.5 N), while GD_C had the lowest (38.7 ± 3.9 N). A Significant difference ($p<0.05$) in the edge strength values was found among the groups irrespective of the incorporated FRC. FRC orientation had a significant influence on the edge-strength ($p<0.001$).

Conclusions: Incorporating FRC improves the edge strength for all PRCs. The degree of this improvement is dependent on PRC type and FRC orientation. Bidirectional FRC tends to improve the edge strength better than unidirectional FRC.

5.2 INTRODUCTION:

In the modern era of metal-free dentistry, there is a growing tendency toward using metal-free restorative alternatives that provide not only excellent aesthetics but also enable superior durability. Fibre-reinforced composite (FRC) is one of such alternatives that allows favourable reinforcement of several materials without compromising their aesthetics [1-7].

FRC is a polymeric composite material composed primarily of fillers embedded in a resin matrix. In contrast to the widely used particulate-reinforced composite (PRC), the fillers in FRC are in form of fibres, long or short, rather than traditional particles [6, 8, 9]. This modification in filler form is intended to improve the physic–mechanical properties of PRCs and expand their clinical applications, especially under high-demanding oral conditions [10-12]. Previous studies have confirmed some enhancements in strength and durability of PRC once reinforced with FRC [12-22]. However, most of these enhancements have been proven *in-vitro* using the ISO-4049 standards, which are designed to examine the strength of relatively large surface areas and preclude edges. From a clinical perspective, this is not always relevant as the strength of restoration edge, or the so-called marginal integrity, can be crucial for restoration longevity, especially when minimal material thickness is employed [23, 24].

Restorative materials are relatively weaker at the edge, in comparison with other places [8]. The edge also tends to be highly-susceptible to temperature changes and frequent mechanical loadings that promote fracture [25]. In view of this, clinical precautions to avoid materials being loaded at their margins are always advisable. Nevertheless, this is not always achievable, especially when margins are subjected to heavy unanticipated eccentric loading that would disrupt the integrity and cause fracture [26]. Although marginal fracture is often a minimal chipping and could cause no detrimental effect on restoration retention, the resulted disruption in marginal integrity alone might have several negative consequences. Marginal microleakage, tooth sensitivity, secondary caries, staining and aesthetic problems, as well as increasing the tendency of catastrophic marginal fracture, are all complications that would necessitate clinical intervention [26, 27]. Therefore, it is essential to use a restorative material that offers not only excellent bulk strength but also allows superior marginal integrity.

The marginal integrity of restorative materials can be investigated *in-vitro* by using the concept of edge-strength. This concept indicates the ability of material fine margins to

resist fracture [26-29], and predicts how marginal integrity would be maintained upon loading *in-vivo* [29, 30]. It is mainly influenced by material strength as well as other experimental factors. [25-28, 31-34].

As FRC has the ability to improve the strength of PRCs [35], it can be hypothesized that it would also enhance the edge strength. To date, one study has investigated this assumption on indirect PRCs, and reported an enhancement in the edge strength [27]. Therefore, the aims of this study were i) to measure and compare the edge-strength of three commercial direct PRCs reinforced with differently-oriented FRCs, and ii) to investigate the effect of ‘FRC orientation’ and ‘PRC type’. Two null hypotheses were formulated: i) FRC and its orientation have no significant effect on the edge-strength, and ii) material type reinforced has no significant influence on edge strength or reinforcement efficiency effectiveness of reinforcement.

5.3 MATERIALS AND METHODS:

Three commercial direct PRCs, representative of three different categories, were reinforced with two differently-oriented FRCs and assessed for their edge-strength. Descriptions of all the materials used, their composition and manufacturer are listed in Table 5.1.

Table 5.1: Materials used to prepare all specimens.

Materials	Description	Composition	Lot No./ Shade	Manufacturer
Grandio® (GD)	Packable nanohybrid composite (increment-fill)	87 wt% fillers: SiO ₂ (20–50nm), glass-ceramic particles (1µm) Bis-GMA, TEGDMA.	630878 A2	<i>Voco, Cuxhaven, Germany</i>
Herculite Ultra® (HT)	Packable nanohybrid composite for Enamel replacement (Increment-fill)	78 wt% fillers: SiO ₂ (20–50nm), barium silicate glass (0.4µm), prepolymerized aggregate (30–50µm). Bis-GMA, TEGDMA, Bis-EMA	3278584 A2-Enamel	<i>Kerr, CA, USA</i>
X-tra Base® (XB)	Flowable nanohybrid composite. (Bulk-fill)	75 wt% fillers. UDMA, Bis-EMA	1208392 U	<i>Voco, Cuxhaven, Germany</i>
EverStick® C&B (U)	Unidirectional FRC	Pre-impregnated unidirectional E-glass fibres, PMMA, Bis-GMA	120507V	<i>Stick Tech Ltd, Turku, Finland</i>
EverStick® Net (B)	Bidirectional FRC	Pre-impregnated bidirectional E-glass fibres, PMMA, Bis-GMA	120424	<i>Stick Tech Ltd, Turku, Finland</i>
<i>Bis-GMA: bisphenol A diglycidyl dimethacrylate, TEGDMA: triethylene glycol dimethacrylate, UDMA: urethane dimethacrylate, Bis-EMA: ethoxylated bisphenol A dimethacrylate, PMMA: poly methyl methacrylate.</i>				

5.3.1 Specimen preparation:

Forty five bar specimens (12.5 x 4 x 2 mm) were fabricated from FRC and PRC using a sectional stainless steel (SS) mould. All specimens were allocated into three equal groups (n=15) according to the used PRC. In Group GD, Grandio (*Voco*) and Herculite Ultra (*Kerr*) were respectively used to prepare specimens, while Herculite Ultra (*Kerr*) was used to prepare specimens in Group HT. In Group XB, X-tra base (*Voco*) was used to prepare the specimens. Each group was further divided into three subgroups according to the incorporated FRC. Specimens in subgroup C (Control) were made purely of PRC with no fibre reinforcement, while pre-impregnated unidirectional (*Everstick C&B, Stick Tech Ltd*) and bidirectional (*Everstick Net, Stick Tech Ltd*) E-glass FRCs were used to reinforce specimens in Subgroup U and B, respectively.

All the tested specimens were prepared using a standardised layering technique. After the application of a separating medium (petroleum jelly) to the mould, an initial increment of PRC (0.5mm thickness) was packed into the base. The designated intermediate FRC layer was then incorporated and spread to the entire area to ensure

appropriate adaptation prior to light curing (40s). The final PRC increment was subsequently adapted using glass slide and pressure on the top of the mould before being light-cured for another 40 seconds. All specimens were cured using the same handheld curing device (*Optilux-501, Optilux, Demetron, USA*) with an irradiance output of 540 mW/cm². After curing, all specimens were abraded with 800 grit silicon carbide sandpaper to remove any excess flash and then stored in distilled water (37 °C) for one week prior to testing.

5.3.2 Edge strength testing:

Specimens were dried for 1h at room temperature (22±1°C) prior to testing. The measurement of edge-strength was executed using CK10 instrument (*Engineering Systems, Nottingham, UK*). A customized specimen locator made of epoxy resin was employed to ensure standardized positioning among specimens. A Vickers diamond indenter was used to apply vertical compressive load (1 mm/min crosshead speed) to the top surface of each specimen at 0.5mm distance from each edge, and the force-to-failure (N) was recorded. Two measurements per specimen were taken and the mean value was calculated.

5.3.3 Fractography:

The mode of failure for each specimen was microscopically examined under magnification (x40) using an optical microscope (*Meiji EMZ-TR, Meiji Techno Co. Ltd, Tokyo, Japan*). Three patterns of fracture were observed and classified accordingly into: i) minimal chipping, ii) edge fracture and iii) edge fracture with bulk cracking (Figure 5.2, Figure 5.3 and Figure 5.4).

5.3.4 Statistical analysis:

All data were collected and analysed statistically using SPSS software (*SPSS 19.0, SPSS Statistics, SPSS Inc., Chicago, IL, USA*). A series of one-way and two-way ANOVA followed by Tukey's post hoc were used to detect the significance of experimental factors on the edge-strength ($\alpha=0.05$). Size effect calculations were performed to assess effectiveness of fibre reinforcement, and the effect-size correlation (r_{YX}) and Cohen's d were reported for each reinforced subgroup.

5.4 RESULTS:

The mean force-to-failure (N) and standard deviation for each tested group is shown in Table 5.2, and presented graphically in Figure 5.1. The mode of failure for each tested specimen is reported in Table 5.3. Three representative fractured specimens demonstrating the different failure modes are shown in Figure 5.2 and Figure 5.3.

Table 5.2 : Mean (SD) edge-strength values (N) for all groups.			
PRC	FRC orientation		
	Control (C)	Unidirectional (U)	Bidirectional (B)
GD: Grandio	38.7±3.9 ^{a,1}	56.8±5.9 ^{a,2}	67.7±8.2 ^{a,3}
HT: Herculite	82.3±6.4 ^{b,1}	89.8±10.6 ^{b,1,2}	105.4±17.0 ^{b,2}
XB: X-tra Base	255.7±39.5 ^{c,1}	186.7±28.3 ^{c,2}	420.2±47.5 ^{c,3}

** Different superscripts letters and numbers indicate statistical significance (p<0.05) within the same column and row, respectively.*

Table 5.3: The mode of fracture for all groups.

Fracture mode	Grandio			Herculite			X-tra Base		
	GD_C	GD_U	GD_B	HT_C	HT_U	HT_B	XB_C	XB_U	XB_B
<i>Minimal chipping</i>	8	7	4	8	6	8	-	-	-
<i>Edge fracture</i>	2	3	6	2	4	4	4	1	3
<i>Edge and bulk fracture</i>	-	-	-	-	-	-	6	9	7

XB had the highest edge strength values with ‘edge/bulk fracture’ as the main mode of failure, while GD had the lowest values with ‘minimal chipping’ as the main fracture mode. Subgroup B exhibited the highest edge strength values in all three groups. Both experimental factors (FRC orientation and PRC type) had a significant influence on the edge strength ($p < 0.001$).

The effect size parameters for both FRC types in each main group are reported in Table 5.4. Both FRCs exhibited a large effect on the edge strength but bidirectional FRC had the most effect. For the same FRC, different size effect values were found between the main groups. Bidirectional FRC had the highest effect when combined with GD. Unidirectional FRC exhibited a positive effect when combined with GD and HT, whereas it showed a negative effect with XB.

Table 5.4: The efficiency of different fibre reinforcement represented by Cohn’s d ($r_{y\lambda}$) values for every main group.

FRC orientation	GD	HT	XB
Unidirectional	3.62(0.875)	0.86(0.393)	-2.00(-0.708)
Bidirectional	4.50(0.913)	1.80(0.668)	3.77(0.883)

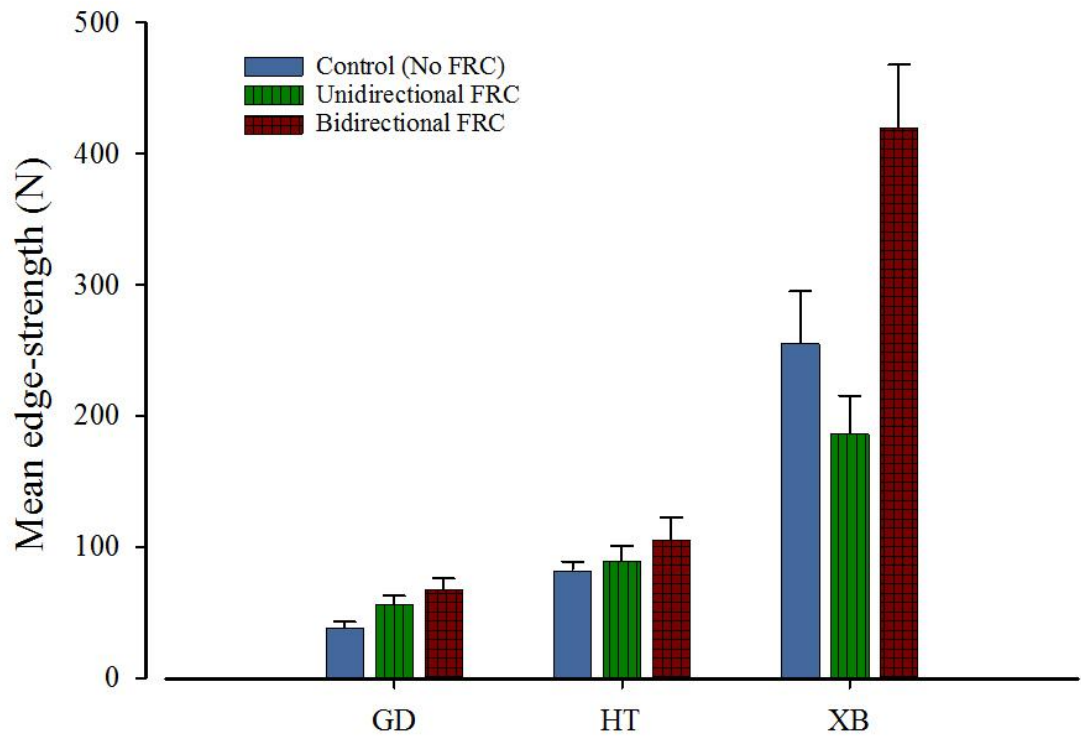


Figure 5.1: Bar chart showing the mean (SD) edge strength for all tested groups.

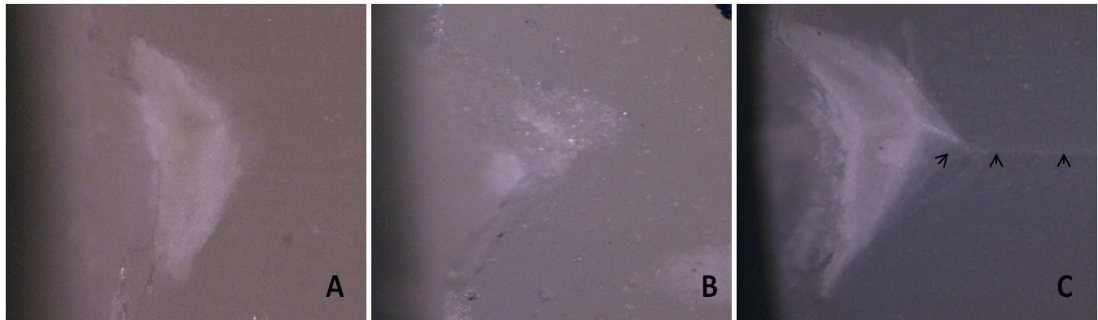


Figure 5.2: Mode of failure for three representative specimens (top view where the load was perpendicularly applied), A) minimal chipping, B) edge fracture and C) edge/bulk fracture. Arrow head \blacktriangleright indicates crack propagation within specimen bulk.

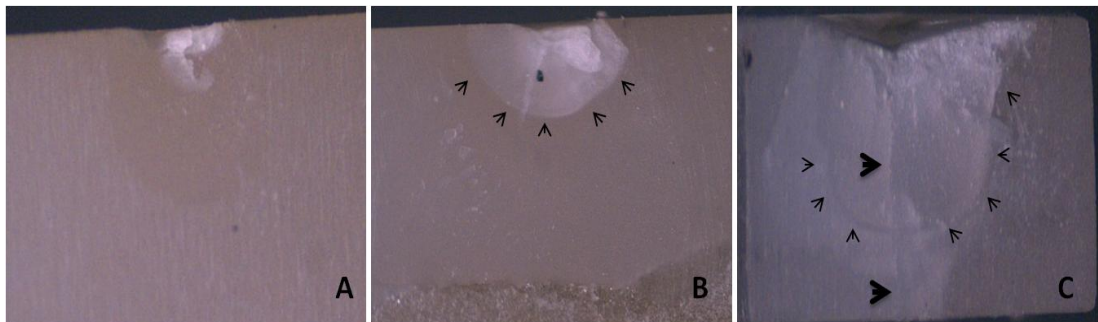


Figure 5.3: Mode of failure for three representative specimens (side view of specimen edge), A) minimal chipping, B) edge fracture and C) edge/bulk fracture. Large arrow head \blacktriangleright indicates crack propagation within specimen bulk. Small arrow head \blacktriangleright indicates fracture line at edge surface.

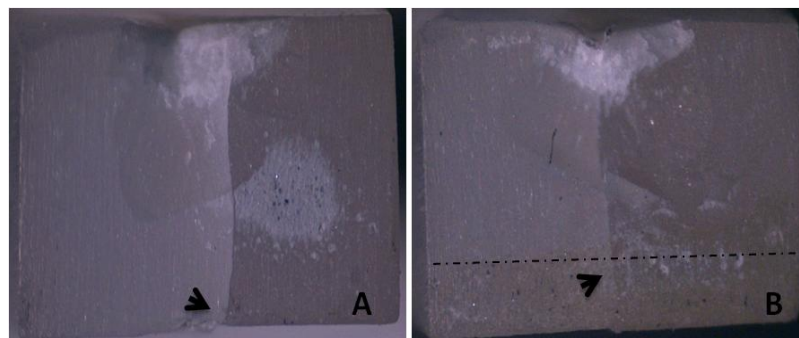


Figure 5.4: Two representative fractured specimens made of XB with A) no reinforcement (control) and B) unidirectional FRC.

5.5 DISCUSSION:

The reinforcement of resin-composites by using an intermediate FRC layer has been advocated in the literature to enhance mechanical properties [7, 12]. Many authors have confirmed this positive enhancement in terms of flexural strength, modulus of elasticity and fracture toughness [2, 6, 15-20]. However, the effect of such reinforcement on marginal integrity has not been investigated. Accordingly, this study aimed to examine the influence of fibre reinforcement on the edge-strength of resin composite materials.

The first null hypothesis was rejected since the results showed a statistically significant difference ($p < 0.05$) between the reinforced and unreinforced subgroups. All groups exhibited an improvement in edge-strength as a consequence of incorporating FRC, which means that fibre reinforcement has a positive influence on the edge strength irrespective of PRC type. This improvement can be explained by the fact that the presence of reinforcing-fibres within a resin-composite material enhances the overall strength by altering stress dynamics and increasing filler size and fraction [8, 21, 24, 36, 37]. Owing to their small diameter and preferential microstructure alignment, reinforcing-fibres can reduce crack propagation and enhance stress distribution when tested under a three-point bending configuration [2, 8, 21]. The same principle can be applied to the edge-strength testing as the compressive load seems to be partially absorbed by the incorporated FRC layer, which acts as a stress breaker to reduce crack propagation. An increased filler fraction also results from the incorporation of FRC, leading to an improvement in material toughness and edge strength [3, 27, 33]. This is also consistent with previous studies confirming the dependency of marginal integrity on material toughness, filler size and content [25], and reporting a lesser degree of marginal deterioration with the coarser and more heavily-filled composite materials [26, 28, 30, 33, 38].

The present study also found that FRC orientation has a significant influence on edge strength. A significant difference was detected between the reinforced subgroups in GD ($p = 0.043$) and XB ($p < 0.001$) but not in HT ($p = 0.147$). Subgroup B had higher edge strength and effect size values than subgroup U in all main groups, which indicates that bidirectional FRC tends to reinforce material margins better than unidirectional FRC. Such a variation in values can be explained by the dissimilar levels of anisotropy induced as a consequence of different fibre orientation [8]. Unidirectional reinforcing-fibres induce anisotropic properties within polymeric materials [24], which means that

mechanical properties are altered according to the direction of loading, and the reinforcement is mainly in one plane. In contrast, bidirectional reinforcing-fibres induce orthotropic properties and the resultant reinforcement tend to be similar in two planes [22]. Previous studies have confirmed the superiority of unidirectional FRC under three- and four-point bending tests, and so advocated their use in applications where the direction of the highest load is known or likely to be single, like fixed partial dentures [11, 21, 22, 37, 39]. However, bidirectional FRCs have been reported to enable better toughness by acting as a crack stopper [15, 24, 35], and suggested in situations where extra toughness is mandatory, such as the margins of composite restorations [14, 40], which concurs with the findings of this study.

The second null hypothesis was also rejected as edge strength values were significantly different between the main groups ($p < 0.001$), which indicates the dependency of edge strength on PRC type. This finding coincides with previous studies which have reported dissimilarity in edge strength values corresponding to the compositional variations in fillers (size, morphology and fraction) and polymeric network [26, 28, 30, 33]. Comparing the conventional PRCs, HT exhibited better edge-strength values than GD although their filler fractions indicate the contrary (78 wt% and 87 wt% respectively). This can be explained by the variation in filler size and morphology which are more influential on edge strength than filler content [26]. GD is formulated from irregular inorganic particles and heterogenous fillers, while HT is composed of homogenous spherical particles with large aggregates [41, 42]. Irregular fillers concentrate mechanical stresses on their angles and protuberances, whereas spherical-shaped particles and large aggregates are better in stress distribution [42, 43]. Likewise, XB exhibited the highest edge-strength values between the tested PRCs although its filler fraction is the lowest. This can be attributed to the differences in other parameters such as particle size, filler density and polymeric network, which cumulatively tend to alter fracture dynamics [44]. Monomer type and content also differ in XB, which can influence the edge strength [28, 45]. Interestingly, the efficiency of fibre reinforcement was also influenced by PRC type since different size effect values were demonstrated between the main groups. FRCs exhibited the best effectiveness in GD specimens, while the least effectiveness was demonstrated in HT specimens. This variation could also be attributable to the compositional difference between PRCs as well as the variation in fracture dynamics at margins [33, 46].

Minimal chipping was the most observed fracture mode in subgroups GD_C and HT_C, while edge/bulk fracture was the most frequent failure in subgroup XB_C. However, after FRC incorporation, the main mode of fracture had changed. Edge fracture became more evident in groups GD and HT, while the frequency of edge/bulk fracture in XB had increased. These observations support the idea that the reinforcing fibres are capable of altering the fracture dynamics at the margins. However, this alteration is not always desirable. For example, the reinforcement of XB with unidirectional FRC led to significant reduction in the edge strength in comparison with the control. This reduction could be attributed to the large thickness of incorporated unidirectional fibres which considerably reduced material bulk and negatively affected crack propagation (Figure 5.4). In contrast, the minimal thickness of bidirectional FRCs favourably reinforced PRCs without reducing their bulk. Therefore, it is recommended to characterise the mechanical behaviour of a material before attempting to reinforce its margins.

Some limitations were encountered in this study. The major obstacle was to spread the unidirectional fibres evenly at the margins and the required depth as the fibres were strongly attracted to each other in the bundle form. However, a careful adaptation was performed to ensure standardized amount of fibres at the margins. Another limitation was only comparing two orientations of FRC made from the same material type (E-glass) and preimpregnated by the same manufacturer. This can limit the results obtained to that specific type of fibres. Potential studies comparing different FRC types, orientations and impregnations are suggested in the future.

Overall, the marginal integrity of direct resin-composite materials could be enhanced by incorporating FRC in their bulk. However, this enhancement is dependent on FRC orientation and material type. From a clinical perspective, incorporating FRC in composite restorations could be an option to enhance their marginal integrity, especially in situations where high masticatory force and consequent marginal deteriorations are expected. A bulk-fill PRC reinforced with bidirectional FRC seems to be the best material combination to achieve excellent marginal integrity.

5.6 CONCLUSIONS:

Within the limitations of this study the following can be concluded:

- 1- Fibre reinforcement of direct resin-composite materials significantly influences their edge strength.
- 2- The efficiency of marginal reinforcement is dependent on PRC type and FRC orientation.
- 3- Bidirectional FRC causes a significantly better marginal reinforcement than unidirectional FRC.

5.7 REFERENCES:

1. Yokoyama D, Shinya A, Lassila LV, Gomi H, Nakasone Y, Vallittu PK. Framework Design of an Anterior Fiber-Reinforced Hybrid Composite Fixed Partial Denture: A 3D Finite Element Study. *Int J Prosthodont*, 2009; **22**: 405-412.
2. van Heumen CC, Kreulen CM, Bronkhorst EM, Lesaffre E, Creugers NH. Fiber-Reinforced Dental Composites in Beam Testing. *Dent Mater*, 2008; **24**: 1435-1443.
3. Turkaslan S, Tezvergil-Mutluay A, Bagis B, Shinya A, Vallittu PK, Lassila LV. Effect of Intermediate Fiber Layer on the Fracture Load and Failure Mode of Maxillary Incisors Restored with Laminate Veneers. *Dent Mater J*, 2008; **27**: 61-68.
4. Garoushi SK, Vallittu PK, Lassila LV. Short Glass Fiber-Reinforced Composite with a Semi-Interpenetrating Polymer Network Matrix for Temporary Crowns and Bridges. *J Contemp Dent Pract*, 2008; **9**: 14-21.
5. Lassila LV, Tezvergil A, Dyer SR, Vallittu PK. The Bond Strength of Particulate-Filler Composite to Differently Oriented Fiber-Reinforced Composite Substrate. *J Prosthodont*, 2007; **16**: 10-17.
6. Garoushi S, Vallittu PK, Lassila LV. Short Glass Fiber Reinforced Restorative Composite Resin with Semi-Inter Penetrating Polymer Network Matrix. *Dent Mater*, 2007; **23**: 1356-1362.
7. van Heumen CC, Kreulen CM, Creugers NH. Clinical Studies of Fiber-Reinforced Resin-Bonded Fixed Partial Dentures: A Systematic Review. *Eur J Oral Sci*, 2009; **117**: 1-6.
8. Hull D, Clyne TW. *An Introduction to Composite Materials*. 2nd ed. Cambridge: Cambridge University Press; 1996.
9. Goldberg AJ, Burstone CJ. The Use of Continuous Fiber Reinforcement in Dentistry. *Dent Mater*, 1992; **8**: 197-202.
10. Eisenburger M, Riechers J, Borchers L, Stiesch-Scholz M. Load-Bearing Capacity of Direct Four Unit Provisional Composite Bridges with Fibre Reinforcement. *J Oral Rehabil*, 2008; **35**: 375-381.
11. Dyer SR, Sorensen JA, Lassila LV, Vallittu PK. Damage Mechanics and Load Failure of Fiber-Reinforced Composite Fixed Partial Dentures. *Dent Mater*, 2005; **21**: 1104-1110.
12. Freilich MA, Meiers JC. Fiber-Reinforced Composite Prostheses. *Dent Clin North Am*, 2004; **48**: viii-ix, 545-562.
13. Bohlsen F, Kern M. Clinical Outcome of Glass-Fiber-Reinforced Crowns and Fixed Partial Dentures: A Three-Year Retrospective Study. *Quintessence Int*, 2003; **34**: 493-496.
14. Behr M, Rosentritt M, Handel G. Fiber-Reinforced Composite Crowns and FPDs: A Clinical Report. *Int J Prosthodont*, 2003; **16**: 239-243.
15. Garoushi S, Lassila LV, Tezvergil A, Vallittu PK. Static and Fatigue Compression Test for Particulate Filler Composite Resin with Fiber-Reinforced Composite Substructure. *Dent Mater*, 2007; **23**: 17-23.
16. Dyer SR, Lassila LV, Jokinen M, Vallittu PK. Effect of Cross-Sectional Design on the Modulus of Elasticity and Toughness of Fiber-Reinforced Composite Materials. *J Prosthet Dent*, 2005; **94**: 219-226.
17. Bae JM, Kim KN, Hattori M, Hasegawa K, Yoshinari M, Kawada E, Oda Y. Fatigue Strengths of Particulate Filler Composites Reinforced with Fibers. *Dent Mater J*, 2004; **23**: 166-174.

18. Tsue F, Takahashi Y, Shimizu H. Reinforcing Effect of Glass-Fiber-Reinforced Composite on Flexural Strength at the Proportional Limit of Denture Base Resin. *Acta Odontol Scand*, 2007; **65**: 141-148.
19. Ellakwa A, Shortall A, Marquis P. Influence of Fibre Position on the Flexural Properties and Strain Energy of a Fibre-Reinforced Composite. *J Oral Rehabil*, 2003; **30**: 679-682.
20. Lassila LVJ, Nohrström T, Vallittu PK. The Influence of Short-Term Water Storage on the Flexural Properties of Unidirectional Glass Fiber-Reinforced Composites. *Biomaterials*, 2002; **23**: 2221-2229.
21. Nakamura T, Ohyama T, Waki T, Kinuta S, Wakabayashi K, Takano N, Yatani H. Finite Element Analysis of Fiber-Reinforced Fixed Partial Dentures. *Dent Mater J*, 2005; **24**: 275-279.
22. Vallittu PK. Flexural Properties of Acrylic Resin Polymers Reinforced with Unidirectional and Woven Glass Fibers. *J Prosthet Dent*, 1999; **81**: 318-326.
23. Freilich MA, Meiers JC, Duncan JP, Eckrote KA, Goldberg AJ. Clinical Evaluation of Fiber-Reinforced Fixed Bridges. *J Am Dent Assoc*, 2002; **133**: 1524-1534; quiz 1540-1521.
24. Vallittu PK. Strength and Interfacial Adhesion of FRC-Tooth System. In: *The Second International Symposium on Fibre-Reinforced Plastics in Dentistry, Symposium Book on the Scientific Workshop on Dental Fibre-Reinforced Composite on 13 October 2001*. Edited by Vallittu PK. Nijmegen, Netherlands 2001.
25. Ferracane JL, Condon JR. In Vitro Evaluation of the Marginal Degradation of Dental Composites under Simulated Occlusal Loading. *Dent Mater*, 1999; **15**: 262-267.
26. Watts DC, Issa M, Ibrahim A, Wakiaga J, Al-Samadani K, Al-Azraqi M, Silikas N. Edge Strength of Resin-Composite Margins. *Dent Mater*, 2008; **24**: 129-133.
27. Ereifej N, Silikas N, Watts DC. Edge Strength of Indirect Restorative Materials. *J Dent*, 2009; **37**: 799-806.
28. Baroudi K, Silikas N, Watts DC. Edge-Strength of Flowable Resin-Composites. *J Dent*, 2008; **36**: 63-68.
29. Kim SH, Watts DC. In Vitro Study of Edge-Strength of Provisional Polymer-Based Crown and Fixed Partial Denture Materials. *Dent Mater*, 2007; **23**: 1570-1573.
30. Hoard RJ, Eichmiller FC, Parry EE, Giuseppetti AA. Edge-Bevel Fracture Resistance of Three Direct-Filling Materials. *Oper Dent*, 2000; **25**: 182-185.
31. Quinn JB, Sundar V, Parry EE, Quinn GD. Comparison of Edge Chipping Resistance of Pfm and Veneered Zirconia Specimens. *Dent Mater*, 2010; **26**: 13-20.
32. Quinn J, Mohan R. Geometry of Edge Chips Formed at Different Angles. In: *Mechanical Properties and Performance of Engineering Ceramics and Composites: Ceramic Engineering and Science Proceedings*: John Wiley & Sons, Inc.; 2008. pp. 85-92.
33. Quinn JB, Quinn GD. Material Properties and Fractography of an Indirect Dental Resin Composite. *Dent Mater*, 2010; **26**: 589-599.
34. Flanders LA, Quinn JB, Wilson Jr OC, Lloyd IK. Scratch Hardness and Chipping of Dental Ceramics under Different Environments. *Dent Mater*, 2003; **19**: 716-724.
35. Garoushi S, Lassila LV, Tezvergil A, Vallittu PK. Load Bearing Capacity of Fibre-Reinforced and Particulate Filler Composite Resin Combination. *J Dent*, 2006; **34**: 179-184.

36. Dyer SR, Lassila LV, Jokinen M, Vallittu PK. Effect of Fiber Position and Orientation on Fracture Load of Fiber-Reinforced Composite. *Dent Mater*, 2004; **20**: 947-955.
37. Isaac D. Engineering Aspects of the Structure and Properties of Polymer–Fibre Composites. In: *The First International Symposium on Fibre-Reinforced Plastics in Dentistry*. Edited by Vallittu pK. Turku,Finland; 1998.
38. Bryant RW, Hodge K-LV. A Clinical Evaluation of Posterior Composite Resin Restorations. *Aust Dent J*, 1994; **39**: 77-81.
39. Alander P, Lassila LV, Tezvergil A, Vallittu PK. Acoustic Emission Analysis of Fiber-Reinforced Composite in Flexural Testing. *Dent Mater*, 2004; **20**: 305-312.
40. Shinya A, Yokoyama D, Lassila LV, Vallittu PK. Three-Dimensional Finite Element Analysis of Metal and FRC Adhesive Fixed Dental Prostheses. *J Adhes Dent*, 2008; **10**: 365-371.
41. Mota EG, Horlle L, Oshima HM, Hirakata LM. Evaluation of Inorganic Particles of Composite Resins with Nanofiller Content. *Stomatologija*, 2012; **14**: 103-107.
42. Beun S, Glorieux T, Devaux J, Vreven J, Leloup G. Characterization of Nanofilled Compared to Universal and Microfilled Composites. *Dent Mater*, 2007; **23**: 51-59.
43. Suzuki S, Leinfelder KF, Kawai K, Tsuchitani Y. Effect of Particle Variation on Wear Rates of Posterior Composites. *Am J Dent*, 1995; **8**: 173-178.
44. Leprince JG, Palin WM, Vanacker J, Sabbagh J, Devaux J, Leloup G. Physico-Mechanical Characteristics of Commercially Available Bulk-Fill Composites. *J Dent*, 2014; **42**: 993-1000.
45. Alshali RZ, Salim NA, Sung R, Satterthwaite JD, Silikas N. Qualitative and Quantitative Characterization of Monomers of Uncured Bulk-Fill and Conventional Resin-Composites Using Liquid Chromatography/Mass Spectrometry. *Dent Mater*, 2015; **31**: 711-720.
46. Ellakwa A, Shortall A, Shehata M, Marquis P. Influence of Veneering Composite Composition on the Efficacy of Fiber Reinforced Restorations (Frr). *Oper Dent*, 2001; **26**: 467-475.

**Chapter 6: Influence of Fibre-Reinforced Composite
on Shear Bond strength with Ceramic and Metal
Substrates.**

6.1 ABSTRACT:

Objectives: To i) investigate the effect of incorporating fibre-reinforced composite (FRC) layer on the shear bond strength (SBS) between resin-composite and ceramic/metal substrates *in-vitro*, and ii) examine the influence of ‘substrate material’, ‘surface treatment’ and ‘FRC orientation’ on SBS values.

Methods: Sixty disc-shaped specimens with 120 surfaces (16 x 2 mm) made of ceramic (*e.max press, Ivoclar-Vivadent*) and metal alloy (*Incise LaserPFM, Rainshaw*) were bonded with FRC and particulate-reinforced composite (PRC) after surface treatment. Group-A (ceramic, n=60) were pre-treated with hydrofluoric acid etching (HF: 9.5% *Porcelain etchant, Bisco*, n=30) and tribochemical silica-coating (SC: *Cojet Sand, 3M-ESPE*, n=30), whereas Group-B (metal, n=60) had silica-coating (n=30) and air-abrasion (AA: 50 μ m alumina particles, n=30). Subsequent silanization (*EPSE Sil, 3M-ESPE*) and bonding (*Viso-bond, 3M-ESPE*) were performed for all surfaces. Flowable resin-composite (*GradioSO flow, Voco*) was applied as a thin layer prior to further FRC/PRC adhesion. Three equal subgroups (n=10) were assigned for each group/surface treatment according to the used FRC. Unidirectional (*Everstick C&B, Stick Tech Ltd*) and bidirectional (*Everstick Net, Stick Tech Ltd*) FRCs were incorporated at the interface in subgroups U and B respectively, while subgroup C had no reinforcement (control). A veneering PRC (*X-tra fil, Voco*) was then packed in single increment (5 x 5x 3 mm) and light-cured (20s). All specimens were thermocycled (1000 cycles, 5-55°C, 10s dwell) and water stored (37°C, 48h) prior to SBS testing. A universal testing machine (*Zwick Z020*) was employed to apply shear load (0.5 mm/min crosshead speed) at the interface and calculate SBS (MPa). Statistical analysis using 2-way ANOVA (*Tukey's post hoc*) was performed ($\alpha=0.05$).

Results: FRC and their orientation had a significant influence on SBS independent of surface treatment and material substrate ($p<0.001$). Subgroup C had the highest mean SBS values (15.4-17.96 MPa) while Subgroup U had the lowest (5.38-9.76 MPa). Surface treatments had a significantly different effect with Group A ($p=0.011$), but not with Group-B ($p=0.642$). With silica-coating, the substrate material had no significant effect on SBS ($p=0.418$).

Conclusion: Incorporating FRC at the interface between PRC and ceramic/metal substrates reduces SBS values. Bidirectional FRCs tend to provide superior support for veneering PRCs than unidirectional FRCs under shear loading.

6.2 INTRODUCTION:

Fibre-Reinforced Composites (FRCs) are becoming a popular restorative material in dental practice, partly due to their superior mechanical properties and diverse applications. They are used as removable denture frameworks [1], periodontal splints [2], post-core systems [3, 4], orthodontic retainers [5, 6], single crowns, conventional fixed partial dentures (FPDs) [7] as well as adhesive and implant-supported FPDs [8, 9]. Recently, they have also been employed as an intermediate layer to restore teeth and repair fractured restorations intraorally [10-14]. This application has highlighted the ability of FRC to reinforce repairing structures and withstand stresses at the interface by stopping crack propagation [11, 13, 15, 16].

As a traditional repairing technique, particulate-reinforced composite (PRC) is often bonded to a fractured tooth/restoration [17-19]. A strong adhesion between PRC and fractured substrates is essential for a successful repair. It provides retention for the repairing material, ensures an adequate stress distribution at the interface, improves the longevity and reduces the necessity for replacement [5, 16, 20-22]. However, it is frequently reported that the interface between PRC/substrate is significantly weak and demonstrates many bonding failures, adversely affecting the mechanical properties and long-term durability of restorations [13, 15, 16, 23-26]. Using FRC at the interface is a viable method of reinforcement as it could increase bond strength at the interface by changing stress dynamics and mode of failure [15, 16, 23, 24, 26-28].

The orientation of FRC is also an important factor in relation to reinforcement. Unidirectional fibres offer reinforcement in one direction that leads to anisotropic properties, while bidirectional and random fibres provide orthotropic and isotropic properties, respectively [16, 23]. This suggests that FRCs with different orientation can have a diverse influence on the adhesive interface of repaired substrates. Previous studies have confirmed this diversity when differently-oriented FRCs employed to reinforce the interface between PRC and tooth structures [15, 16, 23, 24, 26-28]. However, the advantages on the bond strength are still uncertain. Some studies investigating the influence of fibre reinforcement on the shear bond strength (SBS) with natural and bovine tooth structures have reported no significant difference between the reinforced and unreinforced substrates [23, 27], while others have exhibited a significant improvement once specific fibre orientation used [26, 28]. Nevertheless, no previous study has investigated the SBS of FRC with ceramic or metal substrates.

Adhesion to ceramic or metal substrates differs from that with tooth substance. Some preparation and subsequent activation for ceramic/metal surfaces are crucial prerequisites to ensure satisfactory micromechanical locking and chemical bonding of resin-composites [21, 29-31]. Acid-etching, air-abrasion with aluminium oxides and tribochemical silica-coating are the most common modalities of surface treatments capable of promoting micromechanical roughness and surface wettability [19, 21, 29, 32-38]. Subsequent silanization is also highly recommended as it activates the prepared surfaces and encourages their chemical adhesion with resin-composite materials [29-31, 34]. Many studies have investigated the effect of different surface treatments on SBS with ceramic/metal substrates but there is no published study that examines such influence with the presence of an intermediate FRC layer at the interface.

In view of that, the main aim of this study was to investigate the effect of incorporating a FRC layer at the interface between resin-composite and ceramic/metal substrates on SBS. The influence of 'FRC orientation', 'surface treatment' and 'substrate material' was also examined. Three null hypotheses were formulated as the following: 1) FRC and their orientation have no significant effect on SBS, 2) Different surface treatments for ceramic and metal substrates have no significantly different effect on SBS, 3) The substrate material has no significant effect on SBS when the same surface treatment employed.

6.3 MATERIALS AND METHODS:

Two differently-oriented FRCs were used to reinforce the bonding interface between a resin-composite material and two crown fabricating materials (lithium disilicate ceramic and cobalt-chrome metal alloy), and then assessed for their bond strength. All the materials used in this study, their compositions and manufacturers, are listed in Table 6.1.

Table 6.1: Materials used in this study

Materials	Description	Composition	Manufacturer
IPS e.max press (A)	Silicate-based ceramic. (LT BL 1 ingot)	70 wt% lithium disilicate crystal ($\text{Li}_2\text{Si}_2\text{O}_5$), 30% glassy matrix (K_2O , MgO , Al_2O_3 , P_2O_5)	<i>Ivoclar Vivadent, Schaan, Liechtenstein</i>
Incise LaserPFM (B)	Laser-sintered Co-Cr metal alloys	Co (65 wt%), Cr (24 wt%), W, Si, Fe, Mn	<i>Renishaw plc, Gloucestershire, UK</i>
EverStick® C&B (ES)	Pre-impregnated unidirectional fibres	E-glass fibres, PMMA, Bis-GMA	<i>Stick Tech Ltd, Turku, Finland</i>
EverStick® Net (EN)	Pre-impregnated bidirectional E-glass fibres	E-glass fibres, PMMA, Bis-GMA	<i>Stick Tech Ltd, Turku, Finland</i>
X-tra fil (C)	Packable bulk-fill micro-hybrid composite	86 wt% filler (barium-boron-alumina-silicate glass), Bis-GMA, UDMA, TEGDMA	<i>VOCO GmbH, Cuxhaven, Germany</i>
GrandioSO flow	Light-cured, flowable Nano-Hybrid Composite	81 wt% filler: (SiO_2 :20–40nm), Bis-GMA, Bis-EMA, TEGDMA,	<i>VOCO GmbH, Cuxhaven, Germany</i>
Porcelain Etchant	9.5% buffered HF acid gel	Hydrofluoric acid, polyacrylamidomethylprpane sulfonic acid	<i>BISCO Inc, Illinois, USA</i>
Cojet® Sand	Silicized airborne sand	30µm silica-modified corundum particles	<i>3M-ESPE, Seefeld, Germany</i>
ESPE Sil®	Silane coupling agent	Silane, Ethanol	<i>3M-ESPE, Seefeld, Germany</i>
Visio-Bond®	One bottle bonding agent	Tricyclodecane diacrylate	<i>3M-ESPE, Seefeld, Germany</i>
<i>Bis-GMA: bisphenol A diglycidyl dimethacrylate, TEGDMA: triethylene glycol dimethacrylate, UDMA: urethane dimethacrylate, Bis-EMA: ethoxylated bisphenol A dimethacrylate, PMMA: poly methyl methacrylate.</i>			

6.3.1 Specimen preparation

Sixty disc-shaped specimens (16 x 2 mm) of IPS e.max press (Group A, n=30) and Incise LaserPFM (Group B, n=30) were prepared by one specialized milling centre using CAD/CAM technology. A virtual 3D model representing the master disc specimen with the required dimensions was digitally generated (in the form of .STL file) and used to fabricate all the specimens. The corresponding specialized CAD/CAM machines were employed to mill the ceramic discs (*CORiTEC 250i, Imes-Core GmbH, Eiterfeld, Germany*) and laser-sinter the metal specimens (*Incise™ DM10, Renishaw plc, Gloucestershire, UK*) according to the manufacturer's instructions. Upon completion, the specimens were finished and polished with a fine grit diamond bur and 100, 600, 1200 grit silicon carbide abrasive discs under water-cooling, using a semi-automatic polishing machine (*Metraserv™ 250, Buehler, UK*). Both surfaces in Group A specimens were ground, while one surface was polished in Group B specimens, leaving the other surface with the macro-roughness induced during the laser-sintering process. Later, all specimens were ultrasonically cleaned for 3min in deionised water prior to subsequent surface treatment and bonding.

6.3.2 Surface treatment and bonding procedure:

Prior to bonding, both surfaces of each specimen were treated differently. In Group A, surfaces (n=60) were treated with either silica-coating (n=30) or hydrofluoric (HF) acid etching (n=30), while Group B surfaces (n=60) were treated with either silica-coating (n=30) or air-abrasion (n=30). To perform silica-coating (SC), CoJet™ sand (*3M-ESPE, Seefeld, Germany*) was perpendicularly applied to the surface (10mm distance, 2.5 bar pressure, 15s) by using a chairside abrader (*Cojet™ Prep Micro-blaster, 3M-ESPE*). Acid-etching (HF) treatment was performed as described by the manufacturer, using 9.5% HF (*Porcelain etchant, Bisco Inc, USA*) for 60s, followed by spray-water rinsing for 30s. Air-abrasion (AA) was performed on the unpolished surface of Group B specimens using aluminium oxide particles (10cm distance, 6 bar pressure, 10s). Subsequent silanization was performed for all surfaces by applying one thin layer of ESPE™ Sil (*3M-ESPE, Seefeld, Germany*) and then air-drying (30s).

6.3.3 Bonding procedure:

A bulk-fill resin composite material was directly bonded to each surface, with the aid of an intermediate FRC layer to reinforce the adhesional interface. According to the FRC layer incorporated, all specimens in each main group were randomly allocated into three

equal subgroups (n=10). Specimens in subgroup EU were reinforced by unidirectional E-glass FRC (*EverStick C&B, Stick Tech Ltd*), while bidirectional E-glass FRC was used in subgroup EN (*EverStick Net, Stick Tech Ltd*) Subgroup C was the control with no FRC incorporated.

A customized Teflon mould (5 x 5 x 3 mm) was employed in order to standardize the shape of bonded resin-composite and resultant specimens. The mould was set on the centre of the bonding surface before the bonding procedure started. A layer of resin bonding agent (*Viso-bond, 3M-ESPE*) was initially applied to the surface and then light-cured (10s). A thin layer of flowable resin composite (*GrandioSO Flow, Voco*) was then applied in all specimens to facilitate the adaptation of the intermediate FRC layer and enhance the bonding. For subgroup EU, one unidirectional fibres bundle (5mm length) was adapted and spread all over the area before being light-cured for 20s using a hand-held LED curing light (*EliparTMSI0, 3M-ESPE*). The mould was then completely filled with one increment of PRC and covered with a glass slide (with 5kg load for 5min) prior to the final light polymerisation (20s). The same technique was followed when a single square sheet (5 x 5 mm) of bidirectional fibres was used as the intermediate layer in subgroup EN. The control subgroup had no intermediate layer, and PRC was directly packed over the flowable resin-composite layer and then light-cured (20s). Upon the completion, all the specimens had a final polish using polishing discs (*Optidisc, Kerr, CA, USA*), and stored in water (37°C, 48h). Figure 6.1 shows one representative specimen for each main group.

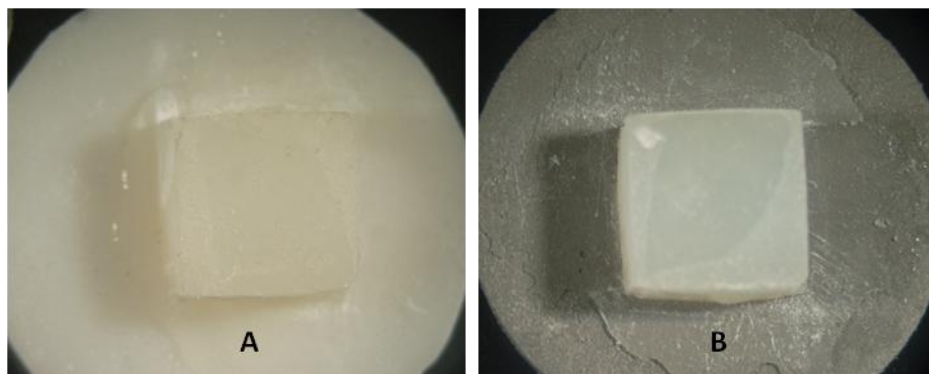


Figure 6.1: Two representative specimens. A) ceramic substrate and B) Co-Cr metal substrate

6.3.4 Thermocycling:

Before testing of the shear bond strength (SBS), accelerated thermocyclic aging for 1000 cycles (10s dwell) in water baths (5-55°C) was performed for all specimens to simulate the adverse effects of the oral environment. Further storing in water (37°C, 24h) and then air drying (1h) were done before SBS testing.

6.3.5 Shear bond testing:

A Zwick/Roell Z020 universal testing machine (*Zwick GmbH, Ulm, Germany*) with a single-sided chisel indenter was employed to apply shear loading (0.5 mm/min crosshead speed) along the adhesive interface between resin composite and metal/ceramic materials in each specimen. The shear bond strength (MPa) was then calculated according the following equation:

$$SBS = \frac{F_{Max}}{A} \quad \text{Equation 6.1}$$

Where F_{Max} is the ultimate load-to failure (N) and A is the bonded area (mm^2) of resin composite. The debonded surfaces were examined under light microscopy with high magnification (x30) in order to assess the failure mode. The mode of failure was reported for each specimen and classified as adhesive failure within substrate interface, adhesive within PRC interface, cohesive failure within FRC and mixed adhesive/cohesive failure.

6.3.6 Statistical analysis:

The data for all subgroups were analysed statistically with SPSS 22.0 (*IBM SPSS Statistics, SPSS Inc., Chicago, IL, USA*). A series of two-way ANOVA was used to investigate the influence of material substrate, surface treatment and FRC orientation on SBS. Post-hoc testing was accomplished with the Tukey's test. The level of significance was set at $\alpha=0.05$.

6.4 RESULTS:

The means and standard deviations of SBS (MPa) for all subgroups are shown in Table 6.2 and graphically presented in Figure 6.2. The control subgroup had the highest mean strength values independent of type of substrate material and surface treatment, while EU had the lowest values. Ceramic specimens treated with HF etchant and without the intermediate FRC layer exhibited the highest shear bond strength among all subgroups (18.0 ± 3.4 MPa).

Table 6.2: Mean (SD) shear bond strength for all the tested groups.				
Subgroup	Ceramic (A)		Metal (B)	
	<i>Silica Coating</i>	<i>HF acid etching</i>	<i>Silica Coating</i>	<i>air-abrasion</i>
C : Control (No FRC)	15.2±3.6 ^{a,1}	18.0±3.4 ^{a,2}	15.0±3.7 ^{a,1}	16.8±4.0 ^{a,1}
EU: Unidirectional FRC	9.1±2.1 ^{b,1}	9.8±2.8 ^{b,1}	9.3±2.7 ^{b,1}	5.4±1.8 ^{b,2}
EN: Bidirectional FRC	10.9±3.1 ^{c,1}	14.1±3.9 ^{c,2}	12.8±2.3 ^{c,1}	13.9±2.3 ^{c,1}
*Different superscript letters indicate a significant difference within same column.				
** Different superscript numbers indicate a significant difference within the same row in each main group.				

The use of intermediate FRC layer and its orientation had a significant influence on SBS regardless of the substrate used and its surface treatment ($p < 0.001$). The influence of substrate material and the interaction with using FRC layer were found non-significant when the same surface treatment was employed ($p = 0.418$, 0.515 respectively). Comparing the main groups separately, surface treatment had a significant influence ($p = 0.011$) on SBS with no significant interaction with fibre content ($p = 0.426$) when the ceramic material was the bonding substrate. For the metal alloy, surface treatment had no significance ($p = 0.642$) but their interaction with fibre content was significant ($p = 0.007$).

Analysis of the fractured specimens exhibited differences in fracture patterns among all the tested subgroups (Table 6.3). Examples of fractured specimens are shown in Figure 6.4. Control subgroups had mostly an adhesional failure while the reinforced subgroups demonstrated more cohesive fractures within their FRC layer. Surface treatment had also an influence on mode of failure. A high percentage (40%) of cohesive failure in ceramic substrate was evident within control subgroups, whereas metal substrate exhibited no cohesive failure.

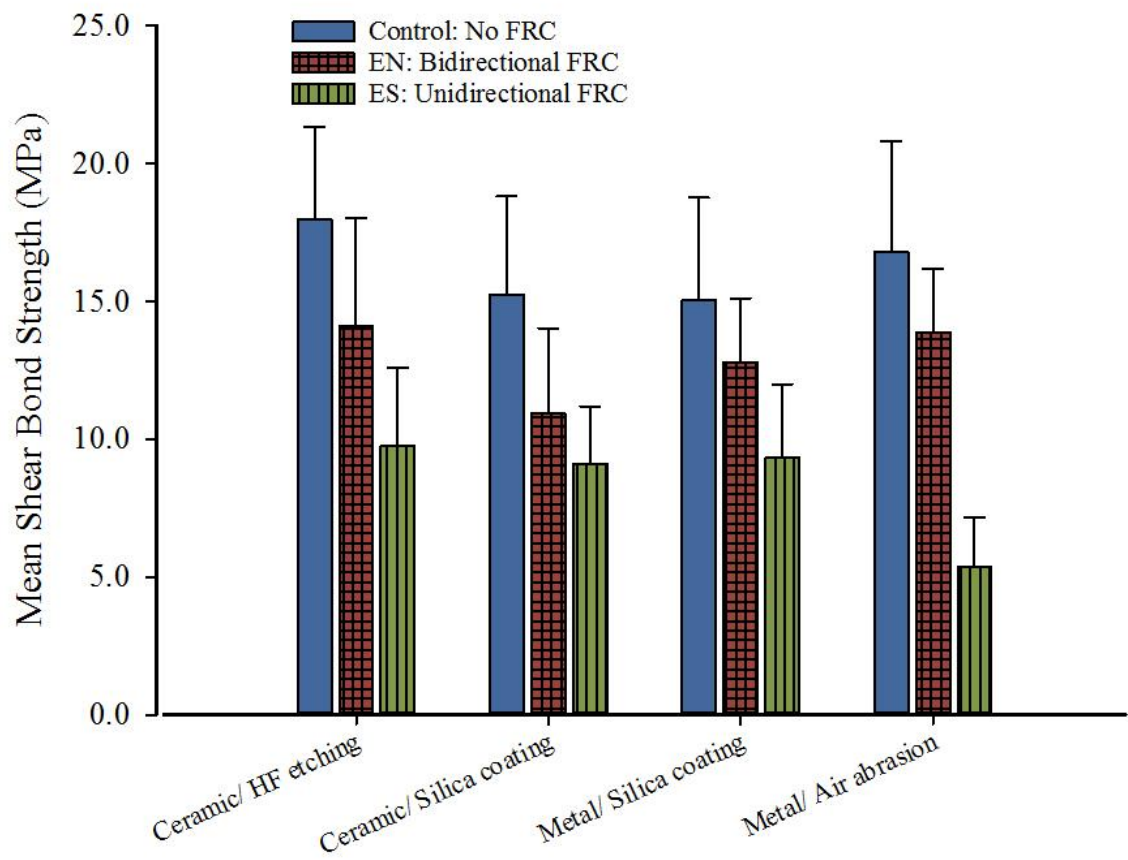


Figure 6.2: Bar chart showing mean (SD) shear bond strength for all groups according to their substrate and surface treatment.

Table 6.3: Fracture mode distribution for all tested groups according to the surface treatment applied.

Group & Treatment	Subgroup	Mode of Fracture			
		<i>Adhesive with substrate</i>	<i>Adhesive with PRC</i>	<i>Cohesive in FRC</i>	<i>Mixed</i>
Ceramic SC (HF)	<i>Control</i>	6 (6)	-	-	4 (4)
	<i>EU</i>	3 (1)	2 (2)	5 (7)	-
	<i>EN</i>	1 (2)	4 (2)	5 (6)	-
Metal SC (AA)	<i>Control</i>	10 (5)	-	-	0 (5)
	<i>EU</i>	1 (6)	2 (1)	7 (3)	-
	<i>EN</i>	1 (5)	4 (3)	5 (2)	-

* SC: silica coating, HF: hydrofluoric acid, AA: air abrasion.
 ** The numbers in and out brackets indicate the frequency of fracture corresponding to the surface treatment in and out brackets, respectively.

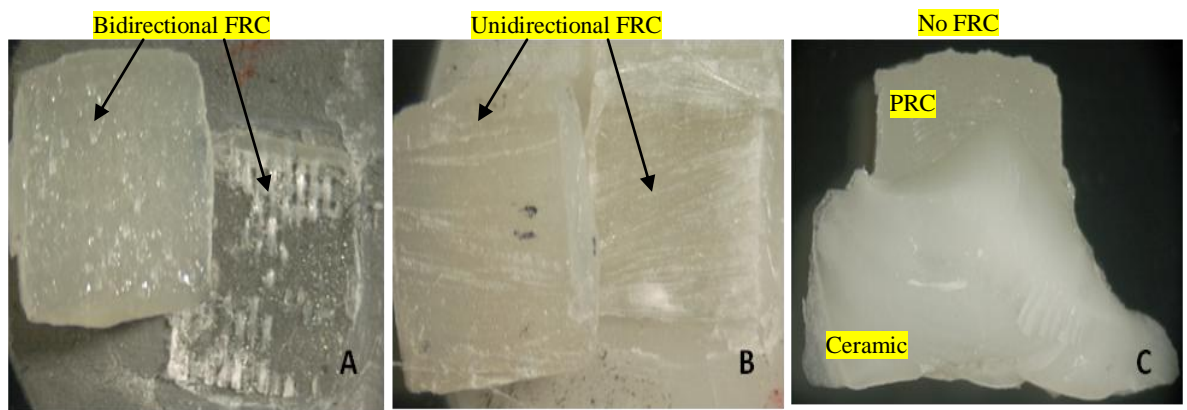


Figure 6.3: Examples of the failure modes observed following SBS testing, A) cohesive fracture in bidirectional FRC layer with metal, B) cohesive fracture in unidirectional FRC layer with ceramic, C) mixed adhesion/cohesion fracture at the ceramic interface with no reinforcement.

6.5 DISCUSSION:

This *in-vitro* study investigated the effect of incorporating FRC as an intermediate layer within resin-composite materials (PRC) when adhesion to ceramics or metal alloys is required. The influence of three experimental factors, namely FRC orientation, surface treatment and substrate material, on the shear bond strength (SBS) was accordingly considered.

The first null hypothesis was rejected since the use of FRC and their orientation significantly influenced SBS irrespective of the substrate material bonded or surface treatment used. Using an intermediate layer of FRC underneath PRC was advocated by many authors, whenever a repair of tooth structure or restoration is indicated, since it would improve fracture resistance and reduce subsequent failures [10, 11, 13, 21]. It was also premised on the idea that the presence of a FRC network would reinforce the relatively-weak substrate/PRC interface, and provide a stress-breaking shield that alters stress dynamics at the adhesive interface and reduces crack initiation and propagation [22, 26]. Studies investigating this technique were able to confirm its positive influence on the fracture resistance of bonded substrates [13, 20-22]. However, the potential benefits on adhesion and shear strength are still controversial. Some studies have reported positive influence of fibre reinforcement on SBS when natural and bovine teeth were used [26, 28], while others have found the effect is not significant [23, 27]. In contrast, the findings of this study show a significantly negative effect on SBS when both unidirectional and bidirectional FRCs were used to bond either ceramic or metal substrates. This could be explained by the fact that different substrate materials have different adhesive properties, and so ceramics and metal alloys are not expected to behave in the same way as natural or bovine teeth.

SBS values for all subgroups with bidirectional FRC were significantly higher than those with unidirectional orientation. This is in accordance with previous studies showing that SBS of resin-composite to FRC substrates relies on the load to fibre direction [16, 23, 26]. The highest shear resistance is reported when FRC orientation corresponds to the direction of shear load, while a lesser degree of resistance is reported for the fibres perpendicular to the load direction [16]. The difference in Krenchel factor (K_{θ}) (which describes the effectiveness of fibre reinforcement in relation to the direction of load) can also explain these findings [1]. According to their Krenchel factor, the unidirectional FRC have the highest effectiveness ($K_{\theta}=1$) when been loaded along their

orientation. However, their effectiveness drops to the minimal ($K_0 = 0$) once they have been perpendicularly loaded [1]. In contrast, bidirectional FRC have fibres oriented along two different directions with ($K_0 = 0.5$), and expected to exhibit better reinforcement than unidirectional FRC under the perpendicular shear load, which agrees with this study.

This study also reported a change in the failure mode of specimens as a consequence of utilizing different FRCs. As anticipated, the mode of fracture for most unreinforced specimens was adhesive in nature (80% for metal, 60% for ceramic) at the substrate/PRC interface. For those with reinforcement, the cohesive fracture within the FRC layer was the most observed failure mode (70% for unidirectional FRC and 50% for bidirectional FRC). This would indicate that the bond with substrates was stronger than the cohesive strength of the FRC. Such observations are in accordance with previous studies which reported similar changes in fracture patterns as a result of using FRC to reinforce enamel and dentine [15, 24, 28]. A considerable reduction in SBS values was found to accompany the cohesive fracture within FRC. This can imply that the incorporated FRC layer tends to be the weakest part in the 'substrate-FRC-PRC' assembly, leading to accelerated crack propagation at the interface. However, this introduced weakness is not entirely hostile since it could be beneficial to prevent undesirable failures in the bonding substrates. For example, the cohesive fractures within the ceramic substrates (Figure 6.3.C) were completely prevented as a consequence of FRC incorporation.

The second null hypothesis was partially rejected as the difference between surface treatments was found statistically significant in case of ceramic substrate ($p=0.011$) but not significant with the metal alloy ($p=0.642$). Comparing the ceramic treatments together, the acid-etching with HF was found to have a more influence on SBS values (17.96, 9.76, 14.08) compared with the tribochemical silica-coating (15.23, 9.10, 10.93). Similar findings have been reported, and the necessity of acid-etching silica-based ceramics in order to obtain a robust SBS with repairing resin-composite materials has been emphasised [29, 32]. However, some studies have reported no significant difference between acid-etching and silica-coating in terms of SBS when used to repair ceramic- and metal-based restorations [21, 25, 33, 35].

As a principle, acid-etching relies on selective dissolving of the glass matrix from ceramic superficial microstructure that causes physical alteration and promotes

micromechanical locking of resin-composite to the porous surface [17, 30]. Additionally, it generates unsaturated oxygen bonds which enhance surface wettability and serve as bonding partners for the subsequent silanization [32]. Silica-coating, on other hand, has a different mechanism of action which relies on the impact of silica modified micro-particles (30µm) to produce micromechanical roughening and tribochemical coating [38]. A blast of silica-modified corundum particles under high air-pressure (2-3 bars) causes not only surface abrasion (up to 15 µm depth) but also releases high levels of heat utilized to generate chemical bonds between silica and the microblasted surface [31]. Such silica coating provides an additional micromechanical roughening within the surface, and also improves the chemical affinity to silane coupling agents [31, 34]. Owing to its unique crystalline microstructure, lithium disilicate ceramic is considered highly susceptible to HF acid-etching which enables a higher degree of surface micromechanical roughening compared with silica-coating [29, 32].

For metal substrates, air-abrasion and silica-coating have been used in order to promote surface micromechanical roughness. Although both techniques share the same mechanism of action, no tribochemical silica-coating occurs with the former technique which is postulated to offer lower values of SBS accordingly [38]. However, both treatments exhibited no significant difference on SBS of metal specimens, but with a relative superiority of the air-abrasion. This can be explained by the macro-roughness induced during the laser-sintering process on the surfaces treated with air-abrasion [39]. This roughness was kept on one side of metal specimens with the intention to represent the porcelain-bonding surface in PFM restorations previous to repairing. This additional roughness demonstrated a positive influence on SBS of the unreinforced metal subgroups by increasing the retention of resin-composite. However, it seems to have an adverse effect on FRC layer as it prevents effective fibre/surface adaptation and causes stresses concentration within FRC. This explains the significant interaction ($p=0.007$) reported between surface treatment and FRC orientation in metal specimens.

The third null hypothesis was accepted as no significantly different effect ($p=0.418$) exhibited between ceramic and metal substrates on SBS when the same surface treatment was employed. It is established that different material substrates have dissimilar adhesional behaviours owing to the variation in their superficial microstructure [36]. Previous studies have reported a variation in SBS values when a resin-composite material bonded to combination substrates, like enamel/dentine or

ceramic/metal, and highlighted the need of using selective surface treatments to ensure adequate adhesion [24, 25, 36, 37, 40]. Although metal alloys are less prone to air-abrasion due to their superior mechanical properties compared with ceramics, the use of silica-coating and silanization tends to produce a comparable effect on their adhesive behaviour with resin-composite. Many studies have supported the use of a silica-coating/silanization technique to repair fractured restorations with exposed metal and ceramic structures [17, 19, 21, 25]. It is claimed that this would standardize the adhesion between both substrates and resin-composite, producing higher SBS values and reducing the need for replacement, in comparison with other repair modalities [25].

The process of silanization itself is considered as the most effective method for improving resin bonding with silica-based ceramics and metal alloys [29, 30]. The bifunctional molecules of silane form chemical bonds with the silica or unsaturated oxygen layers on the bonding substrate from one side, and the resin molecules from the other side through a process of polymerization [31, 34]. Furthermore, the surface wettability is also enhanced by the presence of silane, which promotes resins penetration within a substrate microstructure [25, 30]. Therefore, this study used silanization as a standard subsequent treatment for all the specimens. Low viscosity (flowable) resin composite, as recommended by many authors, was also used in order to facilitate fibre adaptation and enhance resin penetration [5, 13, 26, 27]. However, some studies have reported that there is no significant benefit of using this technique on SBS [24]. Thermocycling and water storage were also used to simulate the adverse effect of oral environment on SBS and confirmed in previous studies [41].

Some limitations were encountered during the fabrication of specimens, especially when air abrasion was used. The macro-roughness induced from the laser sintering process has led to a difficulty during the adaption of FRC to specimen surface. The relatively large spikes on the surface increased the stress concentration and caused a separation of the fibres from its bundle form, leading to some degree of misdistribution, especially when a unidirectional FRC used. This explains the massive reduction of SBS in subgroup B_{EN} (with air abrasion). Another limitation was the only use of preimpregnated E-glass FRC to investigate the effect on SBS, which limits the results to that type of material. Potential studies comparing different FRC types, orientations and impregnations are suggested in the future.

To summarize, the incorporation of an intermediate FRC layer between resin-composite and ceramic/metal substrate tends to have a negative effect on SBS despite the confirmed positive effect on fracture resistance. This seems to be due to the weak cohesion between the reinforcing fibres themselves, which could not withstand high shear stresses and so fractured cohesively. From clinical perspective, this technique could be beneficial when a provisional adhesion to ceramic/metal restorations is indicated since it would reduce the possibility of undesirable fractures in bonding substrates. Moreover, it could be essential to modify the loading direction away from shear when FRC are indicated to repair or bond restorations. The use of bidirectional FRCs instead of unidirectional FRC is also recommended as their reinforcement tends to be more effective against shear loading.

6.6 CONCLUSION:

Within the limitation of this study, the following conclusions were drawn:

- 1- FRC has a negative influence on SBS when incorporated between resin-composite and metal/ceramic substrates.
- 2- Bidirectional FRC performs better than unidirectional FRC under shear loading.
- 3- Acid-etching, as a surface treatment, promotes better adhesion than silica-coating with ceramic substrates. With metal substrates, silica-coating and air-abrasion have the same influence on SBS.
- 4- Using silica-coating, both ceramic and metal substrates has the same influence on SBS.

6.7 REFERENCES:

1. Vallittu PK. Flexural Properties of Acrylic Resin Polymers Reinforced with Unidirectional and Woven Glass Fibers. *J Prosthet Dent*, 1999; **81**: 318-326.
2. Kumbuloglu O, Aksoy G, User A. Rehabilitation of Advanced Periodontal Problems by Using a Combination of a Glass Fiber-Reinforced Composite Resin Bridge and Splint. *J Adhes Dent*, 2008; **10**: 67-70.
3. Asakawa Y, Takahashi H, Kobayashi M, Iwasaki N. Effect of Components and Surface Treatments of Fiber-Reinforced Composite Posts on Bond Strength to Composite Resin. *J Mech Behav Biomed Mater*, 2013; **26**: 23-33.
4. Kurt M, Güler AU, Duran İ, Uludamar A, İnan Ö. Effects of Different Surface Treatments on the Bond Strength of Glass Fiber-Reinforced Composite Root Canal Posts to Composite Core Material. *J Dent Sci*, 2012; **7**: 20-25.
5. Brauchli L, Pintus S, Steineck M, Lüthy H, Wichelhaus A. Shear Modulus of 5 Flowable Composites to the Everstick Ortho Fiber-Reinforced Composite Retainer: An in-vitro Study. *Am J Orthod Dentofacial Orthop*, 2009; **135**: 54-58.
6. Scribante A, Cacciafesta V, Sfondrini MF. Effect of Various Adhesive Systems on the Shear Bond Strength of Fiber-Reinforced Composite. *Am J Orthod Dentofacial Orthop*, 2006; **130**: 224-227.
7. Behr M, Rosentritt M, Handel G. Fiber-Reinforced Composite Crowns and FPDs: A Clinical Report. *Int J Prosthodont*, 2003; **16**: 239-243.
8. Garoushi S, Lassila L, Vallittu PK. Resin-Bonded Fiber-Reinforced Composite for Direct Replacement of Missing Anterior Teeth: A Clinical Report. *Int J Dent*, 2011: 5.
9. Erkmen E, Meriç G, Kurt A, Tunç Y, Eser A. Biomechanical Comparison of Implant Retained Fixed Partial Dentures with Fiber Reinforced Composite Versus Conventional Metal Frameworks: A 3D FEA Study. *J Mech Behav Biomed Mater*, 2011; **4**: 107-116.
10. Bagis B, Ustaomer S, Lassila LV, Vallittu PK. Provisional Repair of a Zirconia Fixed Partial Denture with Fibre-Reinforced Restorative Composite: A Clinical Report. *J Can Dent Assoc*, 2009; **75**: 133-137.
11. Turkaslan S, Tezvergil-Mutluay A, Bagis B, Shinya A, Vallittu PK, Lassila LV. Effect of Intermediate Fiber Layer on the Fracture Load and Failure Mode of Maxillary Incisors Restored with Laminate Veneers. *Dent Mater J*, 2008; **27**: 61-68.
12. Ergun G, Cekic I, Lassila LV, Vallittu PK. Bonding of Lithium-Disilicate Ceramic to Enamel and Dentin Using Orthotropic Fiber-Reinforced Composite at the Interface. *Acta Odontol Scand*, 2006; **64**: 293-299.
13. Badakar CM, Shashibhushan KK, Naik NS, Reddy VV. Fracture Resistance of Microhybrid Composite, Nano Composite and Fibre-Reinforced Composite Used for Incisal Edge Restoration. *Dent Traumatol*, 2011; **27**: 225-229.
14. Turkaslan S, Tezvergil-Mutluay A. Intraoral Repair of All Ceramic Fixed Partial Denture Utilizing Preimpregnated Fiber Reinforced Composite. *Eur J Dent*, 2008; **2**: 63-68.
15. Cekic-Nagas I, Ergun G, Tezvergil A, Vallittu PK, Lassila LV. Effect of Fiber-Reinforced Composite at the Interface on Bonding of Resin Core System to Dentin. *Dent Mater J*, 2008; **27**: 736-743.
16. Lassila LV, Tezvergil A, Dyer SR, Vallittu PK. The Bond Strength of Particulate-Filler Composite to Differently Oriented Fiber-Reinforced Composite Substrate. *J Prosthodont*, 2007; **16**: 10-17.

17. Kimmich M, Stappert CFJ. Intraoral Treatment of Veneering Porcelain Chipping of Fixed Dental Restorations: A Review and Clinical Application. *J Am Dent Assoc*, 2013; **144**: 31-44.
18. Hickel R, Brühshaver K, Ilie N. Repair of Restorations – Criteria for Decision Making and Clinical Recommendations. *Dent Mater*, 2013; **29**: 28-50.
19. Blum IR, Jagger DC, Wilson NH. Defective Dental Restorations: To Repair or Not to Repair? Part 2: All-Ceramics and Porcelain Fused to Metal Systems. *Dent Update*, 2011; **38**: 150-152, 154-156, 158.
20. Fennis WMM, Kreulen CM, Tezvergil A, Lassila LVJ, Vallittu PK, Creugers NHJ. In Vitro Repair of Fractured Fiber-Reinforced Cusp-Replacing Composite Restorations. *Int J Dent*, 2011; **2011**.
21. Ozcan M, van der Sleen JM, Kurunmaki H, Vallittu PK. Comparison of Repair Methods for Ceramic-Fused-to-Metal Crowns. *J Prosthodont*, 2006; **15**: 283-288.
22. Fennis WM, Tezvergil A, Kuijs RH, Lassila LV, Kreulen CM, Creugers NH, Vallittu PK. In Vitro Fracture Resistance of Fiber Reinforced Cusp-Replacing Composite Restorations. *Dent Mater*, 2005; **21**: 565-572.
23. Tezvergil A, Lassila LV, Vallittu PK. The Shear Bond Strength of Bidirectional and Random-Oriented Fibre-Reinforced Composite to Tooth Structure. *J Dent*, 2005; **33**: 509-516.
24. Tezvergil A, Lassila LV, Vallittu PK. Strength of Adhesive-Bonded Fiber-Reinforced Composites to Enamel and Dentin Substrates. *J Adhes Dent*, 2003; **5**: 301-311.
25. Ozcan M. Evaluation of Alternative Intra-Oral Repair Techniques for Fractured Ceramic-Fused-to-Metal Restorations. *J Oral Rehabil*, 2003; **30**: 194-203.
26. Meiers JC, Kazemi RB, Donadio M. The Influence of Fiber Reinforcement of Composites on Shear Bond Strengths to Enamel. *J Prosthet Dent*, 2003; **89**: 388-393.
27. Juloski J, Beloica M, Goracci C, Chieffi N, Giovannetti A, Vichi A, Vulicevic ZR, Ferrari M. Shear Bond Strength to Enamel and Flexural Strength of Different Fiber-Reinforced Composites. *J Adhes Dent*, 2013; **15**: 123-130.
28. Ilday N, Seven N. The Influence of Different Fiber-Reinforced Composites on Shear Bond Strengths When Bonded to Enamel and Dentin Structures. *J Dent Sci*, 2011; **6**: 107-115.
29. Liang Chen, Suh BI. Bonding of Resin Materials to All-Ceramics: A Review. *Curr. Res. Dent*, 2012; **3**: 7-17.
30. Matinlinna JP, Vallittu PK. Bonding of Resin Composites to Etchable Ceramic Surfaces - an Insight Review of the Chemical Aspects on Surface Conditioning. *J Oral Rehabil*, 2007; **34**: 622-630.
31. Özcan M, Vallittu PK. Effect of Surface Conditioning Methods on the Bond Strength of Luting Cement to Ceramics. *Dent Mater*, 2003; **19**: 725-731.
32. Yucel MT, Aykent F, Akman S, Yondem I. Effect of Surface Treatment Methods on the Shear Bond Strength between Resin Cement and All-Ceramic Core Materials. *J Non-Cryst Solids* 2012; **358**: 925-930.
33. Attia A. Influence of Surface Treatment and Cyclic Loading on the Durability of Repaired All-Ceramic Crowns. *J Appl Oral Sci*, 2010; **18**: 194-200.
34. Matinlinna JP, Vallittu PK. Silane Based Concepts on Bonding Resin Composite to Metals. *J Contemp Dent Pract*, 2007; **8**: 1-8.

35. de Melo RM, Valandro LF, Bottino MA. Microtensile Bond Strength of a Repair Composite to Leucite-Reinforced Feldspathic Ceramic. *Braz Dent J*, 2007; **18**: 314-319.
36. de Melo RM, Travassos AC, Neisser MP. Shear Bond Strengths of a Ceramic System to Alternative Metal Alloys. *J Prosthet Dent*, 2005; **93**: 64-69.
37. Almilhatti HJ, Giampaolo ET, Vergani CE, Machado AL, Pavarina AC. Shear Bond Strength of Aesthetic Materials Bonded to Ni–Cr Alloy. *J Dent*, 2003; **31**: 205-211.
38. Fonseca RG, Martins SB, de Oliveira Abi-Rached F, dos Santos Cruz CA. Effect of Different Airborne-Particle Abrasion/Bonding Agent Combinations on the Bond Strength of a Resin Cement to a Base Metal Alloy. *J Prosthet Dent*, 2012; **108**: 316-323.
39. Akova T, Ucar Y, Tukay A, Balkaya MC, Brantley WA. Comparison of the Bond Strength of Laser-Sintered and Cast Base Metal Dental Alloys to Porcelain. *Dent Mater*, 2008; **24**: 1400-1404.
40. Liu J, Qiu XM, Zhu S, Sun DQ. Microstructures and Mechanical Properties of Interface between Porcelain and Ni–Cr Alloy. *Mater Sci Eng*, 2008; **497**: 421-425.
41. Mair L, Padipatvuthikul P. Variables Related to Materials and Preparing for Bond Strength Testing Irrespective of the Test Protocol. *Dent Mater*, 2010; **26**: e17-23.

**Chapter 7: Fracture Load of Fibre-Reinforced
Composite Bridges after *in-vitro* Chewing
Simulation**

7.1 ABSTRACT

Objectives: To investigate the effects of framework design and dynamic fatigue on initial fracture (IF) and final fracture (FF) loads of directly-fabricated 3-unit inlay-retained fibre-reinforced composite fixed partial dentures (FRC-FPDs).

Methods: Twenty FRC-FPDs (n=20), replacing a lower first molar by two inlay-retainers, were directly fabricated over duplicated acrylic teeth. Woven polyethylene fibres (Construct, Kerr) were used to fabricate the main framework of all samples. Type-I specimens (n=10) had one additional bidirectional E-glass fibre sheet (*Everstick Net, Stick Tech Ltd*) perpendicularly-embedded within the pontics, while Type-II had an additional woven fibre bundle (*Construct, Kerr*). Two equal subgroups were allocated from each group. Subgroup A (n=5) was the control, while subgroup B (n=5) specimens were cyclically-loaded in a chewing simulator (240,000 cycles, 5 kg). All specimens were loaded in a universal testing machine with a compressive load (N) applied along the central fossa (1 mm/min crosshead speed) until fracture. IF and FF values were recorded for each specimen. A series of paired and independent t-tests were used to detect any statistical difference within subgroups ($\alpha=0.05$).

Results: All specimens in subgroup B survived the dynamic fatigue with no signs of fracture. Under static loading, Type-I_A specimens exhibited the highest mean IF (623.8±115.2 N) and FF values (1598.6±361.8 N), while specimens of Type-II_B scored the lowest (421.6±121.9 N and 716.0±72.1 N respectively). Both ‘framework type’ and ‘dynamic fatigue’ had a significant influence on FF ($p<0.001$), but IF was significantly affected by ‘framework type’ alone ($p<0.001$).

Conclusion: Modifying the framework of FRC-FPDs by incorporating additional reinforcing fibres within the pontic improves load-bearing capacity. The design of this modification significantly affects the outcome values, and the perpendicular configuration of incorporated bidirectional fibres provides the best fracture resistance.

7.2 INTRODUCTION:

In the modern era of metal-free minimally-invasive dentistry, replacing missing posterior teeth with a conventional porcelain fused-to-metal fixed partial denture (FPD) has become undesirable. An implant-supported prosthesis is often considered a ‘gold standard’ although it is not always feasible due to contraindications and patient preference [1]. All-ceramic materials and fibre-reinforced composite resins (FRC) are alternatives that have been clinically well-practiced as adhesive inlay-retained FPDs, especially where abutment teeth have carious lesions or existing fillings adjacent to the saddle area [2]. Both materials are considered as metal-free, minimal-invasive, yet durable for replacing missing teeth in anterior and posterior areas. They are advocated to provide restorations with excellent aesthetics, good adhesion and favourable mechanical strength [3, 4]. However, the brittleness of all-ceramic materials means that a larger amount of tooth substance removal is needed in order to accommodate sufficient connector dimensions, thus limiting their clinical application [5]. On the contrary, FRC-FPDs retain the advantage of minimal invasion, provide broader applications, directly or indirectly, with better cost-effectiveness and maintainability [6]. Consequently, their implementation has gained increasing interest recently.

FRC-FPDs are generally made from supporting FRC frameworks veneered by particulate-reinforced composite (PRC) to reproduce the anatomical morphology, and then resin-bonded to the abutments. Many factors have been identified to have an influence on the clinical performance and lifespan of such restorations, including fibre type [7], orientation [8], position [9, 10], volume fraction [11, 12], abutment preparation [13-15] and also framework design [16]. High-volume fraction frameworks have been found to provide better clinical performance than low-volume fraction frameworks due to their better support for the veneering composite [11]. A framework with a curved bundle of fibres following the contour of the tension side of the pontic has also been reported to enable a better stress distribution than the ‘traditional’ straight fibres connecting abutments together [17]. This design of framework has recently been advocated and validated using finite element analysis [5, 10, 18]. However, no study has attempted to investigate the influence of combining the two bundles together. Superior strength and load-bearing capacity are also reported when FRC frameworks with unidirectional fibres are used since they have the highest Krenchel factor [7]. However, fibres with bidirectional or woven orientations have a better potential to arrest crack propagation and support veneering composite, respectively [8, 19].

In a recent systematic reviews, the mean survival rate of FRC-FPDs was reported to be 77.5% for 5 years [20], while it is 88.6% for all-ceramic FPDs [21], 94.3% for zirconia-ceramic [22] and 94.4% metal-ceramic FPDs [21]. Delamination at the interface between the fibres and matrix of veneering composite represents the main mode of failure [14, 20, 23]. The connectors, loading points and pontics are also reported as the weakest parts where most fractures were observed [2, 14, 15]. All of that implies the necessity for further reinforcements. A few studies have attempted to address these problems, either by embedding additional reinforcing fibres within pontics to limit delamination [16, 24], or by altering the layout of the constituent materials within pontics or connectors to improve stress distribution [5, 10, 16], or even using different pontic materials and occlusal morphologies [25, 26]. To the authors' knowledge, no study investigates the effect of combining such modifications on the performance of FRC-FPDs.

The aims of this study were i) to propose two new framework designs for direct inlay-retained FRC-FPDs, and ii) to investigate their performance after chewing simulation *in-vitro*. The effect of two experimental factors, namely 'framework design' and 'dynamic fatigue', on initial (IF) and final fracture (FF) load values was investigated. The null hypothesis tested was that neither 'framework design' nor 'fatigue condition' would demonstrate a significant influence on IF nor FF loads.

7.3 MATERIALS AND METHODS:

Twenty specimens (n=20), representing directly-fabricated inlay-retained fibre-reinforced composite fixed partial dentures (FRC-FPD), replacing a lower first molar by two inlay-retainers, were tested for their initial (IF) and final fracture (FF) load values *in-vitro*. The materials used to fabricate specimens are all listed in Table 7.1

Table 7.1: Materials used to fabricate all specimens.

Material	Description	Composition	Lot No. /Shade	Manufacturer
X-tra® Fill (XF)	Bulk-fill nanohybrid composite	86 wt% filler, Bis-GMA, UDMA,TEGDMA	1209351 U	<i>Voco GmbH, Cuxhaven, Germany</i>
X-tra® Base (XB)	Flowable bulk-fill nanohybrid composite	75 wt% filler, Aliphatic dimethacrylate, Bis-EMA	1208392 U	<i>Voco GmbH, Cuxhaven, Germany</i>
Construct™ (P)	Non-impregnated woven FRC	Cold gas plasma-treated pre-silanated ultra-high strength polyethylene fibres (1mm).	2944115	<i>Kerr, USA</i>
EverStick® Net (EN)	Pre-impregnated bidirectional FRC	E-glass mesh, PMMA, Bis-GMA,	120424	<i>Stick Tech Ltd, Turku, Finland</i>
Stick Resin	Unfilled light-cured resin	Bis-GMA, TEGDMA	1203211	<i>Stick Tech Ltd, Turku, Finland</i>
ESPE™ Sil	Silane coupling agent	3-methacryloxypropyl trimethoxysilain, ethanol	529392	<i>3M-ESPE, Seefeld, Germany</i>
Visio-Bond	Light-curing bonding agent	Dicyclopentyl dimethylene diacrylate, 2-propenoic acid, 2-methyl, 2-(2-hydroxyethyl)(3-methoxypropyl) (amin P ethyl ester)	526323	<i>3M-ESPE, Seefeld, Germany</i>
Cojet™ Sand	Blast-coating agent	corundum particles coated with silica, particles size 30µm	534151	<i>3M-ESPE, Seefeld, Germany</i>
<i>PMMA: poly methyl methacrylate, Bis-GMA: bisphenol-A-glycidyl dimethacrylate, TEGDMA: triethylene glycol dimethacrylate, BisEMA: bisphenol-A-dyethoxy dimethacrylate, UDMA: urethane dimethacrylate.</i>				

7.3.1 Specimen preparation:

A mandibular artificial model with plastic teeth (*KaVo model, KaVo dental GmbH, Biberach, Germany*) was used with a missing lower right first molar. Two box-shaped inlay cavities, representing the future bridge retainers, were prepared on the second premolar and molar, using a high speed air turbine with coarse grit shoulder end diamond bur, according to specific dimensions (Figure 7.1). Following the duplication of both prepared teeth with silicon duplicating material (*Gemini, Bracon, East Sussex, UK*), twenty identical premolars and molars were constructed from cold-cure acrylic resin. To simulate the periodontal ligament (PDL) space within the future specimens, the duplicated teeth were pre-coated with 0.2mm-thickness wax, prior to mounting within epoxy-resin (*B&K Resins Ltd, Bromley, UK*). A standardised position of abutment teeth, with 11mm pontic space and 2mm base support below CEJ, was ensured through the mounting process using a custom-made holder made from a vacuum-formed matrix. Once the epoxy-resin was set, the wax coatings were replaced by light-bodied impression material (*Aquasil LV, Dentsply, USA*) to reproduce PDL elasticity.

7.3.2 FRC-FPD fabrication:

Twenty FRC-FPDs (n=20) were directly-fabricated over each of the mounted teeth, utilizing two bundles of woven ultrahigh molecular weight polyethylene (UHMWP) fibres (*Construct, Kerr*) as the main supporting framework (Figure 7.2). Prior to the fibre adaptation, sandblasting (*CojetTMSand, 3M-ESPE*) and silanization (*ESPETMSil, 3M-ESPE*) pre-treatments were performed to the cavities according to the manufacturer's instruction, followed by the application of a bonding agent (*Viso-Bond, 3M-ESPE*) which was cured for 20s. A thin layer of flowable bulk-fill composite (*X-base, Voco*) was then applied to the cavities to facilitate FRC adaptation. The two fibre bundles were impregnated with an unfilled resin (*Stick resin, Stick Tech Ltd*) for 5 minutes before being adapted and cured (20s) within the inlay cavities. One bundle (24mm) was curvedly adapted between the abutments to reinforce the pontic at the tension side, while the other bundle (18mm) was straight. A high-filled bulk resin-composite (*X-tra fill, Voco*) was adapted between the fibres to build the pontic core and then light-cured (20s).

Two types of frameworks with different additional reinforcing fibres were subsequently fabricated. Type-I (n=10) had a bidirectional E-glass fibre sheet (6 X 5 mm) (*Everstick*

Net, Stick Tech Ltd) perpendicularly-adhered to the core, whereas Type-II had an additional bundle (12mm) of the UHMWP fibres (*Construct, Kerr*) wrapped around the core in an inverted U-shape fashion. A thin layer of flowable composite (*X-tra base, Voco*) was used to facilitate fibre adaptation to the core before the additional fibres were light-cured in place. To reproduce the final specimen shape in standardised way, a veneering resin-composite (*X-tra fill, Voco*) was applied and cured through a clear vacuum index produced from the original model. A handheld LED curing light (*EliperTMS10, 3M-ESPE, USA*) was employed to perform all light-curing steps. Coarse/medium finishing discs (*OptiDisc, Kerr, Switzerland*) were used for specimen finishing and polishing. All specimens were stored in water (37°C, 48h) prior to further testing.

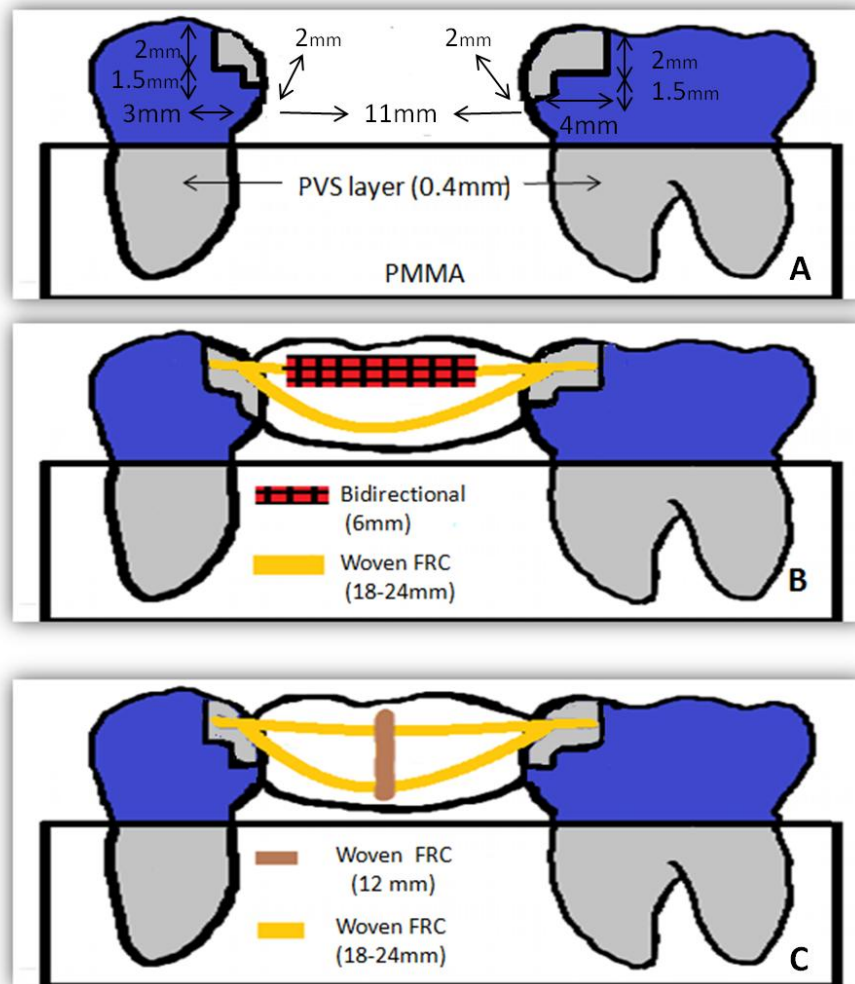


Figure 7.1: Diagrams showing A) the specimen assembly and dimensions of inlay cavities in each abutment, B) Type-I fibre framework, and C) Type-II framework. The dimensions of major connectors were 5mm height, 2.5mm width at premolar side and 3.5mm width at molar side. The clearance of the pontic base from the PMMA base was 3mm, ensured by using a custom silicon index beneath the pontic during fabrication.

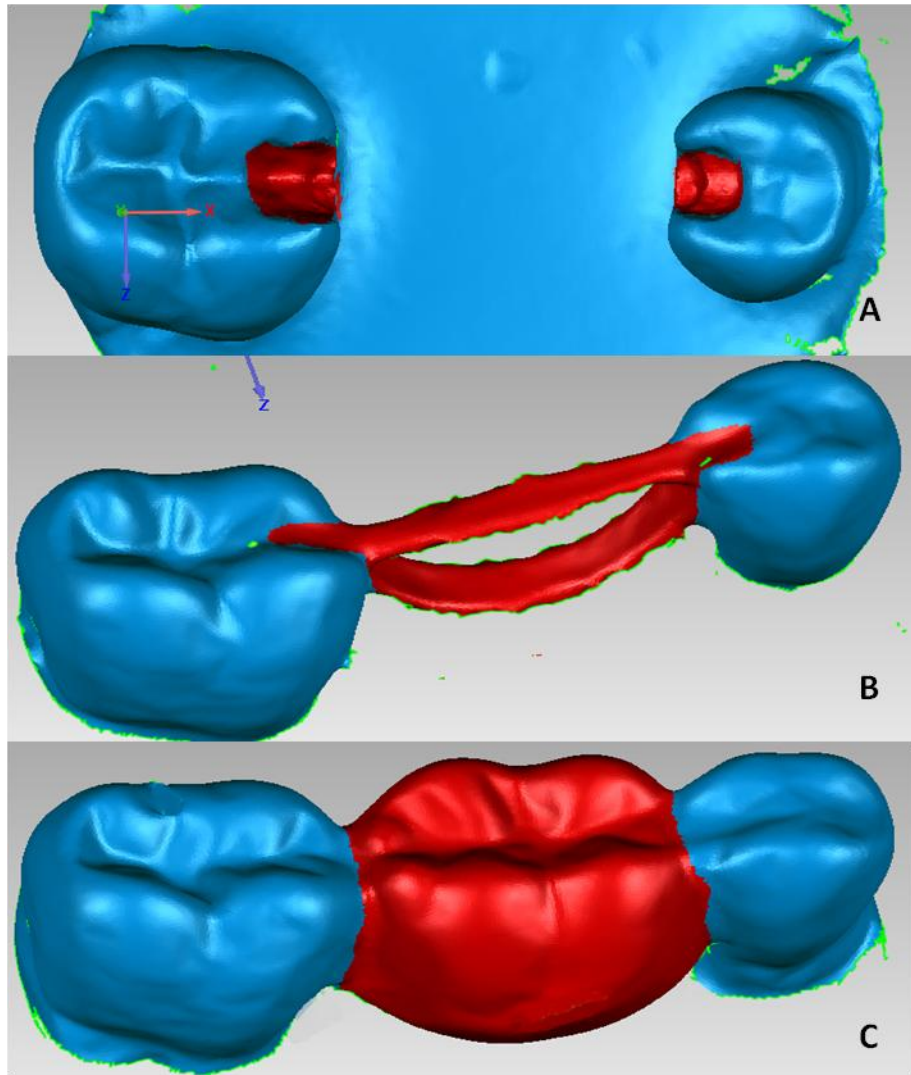


Figure 7.2: 3D representations of a specimen during the preparation, A) silica coating for the cavities to enhance adhesion, B) bonding of the main FRC framework within the inlay retainers using bonding agent (Viso-Bond) and flowable PFC (x-tra Base) , and C) full build-up for the pontic with packable bulk-fill PRC (X-tra fil).

7.3.3 Chewing simulation:

An *in-vitro* chewing simulator machine (CS-4.2, SD Mechatronic, Germany) was employed to simulate the effect of mastication and dynamic fatigue. Two subgroups were allocated equally from each framework type. Subgroup A (n=5) was the control with no pre-cyclic loading applied, whereas subgroup B included specimens were cyclically loaded for 240,000 cycles (5kg, 1.8Hz) in the chewing machine using a stainless steel stylus. The stylus was positioned to axially load the pontic with 2.5mm vertical movement towards the central fossa and then 0.7mm oblique movement over the lingual groove of buccal cusps (Figure 7.3). The contact point and buccal movement were checked by 40µm-thick articulating paper (Hanel, Coltene, Switzerland). To enable periodic recovery of the specimen, the stylus was automatically left off the specimen every 2500 cycles for a 5s period. After the chewing simulation, the specimens were each evaluated for cracks or signs of fracture using an optical microscope (Meiji EMZ-TR, Meiji Techno Co. Ltd., Tokyo, Japan) with high magnification (x40), and then stored in water (37°C) until further testing.

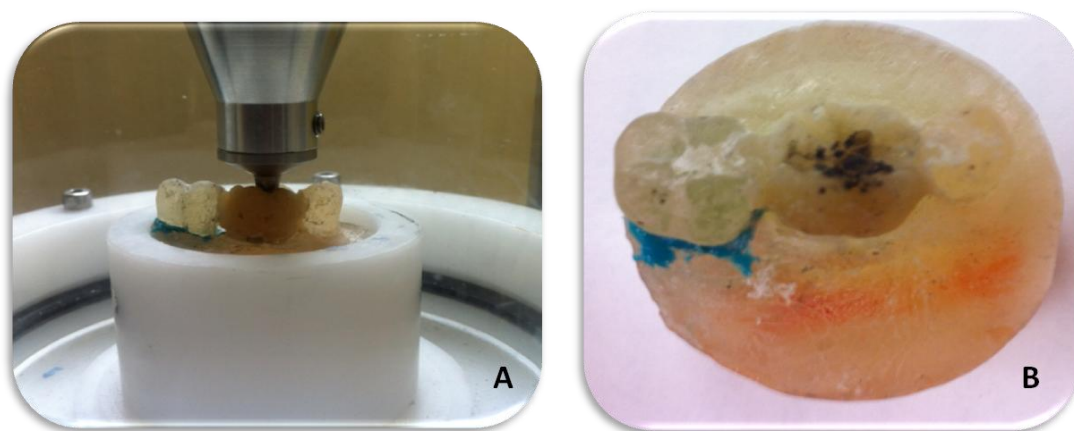


Figure 7.3: One representative specimen mounted in CS 4.2 machine, A) during the cyclic loading with the stylus moving vertically to the central fossa and then obliquely over the buccal groove, and B) after the completion of cyclic loading.

7.3.4 Static loading to fracture:

All the specimens (fatigued and control) were statically loaded to fracture in a universal testing machine (Zwick Z020, *Zwick/Roell GmbH, Germany*). A steel ball indenter (4mm Ø) was used to apply a compressive load along the pontic central fossa, with 1 mm/min crosshead speed. Tin foil (0.2mm thickness) was inserted between the indenter and the tested specimen to enable an even stress distribution. Initial fracture (IF) and final fracture (FF) loads (N) were recorded for each specimen. Fracture initiation was recognised as an initial sharp decline in the stress/strain curve. The mode of fracture was reported for each specimen as horizontal cracks, delamination or vertical midline fracture.

7.3.5 Statistical analysis:

Data collection and statistical analysis were performed with SPSS software (*IBM SPSS statistics 20, Chicago, IL, USA*). Mean and standard deviation (SD) values were calculated for IF and FF loads. The collected data were found homogenous and normally-distributed according to Levene's test ($p > 0.05$) and histograms. A two-way ANOVA was conducted to verify the statistical effect of framework types and dynamic fatigue on the observed fracture values. A series of paired and independent t-tests was performed to detect differences between IF and FF values in the same and different groups, respectively. The Weibull statistics of fracture probability for both framework types were performed to identify the Weibull modulus (m) and the characteristic strength (σ_θ) (the strength value that 63.2% of the specimens would fail up to it) [27].

7.4 RESULTS:

7.4.1 Quantitative findings

Static initial (IF) and final fracture (FF) loads for FRC-FPDs with different framework types and loading condition are shown in Table 7.2, and graphically represented in Figure 7.4. Type-I_A had the highest IF (623.8 N) and FF values (1598.6 N), while Type-II_B had the lowest (421.6-716.0 N respectively). FF values were always significantly higher than IF values ($p < 0.05$) with the highest difference among Type-I_A (974.8 N) and the lowest in Type-II_B (294.4 N). A positive linear correlation was found between IF and FF loads for both framework types (Figure 7.5).

Table 7.2: Mean±SD values for initial fracture (IF) and final fracture (FF) loads for all tested groups.

Group (framework type)	<i>Subgroup A (Control) (without previous fatigue)</i>		<i>Subgroup B (Fatigued) (with previous fatigue)</i>	
	<i>IF</i>	<i>FF</i>	<i>IF</i>	<i>FF</i>
Type-I (with unidirectional FRC)	623.8±115.2 ^a	1598.6±361.8 ^{b,1}	589.2±28.7 ^a	1144.0±270.9 ^{b,1}
Type-II (with bidirectional FRC)	505.2±104.2 ^a	1125.8±278.2 ^{c,2}	421.6±121.9 ^a	716.0±72.1 ^{c,3}

**Different superscript letters and numbers indicate statistical significance with intra- and inter-groups, respectively.*

Both framework type and cyclic loading had a significant influence on FF load ($p=0.002$) with no significant interaction ($p=0.854$), whereas the framework type only had a significant effect on IF load ($p=0.005$). Cyclic loading had no significant effect on IF values ($p=0.204$) nor interaction ($p=0.591$). According to Weibull statistics, represented in Figure 7.6 and Figure 7.7, the FRC-FPD specimens with Type-I framework had a better performance ($m=0.954$, $\sigma_0=1555.4$ N) than those with Type-II framework ($m=0.836$, $\sigma_0=1074.5$ N).

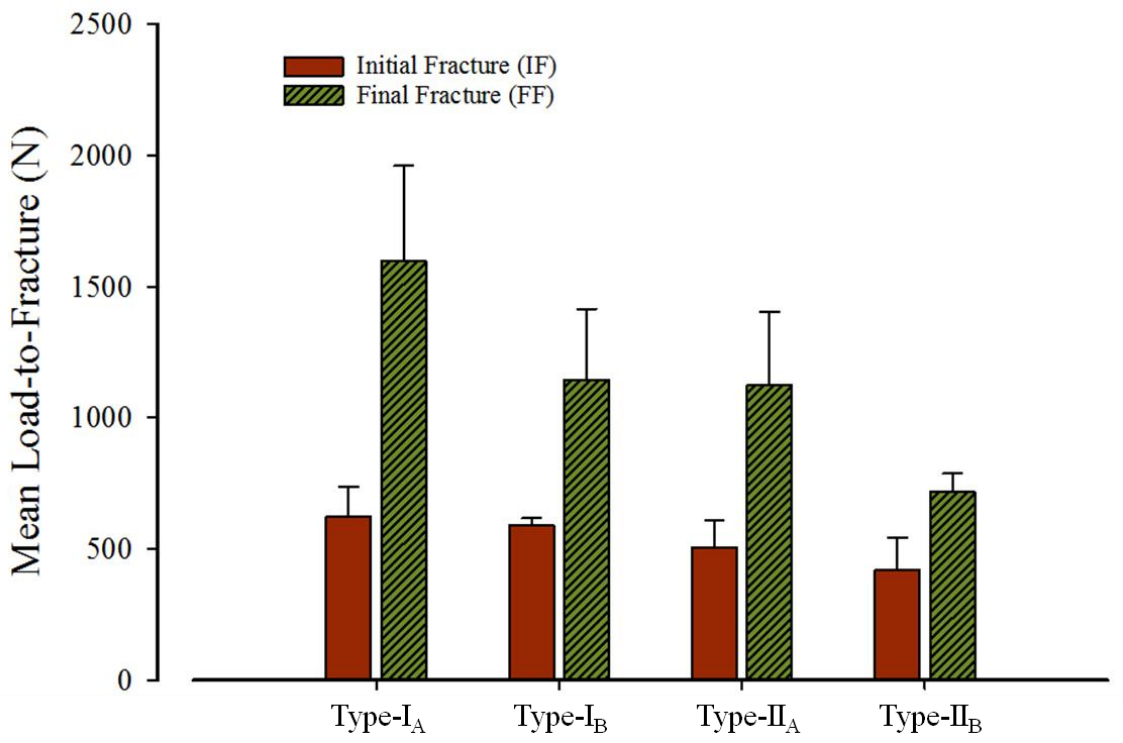


Figure 7.4: Bar chart showing the mean (SD) values of static IF and FF values for all tested groups with (B) and without previous thermocycling and dynamic fatigue (A).

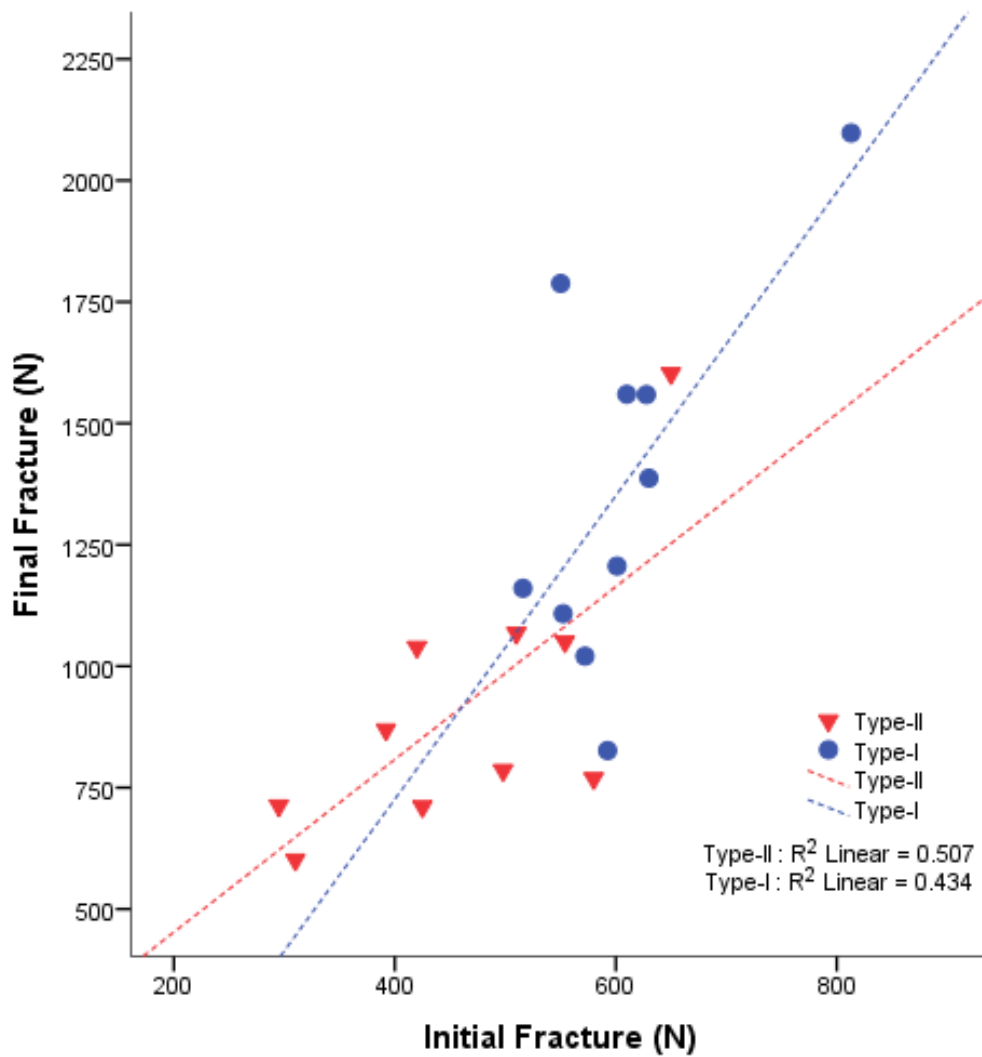


Figure 7.5: Scatter plot showing the positive linear correlation between initial fracture and final fracture in both framework types.

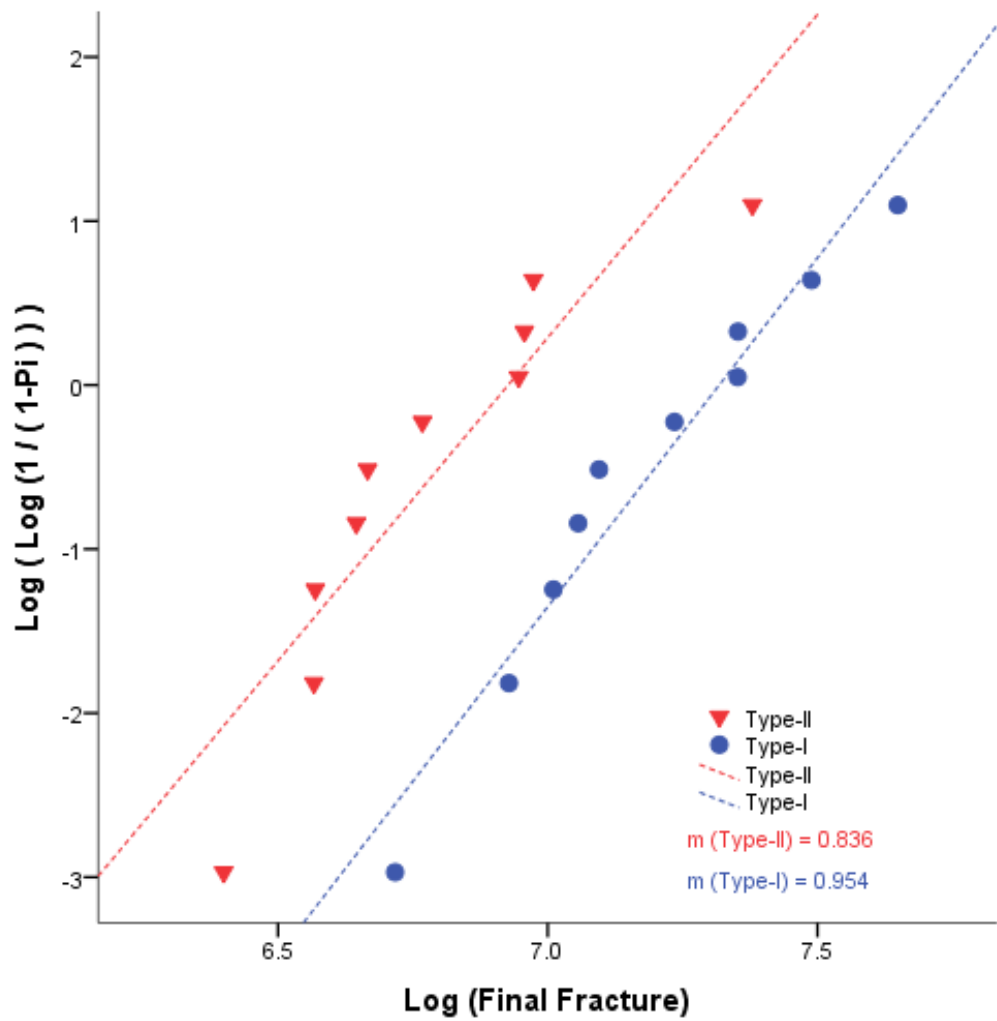


Figure 7.6: Scatter plot showing the Weibull modulus (m) for both framework types.

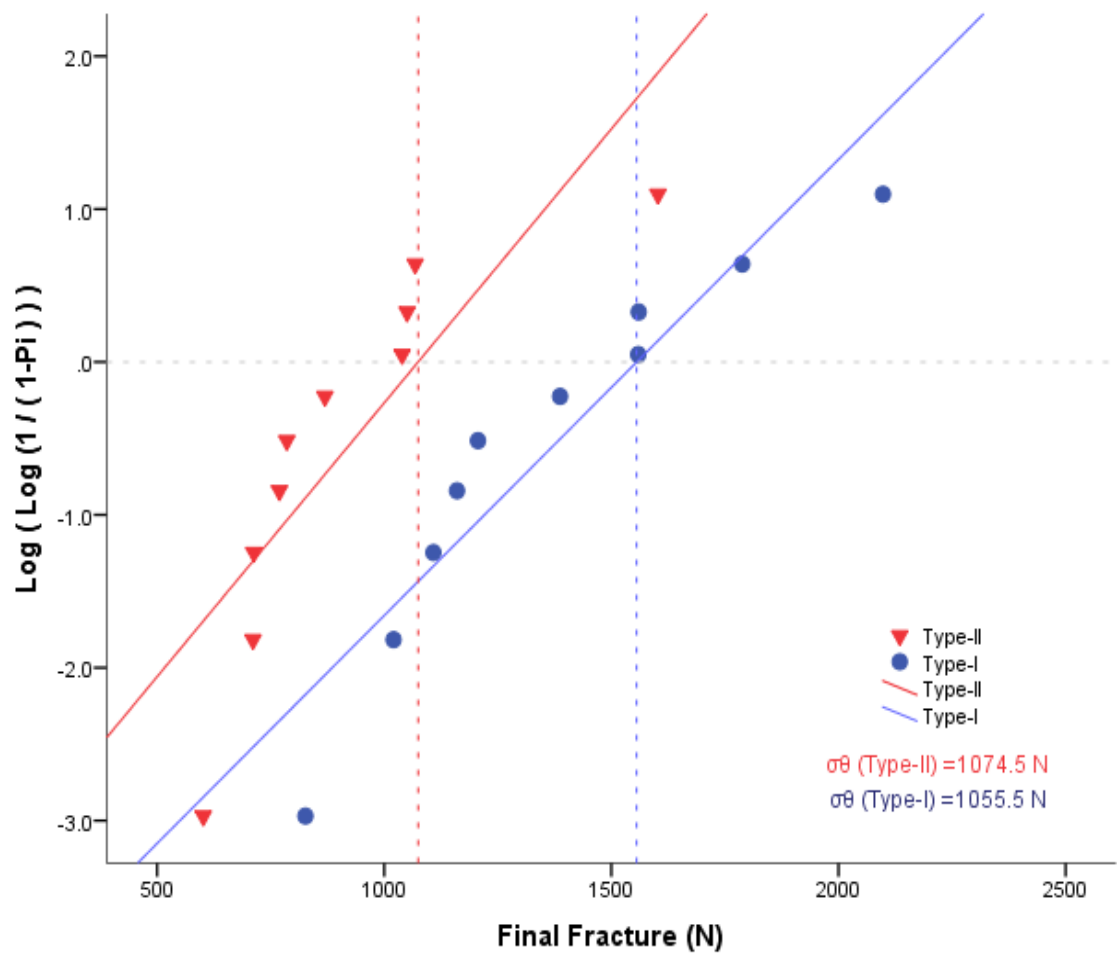


Figure 7.7: Scatter plot showing the characteristic strength (σ_θ) for both framework types.

7.4.2 Qualitative findings:

Subsequent to the chewing simulation, the inspection for subgroup B specimens exhibited 100% survival with no cracks/signs of fracture. Analysis of all the fractured specimens following static loading exhibited various modes of fracture as shown in Table 7.3. Failures within Type-I framework were mainly delamination, while the vertical fracture dominated failures of Type-II framework (Figure 7.8).

Table 7.3: The mode of fracture exhibited in all tested specimens.				
Failure mode	Type-I _A	Type-I _B	Type-II _A	Type-II _B
Horizontal cracks	-	-	1	1
Delamination	3	3	1	-
Midline fracture	2	2	3	4

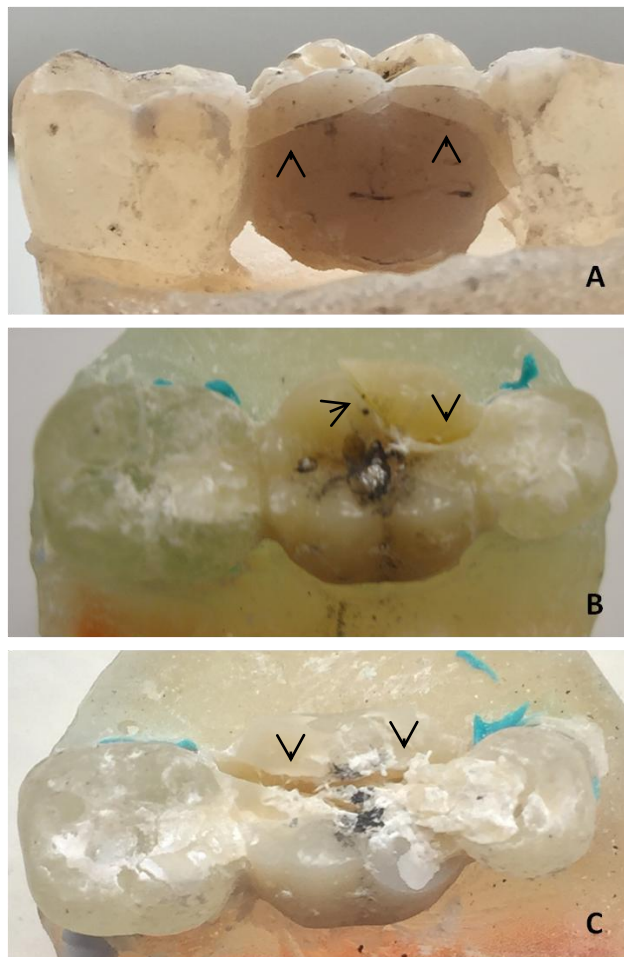


Figure 7.8: Examples of the fracture modes observed in FRC-FPDs after static loading, A) horizontal cracks extending from underneath the major connectors to the central fossa (loading point), B) delamination fracture with a separation of a mesio-lingual veneering PRC and C) midline (catastrophic) fracture extending vertically between both retainers.

7.5 DISCUSSION:

Two new fibre frameworks for FRC-FPDs were proposed and tested based on the current available evidence in the literature. The influence on fracture resistance (represented with IF and FF values) of FRC-FPDs was compared between the frameworks. Both frameworks shared the same layout of the main framework but differed in the form of additional FRCs incorporated to support the veneering resin-composite. A bidirectional fibre sheet incorporated perpendicular to the main FRC framework was used to modify Type-I framework, while Type-II had a woven fibres bundle perpendicularly-incorporated and wrapped around the pontic core. The rationale of such modifications was to allow more effective support for the pontic cusps and overall veneering resin-composite than the main fibre framework could provide alone. Although a high compressive strength can be offered by the main FRC framework, the support for the veneering composite is not as effective since the interface between veneering resin-composite and framework is weak [15, 24], which explains the frequent delamination failure of FRC-FPDs reported in previous studies [4, 10, 14, 16, 20, 23]. Therefore, the present study attempted to overcome this problem by incorporating additional FRC at the interface with the veneering resin-composite to aid in enhancing adhesion, increasing support, conquering shear and tensile stresses, and consequently reducing delamination failures.

Comparing the performance of both frameworks, specimens with Type-I framework had significantly better IF (589-624 N) and FF (1144-1599 N) values than those with Type-II framework (IF: 422-505 N, FF: 716-1126 N) independent of the fatigue condition applied. This variation in fracture resistance means that Type-I framework has higher load-bearing capacity and threshold of fracture than Type-II framework. The Weibull analysis also confirmed the superiority of the Type-I framework and revealed that it had more favourable Weibull modulus and characteristic strength values than Type-II framework, and therefore better failure behaviour and performance [27]. Nevertheless, this does not rule out that both framework types could survive the mean masticatory force that human can produce clinically at the molar region (500-600N) [28]. Consistent load-bearing capacity values have been reported previously with relatively similar pontic span (11mm) and retainer configuration (box inlay-retainers) [15]. However, the literature shows a wide range of load-bearing capacity values reported in previous studies (500N-2500N) [24, 29], which can be explained by the differences in test set-up, pontic span, materials and type of FRC incorporated.

A possible explanation for the variation between groups in the present study can be attributed to the difference in Krenchel factor. According to Krenchel [30], the efficiency of reinforcement for fibres loaded at a given direction, or the so-called 'Krenchel factor (K_{θ})', is highly influenced by the fibre orientation. The higher K_{θ} found for fibres the better efficiency of reinforcement provided in that direction. Consequently, fibres with bidirectional orientation have been reported to have higher K_{θ} ($=0.5$) under a perpendicular loading, and therefore provide better effective reinforcement than those with woven orientation ($K_{\theta} = 0.25$) [2, 8, 31], which supports the findings of the present study. Another potential explanation is the wider area of reinforcement and the more perpendicular occlusal support allowed by the bidirectional fibre sheet compared with the woven bundle. Such configuration of bidirectional FRC tends to stop crack propagation, delay fracture initiation and provide support for the occlusal veneering resin-composite better than the narrow curved woven bundle [8].

Specimens with Type-II framework also experienced more midline pontic fractures, yet, fewer delamination failures than those with Type-I framework. This observation certifies the influence of framework design on fracture dynamics and support for the veneering material. It also suggests that the configuration of Type-I framework tends to provide a wider support for the cusps and occlusal resin-composite, while the configuration of Type-II framework tends to enable a more retention for the buccal/lingual resin-composite. Previous studies comparing the influence of different framework modifications within the pontic of FRC-FPDs have reported similar findings [16, 24, 25, 32]. One study has found that the perpendicular incorporation of additional unidirectional fibre bundles reduces the delamination and provides the highest load-bearing capacity, in comparison with the incorporation of parallel unidirectional bundles or multidirectional fibres veil. [24]. Another study has also claimed reduction in the delamination failure and enhancement in load bearing capacity as a consequence of modifying the pontic framework with double perpendicular unidirectional fibres or short random FRC [16]. Nevertheless, the framework modifications used in the current study have not been previously investigated.

All specimens in this study were supported with two main bundles of FRCs in order to ensure high volume fraction of reinforcing fibres. Enhanced reinforcement and strength have been reported as a consequence of using high volume FRC-FPDs [11, 12]. The curved fibre bundle within the tension side of the pontic provides excellent stress distribution and crack growth resistance [5, 10, 18], while the straight bundle within the

compression side enables the required support for veneering composites and enhances the stiffness [15, 32, 33]. The employment of the box-shaped design for inlay cavities was also beneficial. It was not only a preservative approach but also provided the required space to include the two fibre bundles as needed, which permitted high fibre content and large connectors to resist stress concentrations at that area [15, 33]. This design also hindered crack propagation within the retainers as the small boxes tend to absorb great energy level before failure [14].

The chewing simulator was a valuable tool to investigate the performance of FRC-FPDs *in-vitro* since it allowed an accelerated simulation of the occlusal load in a standardised clinical fashion. The mean biting force (50N) was used to induce dynamic fatigue equivalent to one year of average mastication [34, 35]. Such dynamic fatigue was found critical to the structural integrity of FRC-FPDs as the FF values for subgroup B specimens were significantly lower than those for subgroup A specimens. This detrimental effect is potentially attributed to the cyclic stresses affecting the fibre-matrix interface of FRCs and causing debonding [11, 36]. Upon further static loading, the length of the debonded interface will propagate until abrupt load reduction and large acoustic emission observed. This event represents the point of fracture initiation (IF) which corresponds to the separation of entire fibre length [31, 37]. Despite the non-significant effect of dynamic fatigue on fracture initiation, it may still be responsible for lowering the threshold of fracture initiation in subgroup B.

With the intention of limiting the inconsistency that would result from the use of natural human teeth, this study used duplicated acrylic teeth as abutments. The variability of abutment dimensions, the discrepancies among the multiple preparations and the variation of dentine structures are all possible confounding factors that were omitted [34]. Nevertheless, the adhesion between composite resin and acrylic teeth is not guaranteed. Therefore, a standardised surface pre-treatment was performed to the abutment cavities aiming to enhance the retention. Moreover, an artificial periodontium was incorporated around the abutment roots to simulate the physiological tooth movement and the resultant stresses developing at the gingival part of the connectors. Such movement and stresses have been considered essential for investigating the performance of adhesive FPDs [34].

Nevertheless, this study has some limitations. Only one design of FPD (inlay-retained) has been investigated, and the results can be only applied to that design. Other designs,

including the conventional and prep less FPDs can be considered in future studies. Another limitation was encountered by not using a control group (without additional FRC incorporated in the pontic). Such a group would have emphasised the finding when its load bearing capacity compared with other groups. Moreover, limiting the investigation to one type of FRC as the main framework is an obstacle that prevents generalising the findings to other types of FRC. Accordingly, future studies investigating different types and designs of FRC-FPDs are suggested.

Overall, modifying the framework of FRC-FPDs via incorporating additional reinforcing fibre within pontics tends to enhance fracture resistance. Improved load bearing capacity, superior reinforcement for the veneering layer and reduced delamination fractures were reported. The configuration and orientation of incorporated fibres are also important as they regulate the effectiveness of reinforcement. Significantly different initial and final fracture values were reported as result of using frameworks with bidirectional and woven reinforcing fibres, which supports rejection of the first null hypothesis. The second null hypothesis was partially rejected as the dynamic fatigue significantly affected final fracture alone. From a clinical perspective, improved longevity and enhanced overall performance can be achieved by FRC-FPD with some simple modifications in its framework design, and since it offers versatility, maintainability and minimal invasion, it could be a potential alternative to replace posterior missing teeth.

7.6 CONCLUSIONS:

Within the limitations of this study, the following can be concluded:

- 1- The load-bearing capacity of FRC-FPD is significantly influenced by the framework design of its pontic.
- 2- The additional bidirectional fibres placed perpendicularly on the occlusal surface of the main framework provides better fracture resistance than the woven bundle incorporated around the pontic core.
- 3- Both framework designs provide lower fracture resistance when subjected to prior dynamic fatigue.

7.7 REFERENCES:

1. Fugazzotto PA. Evidence-Based Decision Making: Replacement of the Single Missing Tooth. *Dental Clinics of North America*, 2009; **53**: 97-129.
2. Kolbeck C, Rosentritt M, Behr M, Lang R, Handel G. In Vitro Examination of the Fracture Strength of 3 Different Fiber-Reinforced Composite and 1 All-Ceramic Posterior Inlay Fixed Partial Denture Systems. *J Prosthodont*, 2002; **11**: 248-253.
3. Harder S, Wolfart S, Eschbach S, Kern M. Eight-Year Outcome of Posterior Inlay-Retained All-Ceramic Fixed Dental Prostheses. *J Dent*, 2010; **38**: 875-881.
4. van Heumen CC, Kreulen CM, Creugers NH. Clinical Studies of Fiber-Reinforced Resin-Bonded Fixed Partial Dentures: A Systematic Review. *Eur J Oral Sci*, 2009; **117**: 1-6.
5. Chen Y, Li H, Fok A. In Vitro Validation of a Shape-Optimized Fiber-Reinforced Dental Bridge. *Dent Mater*, 2011; **27**: 1229-1237.
6. Başaran EG, Ayna E, Vallittu PK, Lassila LVJ. Load Bearing Capacity of Fiber-Reinforced and Unreinforced Composite Resin CAD/CAM-Fabricated Fixed Dental Prostheses. *J Prosthet Dent*, 2013; **109**: 88-94.
7. Kolbeck C, Rosentritt M, Behr M, Lang R, Handel G. In Vitro Study of Fracture Strength and Marginal Adaptation of Polyethylene-Fibre-Reinforced-Composite Versus Glass-Fibre-Reinforced-Composite Fixed Partial Dentures. *J Oral Rehabil*, 2002; **29**: 668-674.
8. Vallittu PK. Strength and Interfacial Adhesion of FRC-Tooth System. In: *The Second International Symposium on Fibre-Reinforced Plastics in Dentistry, Symposium Book on the Scientific Workshop on Dental Fibre-Reinforced Composite on 13 October 2001*. Edited by Vallittu PK. Nijmegen, Netherlands 2001.
9. Ellakwa AE, Shortall AC, Shehata MK, Marquis PM. The Influence of Fibre Placement and Position on the Efficiency of Reinforcement of Fibre Reinforced Composite Bridgework. *J Oral Rehabil*, 2001; **28**: 785-791.
10. Shi L, Fok AS. Structural Optimization of the Fibre-Reinforced Composite Substructure in a Three-Unit Dental Bridge. *Dent Mater*, 2009; **25**: 791-801.
11. Freilich MA, Meiers JC, Duncan JP, Eckrote KA, Goldberg AJ. Clinical Evaluation of Fiber-Reinforced Fixed Bridges. *J Am Dent Assoc*, 2002; **133**: 1524-1534; quiz 1540-1521.
12. Abdulmajeed AA, Närhi TO, Vallittu PK, Lassila LV. The Effect of High Fiber Fraction on Some Mechanical Properties of Unidirectional Glass Fiber-Reinforced Composite. *Dent Mater*, 2011; **27**: 313-321.
13. Magne P, Perakis N, Belser UC, Krejci I. Stress Distribution of Inlay-Anchored Adhesive Fixed Partial Dentures: A Finite Element Analysis of the Influence of Restorative Materials and Abutment Preparation Design. *J Prosthet Dent*, 2002; **87**: 516-527.
14. Ozcan M, Breuklander MH, Vallittu PK. The Effect of Box Preparation on the Strength of Glass Fiber-Reinforced Composite Inlay-Retained Fixed Partial Dentures. *J Prosthet Dent*, 2005; **93**: 337-345.
15. Song H-Y, Yi Y-J, Cho L-R, Park D-Y. Effects of Two Preparation Designs and Pontic Distance on Bending and Fracture Strength of Fiber-Reinforced Composite Inlay Fixed Partial Dentures. *J Prosthet Dent*, 2003; **90**: 347-353.
16. Keulemans F, Lassila LV, Garoushi S, Vallittu PK, Kleverlaan CJ, Feilzer AJ. The Influence of Framework Design on the Load-Bearing Capacity of Laboratory-Made

- Inlay-Retained Fibre-Reinforced Composite Fixed Dental Prostheses. *J Biomech*, 2009; **42**: 844-849.
17. Waki T, Nakamura T, Kinuta S, Wakabayashi K, Yatani H. Fracture Resistance of Inlay-Retained Fixed Partial Dentures Reinforced with Fiber-Reinforced Composite. *Dent Mater J*, 2006; **25**: 1-6.
 18. Nakamura T, Ohyama T, Waki T, Kinuta S, Wakabayashi K, Takano N, Yatani H. Finite Element Analysis of Fiber-Reinforced Fixed Partial Dentures. *Dent Mater J*, 2005; **24**: 275-279.
 19. Rosentritt M. Fibre Reinforced Composite in Vitro Behaviour. In: *The Second International Symposium on Fire-Reinforced Plastics in Dentistry, Symposium Book on Scientific Workshop*. Edited by Vallittu PK; 2001.
 20. van Heumen CCM, Tanner J, van Dijken JWV, Pikaar R, Lassila LVJ, Creugers NHJ, Vallittu PK, Kreulen CM. Five-Year Survival of 3-Unit Fiber-Reinforced Composite Fixed Partial Dentures in the Posterior Area. *Dent Mater*, 2010; **26**: 954-960.
 21. Anusavice KJ. Standardizing Failure, Success, and Survival Decisions in Clinical Studies of Ceramic and Metal-Ceramic Fixed Dental Prostheses. *Dent Mater*, 2012; **28**: 102-111.
 22. Schley J-S, Heussen N, Reich S, Fischer J, Haselhuhn K, Wolfart S. Survival Probability of Zirconia-Based Fixed Dental Prostheses up to 5 Yr: A Systematic Review of the Literature. *Eur J Oral Sci*, 2010; **118**: 443-450.
 23. Göhring TN, Roos M. Inlay-Fixed Partial Dentures Adhesively Retained and Reinforced by Glass Fibers: Clinical and Scanning Electron Microscopy Analysis after Five Years. *Eur J Oral Sci*, 2005; **113**: 60-69.
 24. Xie Q, Lassila LV, Vallittu PK. Comparison of Load-Bearing Capacity of Direct Resin-Bonded Fiber-Reinforced Composite FPDs with Four Framework Designs. *J Dent*, 2007; **35**: 578-582.
 25. Perea L, Matinlinna JP, Tolvanen M, Lassila LV, Vallittu PK. Fiber-Reinforced Composite Fixed Dental Prostheses with Various Pontics. *J Adhes Dent*, 2014; **16**: 161-168.
 26. Ozcan M, Breuklander M, Salihoglu-Yener E. Fracture Resistance of Direct Inlay-Retained Adhesive Bridges: Effect of Pontic Material and Occlusal Morphology. *Dent Mater J*, 2012; **31**: 514-522.
 27. Quinn JB, Quinn GD. A Practical and Systematic Review of Weibull Statistics for Reporting Strengths of Dental Materials. *Dent Mater*, 2010; **26**: 135-147.
 28. Hidaka O, Iwasaki M, Saito M, Morimoto T. Influence of Clenching Intensity on Bite Force Balance, Occlusal Contact Area, and Average Bite Pressure. *J Dent Res*, 1999; **78**: 1336-1344.
 29. Behr M, Rosentritt M, Ledwinsky E, Handel G. Fracture Resistance and Marginal Adaptation of Conventionally Cemented Fiber-Reinforced Composite Three-Unit FPDs. *Int J Prosthodont*, 2002; **15**: 467-472.
 30. Krenchel. Fibre Reinforcement: Copenhagen: Technical University of Denmark; 1963.
 31. Dyer SR, Lassila LV, Jokinen M, Vallittu PK. Effect of Fiber Position and Orientation on Fracture Load of Fiber-Reinforced Composite. *Dent Mater*, 2004; **20**: 947-955.
 32. Behr M, Rosentritt M, Taubenhansl P, Kolbeck C, Handel G. Fracture Resistance of Fiber-Reinforced Composite Restorations with Different Framework Design. *Acta Odontol Scand*, 2005; **63**: 153-157.

33. Rappelli G, Scalise L, Procaccini M, Tomasini EP. Stress Distribution in Fiber-Reinforced Composite Inlay Fixed Partial Dentures. *J Prosthet Dent*, 2005; **93**: 425-432.
34. Heintze SD, Cavalleri A, Zellweger G, Buchler A, Zappini G. Fracture Frequency of All-Ceramic Crowns During Dynamic Loading in a Chewing Simulator Using Different Loading and Luting Protocols. *Dent Mater*, 2008; **24**: 1352-1361.
35. Kohyama K, Hatakeyama E, Sasaki T, Azuma T, Karita K. Effect of Sample Thickness on Bite Force Studied with a Multiple-Point Sheet Sensor. *J Oral Rehabil*, 2004; **31**: 327-334.
36. Dyer SR, Sorensen JA, Lassila LV, Vallittu PK. Damage Mechanics and Load Failure of Fiber-Reinforced Composite Fixed Partial Dentures. *Dent Mater*, 2005; **21**: 1104-1110.
37. Dyer SR, Lassila LV, Alander P, Vallittu PK. Static Strength of Molar Region Direct Technique Glass Fibre-Reinforced Composite Fixed Partial Dentures. *J Oral Rehabil*, 2005; **32**: 351-357.

Chapter 8: Quantitative Wear Evaluation of Metal-Free Crowns Using Intraoral Scanner in-vitro.

8.1 ABSTRACT:

Objectives: To monitor the morphological changes of three metal-free crowns after *in-vitro* dynamic fatigue simulation using a 3D intraoral scanner.

Methods: Metal-free crowns (n=15), for a lower first molar, were fabricated using three different materials. In groups LZ (n=5) and LU (n=5), monolithic crowns were manufactured using CAD/CAM technology from zirconia-based ceramic (*Lava Zirconia*, 3M-ESPE) and resin nano-ceramic (*Lava Ultimate*, 3M-ESPE) materials, respectively. In group FRC-S (n=5), experimental fibre-reinforced composite (FRC) crowns were made conventionally from bidirectional reinforcing-fibres (*Stick Net*, *Stick Tech Ltd*) and resin-composite material (*Sinfony*, 3M-ESPE). All crowns were adhesively cemented (*RelyX-UniCem2*, 3M-ESPE) over identical acrylic abutments. Following thermocycling aging (3500 cycles, 5-55°C, 10s), all crowns were cyclically loaded to induce wear using a chewing simulator (*CS-4.2*, *SD-Mechatronic*). A 3D intraoral scanner (*3M True Definition Scanner*, 3M-ESPE) was employed to monitor the resultant morphological changes. 3D scans were taken at baseline (C0: No cyclic loading), after 240K cycles (C1) and 480K cycles (C2) and then compared. The wear analysis was performed using surface matching software (*Geomagic Control*, *Geomagic*). The mean morphological change (μm) was recorded for each specimen after C1 and C2. One-way ANOVA and paired t-test were conducted to detect the significance of experimental factors (material type and loading phase) on the quantitative degree of wear ($\alpha=0.05$).

Results: The highest cumulative wear was detected for LU ($348.2 \pm 52.0 \mu\text{m}$) while LZ had the lowest ($16.4 \pm 1.5 \mu\text{m}$). The degree of wear detected following C1 phase was significantly higher than that detected after C2 phase independent of the constructing material.

Conclusion: Wear rate of metal-free crowns is significantly influenced by the constructing material and number of loading cycles. Lava Zirconia has the most significant resistance, while Lava Ultimate has the least. The initial phase of wear simulation has the most significant effect on the degree of wear.

8.2 INTRODUCTION:

Tooth wear is becoming an increasingly recognised problem due to its growing prevalence and severity [1, 2]. It is an irreversible condition with multi-factorial aetiology that affects both teeth and restorative materials, and represents their cumulative surface loss under operational conditions [3]. It may be a physiological process that has a low estimated annual rate (approximately 20-38 μm); however, can be pathological under certain circumstances, such as parafunctional habits and high acid consumption, which excessively amplify its rate to a degree that adversely affects functionality and appearance of affected structures [3, 4]. Therefore, early diagnosis, regular monitoring and accurate interventions are always necessary.

It has been demonstrated that tooth wear is influenced by many different tribological parameters in the oral cavity. The properties of articulating surfaces, their roughness and topography, the abrasive nature of food, saliva and lubrication, chewing behaviour and biting force as well as other environmental factors are among parameters that simultaneously affect the mechanism of wear [5, 6]. Accordingly, different mechanisms of wear have been identified [7]. Attrition is a wear resulting of direct sliding action between antagonistic teeth or restorations during mastication or any other occlusal movements. It is usually described as two-body wear as long as there is no intermediate layer transmitting forces between the interlocking surfaces [5, 8]. The presence of an intermediate layer (like food or other soft medium) during mastication serves as a third body and causes abrasion wear [8]. In contrast, the repetitive cyclic load of mastication provokes surface micro-cracking which induces chipping and so fatigue wear [5, 9]. Corrosive wear, however, is more related to a chemical reaction that softens superficial microstructures and facilitates their scrapping away by antagonistic contact [10]. Understanding of all these parameters and mechanisms is the key role for tooth wear management.

Selection of restorative materials is also crucial for tooth wear management. The use of materials with high wear resistance may complicate the clinical situation due to their abrasiveness that can cause teeth sensitivity and occlusal imbalance [6, 11, 12]. Ideally, wear behaviour of restorative materials should match that of antagonistic structures in order to preserve occlusal form and prevent instability. Precious metal alloys, irrespective of their poor aesthetics, are the first choice for restoring worn posterior teeth as their wear behaviour is comparable to enamel [11, 13]. Dental resin-composites,

as aesthetic alternatives, have continuously been improved in terms of wear resistance; however, their relatively poor mechanical properties and insufficient wear behaviour limit their application under high-demand situations [14, 15]. Dental ceramics, on the other hand, have been widely used to restore posterior teeth, owing to their high wear resistance and excellent aesthetics. However, their abrasiveness that affects opposing dentition may be enough to enhance pathological tooth wear and generate other complications [12]. In comparison with other ceramics, recent studies have suggested the use of polished monolithic zirconia-based restorations as they offer not only superior mechanical properties but also optimum wear behaviour. However, their abrasiveness is still questionable [6, 16, 17].

Many techniques have been employed to optimize wear resistance and abrasiveness of metal-free restorative materials. Filler size, shape and volume of resin-composites have been modified in order to minimize filler exfoliation and improve wear resistance [5, 18-21]. Incorporation of long or short reinforcing fibres has been also suggested to improve mechanical properties, and so enhance the overall wear behaviour [22, 23]. Microstructures of various ceramics have been also modified with different processing and polishing techniques, leading to a consequent reduction in the abrasiveness [17, 24]. Moreover, new materials combining the favourable properties of resin-composites and ceramics have been recently developed [25-27]. However, limited information on their wear behaviour compared with other materials is available [28].

Monitoring pathological tooth wear and quantifying the consequential changes are also essential steps for management [29]. Many monitoring techniques have been developed, including tooth wear indices, image analysis, cusp-height measurement, scanning electron microscopy, computer graphics and profilometry [30, 31]. However, 3D scanning is currently the most preferable to quantify tooth wear, owing to its accuracy and versatility. Surface mapping systems, like contact/non-contact profilers, micro-CT scanners, laser scanners and CAD/CAM systems, are used to obtain sequential 3D images [30, 32]. Analysis and comparison of such images have been reported as the most accurate method for tooth wear measurement [33]. Nevertheless, these systems depend on impressions, gypsum casts or epoxy-resin dies for image acquisition, which could produce inherent errors [32, 34, 35]. Direct intraoral scanning of worn teeth would be the potential gold standard for wear measurement since it would decrease the number of steps and enhance accuracy, but this area has not been extensively studied.

The aim of this *in-vitro* study was to compare the wear behaviour of three metal-free restorative materials by investigating the effect of sequential chewing simulation and monitoring the morphological changes using a 3D intraoral scanner. The first null hypothesis was that there is no difference between the tested materials in terms of wear resistance, while the second was that there is no difference in the wear rate as a result of sequential chewing simulation.

8.3 MATERIALS AND METHODS:

Fifteen posterior crowns (n=15) constructed from three metal-free crown fabricating materials were dynamically fatigued *in-vitro* and monitored for the resultant morphological changes using an intraoral 3D scanner. The fabricating materials used, their description and manufacturers are listed in Table 8.1.

Table 8.1: Materials used to fabricate all crowns in the study.				
Group	Fabrication Mode	Material	Description	Manufacturer
LZ	CAD/CAM	Lava™ Zirconia	Pre-sintered Zirconia-based ceramic	3M-ESPE, Seefeld, Germany
LU	CAD/CAM	Lava™ Ultimate	Resin nano-ceramic	3M-ESPE, Seefeld, Germany
FRC-S	Conventional	Sinfony	Indirect laboratory micro-hybrid composite	3M-ESPE, Seefeld, Germany
		Stick Net	Bidirectional E-glass reinforcing fibres sheet	Stick Tech Ltd, Turku, Finland

8.3.1 Specimen Preparation:

Fifteen identical specimen assemblies representing a prepared lower first molar tooth and its supporting structure were produced in a standardised manner. A master preparation was performed on a molar plastic tooth (*KaVo dental GmbH, Biberach, Germany*) using a high speed air turbine with coarse grit shoulder end diamond bur, according to specific dimensions (1mm finish line, 1.5–2 mm occlusal clearance). A silicon master mould (*Gemini, Bracon, East Sussex, UK*) was then produced and used to fabricate fifteen identical teeth made of cold-cure acrylic resin (*Metropair Denture Repair, Metrodent Limited, Huddersfield, UK*). All the duplicated teeth were pre-coated with wax before being mounted within an epoxy-resin base (*Epoxy resin, B&K Resins Ltd, Bromley, UK*) in order to reproduce the periodontium and bone support.

Subsequently, the wax coatings were substituted with light-bodied impression material (*Aquasil LV, Dentsply, PA, USA*) to simulate the elasticity of periodontal ligament.

8.3.2 Crown fabrication:

Fifteen mandibular first molar crowns (n=15) with the same occlusal morphology and dimensions were fabricated from three different metal-free materials (Figure 8.1). In groups LZ and LU (n=5 each), monolithic crowns were manufactured using CAD/CAM technology from zirconia-based ceramic (*Lava Zirconia, 3M-ESPE*) and resin nano-ceramic (*Lava Ultimate, 3M-ESPE*) materials, respectively. In group FRC-S (n=5), experimental fibre-reinforced composite (FRC) crowns were made conventionally from bidirectional reinforcing-fibres (*Stick Net, Stick Tech Ltd*) and resin-composite material (*Sinfony, 3M-ESPE*).

Prior to preparing the master plastic tooth, digital impression and transparent vacuum-formed matrix were created to standardise the morphology of all crowns. An intraoral 3D scanner (*3MTM True definition scanner, 3M-ESPE, USA*) was used to obtain the digital impressions for the master tooth, before and after preparation, in order to be utilized in the fabrication of the CAD/CAM crowns. All the CAD/CAM crowns were milled by one milling centre using the same set of 3D digital impressions for designing and processing. The vacuum-formed matrix and one master tooth were used by one trained technician to fabricate the experimental FRC crowns. A standardized 2-coat thickness of die spacer (*blue die spacer 20µm, Kerr, USA*) was ensured for all crowns by painting-on the master tooth before crown fabrication. Upon completion, all crowns were hand-polished (with no glaze application), inspected and then tried on the master tooth. The crowns were then adhesively cemented to the corresponding specimen assemblies using self-adhesive resin cement (*RelyX UniCem 2, 3M-ESPE, Seefeld, Germany*). In order to improve adhesion, the teeth and the intaglio (inner) surfaces of the crowns were sandblasted (2.5 bar pressure, 15s) and silanated (30s) using CojetTM repair system (*3M-ESPE, Seefeld, Germany*) before cementation. A standardized load (5kg for 5 min) was used to ensure optimal seating. All the specimens were then stored in water (37°C, 24h) prior to further testing.

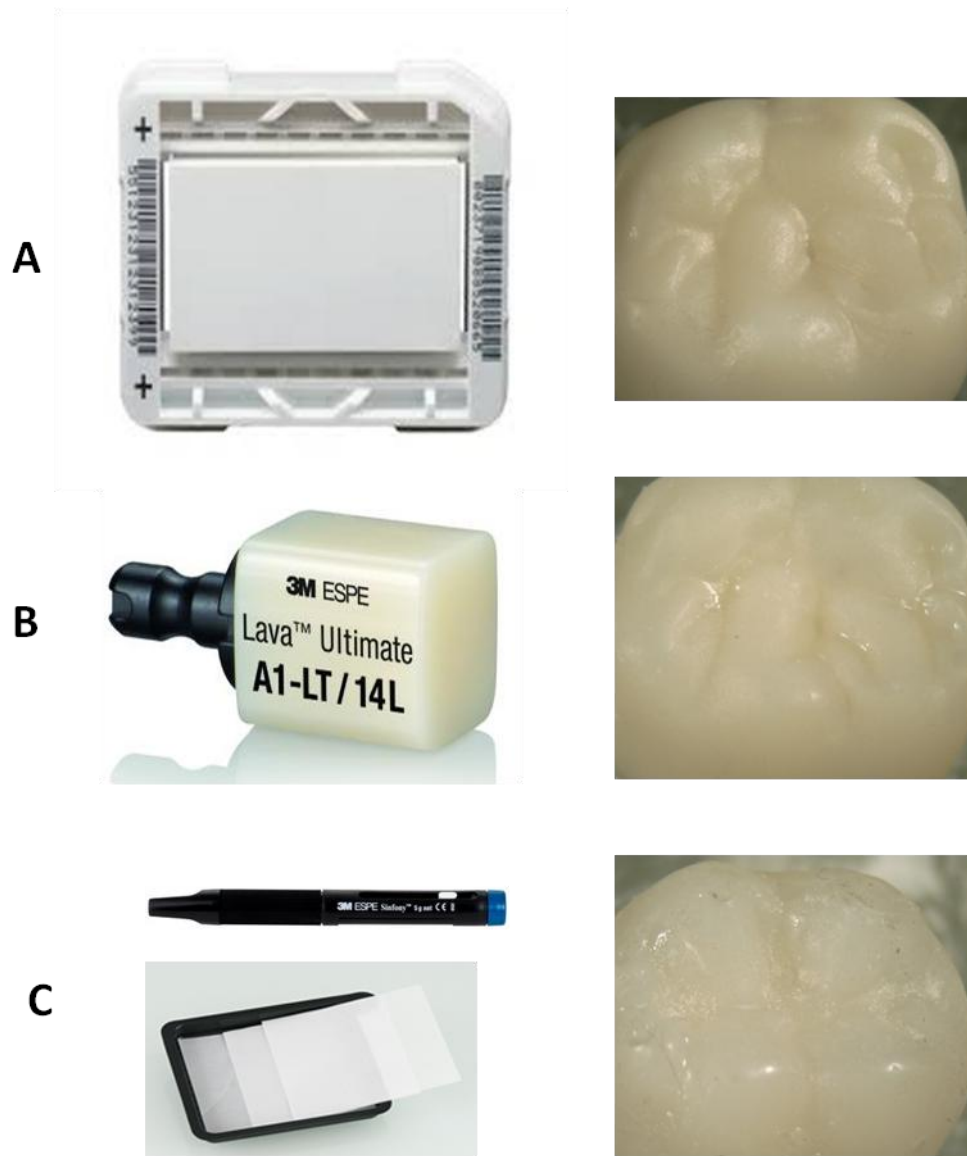


Figure 8.1: Fabricating materials used to prepare all specimens, A) Lava Zirconia, B) Lava Ultimate and C) Stick Net & Sinfony.

8.3.3 Wear simulation:

The *in-vitro* wear simulation was performed in three distinctive phases. In the first phase (C₀), thermocycling (3500 cycles) was performed in hot/cold water baths (5 -55 °C, 10s dwell time) for all crowns. A digital impression was then taken for each crown to register the baseline occlusal morphology without any wear. *3M™ True definition scanner* was used to obtain all the required digital impressions (as .STL files) for future wear analysis. Before taking the impressions, a dusting layer (10µm) of titanium dioxide-based powder (*3M™ High-Resolution Scanning Spray, 3M-ESPE*) was sprayed all over the specimen in order to enhance accuracy and speed of capture. This was followed by washing and drying to ensure no residual powder left.

The successive two phases (C₁, C₂) simulated mechanical wear in a clinically-relevant approach. A chewing simulator machine (CS-4.2, *SD Mechatronic, Germany*) was used to introduce wear by mimicking parafunctional mastication. A stainless steel stylus, representing the opposing working cusp, was used as an antagonist that transmitted the biting load (5Kg) into the specimens and induced wear. The stylus motion was adjusted to initially contact crowns in the deepest point of the central fossa with a vertical movement (2.5mm), followed by a further oblique sliding movement (2.0mm) along the buccal groove. The point of contact between stylus and crown was verified using 40µm-thick articulating paper (*Hanel, Coltene, Switzerland*). The same motion was repeated cyclically (1.8Hz frequency) with a total of 240,000 cycles for each phase. Digital impressions, as previously described, were taken at the end of each phase and saved for future analysis.

8.3.4 Wear analysis:

Geomagic Control 2014 software (*Geomagic, 3D System Corporation, USA*) was used to digitally inspect all the specimens and monitor the resultant morphological changes. The specimens were analysed one at a time via inspecting the three sequential impressions (at C₀, C₁ and C₂) simultaneously (Figure 8.2). The morphological changes were visualised as deviations from the baseline impression using ‘Best fit alignment’ and ‘3D comparison’ functions in the software (Figure 8.3). The mean vertical deviation was measured at one particular area (0.5mm radius) within the wear facets (Figure 8.4). Three wear values (W₁, W₂ and W_C) were recorded per specimen; W₁ represents the resultant wear of phase C₁, W₂ represents the resultant wear of phase C₂, and W_C is the cumulative vertical wear.

8.3.5 Statistics:

Data collection and statistical analysis were performed with SPSS software (IBM SPSS statistics 20, Chicago, IL, USA). Mean and standard deviation (SD) values were calculated for each group. The assumption of homogeneity and normal distribution was granted according to Levene's test ($p > 0.05$) and histograms. One-way ANOVA (Tukey's post hoc) and paired t-test were conducted to detect the significance of 'material type' and 'loading phase' on the degree of wear ($\alpha = 0.05$).

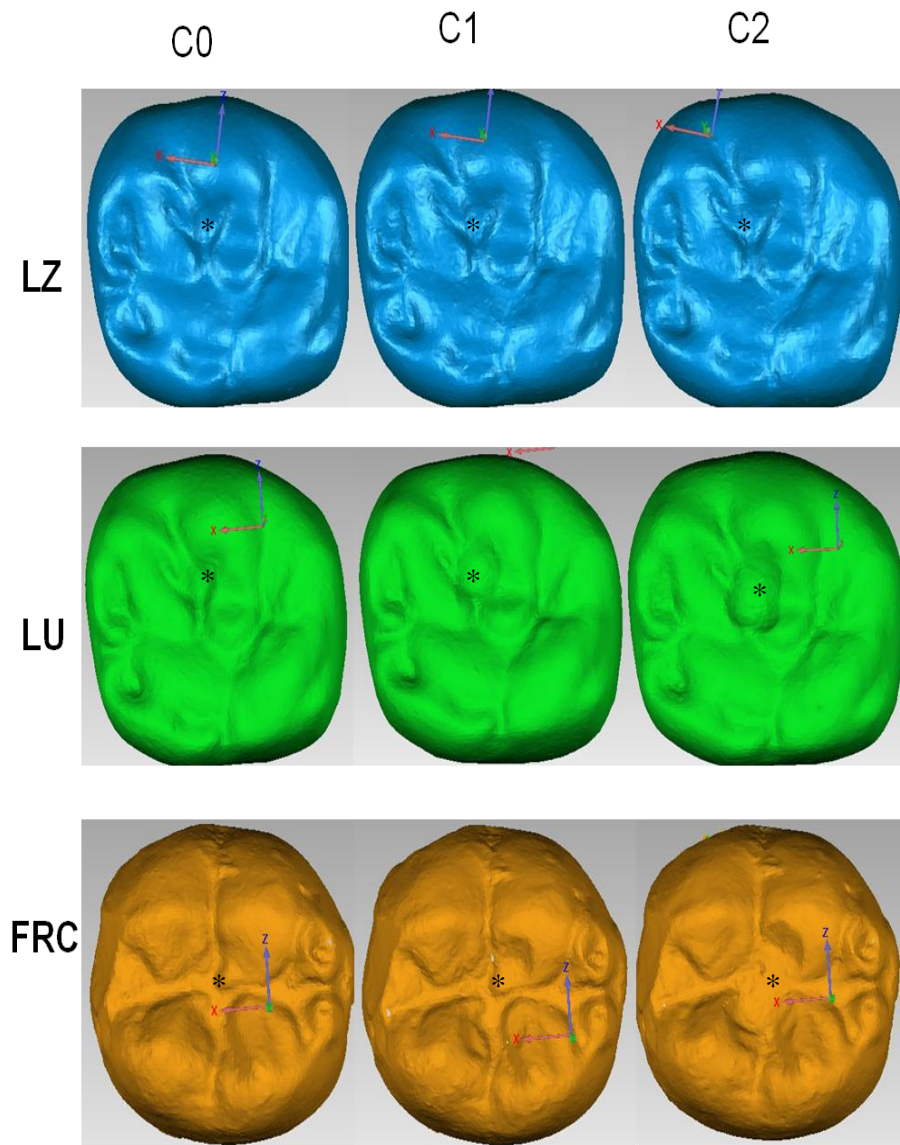


Figure 8.2: Occlusal views for one representative specimen from each group showing the wear facet (*) and its morphological changes after C0, C1 and C2 phases (using Geomagic Control software). LZ had the modest morphological changes, while LU had the largest.

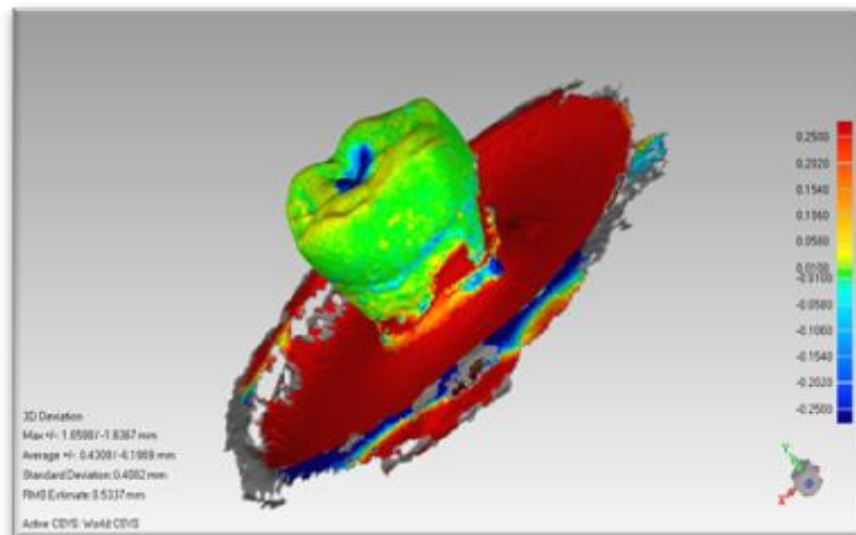
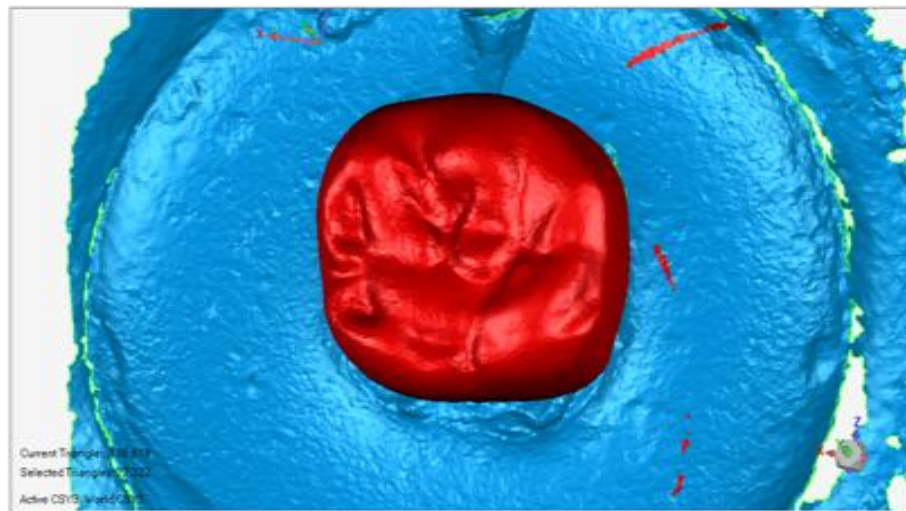
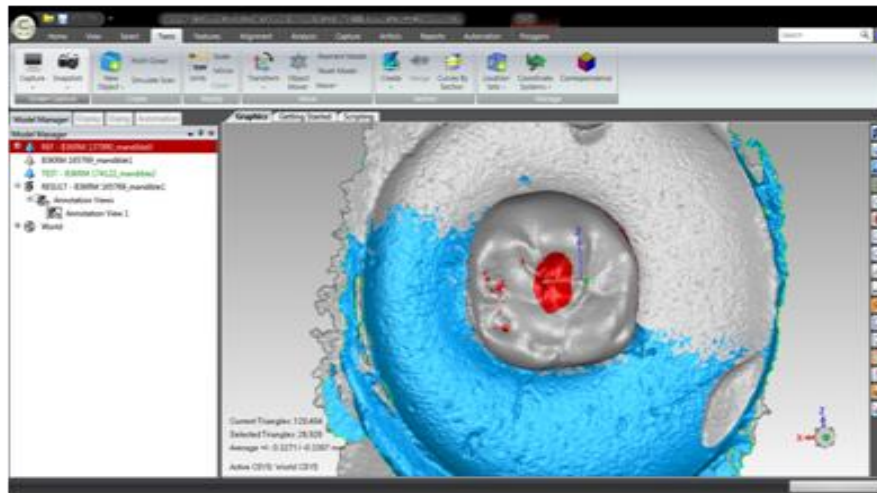


Figure 8.3: A snapshot from the Geomagic software after the ‘Best Fit Alignment’ function was performed (top), the area of interest ‘common area’ was selected prior to the alignment (middle), and then the 3D Comparison performed and the deviations visualised via deviation spectrum (bottom).

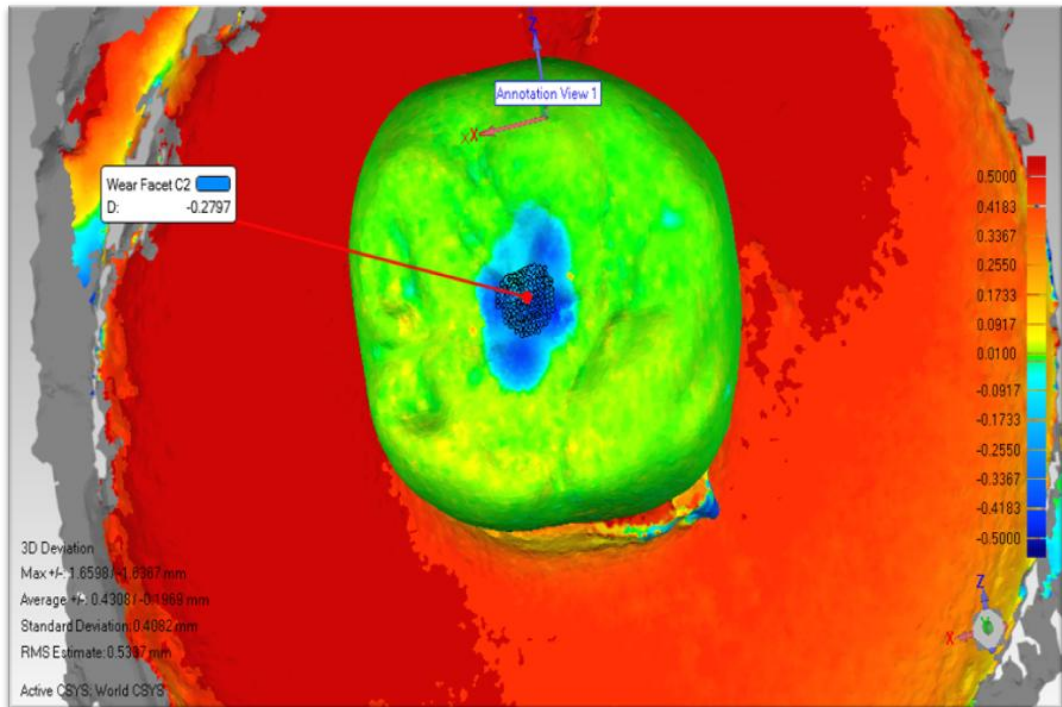
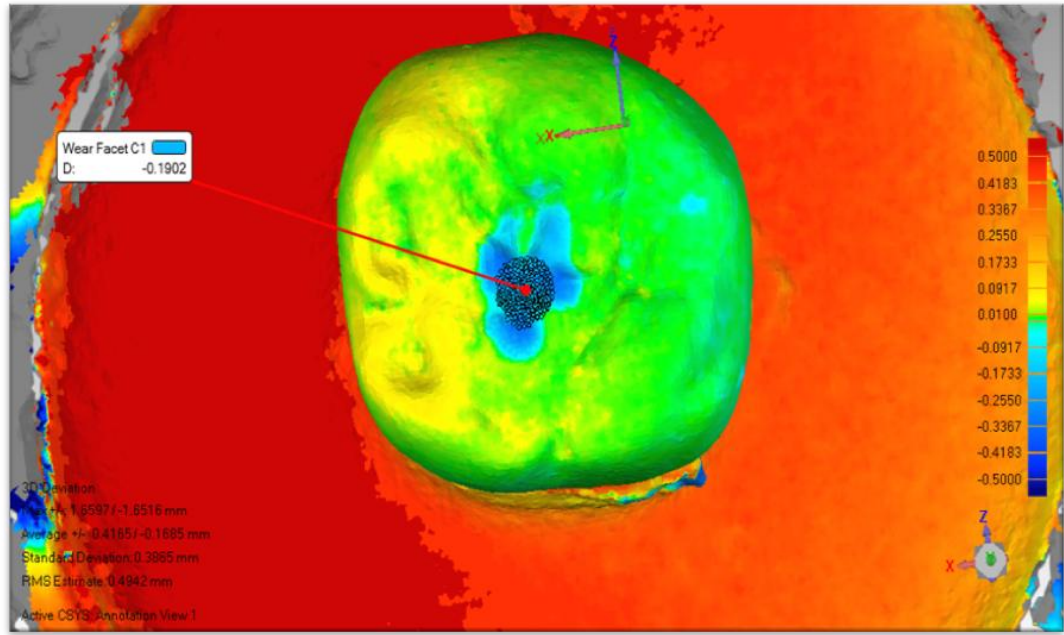


Figure 8.4: 3D comparisons for one representative specimen in group LU, (Top) shows the mean wear value 'W1' within the wear facet (0.5mm radius) after phase C1, while (bottom) shows the cumulative wear W_C at the end of phase C2.

8.4 RESULTS:

The mean wear values for all the tested groups are shown in Table 8.2, and graphically represented in Figure 8.5. The highest cumulative wear (W_C) was detected for LU ($348.2 \pm 52.0 \mu\text{m}$) while LZ had the lowest ($16.4 \pm 1.5 \mu\text{m}$). The fabricating material had a statistically significant influence on the degree of wear independent of the loading phase. Moreover, both loading phases had a significantly different impact on the cumulative wear. Phase C1 had the most influence on the cumulative wear irrespective of the fabricating material. Both fabricating material and loading phase significantly influenced the degree of wear detected.

Table 8.2: Wear measurements (μm) for all specimens, using 3D analysis.			
Group	Mean \pm SD		
	W_1	W_2	W_C
LZ	$11.0 \pm 4.4^{a,1}$	$5.4 \pm 5.2^{a,1}$	16.4 ± 1.5^a
LU	$215.1 \pm 95.2^{b,1}$	$133 \pm 45.5^{b,2}$	348.2 ± 52.0^b
FRC-S	$177.6 \pm 105.8^{b,1}$	$56.3 \pm 31.3^{c,2}$	233.9 ± 100.4^c

**Different superscript letters and numbers indicate statistical significance within the same columns (one-way ANOVA/post hoc), and rows (Paired t-test) respectively.*

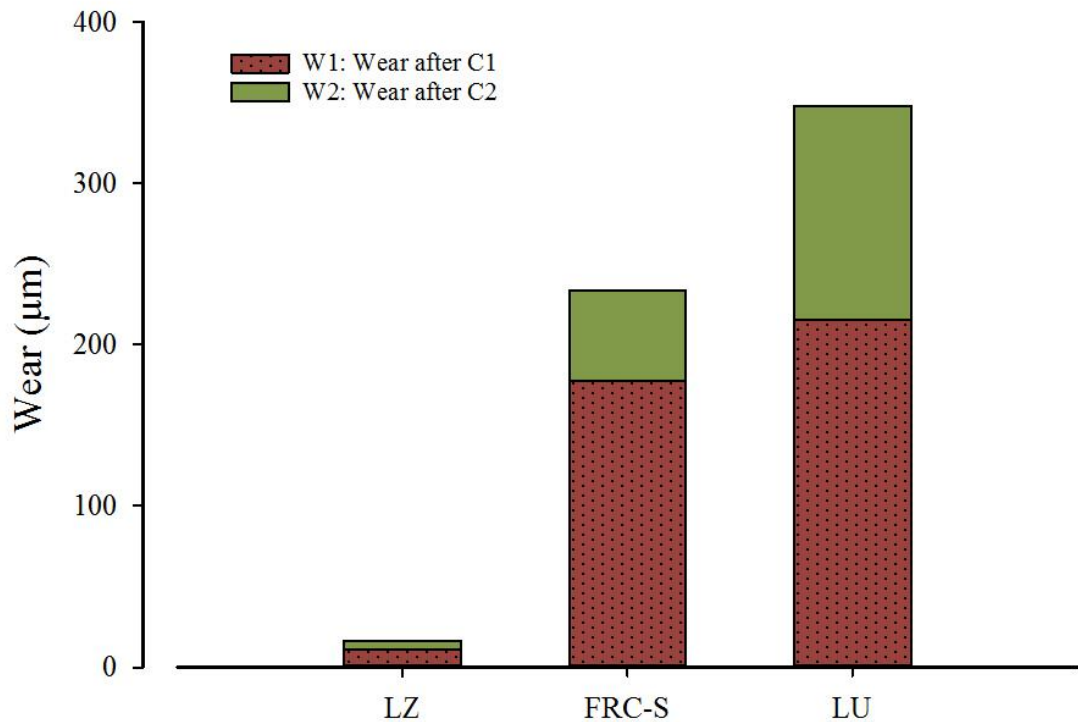


Figure 8.5: Graph showing the mean cumulative wear (μm) for all the tested groups.

8.5 DISCUSSION:

This study monitored the morphological changes and quantified the progression of wear among three metal-free crown systems following *in-vitro* dynamic fatigue simulation, and using a 3D intraoral scanner. The results demonstrated that the fabricating material significantly influences the wear resistance independent of the loading condition. Lava Zirconia was ranked as the most wear-resistant in comparison with FRC-Sinfony and Lava Ultimate. This supports rejection of the first null hypothesis. Furthermore, the successive phases of chewing simulation did not exhibit the same wear rate since the earlier loading phase (C1) induced the most significant material loss, leading to the rejection of the second null hypothesis.

The materials were chosen as representatives of their main categories, and compared in terms of wear behaviour. A significant difference was found in their wear resistance, which can be explained by the variation in their mechanical properties and tribological behaviours [5, 6, 9]. Other possible influencing factors, including lubrication, testing environment, surface polishing and specimen topography, were all standardised in this study. Materials with high mechanical strength are wear-resistant as they are less susceptible to surface fatigue and chipping [9]. As reported by the manufacturers, Lava Zirconia with its flexural strength (1100 MPa), E-modulus (210 GPa) and hardness (1200 VKH) demonstrates far more strength than Sinfony (105 MPa, 3.1 GPa, 250 VKH) and Lava Ultimate (204 MPa, 12.7 GPa, 280 VKH) [36]. This superiority in strength was clearly reflected by wear resistance as it exhibited the least degree of wear. Many studies comparing dental ceramics in terms of wear-resistance have also confirmed the superiority of zirconia-based ceramics due to their high overall strength, and therefore recommended their use as monolithic restorations [6, 24, 28].

Surprisingly, one unanticipated finding was that the crowns made of Sinfony revealed less obvious wear facets and higher wear resistance than those made of Lava Ultimate despite the latter having superior mechanical properties. This inconsistency can be attributed to the FRC layer incorporated within the occlusal bulk of FRC-S crowns. This incorporation enhances the overall strength of resin-composites by increasing filler content and reinforcement efficiency [23, 37-39]. Superior support and reduced crack propagation are also achieved within the veneering resin-composite, which tend to reduce the influence of cyclic loading and the consequent wear [38].

Another possible explanation of this variation is based on material microstructure. Both Sinfony and Lava Ultimate are composed of inorganic fillers embedded in a resin matrix. The resin matrix will be worn away at some point during the wear simulation, leaving the inorganic particles unsupported and promoting surface roughness. Subsequently, the inorganic particles become separated and accumulate between the antagonist and crown surface, causing gradual increase in 'self-abrasion' [40]. The larger and harder the particles accumulated, the higher surface roughness induced, and the higher the abrasion rate [5, 41, 42]. Accordingly, Lava Ultimate, which is formulated from a combination of ceramic nanomer (silica: 20nm, zirconia: 4-11nm) and nanocluster (0.6-10 μm) fillers, would be more affected by self-abrasion than Sinfony, which is composed of relatively smaller particles (0.5-0.7 μm). Conversely, Lava Zirconia is believed to show no notable self-abrasion due to its persistent superficial microstructure [28]. It is composed of tough yttria partially-stabilized tetragonal zirconium dioxide polycrystals (Y-TZP) that maintain their structure over time. The phase transformation of such crystals from tetragonal to monoclinic crystalline states (transformation toughening) during cyclic loading hinders crack propagation and prevents consequent grains separation, which explains the trivial morphological changes among LZ crowns [43].

In an attempt to simulate clinical conditions, this study used a dual-axis chewing simulator and anatomical crowns in order to reproduce wear. The chewing simulator allowed an accelerated simulation of the chewing load and induced clinically-relevant wear patterns [42]. The chewing force used here was adjusted to match the mean physiological biting force (50 N) exhibited in a non-bruxist patient [42]. Its vertical application as well as an additional lateral movement was cyclically repeated to induce fatigue wear and attrition. Given that no abrading medium was initially included in such simulation, a possible abrasive wear was considered absent at the commencement. However, this abrasive wear became obtainable when particles of the interfacing material have been worn away. The number of cycles performed was set, in accordance with previous studies, to be equivalent to two years of clinical mastication, and the subsequent wear pattern was as indicated in clinical studies [8, 44]. A stainless steel stylus was used as antagonist to exert the masticatory movement owing to its enamel-comparable properties [45]. Ideally, antagonists made of enamel should be used due to their relevancy, but difficulties in the machining and shaping process as well as

variations in the natural composition make them less precise compared to synthetic materials (stainless steel, steatite, ceramic) [9]

Two distinctive phases of mechanical simulation were performed in order to compare the wear rate. The phase C1, which is equivalent to one-year performance, was found the most influential. This complies with a previous study which found that most restoration wear is noticeable during the first 6 months of performance [46]. A possible explanation for this might be that the surface topography for interfacing materials will change after a certain degree of wear. Wider contact areas and more stress distribution will be produced gradually, diminishing the wear rate. This is applicable for softer materials like Lava Ultimate and Sinfony; however, harder materials like Lava Zirconia are less susceptible to change. This explains the minor wear percentages exhibited after the phase C2 (LZ: 33%, LU: 38%, FRC-S: 24%).

This study also described a novel method to monitor tooth wear and quantify the changes using intraoral digital scanner and surface matching software. The 3M True definition scanner, a chairside intraoral scanner conventionally used for taking digital impressions, was used in this study as a tool for direct mapping of tooth surfaces. Many previous tribology studies have also used surface mapping systems to investigate wear [30-32, 34, 35]. However, they have relied on an indirect technique by scanning impressions, gypsum casts or epoxy-resin dies to acquire viable scans. Such an indirect technique is subject to inherent errors that might lead to inaccuracy and misinterpretation, while the direct technique used in the current study had no intermediate steps for the digital acquisition, and hence it is more precise, feasible and convenient. High degree of trueness and repeatability is also achievable by the use of powder coating since it reduces the coefficient of reflectance for tooth surfaces and enhances signal to noise ratio. Measurement discrepancies that arise from powder particles (10 μ m maximum diameter) are also negligible, and would be minimized by using a standardized technique for powder application. Surface matching software (Geomagic Control), whose accuracy has been previously verified in the literature, was also used for tooth wear analysis [32]. Wear measurements were performed through the software by superimposing the sequential 3D scans together, a technique that is considered as the most accurate way for wear quantification [33]. This technique has been previously validated and a high level of accuracy reported (uncertainty= 2.7 μ m) [32]. Nevertheless, future studies investigating this technique clinically are still recommended.

Some limitations were encountered in this study. One limitation was restricting the investigation to a single type and design of FRC crowns, and comparing them to only two different material types. Studies comparing more materials and designs together are recommended in the future. Moreover, the wear behaviour of the experimental FRC crowns has not been compared with that of composite crowns conventionally-made without fibre reinforcement. Such a comparison in the future would emphasize the role of fibre reinforcement and its effect on wear behaviour.

Overall, this study with its specific methodology was able to discriminate three different crown systems according to their wear resistance. Crowns made from Lava Zirconia have the most resistant; however, they might be still the least favourable due to their abrasiveness. They are not subject to appreciable abrasive wear, which means their anatomical shape will be maintained over time. This could be significant when considering a treatment plan for patients with parafunctional habits or active wear. Alternatives, like Lava Ultimate or FRC crowns, with lesser wear-resistance and abrasiveness would be preferable.

8.6 CONCLUSIONS:

Within the limitation of this study, the following conclusions were drawn:

1. Wear resistance of metal-free crowns is significantly influenced by the fabricating material. Lava Zirconia has the most significant resistance, while Lava Ultimate has the least.
2. The initial phase of mechanical wear simulation has the most significant effect on the cumulative wear independent of the fabricating material.
3. The *3MTM True definition scanner*, combined with surface matching software, is a valid methodology to quantify wear *in-vitro*.

8.7 ACKNOWLEDGEMENTS:

The authors thank 3M-ESPE (Seefeld, Germany) for the loan of the *3MTM True definition Scanner* to perform this study, and for all the valuable assistance with the software.

8.8 REFERENCES:

1. Van't Spijker A, Rodriguez JM, Kreulen CM, Bronkhorst EM, Bartlett DW, Creugers NH. Prevalence of Tooth Wear in Adults. *Int J Prosthodont*, 2009; **22**: 35-42.
2. Barbour ME, Rees GD. The Role of Erosion, Abrasion and Attrition in Tooth Wear. *J Clin Dent*, 2006; **17**: 88-93.
3. Mehta SB, Banerji S, Millar BJ, Suarez-Feito JM. Current Concepts on the Management of Tooth Wear: Part 4. An Overview of the Restorative Techniques and Dental Materials Commonly Applied for the Management of Tooth Wear. *Br Dent J*, 2012; **212**: 169-177.
4. Lambrechts P, Braem M, Vuylsteke-Wauters M, Vanherle G. Quantitative in Vivo Wear of Human Enamel. *J Dent Res*, 1989; **68**: 1752-1754.
5. Hahnel S, Schultz S, Trempler C, Ach B, Handel G, Rosentritt M. Two-Body Wear of Dental Restorative Materials. *J Mech Behav Biomed Mater*, 2011; **4**: 237-244.
6. Wang L, Liu Y, Si W, Feng H, Tao Y, Ma Z. Friction and Wear Behaviors of Dental Ceramics against Natural Tooth Enamel. *J Eur Ceram Soc*, 2012; **32**: 2599-2606.
7. Kim SK, Kim KN, Chang IT, Heo SJ. A Study of the Effects of Chewing Patterns on Occlusal Wear. *J Oral Rehabil*, 2001; **28**: 1048-1055.
8. Mehl C, Scheibner S, Ludwig K, Kern M. Wear of Composite Resin Veneering Materials and Enamel in a Chewing Simulator. *Dent Mater*, 2007; **23**: 1382-1389.
9. Heintze SD, Zellweger G, Cavalleri A, Ferracane J. Influence of the Antagonist Material on the Wear of Different Composites Using Two Different Wear Simulation Methods. *Dent Mater*, 2006; **22**: 166-175.
10. Correr GM, Bruschi Alonso RC, Correr Sobrinho L, Puppini-Rontani RM, Ferracane JL. In Vitro Wear of Resin-Based Materials--Simultaneous Corrosive and Abrasive Wear. *J Biomed Mater Res B Appl Biomater*, 2006; **78**: 105-114.
11. Yip KH, Smales RJ, Kaidonis JA. Differential Wear of Teeth and Restorative Materials: Clinical Implications. *Int J Prosthodont*, 2004; **17**: 350-356.
12. Etman MK, Woolford M, Dunne S. Quantitative Measurement of Tooth and Ceramic Wear: In Vivo Study. *Int J Prosthodont*, 2008; **21**: 245-252.
13. Ekfeldt A, Oilo G. Wear of Prosthodontic Materials--an in Vivo Study. *J Oral Rehabil*, 1990; **17**: 117-129.
14. Jandt KD, Sigusch BW. Future Perspectives of Resin-Based Dental Materials. *Dent Mater*, 2009; **25**: 1001-1006.
15. Bartlett D, Sundaram G. An up to 3-Year Randomized Clinical Study Comparing Indirect and Direct Resin Composites Used to Restore Worn Posterior Teeth. *Int J Prosthodont*, 2006; **19**: 613-617.
16. Park JH, Park S, Lee K, Yun KD, Lim HP. Antagonist Wear of Three CAD/CAM Anatomic Contour Zirconia Ceramics. *J Prosthet Dent*, 2014; **111**: 20-29.
17. Janyavula S, Lawson N, Cakir D, Beck P, Ramp LC, Burgess JO. The Wear of Polished and Glazed Zirconia against Enamel. *J Prosthet Dent*, 2013; **109**: 22-29.
18. Yesil ZD, Alapati S, Johnston W, Seghi RR. Evaluation of the Wear Resistance of New Nanocomposite Resin Restorative Materials. *J Prosthet Dent*, 2008; **99**: 435-443.
19. Cavalcante LM, Schneider LF, Hammad M, Watts DC, Silikas N. Degradation Resistance of Ormocer- and Dimethacrylate-Based Matrices with Different Filler Contents. *J Dent*, 2012; **40**: 86-90.

20. Cavalcante LM, Masouras K, Watts DC, Pimenta LA, Silikas N. Effect of Nanofillers' Size on Surface Properties after Toothbrush Abrasion. *Am J Dent*, 2009; **22**: 60-64.
21. Kakaboura A, Fragouli M, Rahiotis C, Silikas N. Evaluation of Surface Characteristics of Dental Composites Using Profilometry, Scanning Electron, Atomic Force Microscopy and Gloss-Meter. *J Mater Sci Mater Med*, 2007; **18**: 155-163.
22. Garoushi S, Vallittu PK, Lassila LV. Fracture Resistance of Short, Randomly Oriented, Glass Fiber-Reinforced Composite Premolar Crowns. *Acta Biomater*, 2007; **3**: 779-784.
23. Garoushi S, Vallittu PK, Lassila LV. Short Glass Fiber Reinforced Restorative Composite Resin with Semi-Inter Penetrating Polymer Network Matrix. *Dent Mater*, 2007; **23**: 1356-1362.
24. Lawson NC, Janyavula S, Syklawer S, McLaren EA, Burgess JO. Wear of Enamel Opposing Zirconia and Lithium Disilicate after Adjustment, Polishing and Glazing. *J Dent*, 2014; **42**: 1586-1591.
25. Zandinejad AA, Atai M, Pahlevan A. The Effect of Ceramic and Porous Fillers on the Mechanical Properties of Experimental Dental Composites. *Dent Mater*, 2006; **22**: 382-387.
26. Belli R, Geinzer E, Muschweck A, Petschelt A, Lohbauer U. Mechanical Fatigue Degradation of Ceramics Versus Resin Composites for Dental Restorations. *Dent Mater*, 2014; **30**: 424-432.
27. Koller M, Arnetzl GV, Holly L, Arnetzl G. Lava Ultimate Resin Nano Ceramic for CAD/ CAM: Customization Case Study. *Int J Comput Dent*, 2012; **15**: 159-164.
28. Dupriez ND, von Koeckritz AK, Kunzelmann KH. A Comparative Study of Sliding Wear of Nonmetallic Dental Restorative Materials with Emphasis on Micromechanical Wear Mechanisms. *J Biomed Mater Res B Appl Biomater*, 2014.
29. Satterthwaite JD. Tooth Surface Loss: Tools and Tips for Management. *Dent Update*, 2012; **39**: 86-90, 93-86.
30. Al-Omiri MK, Sghaireen MG, Alzarea BK, Lynch E. Quantification of Incisal Tooth Wear in Upper Anterior Teeth: Conventional Vs New Method Using Toolmakers Microscope and a Three-Dimensional Measuring Technique. *J Dent*, 2013; **41**: 1214-1221.
31. Al-Omiri MK, Harb R, Abu Hammad OA, Lamey PJ, Lynch E, Clifford TJ. Quantification of Tooth Wear: Conventional Vs New Method Using Toolmakers Microscope and a Three-Dimensional Measuring Technique. *J Dent*, 2010; **38**: 560-568.
32. Rodriguez JM, Austin RS, Bartlett DW. A Method to Evaluate Profilometric Tooth Wear Measurements. *Dent Mater*, 2012; **28**: 245-251.
33. DeLong R. Intra-Oral Restorative Materials Wear: Rethinking the Current Approaches: How to Measure Wear. *Dent Mater*, 2006; **22**: 702-711.
34. Schlueter N, Ganss C, De Sanctis S, Klimek J. Evaluation of a Profilometrical Method for Monitoring Erosive Tooth Wear. *Eur J Oral Sci*, 2005; **113**: 505-511.
35. Azzopardi A, Bartlett DW, Watson TF, Sherriff M. The Measurement and Prevention of Erosion and Abrasion. *J Dent*, 2001; **29**: 395-400.
36. Pittayachawan P. Comparative Study of Physical Properties of Zirconia Based Dental Ceramics [Doctoral]: University College London; 2009:352.
37. Dyer SR, Lassila LV, Jokinen M, Vallittu PK. Effect of Fiber Position and Orientation on Fracture Load of Fiber-Reinforced Composite. *Dent Mater*, 2004; **20**: 947-955.

38. Vallittu PK. Strength and Interfacial Adhesion of FRC-Tooth System. In: *The Second International Symposium on Fibre-Reinforced Plastics in Dentistry, Symposium Book on the Scientific Workshop on Dental Fibre-Reinforced Composite on 13 October 2001*. Edited by Vallittu PK. Nijmegen, Netherlands 2001.
39. Hull D, Clyne TW. *An Introduction to Composite Materials*. 2nd ed. Cambridge: Cambridge University Press; 1996.
40. Heintze SD, Zellweger G, Grunert I, Munoz-Viveros CA, Hagenbuch K. Laboratory Methods for Evaluating the Wear of Denture Teeth and Their Correlation with Clinical Results. *Dent Mater*, 2012; **28**: 261-272.
41. Turssi CP, Ferracane JL, Vogel K. Filler Features and Their Effects on Wear and Degree of Conversion of Particulate Dental Resin Composites. *Biomaterials*, 2005; **26**: 4932-4937.
42. Heintze SD, Zellweger G, Zappini G. The Relationship between Physical Parameters and Wear of Dental Composites. *Wear*, 2007; **263**: 1138-1146.
43. Hannink RHJ, Kelly PM, Muddle BC. Transformation Toughening in Zirconia-Containing Ceramics. *J Am Ceram Soc*, 2000; **83**: 461-487.
44. Heintze SD. How to Qualify and Validate Wear Simulation Devices and Methods. *Dent Mater*, 2006; **22**: 712-734.
45. Shortall AC, Hu XQ, Marquis PM. Potential Countersample Materials for in Vitro Simulation Wear Testing. *Dent Mater*, 2002; **18**: 246-254.
46. Mazer RB, Leinfelder KF. Evaluating a Microfill Posterior Composite Resin a Five-Year Study. *J Am Dent Assoc*, 1992; **123**: 32-38.

**Chapter 9: Load-Bearing Capacity of Fibre-Reinforced
Composite Crowns in Comparison with Machined
Alternatives.**

9.1 ABSTRACT:

Objectives: To i) compare the fracture resistance of fibre-reinforced composite (FRC) crowns with other metal-free alternatives *in-vitro*, and ii) investigate the influence of fabricating materials and dynamic fatigue on the load-bearing capacity.

Methods: Identical metal-free crowns (n=30), for a lower first molar, were made of three different materials. In groups LZ (n=10) and LU (n=10), monolithic crowns were manufactured using CAD/CAM technology from zirconia-based ceramic (*Lava Zirconia, 3M-ESPE*) and resin nano-ceramic (*Lava Ultimate, 3M-ESPE*) materials, respectively. In group FRC-S (n=5), experimental fibre-reinforced composite (FRC) crowns were made conventionally from bidirectional reinforcing-fibres (*Stick Net, Stick Tech Ltd*) and resin-composite material (*Sinfony, 3M-ESPE*). All crowns were adhesively cemented (*RelyX-UniCem2, 3M-ESPE*) over identical acrylic teeth. Half of the crowns from each group (n=5) were subjected to thermocycling (3500 cycles, 5-55°C, 10s dwell) before being cyclically fatigued (480k cycles, 5kg) using a dual-axis chewing simulator (*CS-4.2, SD-Mechatronic*). The other half (n=5) was control with no fatigue simulation. Crowns were loaded statically in a universal testing machine (Zwick Z020, Zwick/Roell) with a compressive load (1 mm/min crosshead speed) applied perpendicularly at the central fossa until fracture. The load-bearing capacity (N) was recorded for each crown. Statistical analysis using 2-way ANOVA was conducted to detect the effect of fabricating material and dynamic fatigue on the load-bearing capacity ($\alpha=0.05$).

Results: All the fatigued crowns survived the cyclic loading with no fracture signs detected. LZ had the highest load-bearing capacity values with fatigue (1997.8 ± 260.2 N), or without fatigue (2155.6 ± 181.6 N). LU had the lowest load-bearing capacity values with fatigue (756.5 ± 290.9 N), or without fatigue (1023.9 ± 407.7 N). Both material and dynamic fatigue had a significant influence ($p < 0.001$) on the load-bearing capacity.

Conclusion: Crowns made of fibre-reinforced composite exhibited load-bearing capacity comparable to that of monolithic CAD/CAM alternatives, which confirms its potential as a restorative material for posterior teeth.

9.2 INTRODUCTION:

In the era of metal-free dentistry, dental ceramics are becoming the most widely used restorative materials, owing to their excellent aesthetics and durability. However, their inherent brittleness, low flexural strength and fracture toughness are the major drawbacks of their extensive application [1, 2]. High failure rates are reported when conventional glass and alumina all-ceramic restorations have been used in posterior area [3-7]. Bulk catastrophic fracture is the most prominent mode of failure owing to inherent structural flaws that influence the distribution of tensile stresses and enhance crack propagation [4, 6]. In contrast, zirconia-based ceramics exhibits superior mechanical strength and fracture resistance as a consequence of their inherent 'transformation toughening' mechanism [8, 9]. However, due to the opacity and whitish appearance, they tend to be used as core materials and veneered with translucent porcelains for better aesthetics [2, 5, 10, 11], but this presents weak structural points, introduced by the veneer or the veneer/core interface, causing chipping/delamination cracks that may extend through the core materials [6, 10, 12, 13].

Monolithic ceramic restorations made by CAD/CAM technology have been introduced for solving processing-related problems [12-16]. The CAD/CAM processing of restorations allows an efficient and standardised fabrication with significant reductions in porosities and structural flaws [17, 18]. It also improves the mechanical properties and enables a superior reproduction of anatomy with more shade/translucency optimization [15-21]. For example, the use of CAD/CAM yttria-stabilized tetragonal zirconia polycrystal (Y-TZP) monolithic restoration is advocated under high demanding conditions, as they provide superior mechanical stability compared with layered zirconia or lithium disilicate restorations [2, 11, 22-24]. However, these restorations still have restricted applications due to their limited resiliency, difficult maintainability, long-term degradation, questionable adhesion and undesirable abrasiveness [2, 13, 19, 25-27].

Resin nano ceramic (RNC), which is a material combining the favourable properties of resin-composite and ceramic together, has been developed as a substitution for monolithic Y-TZP ceramic [14, 23, 28]. It is formulated with a high percentage of nano ceramic particles embedded in a resin matrix and produced in millable monolithic blocks. Due to its unique composition, it is claimed to offer not only excellent fatigue and wear behaviour, but also good fracture resistance, superior bonding and simple

maintenance [14, 20, 23, 28-31]. Some studies have confirmed that it could provide a fracture resistance as good as other CAD/CAM ceramics with greater thickness, owing to better stress distribution and less crack propagation in its bulk [14, 23]. However, few studies have investigated its fatigue behaviour.

Particulate-reinforced composite (PRC) is a metal-free restorative material that offers many advantages in terms of aesthetic, adhesion and maintainability. However, their limited durability and insufficient fatigue behaviour restrict their applications [32-34]. Fibre-reinforced composite (FRC) has been developed as a modification of PRC, and confirmed to provide significant improvements in flexural strength, fracture toughness, stiffness and fatigue resistance [32, 34-37]. Accordingly, FRC are used as substructure constructions or beneath the veneering layer of PRC restorations with the intention of enhancing clinical performance [38]. Many parameters have been identified influencing the properties of resultant FRC-PRC restorations, including fibres orientation, position, adhesion and volume fraction as well as PRC type. Yet, scarce information is available on their overall performance [32, 39].

The aim of this study was to evaluate FRC and two CAD/CAM alternatives as posterior metal-free crown systems, and compare their *in-vitro* performance in terms of fracture resistance and fatigue behaviour. The null hypothesis was that neither fabricating material nor dynamic fatigue will affect the load bearing capacity.

9.3 METHODOLOGY:

Thirty metal-free single crowns (n=30) for a lower first molar were fabricated and tested *in-vitro*. Table 9.1 shows the materials used to fabricate the crowns.

Table 9.1: Materials used to fabricate all crowns in the study.				
Group	Fabrication Mode	Material	Description	Manufacturer
LZ	CAD/CAM	Lava™ Zirconia	Pre-sintered Zirconia-based ceramic	3M ESPE, Seefeld, Germany
LU	CAD/CAM	Lava™ Ultimate	Resin nano-ceramic	3M ESPE, Seefeld, Germany
FRC-S	Conventional	Sinfony	Indirect laboratory micro-hybrid composite	3M ESPE, Seefeld, Germany
		Stick Net	Bidirectional E-glass reinforcing fibres sheet	Stick Tech Ltd, Turku, Finland

9.3.1 Specimen Preparation:

Thirty identical specimen assemblies (Figure 9.1) representing a prepared lower first molar tooth and its supporting structure were produced in a standardised manner. A master preparation was performed on a molar plastic tooth (*KaVo dental GmbH, Biberach, Germany*) using a high speed air turbine with coarse grit shoulder end diamond bur, according to specific dimensions (1mm finish line, 1.5-2 mm occlusal clearance). A silicon master mould (*Gemini, Bracon, East Sussex, UK*) was then produced and used to fabricate thirty identical teeth made of cold-cure acrylic resin (*Metropair Denture Repair, Metrodent Limited, Huddersfield, UK*). All the duplicated teeth were pre-coated with wax before being mounted within an epoxy-resin base (*Epoxy resin, B&K Resins Ltd, Bromley, UK*) in upright position. The wax coating was then substituted with light-bodied poly-vinyl siloxane (PVS) impression material (*Aquasil LV, Dentsply, PA, USA*) to simulate the elasticity of periodontal ligament.

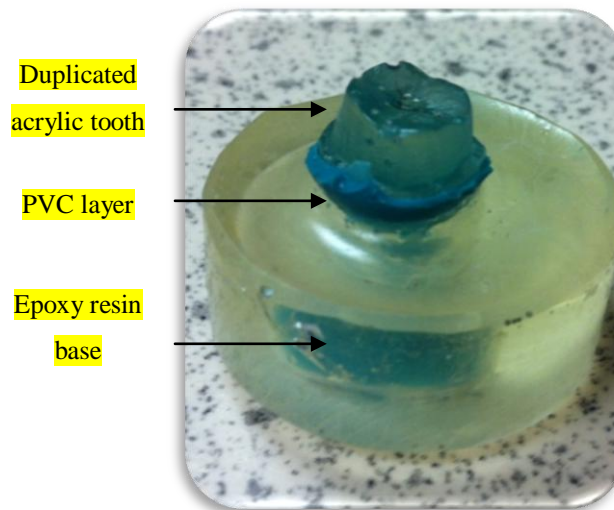


Figure 9.1: Representative specimen assembly showing a duplicated abutment in epoxy resin base (2mm below CEJ) and surrounded with PVS layer (0.2mm thickness) to simulate PDL.

9.3.2 Crown fabrication:

The crown fabrication process started with creating a transparent vacuum-formed matrix in order to register the anatomy of the master tooth previous to any preparation. An intraoral 3D scanner (*3MTM True definition scanner, 3M-ESPE, USA*) was used then to obtain digital impressions for the master tooth, before and after preparation, in order to be utilized in the CAD/CAM crown fabrication (Figure 9.2)

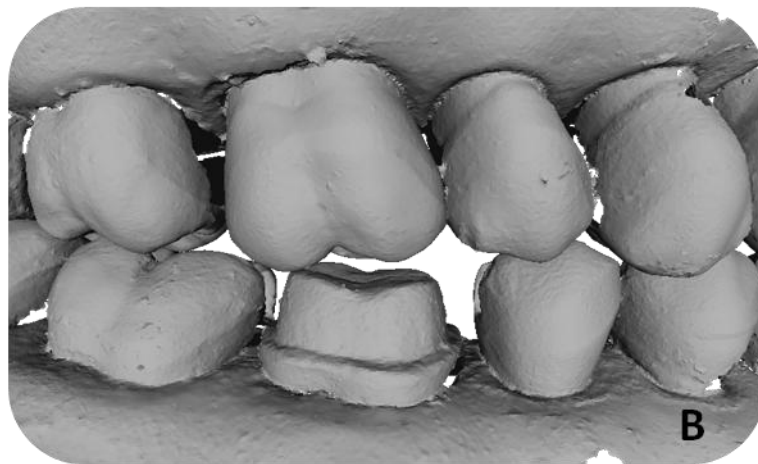
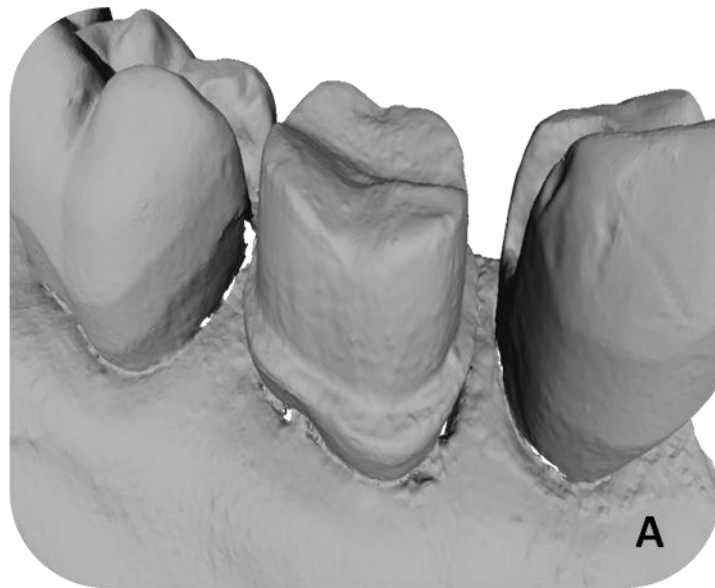


Figure 9.2: 3D impressions for the master preparation using 3M True Definition Scanner, A) Buccal view showing the shoulder finish line (1mm) and buccal cusp bevel, and B) bite registration with 1.5mm interocclusal clearance.

Three materials were chosen to construct thirty identical crowns with the same morphology and dimensions, matching the original master tooth. In groups LZ (n=10) and LU (n=10), zirconia-based ceramic (*Lava™ Zirconia, 3M-ESPE*) and resin nano-ceramic (*Lava™ Ultimate, 3M-ESPE*) were used to manufacture monolithic crowns by CAD/CAM technology, respectively. For Group FRC-S (n=10), bidirectional FRC (*Stick Net, Stick Tech Ltd*) and indirect resin-composite (*Sinfony, 3M-ESPE*) were combined to conventionally fabricate experimental crowns.

For the fabrication of FRC crowns, the prepared master tooth was used as a working die for all crowns. A standardized 2-coat thickness of die spacer (*blue die spacer 20µm, Kerr, USA*) was applied over the entire die to within 0.5mm of the margin. One layer of the bidirectional FRC was cut to an appropriate size (7 x 6 mm), enough to cover the entire occlusal surface, before being impregnated for 5 minutes with filler-free resin (*Stick Resin, Stick Tech Ltd, Turku, Finland*). A thin layer of resin-composite (*Sinfony, 3M-ESPE*) was initially applied over the occlusal third of the die, and the impregnated fibre layer was subsequently adapted and light-cured (20s). A full crown was produced from the resin-composite (*Sinfony, 3M-ESPE*) and shaped using the vacuum-formed matrix. To initiate polymerization, a hand LED curing light (*Elipar™ S10 LED, 3M ESPE, USA*) was used for 20s per surface prior to the 15-minute final vacuum polymerization inside a laboratory curing unit (*Visio™ Beta Vario Light Unit, 3M ESPE, USA*). Final finishing and polishing were manually completed using Sof-Lex™ discs (*3M ESPE, Seefeld, Germany*). At the end, the resulting crowns were thoroughly inspected for any void or discrepancy that could lead to exclusion and remaking. In order to guarantee standardization, all these procedures were performed by one trained operator.

For the fabrication of CAD/CAM crowns, one milling centre was hired to manufacture all the crowns from the same digital impressions. A master 3D crown was virtually designed, and a standardised cement space (40-µm thickness) was digitally incorporated. Crown machining was then performed using a CAD/CAM milling machine (*CORiTEC 250i, Imes-Core GmbH, Eiterfeld, Germany*) according to the manufacturers' instructions. Finishing, shading, sintering and hand polishing (with no glaze) were then performed to produce identical monolithic crowns made from Lava Zirconia and Lava Ultimate.

All crowns were adhesively cemented to the corresponding specimen assemblies using self-adhesive resin cement (*RelyX UniCem2, 3M-ESPE, Seefeld, Germany*). The acrylic teeth and the inner surfaces of the crowns were silica-coated and silanized (*Cojet Repair System, 3M-ESPE, Seefeld, Germany*) before cementation. A 5kg seating-load was used for 5 minutes to ensure standardised cementation. All the specimens were then stored in water (37°C, 24h) before any further testing.

9.3.3 Dynamic fatigue:

Two equal subgroups were allocated randomly for each main group. Subgroup X (LZx, LUx, FRCx, n=5) was artificially fatigued by implementing accelerated thermocycling aging and cyclic loading, whereas subgroup C was the control. The thermocycling process was completed inside water baths (3500 cycles, 5-55°C, 10s dwell) prior to the initiation of cyclic loading. A dual-axis chewing simulator machine (*CS-4.2, SD Mechatronic, Germany*) was used to apply cyclic loading (480,000 cycles, 5kg load, 1.8Hz frequency) (Figure 9.3). A stainless steel stylus was used as an antagonist to transmit the required load into the specimens. The stylus action was adjusted to initially contact the deepest point of central fossa in a vertical motion (2.5mm) prior to a further oblique sliding (2.0mm) along the buccal groove. The points of contact and separation were verified by using articulating paper (*Hanel, Coltene, Switzerland*). The loading cycles were conducted in two subsequent phases (C1 and C2, 240K cycles each). Upon the completion of each phase, an inspection for signs of fracture was performed using optical microscope (*Meiji EMZ-TR, Meiji Techno Co. Ltd., Tokyo, Japan*) with high magnification (x40). Specimens were stored back in water (37°C, 48h) prior to the 'static loading' testing.

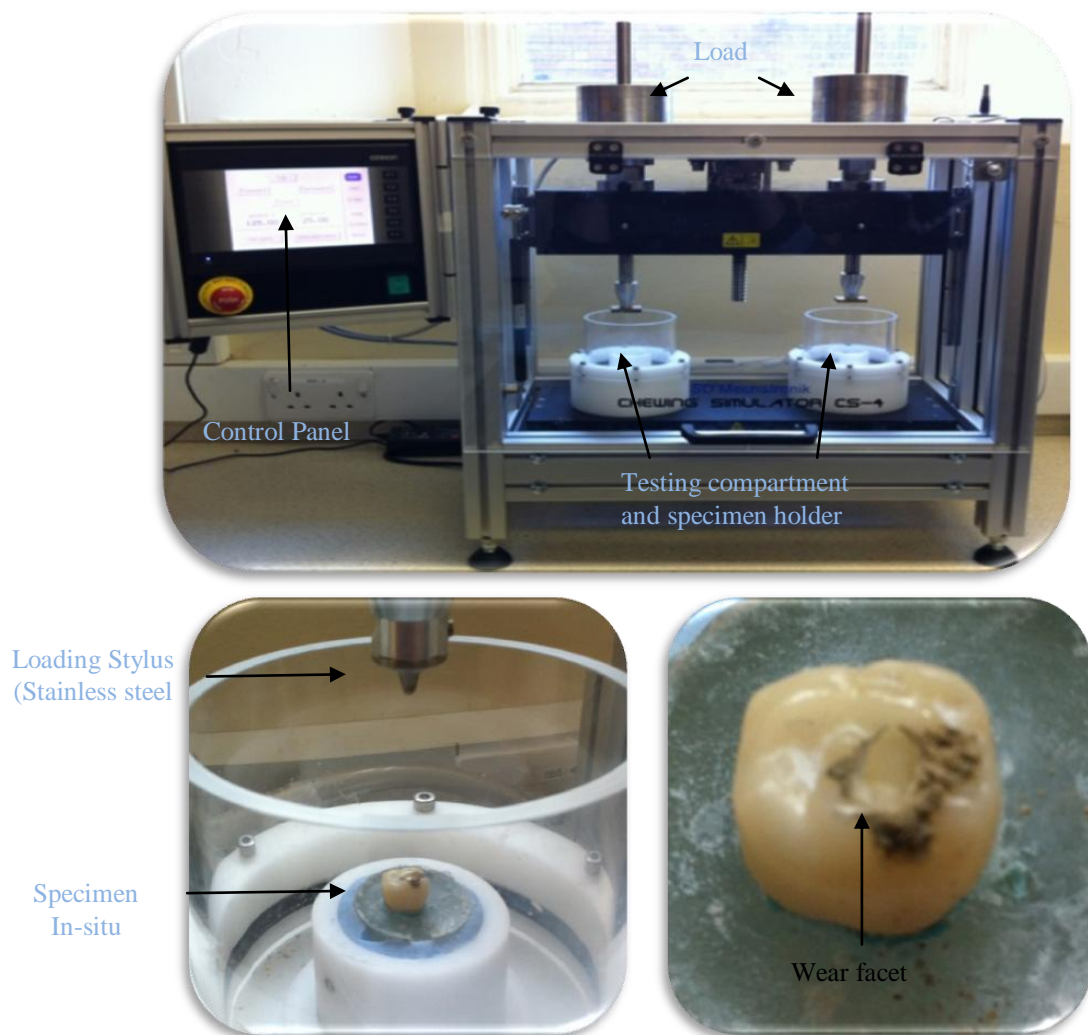


Figure 9.3: CS 4.2 chewing simulator machine with its two compartments (top), one representative specimen mounted in one compartment (left), the same specimen after the completion of cyclic loading with a pronounced wear facet (right).

9.3.4 Static loading:

Specimens were tested for their ultimate fracture strength under a static loading. A Zwick/Roell Z020 universal testing machine (*Zwick GmbH, Ulm, Germany*) with a steel ball indenter (4mm \varnothing) was employed to apply a compressive axial load (1 mm/min crosshead speed) along the specimen central fossa (Figure 9.4). Tin foil (0.2mm thickness) was inserted between the indenter and the specimen to enable even stress distribution. The maximum force-to-fracture (F_{Max}) and fracture pattern were reported for each specimen.

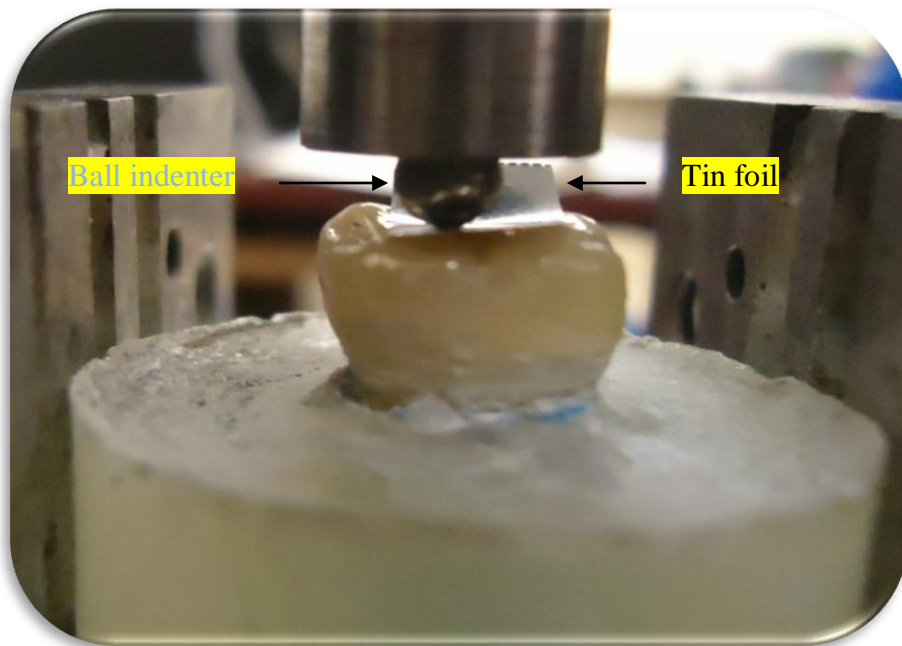


Figure 9.4: One representative crown specimen mounted in the Zwick machine prior to static loading.

9.3.5 Statistical analysis:

Data collection and statistical analysis were performed with SPSS software (*IBM SPSS statistics 20, Chicago, IL, USA*). Mean and standard deviation (SD) values were calculated for each subgroup. The assumption of homogeneity and normal distribution was granted according to Levene's test ($p > 0.05$) and histograms. Two-way ANOVA was conducted to verify the statistical effect of experimental factors (constructing material and dynamic fatigue) on F_{Max} values.

9.4 RESULTS:

All crowns in subgroup X survived the chewing simulation with no fracture signs detected. The mean and SD values of F_{Max} for all groups are listed in Table 9.2, and graphically presented in Figure 9.5. Both constructing material and dynamic fatigue had a significant influence ($p < 0.001$) on the load-bearing capacity but with no significant interactions between the parameters ($p = 0.845$). Group LZ had the highest F_{Max} values, followed by group FRC-S and Group LU, respectively. Dynamic fatigue significantly decreased F_{Max} values independent of the constructing materials used. Examples of fractured specimen are shown in Figure 9.6.

Table 9.2: The mean (SD) load-bearing capacity (N) for all tested groups

Group	Subgroup	
	Control (C)	Fatigued (X)
LZ	2155.6±181.6 ^{a.1}	1997.8±260.2 ^{a.2}
LU	1023.9±407.7 ^{b.1}	756.5±290.9 ^{b.2}
FRC-S	1698.6±373.7 ^{c.1}	1386.5±258.4 ^{c.2}

* Different superscript letters and numbers indicate statistically significant difference within the same column and row respectively.

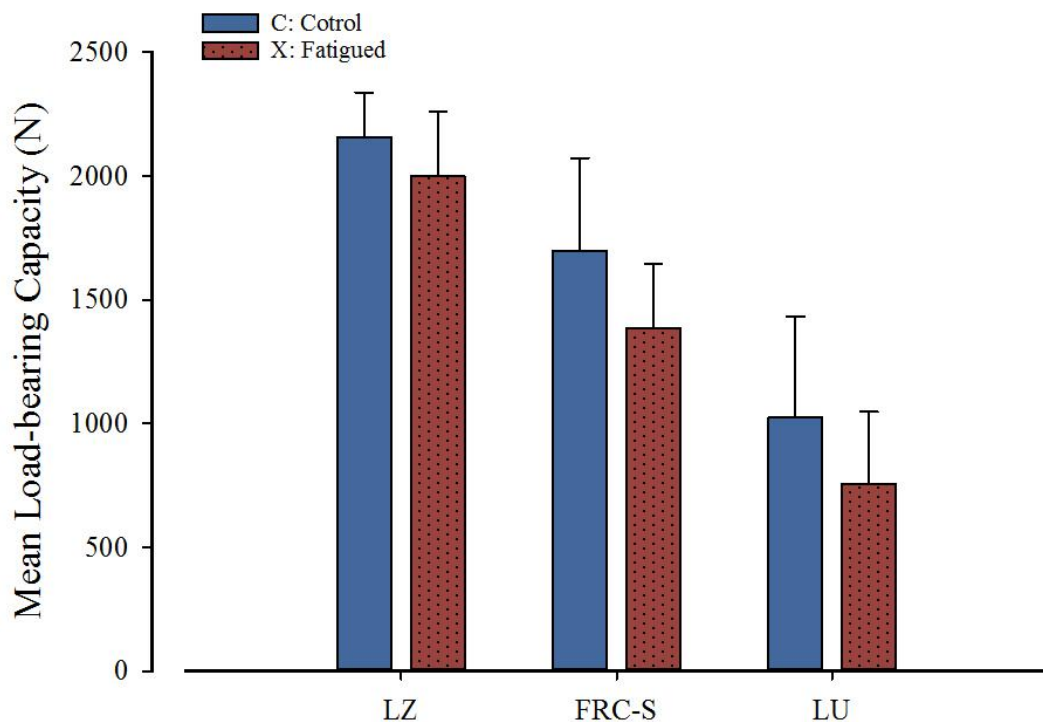


Figure 9.5: Bar chart showing the mean load bearing capacity for all tested groups.



Figure 9.6: Fractured representative specimens from each group. Lava Zirconia: LZ (top) Lava Ultimate: LU (mid), FRC-S (bottom)

9.5 DISCUSSION:

This *in-vitro* study examined the performance of three metal-free crown systems and investigated the influence of material and dynamic fatigue on the load-bearing capacity. The null hypothesis that no experimental factor has an effect on the ultimate fracture strength was rejected since both material and dynamic fatigue were found statistically significant.

Specimens made of Lava Zirconia were found to have the highest F_{Max} values, in comparison with those made of FRC or Lava Ultimate, irrespective of the fatigue condition. This can be explained by the fact that Lava Zirconia has a robust crystalline microstructure (Y-TZP) that provides not only superior mechanical properties but also enables excellent resistance to fracture and surface degradation as a result of its transformation toughening [2]. Upon its loading, a consequential stress-generated transformation of the metastable tetragonal phase to the monoclinic phase occurs and escorts a volumetric expansion that tends to increase toughness, suppress crack propagation and prevent degradation [9, 27]. In contrast, materials with composite microstructure, like Lava Ultimate and FRC-Sinfony, are more susceptible to fracture owing to their limited ability of deformation that reduces stress concentration at a crack tip [16]. Accordingly, the structural flaws within composite materials tend to expand under constant loading, and penetrate deeper through the resin matrix and around the fillers, causing ultimate failure.

Specimens made of Lava Ultimate significantly exhibited lower load-bearing capacity than those made of Sinfony. Theoretically, Lava Ultimate material is expected to provide superior fracture resistance owing to its higher filler content (80 wt%) and larger particles (0.6-10 μm), in comparison with Sinfony (50 wt%, 0.5-0.7 μm) [40]. However, this study found that latter material performs better as a posterior crown, irrespective of the loading condition. This unanticipated behaviour can be attributed to the FRC layer incorporated within the occlusal bulk of Sinfony crown. Such a layer can enhance the support for the veneering material, and hence improve fracture resistance [32, 34]. It can also act as a physical barrier in the direction of crack, which hinders crack propagation and reduces loading impact [32, 34, 39]. This also explains the more maintainable fracture modes observed in FRC-S crowns.

All specimens in the present study exhibited a reduction in the load-bearing capacity when subjected to prior dynamic fatigue, which is in agreement with previous studies

[12, 16, 21, 35]. However, different fatigue behaviour and degree of reduction were found among the tested groups. In LZ, the reduction is attributed to the transformed monoclinic layer that tends to increase as a consequence of moisture, thermal fluctuation and dynamic loading [11, 27, 41]. This unfavourable layer increases the susceptibility for fracture since it accommodates the residual microcracks resulted from the transformation toughening and responsible for fatigue failure [27]. The findings of recent studies investigating the performance of monolithic Y-TZP crowns also confirm this observation as increased spontaneous transformation to the monoclinic phase and reduced fracture resistance exhibited following cyclic loading or water storage [11, 27, 42]. In the resin-based crowns (LU, FRC-S), thermal fluctuation and dynamic loading enhance crack propagation from the inherent flaws, which will eventually combine together to form microcracks. Under further loading, such microcracks reach a critical dimension that could initiate spontaneous (fatigue) failure or reduce load-bearing capacity [16, 43]. The superior durability and fatigue resistance of Lava Zirconia were also demonstrated by the wear behaviour. Upon chewing simulation, wear facets were not obvious in LZ_x crowns, while prominent wear facets and wide surface degradation were noticed in LU_x and FRC-S_x crowns. This surface degradation could influence the load-bearing capacity and explain the degree of strength reduction among groups (LZ: 7.4%, LU: 26.1%, FRC-S: 18.4%).

A clinically-relevant testing protocol was followed in this study to compare the fatigue behaviour among the three groups. The specimens subjected to a definite number of thermocyclic and cyclic loading equivalent to two years of clinical mastication [44, 45]. A dual-axis chewing simulator was used to simulate the masticatory force, as indicated by previous studies, in a clinically-relevant fashion. The stylus moved from the central fossa of the crown upwards on the inclined buccal groove to simulate balancing contacts during the mastication. Steel stylus material was chosen since it is rigid and reliable to avoid breakage during the lateral movement. The chewing force was chosen to match the mean physiological biting force (50 N) exhibited in a non-bruxist patient. The exaggerated lateral movement of 2mm is, however, in contrast with the clinical situation and average sliding movement (0.3-0.7 mm) but is needed to synergise the impact of the lateral tensile stresses and accelerate the fatigue process [45]. This lateral movement may increase the force acting on the crown 2-3 times more than the force of static weight [44]. Anatomical crowns were used as specimens in this study in order to reproduce the stresses generated from restoration geometry [22, 46].

The possible inconsistencies and confounding factors that might arise from using natural teeth, like the variations of abutment dimension and adhesion, were omitted by the employment of duplicated acrylic teeth [45]. Nevertheless, their adhesion with the resin cement is not guaranteed. Therefore, this study used silica-coating and silanization in order to enhance tooth wettability prior to cementation [26]. An artificial periodontium was also used around the roots to simulate damping of periodontal ligament. The effect of moisture on fracture resistance was also simulated by using water storage [24].

Some limitations were encountered in this study. One limitation was restricting the fatigue cycles to two year equivalence of cycles because of an overall time limit. Future studies investigating the fatigue behaviour up to 5 years and generating survival analysis would be more clinically relevant. Another limitation was the use of a single design of FRC crowns in the comparison. Studies comparing more designs of FRC crowns together with composite crowns conventionally-made without fibre reinforcement are suggested in the future to emphasis the role of fibre reinforcement and its design on fatigue behaviour, load bearing capacity and fracture resistance.

Overall, crowns made from monolithic Y-TZP have the highest values; however, they might be not favourable in terms of abrasiveness, translucency and maintainability. Modified-resin composite material, like Lava Ultimate and FRC, would be a potential alternative despite its lower load-bearing capacity. Future studies comparing the clinical performance of such materials are recommended for improving clinical practice.

9.6 CONCLUSION:

Within the limitation of this study, the following conclusions were drawn:

1. Material and dynamic fatigue significantly influence the load-bearing capacity of metal-free crowns.
2. Lava Zirconia has the best fatigue resistance and load bearing capacity, while Lava Ultimate has the worst.
3. FRC offers significantly lower fatigue and fracture resistance than Lava Zirconia but higher than Lava Ultimate.

9.7 REFERENCES:

1. Pjetursson BE, Sailer I, Zwahlen M, Hammerle CH. A Systematic Review of the Survival and Complication Rates of All-Ceramic and Metal-Ceramic Reconstructions after an Observation Period of at Least 3 Years. Part I: Single Crowns. *Clin Oral Implants Res*, 2007; **18 Suppl 3**: 73-85.
2. Miyazaki T, Nakamura T, Matsumura H, Ban S, Kobayashi T. Current Status of Zirconia Restoration. *J Prosthodont Res*, 2013; **57**: 236-261.
3. Conrad HJ, Seong W-J, Pesun IJ. Current Ceramic Materials and Systems with Clinical Recommendations: A Systematic Review. *J Prosthet Dent*, 2007; **98**: 389-404.
4. Thompson VP, Rekow DE. Dental Ceramics and the Molar Crown Testing Ground. *J Appl Oral Sci*, 2004; **12**: 26-36.
5. Raigrodski AJ. Contemporary Materials and Technologies for All-Ceramic Fixed Partial Dentures: A Review of the Literature. *J Prosthet Dent*, 2004; **92**: 557-562.
6. Rekow ED, Silva NRFA, Coelho PG, Zhang Y, Guess P, Thompson VP. Performance of Dental Ceramics: Challenges for Improvements. *J Dent Res*, 2011; **90**: 937-952.
7. Tinschert J, Zvez D, Marx R, Anusavice KJ. Structural Reliability of Alumina-, Feldspar-, Leucite-, Mica- and Zirconia-Based Ceramics. *J Dent*, 2000; **28**: 529-535.
8. Sailer I, Gottnerb J, Kanelb S, Hammerle CH. Randomized Controlled Clinical Trial of Zirconia-Ceramic and Metal-Ceramic Posterior Fixed Dental Prostheses: A 3-Year Follow-Up. *Int J Prosthodont*, 2009; **22**: 553-560.
9. Mochales C, Maerten A, Rack A, Cloetens P, Mueller WD, Zaslansky P, Fleck C. Monoclinic Phase Transformations of Zirconia-Based Dental Prostheses, Induced by Clinically Practised Surface Manipulations. *Acta Biomater*, 2011; **7**: 2994-3002.
10. Stawarczyk B, Ouml, Zcan M, Roos M, Trottmann A, Auml, Mmerle CHF. Fracture Load and Failure Analysis of Zirconia Single Crowns Veneered Withpressed and Layered Ceramics after Chewing Simulation. *Dent Mater J*, 2011; **30**: 554-562.
11. Beuer F, Stimmelmayer M, Gueth JF, Edelhoff D, Naumann M. In Vitro Performance of Full-Contour Zirconia Single Crowns. *Dent Mater*, 2012; **28**: 449-456.
12. Zahran M, El-Mowafy O, Tam L, Watson PA, Finer Y. Fracture Strength and Fatigue Resistance of All-Ceramic Molar Crowns Manufactured with CAD/CAM Technology. *J Prosthodont*, 2008; **17**: 370-377.
13. Tsalouchou E, Cattell MJ, Knowles JC, Pittayachawan P, McDonald A. Fatigue and Fracture Properties of Ytria Partially Stabilized Zirconia Crown Systems. *Dent Mater*, 2008; **24**: 308-318.
14. Chen C, Trindade FZ, de Jager N, Kleverlaan CJ, Feilzer AJ. The Fracture Resistance of a CAD/CAM Resin Nano Ceramic (RNC) and a CAD Ceramic at Different Thicknesses. *Dent Mater*, 2014; **30**: 954-962.
15. Zhang Y, Lee JJW, Srikanth R, Lawn BR. Edge Chipping and Flexural Resistance of Monolithic Ceramics. *Dent Mater*, 2013; **29**: 1201-1208.
16. Attia A, Abdelaziz KM, Freitag S, Kern M. Fracture Load of Composite Resin and Feldspathic All-Ceramic CAD/CAM Crowns. *J Prosthet Dent*, 2006; **95**: 117-123.
17. Harder S, Kern M. Survival and Complications of Computer Aided-Designing and Computer-Aided Manufacturing vs. Conventionally Fabricated Implant-Supported Reconstructions: A Systematic Review. *Clin Oral Implants Res*, 2009; **20 Suppl 4**: 48-54.
18. Beuer F, Schweiger J, Edelhoff D. Digital Dentistry: An Overview of Recent Developments for CAD/CAM Generated Restorations. *Br Dent J*, 2008; **204**: 505-511.

19. Liu M-C, Aquilino SA, Gratton DG, Ou K-L, Lin C-C. Relative Translucency and Surface Roughness of Four Yttrium-Stabilized Tetragonal Zirconia Polycrystalline-Based Dental Restorations. *J Exp Clin Med*, 2013; **5**: 22-24.
20. Awad D, Stawarczyk B, Liebermann A, Ilie N. Translucency of Esthetic Dental Restorative CAD/CAM Materials and Composite Resins with Respect to Thickness and Surface Roughness. *J Prosthet Dent*, 2015.
21. Chen HY, Hickel R, Setcos JC, Kunzelmann KH. Effects of Surface Finish and Fatigue Testing on the Fracture Strength of CAD-CAM and Pressed-Ceramic Crowns. *J Prosthet Dent*, 1999; **82**: 468-475.
22. Sun T, Zhou S, Lai R, Liu R, Ma S, Zhou Z, Longquan S. Load-Bearing Capacity and the Recommended Thickness of Dental Monolithic Zirconia Single Crowns. *J Mech Behav Biomed Mater*, 2014; **35**: 93-101.
23. Belli R, Geinzer E, Muschweck A, Petschelt A, Lohbauer U. Mechanical Fatigue Degradation of Ceramics Versus Resin Composites for Dental Restorations. *Dent Mater*, 2014; **30**: 424-432.
24. Dhima M, Assad DA, Volz JE, An K-N, Berglund LJ, Carr AB, Salinas TJ. Evaluation of Fracture Resistance in Aqueous Environment of Four Restorative Systems for Posterior Applications. Part 1. *J Prosthodont*, 2013; **22**: 256-260.
25. Duan Y, Griggs JA. Effect of Elasticity on Stress Distribution in CAD/CAM Dental Crowns: Glass Ceramic vs. Polymer-Matrix Composite. *J Dent*, 2015.
26. Han I-H, Kang D-W, Chung C-H, Choe H-C, Son M-K. Effect of Various Intraoral Repair Systems on the Shear Bond Strength of Composite Resin to Zirconia. *J Adv Prosthodont*, 2013; **5**: 248-255.
27. Flinn BD, deGroot DA, Mancl LA, Raigrodski AJ. Accelerated Aging Characteristics of Three Yttria-Stabilized Tetragonal Zirconia Polycrystalline Dental Materials. *J Prosthet Dent*, 2012; **108**: 223-230.
28. Johnson AC, Versluis A, Tantbirojn D, Ahuja S. Fracture Strength of CAD/CAM Composite and Composite-Ceramic Occlusal Veneers. *J Prosthodont Res*, 2014; **58**: 107-114.
29. Arocha MA, Basilio J, Llopis J, Di Bella E, Roig M, Ardu S, Mayoral JR. Colour Stainability of Indirect CAD-CAM Processed Composites vs. Conventionally Laboratory Processed Composites after Immersion in Staining Solutions. *J Dent*, 2014; **42**: 831-838.
30. Dupriez ND, von Koeckritz AK, Kunzelmann KH. A Comparative Study of Sliding Wear of Nonmetallic Dental Restorative Materials with Emphasis on Micromechanical Wear Mechanisms. *J Biomed Mater Res B Appl Biomater*, 2014.
31. Koller M, Arnetzl GV, Holly L, Arnetzl G. Lava Ultimate Resin Nano Ceramic for CAD/ CAM: Customization Case Study. *Int J Comput Dent*, 2012; **15**: 159-164.
32. Garoushi S, Lassila LV, Tezvergil A, Vallittu PK. Load Bearing Capacity of Fibre-Reinforced and Particulate Filler Composite Resin Combination. *J Dent*, 2006; **34**: 179-184.
33. Garoushi S, Vallittu PK, Lassila LV. Fracture Resistance of Short, Randomly Oriented, Glass Fiber-Reinforced Composite Premolar Crowns. *Acta Biomater*, 2007; **3**: 779-784.
34. Keulemans F, Palav P, Aboushelib M, van Dalen A, Kleverlaan CJ, Feilzer AJ. Fracture Strength and Fatigue Resistance of Dental Resin-Based Composites. *Dent Mater*, 2009; **25**: 1433-1441.

35. Drummond JL, Bapna MS. Static and Cyclic Loading of Fiber-Reinforced Dental Resin. *Dent Mater*, 2003; **19**: 226-231.
36. Garoushi S, Lassila LV, Tezvergil A, Vallittu PK. Static and Fatigue Compression Test for Particulate Filler Composite Resin with Fiber-Reinforced Composite Substructure. *Dent Mater*, 2007; **23**: 17-23.
37. Garoushi SK, Lassila LV, Vallittu PK. Fatigue Strength of Fragmented Incisal Edges Restored with a Fiber Reinforced Restorative Material. *J Contemp Dent Pract*, 2007; **8**: 9-16.
38. Behr M, Rosentritt M, Handel G. Fiber-Reinforced Composite Crowns and FPDs: A Clinical Report. *Int J Prosthodont*, 2003; **16**: 239-243.
39. Dyer SR, Lassila LV, Jokinen M, Vallittu PK. Effect of Fiber Position and Orientation on Fracture Load of Fiber-Reinforced Composite. *Dent Mater*, 2004; **20**: 947-955.
40. Ornaghi BP, Meier MM, Rosa V, Cesar PF, Lohbauer U, Braga RR. Subcritical Crack Growth and in Vitro Lifetime Prediction of Resin Composites with Different Filler Distributions. *Dent Mater*, 2012; **28**: 985-995.
41. Raigrodski AJ, Hillstead MB, Meng GK, Chung KH. Survival and Complications of Zirconia-Based Fixed Dental Prostheses: A Systematic Review. *J Prosthet Dent*, 2012; **107**: 170-177.
42. Pihlaja J, Napankangas R, Raustia A. Early Complications and Short-Term Failures of Zirconia Single Crowns and Partial Fixed Dental Prostheses. *J Prosthet Dent*, 2014; **112**: 778-783.
43. Attia A, Kern M. Influence of Cyclic Loading and Luting Agents on the Fracture Load of Two All-Ceramic Crown Systems. *J Prosthet Dent*, 2004; **92**: 551-556.
44. Heintze SD, Albrecht T, Cavalleri A, Steiner M. A New Method to Test the Fracture Probability of All-Ceramic Crowns with a Dual-Axis Chewing Simulator. *Dent Mater*, 2011; **27**: e10-19.
45. Heintze SD, Cavalleri A, Zellweger G, Buchler A, Zappini G. Fracture Frequency of All-Ceramic Crowns During Dynamic Loading in a Chewing Simulator Using Different Loading and Luting Protocols. *Dent Mater*, 2008; **24**: 1352-1361.
46. Zhang Y, Chai H, Lee JJW, Lawn BR. Chipping Resistance of Graded Zirconia Ceramics for Dental Crowns. *J Dent Res*, 2012; **91**: 311-315.

**Chapter 10: General Discussion, Implications,
Recommendations for Future Work and
Conclusions.**

10.1 GENERAL DISCUSSION:

The concept of fibre reinforcement and its implementation in dentistry were discussed extensively in the literature review (Chapter 1). Briefly, this engineering concept, which relies on incorporating fibres to reinforce overlaying polymeric materials, has been implemented to potentially address the physico-mechanical inadequacies resin-composite materials would endure under high-demanding clinical conditions. Significant desirable developments in terms of strength, stiffness and toughness have been confirmed as a consequence of reinforcement, allowing the use of resin-composites in many untraditional applications, like fixed partial dentures [1-6]. However, some uncertainties regarding the design, longevity and clinical performance of reinforced resin-composite restorations limit their everyday practice, in comparison with the other well-established alternatives, such as dental ceramic [7-15]. Accordingly, this research set out to address such uncertainties and explore the influence of fibre reinforcement on the performance of resin-composite restorations by characterising some mechanical properties.

As the literature was inconclusive with regard to some clinical aspects of fibre reinforcement, particular gaps of knowledge were identified. The effect of fibre reinforcement on surface mechanical properties, like hardness and marginal strength, has not been previously established. From a clinical perspective, it is essential to understand such effects as it would influence the clinical performance of FRC restorations by determining their ability to resist plastic deformation and marginal breakage [16, 17]. Furthermore, the effect of fibre reinforcement on the bond strength between restorative materials and different bonding substrates is also important to comprehend. This is due to the fact that the strength of bonding interface regulates the effectiveness of stress distribution between bonding structures, and so aids in determining restoration overall performance [18, 19]. Moreover, investigating the influence of fibre reinforcement on the fatigue and corresponding wear was also needed as these properties regulate the clinical longevity of restorations subjected to the dynamic force of mastication[20-23]. The effect of design and orientation of reinforcing fibres on the overall performance has been also considered and highlighted in order to establish guidelines for the fabrication of FRC restorations. Likewise, a performance comparison between FRC restorations and other well-practiced alternatives was established in order to give more meaningful context to the findings.

A systematic approach of testing has been followed to address knowledge gaps. Six consecutive experiments were carried out *in-vitro* to particularly answer the research questions by measuring particular mechanical properties in specific testing configurations. The initial three experiments applied the relevant standardised testing configuration to investigate the influence of fibre reinforcement on three elementary mechanical properties of resin-composite materials, namely surface microhardness, edge-strength and shear bond strength. The remaining experiments utilized testing configurations relevant to the clinical situation to investigate the performance of anatomically-shaped FRC restorations while considering properties such as wear resistance, fatigue and load-bearing capacity.

FRCs with different structural parameters (fibre type, orientation and impregnation) were examined in this research as such parameters significantly influence the mechanical properties and overall performance (Section 1.2.5). Both E-glass and UHMWP reinforcing fibres were employed in this research due to their superior mechanical properties, excellent aesthetics and common applications (Section 1.2.5.1). FRCs with unidirectional, bidirectional and woven orientation were also utilized and compared herein since they have different reinforcement efficiency; and hence impact on the mechanical properties (Section 1.2.5.5). Direct FRC restorations were the main interest of this research in order to investigate and understand their clinical performance (Chapter 4-7). However, the performance of indirect FRC restorations, which follow the same principle of direct fibre reinforcement, was also investigated to validate the comparison with ceramic alternatives (Chapter 8 and 9).

The effect of incorporating differently-oriented FRCs on the surface microhardness of direct resin-composite material was evaluated (Chapter 4). Top and bottom, initial and post-storage Vickers hardness numbers (VHNs) were also measured to study the influence on 'depth of cure' and 'post-cure polymerization'. The findings showed that all VHNs significantly increased as a consequence of fibre reinforcement. This indicates that FRC, irrespective of its orientation, has a positive effect on the immediate and post-storage microhardness of direct resin-composites, and so an improvement in the overall performance would be expected. However, the effect on depth of cure was not favourable since a significant reduction in the bottom/top hardness ratio was detected after reinforcement. Although this reduction was not beyond the minimal acceptable percentage (80%), it still indicates that the presence of reinforcing fibres would attenuate the light transmittance and affect the properties of bottom surface.

To confirm this observation, the light irradiance (I_R) and total energy (E_T) delivered to specimen bottom surface were measured during curing. As expected, a significant reduction in I_R and E_T values as a result of incorporating FRC was detected, which confirms that FRCs attenuate light transmittance. This finding has clinical relevance as FRC restorations would need additional curing time in order to account for the attenuation effect of fibre reinforcement. Interestingly, the orientation of incorporated FRC also seems to have an influence on hardness and light transmittance since bidirectional FRCs exhibited the highest VHNs and lowest attenuation effect. This means that FRC with bidirectional orientation is favourable to incorporate in direct resin-composite restorations as it would provide excellent reinforcement for whole restoration thickness. Accordingly, bidirectional FRCs were mainly employed during the designing process of anatomical FRC restorations in the later experiments (Chapter 7-9).

Similar findings were also established when the effect of FRC orientation on the edge-strength was investigated (Chapter 5). The effect on edge-strength was important to consider as it would give a useful indication about the integrity of restoration margins and their susceptibility to deteriorate throughout the clinical service [17, 24]. Significant improvement in the edge-strength values was seen as a consequence of fibre reinforcement. The efficiency of marginal reinforcement, however, was influenced by fibre orientation since the bidirectional FRC reinforced the margins more effectively than unidirectional FRC. These findings are in accordance with those of the previous experiment, indicating the superiority of bidirectional FRC in terms of marginal integrity and deformation resistance. Additionally, this experiment exhibited that bulk-fill resin-composite materials tend to have better marginal integrity than the conventional ones, hence their use in the later experiments.

The shear bond strength (SBS) between FRC restorations and other restorative materials is also another significant clinical parameter to consider (Chapter 6). This is because that FRCs are clinically indicated to be used as an intermediate layer to reinforce the bonding interface between resin-composite and other restorative materials [25-28]. Accordingly, this research investigated the effect of differently-oriented FRCs on SBS between veneering resin-composite and two crown-fabricating materials (lithium disilicate and Co-Cr alloys) with different surface treatments. This testing set-up is equivalent to clinical situations where FRC restorations have to be bonded to other substrates in order to be functional.

The main finding of the SBS experiment was that FRCs significantly reduced the SBS irrespective to the type of bonding material or surface treatment, which indicates the poor performance of FRC under shear loading. However, FRCs did reinforce the veneering material by favourably altering stress dynamics at the interface and preventing cohesive and catastrophic failures. Once again, bidirectional FRCs exhibited better SBS values than unidirectional FRCs, and performed better under shear loading. One clinical implication of these findings is to consider supporting the veneering material by incorporating a bidirectional reinforcing layer away from pure shear loading. This technique was used later in this research (Chapter 7) in an attempt to prepare FRC restorations with a design that would reduce delamination failures and improve longevity.

Delamination of the veneering composite layer from the reinforcing fibre framework has been clinically reported as the main mode of failure in FRC restorations, especially FPDs [15, 29, 30]. From a clinical perspective, this means that a reduced clinical longevity would be predicted for such restorations. However, from an engineering perspective, this indicates that the stress distribution along the interfaces during loading is not desirable, and so the restoration framework needs to be redesigned in order to provide more support for the veneering material. Inspired by this, as well as the need to provide some guidelines for the designing of FRC restoration, two designs of FRC-FPDs were proposed and tested for their load-bearing capacity and performance (Chapter 7). An additional layer of bidirectional FRC was incorporated perpendicularly to the loading in Type-I design in order to mainly support the occlusal veneering resin-composite. In contrast, Type-II had an additional woven FRC bundle in an inverted-U configuration that was supposed to change stress distribution and entirely support the veneering material. Both types were tested in a clinically-relevant environment and subjected to cyclic eccentric (chewing) loading. This form of loading was important to employ since it simulates not only the clinical masticatory force with its both components but also the corresponding fatigue.

The effect of fatigue on the performance of FRC-FPDs was also explored since it has been believed to be detrimental, yet design-dependent [20, 22, 23, 31-35]. As anticipated, the fatigue was found to have a significant negative effect on the performance of both designs, especially on Type-II. Type-I had significantly better overall performance which was attributed to the superior properties of bidirectional FRC. Nevertheless, the failure analysis showed that Type-II FRC-FPDs had fewer

delamination failures owing to the unique fibre configuration that allowed better support to the veneering layer buccally and lingually. In view of that, it is confirmed that the design of the fibre framework would significantly influence the overall performance of FRC restorations since it controls the crack propagation and fatigue behaviour. The design with bidirectional reinforcing-fibres incorporated perpendicular to the loading direction on a wide area is recommended for use as it improves the fatigue behaviour and allows superior reinforcement with excellent stress distribution.

The above principle of designing was also followed later to prepare indirect FRC crowns whose wear performance and fatigue behaviour were compared in relation to other metal-free restorations (Chapter 8 and Chapter 9). Two established CAD/CAM restorations (Lava Zirconia and Lava Ultimate) were chosen to set a reference for the comparison, which would put the findings into a meaningful context that improves the clinical recognition of FRC restorations. Again, a clinically-relevant protocol was employed during the testing, taking into account the effect of thermal aging, fatigue and dynamic loading. Importantly, the wear performance of FRC restoration was also considered in order to give an indication about the clinical longevity of FRC restorations, their resistance to deterioration and abrasiveness. Novel methodology using an intraoral scanner was followed to quantify the wear, and was found to be simple, feasible and reliable for future use. The findings were promising as the FRC crown showed desirable load-bearing capacity and fatigue behaviour better than Lava Ultimate and comparable to the robust Lava Zirconia restorations. This gives insight about the performance of FRC restorations in relation to other alternatives under high-demanding condition. Also, the wear values were indicative of the reasonable deterioration resistance, longevity and abrasiveness of FRC restorations, which cumulatively would advocate the use of FRC restoration instead of ceramic in certain clinical situations, especially with natural teeth as the opposing structures.

10.2 IMPLICATIONS:

Several noteworthy contributions have been made to the current literature and clinical practice by addressing many uncertainties about FRC restorations and providing practical guidelines.

Firstly, the findings imply that incorporating a layer of FRC within a resin-composite restoration can effectively enhance many properties, including hardness, marginal integrity and fracture resistance. Fatigue behaviour and wear performance also tend to be improved in comparison with non fibre-reinforced composites, like Lava Ultimate. Clinically, this can be a valuable technique to strengthen many restorative modalities (e.g. class-I, class-II, inlays, onlays, crowns and FPDs) under high-demanding conditions. Importantly, the incorporated FRC layers should be well-adapted between the restoration layers and include the margins as this would ensure optimum reinforcement and marginal integrity.

Secondly, this research suggests that the orientation of reinforcing fibres seems to regulate the efficiency of reinforcement in resin-composite restorations, and so affect the overall performance. According to the current literature, unidirectional FRCs are the most effective in reinforcing bulk properties, like flexural strength and modulus of elasticity. Nevertheless, this research suggests that bidirectional FRCs seem to be better in terms of surface properties, including hardness, and edge-strength. From a clinical perspective, the use of unidirectional FRC can be advocated within the main frameworks of restorations to support against the flexural loading, whereas bidirectional FRCs are more recommended in situations where an additional reinforcement is required to enhance the surface resistance against deterioration.

Thirdly, this research also suggests that the performance of FRC restoration is dependent on the design of fibre framework as well as its configuration in relation to the direction of loading. The perpendicular incorporation of FRC is recommended as it is the best to counteract the loading forces and enhance the mechanical properties. Therefore, this research highlights the importance of understanding how the stress would distribute in FRC restorations in order to tailor their frameworks in a way that hinders crack propagation and ultimately enhances the clinical performance. Using multiple reinforcements with different configurations might be an option to support extensive restorations in different places.

Fourthly, this research also suggests that the incorporation of FRC within PRC can affect light transmittance and reduce the irradiance and energy delivered to deep layers. This can affect the depth of cure, degree of conversion and so some physico-mechanical properties. From a clinical perspective, curing time longer than that suggested by manufacturers is needed to compensate the energy lost by the reinforcing fibres.

Fifthly, this research shows that the performance of FRC under shear loading is poor, as it leads to significant reduction in shear bond strength. However, its incorporation at the bonding interface can change the stress dynamics and prevent unfavourable fractures in bonding substrates. Clinically, this can be a valuable technique to limit the destruction of functional restorations used as abutments during the provisionalization of adjacent restorations.

10.3 RECOMMENDATION FOR FUTURE WORK:

This *in-vitro* research has expanded our understanding of FRC restorations, and established fundamentals for future studies aiming to develop further knowledge and understanding.

Future proposed *in-vitro* studies include:

- Identifying different designs of FRC restorations and investigating their fatigue behaviour under prolonged or accelerated loading
- Investigating the effect of FRC incorporation on the optical properties of resin-composite restoration, such as translucency and colour stability.

Investigating the performance of restorations made of short FRC material further reinforced with long FRC layer as a framework.

Further *in-vivo* research proposals include:

- Randomised control trials investigating the clinical performance of FRC restoration in relation to other alternatives in terms of wear behaviour, and longevity.
- Prospective clinical cohort studies investigating the effectiveness of incorporating FRC with different orientation on the surface integrity of resin-composite restorations and their resistance to surface deteriorations.
- Randomised control trials comparing the performance of different designs of FRC-FPDs.
- Clinical setups validating the use of intraoral 3D scanners as direct tooth wear monitoring instruments.

10.4 CONCLUSIONS:

I. Based on the initial three experiments and within their limitations, the following conclusions can be drawn:

- FRC incorporation significantly improves the surface hardness and edge-strength of direct resin-composite materials.
- The presence of FRC within direct resin-composite restorations significantly reduces the transmittance of light as well as the bond strength with metal/ceramic substrates.
- The effectiveness of fibre reinforcement is significantly influenced by the orientation of reinforcing fibres.
- Bidirectional FRC has significantly more effective reinforcement than unidirectional FRC in terms of surface properties (edge-strength, hardness and bond strength).

II. Based on testing the performance of anatomical FRC restorations in the later experiments and within their limitations, the following conclusions can be drawn:

- The design of fibre framework and its configuration in relation to the direction of loading significantly influence the fatigue behaviour and load bearing capacity of FRC restorations.
- The perpendicular incorporation of additional reinforcing fibres within FRC-FPDs is the most beneficial to encounter loading force and support the occlusal veneering material.
- Dynamic fatigue significantly reduces the load bearing capacity of FRC restorations.
- FRC crowns demonstrate fracture and fatigue resistances better than Lava Ultimate but lesser than Lava Zirconia crowns.
- FRC and Lava Ultimate crowns exhibit lesser wear resistance and abrasiveness in relation to Lava Zirconia.
- The use of 3M True definition scanner is a reliable method to monitor and quantify tooth wear.

10.5 REFERENCES:

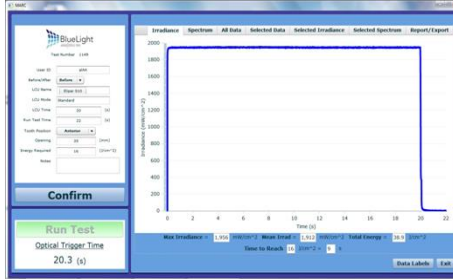
1. Dyer SR, Lassila LV, Alander P, Vallittu PK. Static Strength of Molar Region Direct Technique Glass Fibre-Reinforced Composite Fixed Partial Dentures. *J Oral Rehabil*, 2005; **32**: 351-357.
2. Garoushi S, Vallittu PK, Lassila LV. Fracture Toughness, Compressive Strength and Load-Bearing Capacity of Short Glass Fibre-Reinforced Composite Resin. *Chin J Dent Res*, 2011; **14**: 15-19.
3. Oberholzer TG, du Preez IC, Lombard R, Pitout E. Effect of Woven Glass Fibre Reinforcement on the Flexural Strength of Composites. *SADJ*, 2007; **62**: 386, 388-389.
4. Vallittu PK. Some Aspects of the Tensile Strength of Unidirectional Glass Fibre-Polymethyl Methacrylate Composite Used in Dentures. *J Oral Rehabil*, 1998; **25**: 100-105.
5. Dyer SR, Sorensen JA, Lassila LV, Vallittu PK. Damage Mechanics and Load Failure of Fiber-Reinforced Composite Fixed Partial Dentures. *Dent Mater*, 2005; **21**: 1104-1110.
6. Jokstad A, Gokce M, Hjortsjo C. A Systematic Review of the Scientific Documentation of Fixed Partial Dentures Made from Fiber-Reinforced Polymer to Replace Missing Teeth. *Int J Prosthodont*, 2005; **18**: 489-496.
7. van Heumen CC, Kreulen CM, Creugers NH. Clinical Studies of Fiber-Reinforced Resin-Bonded Fixed Partial Dentures: A Systematic Review. *Eur J Oral Sci*, 2009; **117**: 1-6.
8. Dyer SR, Lassila LV, Jokinen M, Vallittu PK. Effect of Cross-Sectional Design on the Modulus of Elasticity and Toughness of Fiber-Reinforced Composite Materials. *J Prosthet Dent*, 2005; **94**: 219-226.
9. Ootaki M, Shin-Ya A, Gomi H, al e. Optimum Design for Fixed Partial Dentures Made of Hybrid Composite with Glass Fiber Reinforcement by Finite Element Analysis: Effect of Vertical Reinforced Thickness on Fiber Frame. *Dent Mater J*, 2007; **26**: 280-289.
10. Xie Q, Lassila LV, Vallittu PK. Comparison of Load-Bearing Capacity of Direct Resin-Bonded Fiber-Reinforced Composite FPDs with Four Framework Designs. *J Dent*, 2007; **35**: 578-582.
11. Başaran EG, Ayna E, Vallittu PK, Lassila LVJ. Load Bearing Capacity of Fiber-Reinforced and Unreinforced Composite Resin CAD/CAM-Fabricated Fixed Dental Prostheses. *J Prosthet Dent*, 2013; **109**: 88-94.
12. Garoushi S, Lassila LV, Tezvergil A, Vallittu PK. Load Bearing Capacity of Fibre-Reinforced and Particulate Filler Composite Resin Combination. *J Dent*, 2006; **34**: 179-184.
13. Anusavice KJ. Standardizing Failure, Success, and Survival Decisions in Clinical Studies of Ceramic and Metal-Ceramic Fixed Dental Prostheses. *Dent Mater*, 2012; **28**: 102-111.
14. Vallittu PK. Survival Rates of Resin-Bonded, Glass Fiber-Reinforced Composite Fixed Partial Dentures with a Mean Follow-up of 42 Months: A Pilot Study. *J Prosthet Dent*, 2004; **91**: 241-246.
15. van Heumen CCM, Tanner J, van Dijken JWV, Pikaar R, Lassila LVJ, Creugers NHJ, Vallittu PK, Kreulen CM. Five-Year Survival of 3-Unit Fiber-Reinforced Composite Fixed Partial Dentures in the Posterior Area. *Dent Mater*, 2010; **26**: 954-960.

16. Garoushi S, Vallittu PK, Lassila LV. Depth of Cure and Surface Microhardness of Experimental Short Fiber-Reinforced Composite. *Acta Odontol Scand*, 2008; **66**: 38-42.
17. Ereifej N, Silikas N, Watts DC. Edge Strength of Indirect Restorative Materials. *J Dent*, 2009; **37**: 799-806.
18. Ilday N, Seven N. The Influence of Different Fiber-Reinforced Composites on Shear Bond Strengths When Bonded to Enamel and Dentin Structures. *J Dent Sci*, 2011; **6**: 107-115.
19. Juloski J, Beloica M, Goracci C, Chieffi N, Giovannetti A, Vichi A, Vulicevic ZR, Ferrari M. Shear Bond Strength to Enamel and Flexural Strength of Different Fiber-Reinforced Composites. *J Adhes Dent*, 2013; **15**: 123-130.
20. Bae JM, Kim KN, Hattori M, Hasegawa K, Yoshinari M, Kawada E, Oda Y. Fatigue Strengths of Particulate Filler Composites Reinforced with Fibers. *Dent Mater J*, 2004; **23**: 166-174.
21. Baran G, Boberick K, McCool J. Fatigue of Restorative Materials. *Crit Rev Oral Biol Med*, 2001; **12**: 350-360.
22. Drummond JL. Degradation, Fatigue, and Failure of Resin Dental Composite Materials. *J Dent Res*, 2008; **87**: 710-719.
23. Garoushi S, Lassila LV, Tezvergil A, Vallittu PK. Static and Fatigue Compression Test for Particulate Filler Composite Resin with Fiber-Reinforced Composite Substructure. *Dent Mater*, 2007; **23**: 17-23.
24. Watts DC, Issa M, Ibrahim A, Wakiaga J, Al-Samadani K, Al-Azraqi M, Silikas N. Edge Strength of Resin-Composite Margins. *Dent Mater*, 2008; **24**: 129-133.
25. Bagis B, Ustaomer S, Lassila LV, Vallittu PK. Provisional Repair of a Zirconia Fixed Partial Denture with Fibre-Reinforced Restorative Composite: A Clinical Report. *J Can Dent Assoc*, 2009; **75**: 133-137.
26. Turkaslan S, Tezvergil-Mutluay A, Bagis B, Shinya A, Vallittu PK, Lassila LV. Effect of Intermediate Fiber Layer on the Fracture Load and Failure Mode of Maxillary Incisors Restored with Laminate Veneers. *Dent Mater J*, 2008; **27**: 61-68.
27. Turkaslan S, Tezvergil-Mutluay A. Intraoral Repair of All Ceramic Fixed Partial Denture Utilizing Preimpregnated Fiber Reinforced Composite. *Eur J Dent*, 2008; **2**: 63-68.
28. Ergun G, Cekic I, Lassila LV, Vallittu PK. Bonding of Lithium-Disilicate Ceramic to Enamel and Dentin Using Orthotropic Fiber-Reinforced Composite at the Interface. *Acta Odontol Scand*, 2006; **64**: 293-299.
29. Göhring TN, Roos M. Inlay-Fixed Partial Dentures Adhesively Retained and Reinforced by Glass Fibers: Clinical and Scanning Electron Microscopy Analysis after Five Years. *Eur J Oral Sci*, 2005; **113**: 60-69.
30. Ozcan M, Breuklander MH, Vallittu PK. The Effect of Box Preparation on the Strength of Glass Fiber-Reinforced Composite Inlay-Retained Fixed Partial Dentures. *J Prosthet Dent*, 2005; **93**: 337-345.
31. Dyer KP, Isaac DH. Fatigue Behaviour of Continuous Glass Fibre Reinforced Composites. *Composites Part B: Engineering*, 1998; **29**: 725-733.
32. Keulemans F, Palav P, Aboushelib M, van Dalen A, Kleverlaan CJ, Feilzer AJ. Fracture Strength and Fatigue Resistance of Dental Resin-Based Composites. *Dent Mater*, 2009; **25**: 1433-1441.
33. Lohbauer U, Belli R, Ferracane JL. Factors Involved in Mechanical Fatigue Degradation of Dental Resin Composites. *J Dent Res*, 2013; **92**: 584-591.

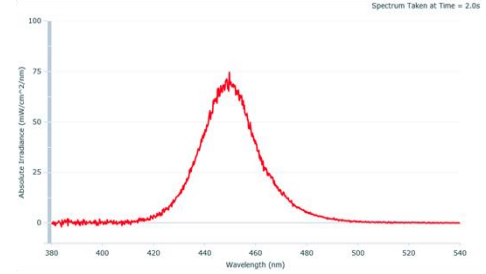
34. Rantala LI, Lastumaki TM, Peltomaki T, Vallittu PK. Fatigue Resistance of Removable Orthodontic Appliance Reinforced with Glass Fibre Weave. *J Oral Rehabil*, 2003; **30**: 501-506.
35. Shah MB, Ferracane JL, Kruzic JJ. Mechanistic Aspects of Fatigue Crack Growth Behavior in Resin Based Dental Restorative Composites. *Dent Mater*, 2009; **25**: 909-916.

Appendix I:

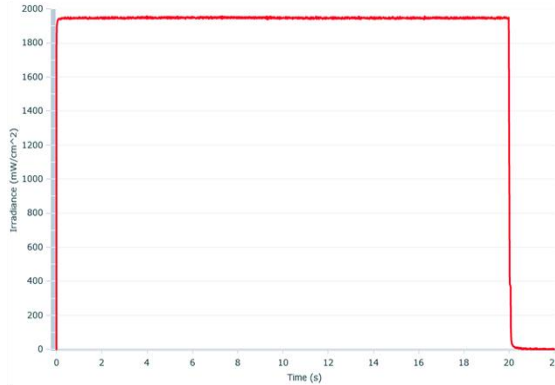
Irradiance measurement of LED curing unit (Eliper S10, 3M-ESPE).



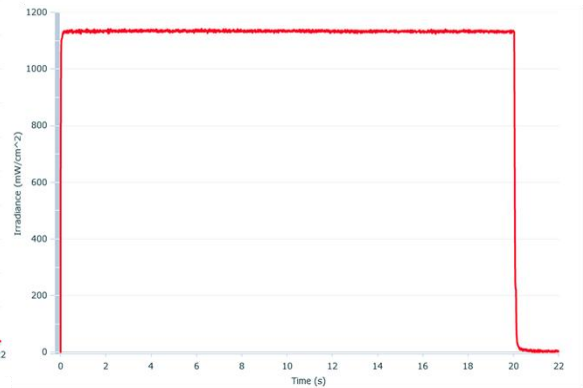
Baseline irradiance measurement
Curing time : 20s, Mode: standard



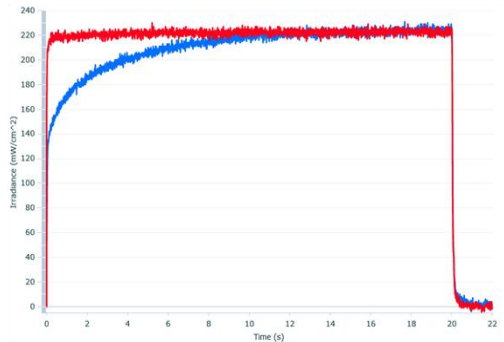
Wave Length 420-480 nm (Single peak)



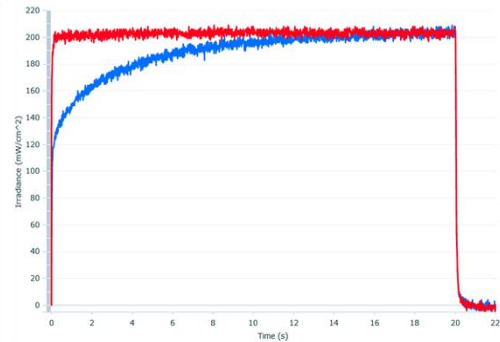
Direct contact with sensor
Irradiance output: 1943 mW/cm²



1mm glass separation:
1764 mW/cm²
3mm space+1mm glass separation:
1032 mW/cm²



3mm-thickness PRC specimen
During curing 200 mW/cm²
After curing: 220 mW/cm²



3mm-thickness FRC-PRC specimen
During curing 185 mW/cm²
After curing: 200 mW/cm²